OCCURRENCE AND BEHAVIOUR OF SILVER NANOPARTICLES IN THE ENVIRONMENT: ANALYTICIAL METHODOLOGIES AND LABORATORY STUDIES

Laura Torrent Fàbrega

Universitat de Girona

Doctoral thesis

Occurrence and behaviour of silver nanoparticles in the environment: Analytical methodologies and laboratory studies

Laura Torrent Fàbrega

2019

Doctoral program in Chemistry

Supervised by Dr. Mònica Iglesias Juncà and Dr. Eva Marguí Grabulosa

(Tutor: Dr. Mònica Iglesias Juncà)

Thesis submitted in fulfilment of the requirements for the degree of Doctor from the University of Girona

Universitat de Girona

Dr. Mònica Iglesias Juncà and Dr. Eva Marguí Grabulosa, from the University of Girona,

WE DECLARE:

That the thesis titled "Occurrence and behaviour of silver nanoparticles in the environment: Analytical methodologies and laboratory studies", presented by Laura Torrent Fàbrega to obtain a doctoral degree, has been completed under our supervision and meets the requirements to opt for an International Doctorate.

For all intents and purposes, we hereby sign this document.

Dr. Mònica Iglesias Juncà

Dr. Eva Marguí Grabulosa

Girona, July 24th 2019

This thesis was financially supported by the Spanish Ministry of Economy and Competitiveness through the national reserch project CGL2013-48802-C3-2-R and by the project MPCUdG2016/103 from the University of Girona. Laura Torrent Fàbrega gratefully acknowledged a FPI grant from the Spanish Ministry of Economy and Competitiveness (BES-2014-070625) and two FPI mobility scholarships for her research stages in the University of Zaragoza (EEBB-I-17-12391) and in the University of Ljubljana (EEBB-I-18-13040).

A la meva mare, al meu pare i a la meva germana

"Life is the art of drawing sufficient conclusions from insufficient premises"

BUTLER, *Samuel*

Agraïments

Agradecimientos/Acknowledgments

Aquest moment representa el final d'una nova etapa en la meva formació com a química, després de rebre fa poc més de quatre anys una trucada que va fer canviar el meu rumb professional. Després d'aquests anys, puc dir que no me'n penedeixo de la decisió que vaig prendre en aquell moment ja que estic satisfeta amb les experiències viscudes tant a nivell professional com a nivell personal.

En primer lloc vull agrair de manera molt especial a les meves directores de tesi, la Dra. Mònica Iglesias i la Dra. Eva Marguí, per haver-me ajudat durant el transcurs d'aquesta tesi. Moltes gràcies per tot el que m'heu ensenyat durant aquests anys en el camp del ICPMS i de la fluorescència, per la vostra paciència i implicació, pel vostre suport en els mals moments, per transmetre'm la vostra passió per la recerca, per deixar-me viure noves experiències lluny de casa que m'han ajudat a créixer tant professionalment com personalment, i sobretot per tots els moments que hem viscut juntes. També vull agrair de forma molt especial a la responsable que fes que emprengués aquest camí, la Prof. Manuela Hidalgo. Gràcies per confiar en mi des dels meus inicis en el món de la química i donar-me l'oportunitat de continuar formant-me a través d'aquesta experiència inoblidable. Ha estat un plaer treballar amb vosaltres i sense la vostra ajuda res d'això hagués estat possible!

També voldria donar les gràcies al Dr. Ignasi Queralt per transmetre'm els seus coneixements tant del món de la ciència com de la vida en general, però sobretot per ajudar-nos amb un dels articles presentats en aquesta tesi a través de les seves nocions sobre mineralogia dels sòls. A la Dra. Dolors Verdaguer i a la Dra. Laura Llorens per contribuir en la realització de l'anàlisi fisiològic de les plantes en un dels estudis duts a terme durant aquesta tesi. Agrair també a la Dra. Lluïsa Matas, a l'Imma Arrom, a en Daniel Reyes i a la Carme Carulla, membres dels Serveis Tècnics de Recerca de la Universitat de Girona, per la seva dedicació i ajuda amb l'ICPMS, l'ICPOES i els microscopis.

A la resta de membres del Grup de Química Analítica i Ambiental del departament de química de la Universitat de Girona agrair-los el suport que m'han donat durant aquests anys. Gràcies Prof. Victòria Salvadó, Dra. Enriqueta Anticó, Dra. Clàudia Fontàs i Dr. Juanma Sánchez. I espero que ningú s'enfadi si destaco els meus dos companys de batalles durant aquests quatre anys, el Dr. Rubén Vera i la Dra.

Gemma Elías. Rubén, ens vam conèixer en el màster i després vam iniciar aquest camí plegats. Noi del "gym" i de l'entrepà de "pavo" només dir-te que moltes gràcies per les xerrades en el despatx, més freqüents durant aquesta última etapa, sobre la feina però també sobre la música, la vida i sobretot el Girona FC! Gemma, amb tu ens vam conèixer pràcticament en els inicis de les nostres tesis. Moltíssimes gràcies per saber-me escoltar i donar-me suport moral en els meus moments d'estrès, d'angoixa i frustració, que n'han estat uns quants! També agrair-te que hagis estat la impulsora en moltes ocasions dels nostres moments d'oci, sense tu crec que no hauríem fet res. A tots dos només dir-vos que ha estat un plaer poder treballar amb vosaltres durant aquesta etapa de la nostra vida professional i us desitjo el millor tant en l'àmbit professional com en el personal! Tot i que ara els nostres camins es separen, tenim un sopar pendent els tres i també espero que de tant en tant anem a fer un dels nostres "vinillos"! Tampoc vull deixar-me a la Gemma Mostazo i a la Dra. Aida García. Gemma , tot i que vas estar un període curtet amb nosaltres, la teva simpatia i saber estar ens va captivar a tots. Encara que al final decidissis no emprendre el camí del doctorat, a la vida hi ha moments que has de prendre decisions difícils però que la decisió que prenguis sempre has de pensar que serà la correcta. Per cert, en els "vinillos" també t'hi esperem i no oblidis que tenim una aventura pendent de les nostres amb la Dra. Elías! Aida, tot i que vam coincidir en el final de la teva tesi, només donar-te les gràcies pels consells que em vas donar per afrontar aquesta etapa i també per ajudar-me en l'organització de la part més festiva de les tesis dels meus companys. A totes dues us desitjo el millor en el futur!

Aquest treball tampoc hauria estat possible sense l'ajuda dels estudiants de grau que han contribuït en la part experimental d'aquesta tesi. Andreu, Lourdes, Albert, Miquel i Guillem us vull agrair el vostre interès i implicació en el vostre i alhora el meu treball. Però sobretot us vull donar les gràcies per la vostra complicitat i els bons moments viscuts en el laboratori. A tots vosaltres us desitjo el millor! A la resta d'estudiants que han passat pel grup per realitzar el seu treball de final de grau també us desitjo el millor! Durant aquesta etapa també he tingut l'oportunitat de conèixer altres estudiants de doctorat o doctors que han passat pel grup a través de les seves estàncies. Rogerta it was so nice to meet you during this period, when you were in Girona as a PhD student. It was great to come to your PhD dissertation in Italy and subsequently to visit you during my holidays to know more about north Italy. I desire all your best as a researcher and in your personal life! I hope to have more opportunities to meet you in Girona, in Brescia or in Albania! Cristina fuiste un gran descubrimiento para mi y mis compañeros. ¡Gracias por tu espontaneidad y tu forma de ser, transmites alegría allá dónde vas! Pero sobretodo, "Eskerrik

asko" por compartir las tardes de confesiones, de cantos (para que lloviera) y bailoteos, de cocina y de enseñarme vasco. Aunque el Girona ya no esté en primera, sé qué aún te debo una visita en Durango para que me enseñes tu tierra y a tu amado Rusti cómo se hace el muerto. ¡Te deseo todo lo mejor en tu vida profesional y personal! Zek it was a short period of time that I shared with you when you were in Girona as a post-doctoral student, but it was sufficient to have a scientific paper together. Thank you for being a funny man and I desire all the best in the future! Donatella también fue un período corto pero intenso el que compartimos en Girona. ¡Contigo tuve la oportunidad de conocer más cosas sobre la "Bella Italia" y su gastronomía a través de la cena que nos preparaste! Solamente decirte que "È stato un vero piacere conoscerti", te deseo todo lo mejor en tu tesis y espero poder hacerte una visita en breve a la "tua Sicilia". Jasna, I remember that my first contact with you was in Gothenburg in the European X-ray spectrometry conference. Later you came to our laboratories to work with my supervisor Eva and through TXRF analysis our friendship started. Thank you for your kindness and our talks about my future, life and other topics. I desire all your best on your great research and I hope to visit you soon in Zagreb! María Martha y Dimitra, aunque os he conocido en el peor momento de la tesis (la etapa de escribir), gracias por vuestra comprensión y ayuda en los momentos de dificultades. ¡También gracias María Martha por la cena argentina que nos preparaste con tanto cariño para despedirnos de nosotros! ¡Os deseo a las dos lo mejor en vuestro futuro laboral y personal, y espero poderos visitar en vuestras respectivas ciudades en un futuro! To the rest of the people who have been in the research group for their research stages during these years, I also desire to them the best!

Una parte de mi trabajo experimental presentado en esta tesis se realizó en el Grupo de Espectroscopía Analítica y Sensores (GEAS) del departamento de química analítica de la Universidad de Zaragoza y que también forma parte del Área de Ciencia y Tecnología Química del Instituto de Investigación en Ciencias Ambientales de Aragón de la Universidad de Zaragoza (IUCA). Quiero agradecer especialmente al Prof. Francisco Laborda su hospitalidad y generosidad en ofrecerme la posibilidad de trabajar durante tres meses en su grupo. Gracias por transmitirme tus conocimientos en el ámbito del análisis de las nanopartículas por SP-ICPMS, por contar conmigo en los eventos académicos que organizaba el grupo, por informarme de los congresos, por quedarte hasta las ocho de la tarde para analizar muestras y por preocuparte que estuviera bien durante mi breve estancia en tus laboratorios. ¡Sin ti y Mònica no hubiera sido posible la publicación de uno de los artículos presentados en esta tesis! También agradecer a los otros miembros del grupo de investigación su amabilidad y hacerme sentir

como una más del grupo durante este corto período de tiempo: Prof. Juan R. Castillo, Dr. Eduardo Bolea, Dra. María S. Jiménez, Dra. María T. Gómez, Dra. Josefina Pérez, Dr. José M. Mir y Juan C. Vidal. Y aunque ya no esté con nosotros también quiero dar las gracias a la simpatiquísima Dra. Gemma Cepriá por sus recomendaciones durante la comida sobre los sitios con encanto que podía visitar en territorio aragonés. A las miembros de los Servicios Técnicos, Maite, Ana y Teresa gracias por vuestra paciencia, atención y ayuda durante los análisis que realicé con el ICPMS durante mi estancia. Obviamente no quiero dejar de mencionar a mis "mañicos" favoritos: Ana Cris, Celia, David y Dani. Ana Cris y Celia, aunque solo compartía con vosotras las mañanas ya que en aquel momento estabais cursando el máster, gracias por hacerme reír con vuestras ocurrencias, por recordarme que llegaba 5 minutos más tarde de lo normal y sobretodo por corregirme mi brillante castellano. David, el único doctorando en aquel momento, gracias por las charlas de las tardes sobre trabajo, libros, fútbol, etcétera; cuando te venías a despedir. Dani, mi DJ favorito y estudiante de máster en aquel momento, gracias por amenizar el ambiente mientras yo trataba los datos y tu jugabas al Buscaminas. En general, agradeceros a todos vuestra ayuda en el laboratorio cuando lo necesitaba. Además, gracias por hacerme sentir una más del grupo a través de los cafés mañaneros, de las comidas, de las cervezas para levantar el ánimo después de un día pésimo en el trabajo y de las cenas que organizasteis. Durante esta etapa también tuve el placer de conocer a Vanesa y a Angélica. Vanesa mi "galleguiña" favorita, muchas gracias por los momentos compartidos en los cafés y las comidas durante tu mini estancia en Zaragoza. ¡Sé que te debemos junto a David venir a ver el Dépor-Girona a Coruña! Angélica, a ti agradecerte también las comidas compartidas, las excursiones por Zaragoza durante el fin de semana y tu visita a Girona donde tuviste el gran detalle de traer una botella de tequila de tu país. Espero que en un futuro me lo pueda venir a tomar a Méjico. ¡Solamente desearos a todos lo mejor en vuestras tesis o en vuestro trabajo y en vuestra vida personal! ¡Y por cierto, aún espero vuestra visita en Girona!

Another part of the experimental work presented in this thesis has been performed in the Plant Physiology Research Group of the Biology Department from the University of Ljubljana. I want to give my deepest gratitude to Dr. Katarina Vogel-Mikuš for accepting me to work in her group during three months and a half. Thank you for teaching me how to work in your laboratories, to transmit me your knowledge in plant physiology and in sample preparation of vegetal samples to analyse by synchrotron radiation XAS, μ-PIXE and LA-ICPMS, and for taking care of me during my stage. Without you and Eva it couldn't be possible the scientific contribution presented in this thesis! I want also thank to other

members of the group for their kind hospitality: Prof. Marjana Regvar, Dr. Matevž Likar and Milena Kubelj. Thanks also to Dr. Alojz Kodre for his support in the data treatment of ALBA synchrotron results. Also thanks to the post-doctoral researchers, Carla and his husband, for giving me some recommendations in my experiments and for showing me some places of Ljubljana. But I want to sincerely thanks to the PhD student Anja Kavčič and the students Anja Mavrič, Petra and Max for helping me in the laboratory and giving me advices during the experiments with plants. Anja Kavčič and Petra "hvala" for your nice farewell showing me the "Salsa" events that are organized in Ljubljana and sharing with me a nice dinner. Anja Mavrič "hvala" for your patience and your kindness to help me in the laboratory until evening, for teaching me some words in Slovenian, for sharing with me several lunches when I was alone, for the fantastic moments that we spent listening Spanish and Slovenian music and for having a beautiful Spanish-Slovenian dinner at my home. I desire all your best in the future! Anja's and Petra, I wait for your visit in Girona! Thank you to Dr. Johannes T. Van Elteren and their colleagues, Dr. Martin Šala and Dr. Vid Simon Šelih, members of the Department of Analytical Chemistry from the National Institute of Chemistry of Ljubljana for their interest in preforming LA-ICPMS analysis with plants contaminated with AgNPs. Special thanks to their PhD student Dino Meterapi for his kindness during our meetings deciding the performance of the experiment and for being able to cooperate in my research. I hope to finish the work that we started together in brief and I desire all your best in your PhD thesis! Also thanks Dino and Dr. Vasko Jovanovski for receiving me always with a smile on their faces, for our pleasant and fun conversations about research and our countries, and for the nice farewell showing me the tasty "piva" that you have in your country. I know that I have to come back for the guided tour in Slovenia, but you have also to come to Girona! I want also to thanks the PhD student Mitja Klemen from the Josef Stefan Institute of Ljubljana for his cooperation in the analysis of the samples by μ-PIXE and for recommending me to go to Velika Planina. It was an amazing place! Best wishes in your PhD thesis! During this period, I had the opportunity to spend many hours with my favourite Tunisian and Italian girls, Mariem and Laura. Mariem thank you for sharing with me all the lunches, some dinners and the nice excursions that we did in the Zoo, in Bled and in Trieste. Laura "grazie mille" for organizing some excursions in the beautiful Tivoli Park during my stage, for preparing for me and Mariem some typical Italian food for our dinners at your home, for watching the football together and for dancing some Italian songs after the dinners. Thank you also to your nice family for receiving me to your beautiful town Chioggia in my last weekend of my stage! I desire all the best in your thesis and I hope to see you in a near future in Girona, Tunis or Chioggia!

Moltíssimes gràcies a les meves estimades “Mosquetes”! Gràcies per entendre els dies que no podia quedar per feina, per entendre que havia de marxar per viure una nova experiència professional, per la vostra visita a Saragossa, pels viatges juntes, etc. Ara que s’acaba aquesta etapa espero poder passar més temps amb vosaltres i encara que no sàpiga quin serà el meu destí professional, espero que aquesta amistat que ens ha unit des de que érem unes adolescents perduri per tota la vida. Us estimo nenes!

Finalment voldria agrair de tot cor a la meva petita però bonica família que son els tres pilars fonamentals de la meva vida. Mama, papa i Eva gràcies per haver-me ajudat en els moments que més ho necessitava i pel vostre suport incondicional que m’heu donat en tot allò que m’he proposat des dels inicis de la meva carrera professional. Mama gràcies per ser tant forta i donar-me un cop més una lliçó de vida. Per nosaltres ets la nostra campiona! Tampoc vull deixar-me en Bernat, moltes gràcies per preocupar-te sempre per la meva germana i per mi. Aquest camí no hagués estat el mateix sense vosaltres i només tinc paraules d’agraïment per haver-me acompanyat durant tot aquest temps! Això va per vosaltres família i en especial per tu mama! Us estimo família!

List of publications

This thesis is based on a compendium of the followed published or submitted scientific papers:

L. Torrent, M. Iglesias, M. Hidalgo, E. Marguí, *Analytical capabilities of total reflection X-ray fluorescence spectrometry for silver nanoparticles determination in soil adsorption studies*. Spectrochim. Acta Part B, Atomic spectroscopy 126 (2016) 71-78. doi: 10.1016/j.sab.2016.10.019. (Impact factor: 3.241, 1st quartile).

L. Torrent, M. Iglesias, M. Hidalgo, E. Marguí, *Determination of silver nanoparticles in complex aqueous matrices by total reflection X-ray fluorescence spectrometry combined with cloud point extraction*. J. Anal. At. Spectrom. 33 (2018) 383-394. doi: 10.1039/C7JA00335H. (Impact factor: 3.646, 1st quartile).

L. Torrent, E. Marguí, I. Queralt, M. Hidalgo, M. Iglesias, *Interaction of silver nanoparticles with mediterranean agricultural soils: Lab-controlled adsorption and desorption studies*. J. Environ. Sci. 83 (2019) 205-216. doi: 10.1016/j.jes.2019.03.018. (Impact factor: 3.556, 2nd quartile).

L. Torrent, F. Laborda, E. Marguí, M. Hidalgo, M. Iglesias, *Combination of cloud point extraction with single particle inductively coupled plasma mass spectrometry to characterize silver nanoparticles in soil leachates*. Anal. Bioanal. Chem. 411 (2019) 5317-5329. doi: 10.1007/s00216-019-01914-y. (Impact factor: 3.286, 1st quartile).

L. Torrent, M. Iglesias, E. Marguí, D. Verdaguer, L. Llorens, A. Kodre, A. Kavčič, K. Vogel-Mikuš, *Uptake, translocation and ligand of silver in Lactuca sativa exposed to silver nanoparticles of different size, coatings and concentration*. Journal of Hazardous Materials (under revision).

OTHER RELATED CONTRIBUTIONS

Additionally to the scientific papers presented in this work, three more scientific contributions related to the studies carried out in this thesis have been published:

L. Torrent, F. Laborda, M. Iglesias, E. Marguí, M. Hidalgo, *Combinación de la extracción en punto*

de nube con TXRF y SP-ICPMS para la determinación de nanopartículas de plata en muestras acuosas. Boletín de la Sociedad Española de Química Analítica, 61 (2018) 25-28.

L. Torrent, M. Iglesias, F. Laborda, E. Marguí, M. Hidalgo, *Estudi del comportament de les nanopartícules de plata en sòls agrícoles*, Revista de la Societat Catalana de Química, 17 (2018) 74-85.

Z. Bahadir, L. Torrent, M. Hidalgo, E. Marguí, *Simultaneous determination of silver and gold nanoparticles by cloud point extraction and total refection X-ray fluorescence analysis*, Spectrochim. Acta Part B, Atomic spectroscopy 149 (2018) 22-29. doi: 10.1016/j.sab.2018.07.016. (Impact factor: 3.101, 1st quartile).

List of abbreviations

Anodic particle coulometry	APC
Apparent electron transport rate	ETR
Atomic force microscopy	AFM
Attachment efficiency	α
Attenuated total reflectance fourier transformed infrared spectroscopy	ATR-FTIR
Avogadro number	N_{Av}
Capillary electrophoresis	CE
Carotenoid	*Car*
Cation exchange capacity	CEC
Certified reference materials	CRM
Charge-coupled device	CCD
Chlorophyll	*Chl*
Cloud point extraction	CPE
Complexing agent	CA
Compound annual growth rate	CAGR
Confocal microscopy	CM
Consumer Products Inventory	CPI
Critical micellar concentration	cmc
Deoxyribonucleic acid	DNA
Derjaguin-Landau-Verwey Overweek	DLVO
Diethylenetriaminepentaacetic acid	DTPA
Disodium dihydrogen ethylenediaminetetraacetate	EDTA
Dissolved organic matter	DOM
Dry weight	DW
Dynamic light scattering	DLS
Electrical conductivity	EC
Electrical double layer	EDL
Electron-energy loss spectroscopy	EELS
Electron microscopy	EM
Electrothermal atomic absorption spectrometry	ETAAS
Energy dispersive X-ray fluorescence	EDXRF
Energy dispersive X-ray spectroscopy	EDX
Engineered nanomaterials	ENMs
Engineered nanoparticles	ENPs
Environmental fate model	EFM
Environmental scanning electron microscopy	ESEM

European Chemicals Agency	ECHA
European Commission	EC
European Food Safety Authority	EFSA
European Medicines Agency	EMA
European Union	EU
Extended X-ray absorption fine structure	EXAFS
Field flow fractionation	FFF
Flame atomic absorption spectrometry	FAAS
Fourier-transformed infrared spectroscopy	FTIR
Glutathione	GSH
Gold nanoparticles	AuNPs
High-resolution continuum source electrothermal atomic absorption spectroscopy	HR-CS ETAAS
Hydrodynamic chromatography	HDC
Inductively coupled plasma	ICP
Inductively coupled plasma mass spectrometry	ICPMS ICP-MS
Inductively coupled plasma optic emission spectrometry	ICP-OES
International Organization for Standardization	ISO
Intrinsic water use efficiency	*WUE*
Instantaneous water use efficiency	WUE_i
Ion selective electrode	ISE(s)
Ionic silver	Ag^+ Ag(I)
Laser ablation	LA
Laser ablation inductively coupled plasma mass spectrometry	LA-ICPMS
Laser-induced breakdown spectroscopy	LIBS
Laser-scanning confocal microscopy	LSCM
Limits of detection	LOD(s)
Liquid-liquid extraction	LLE
Magnetic solid-phase extraction	MSPE
Malondialdehyde	MDA
Manufactured nanoparticles	MNPs
Material flow analysis	MFA
Mass-to-charge ratio	m/z
Mass spectrometer	MS
Metallic silver	Ag(0)
Micellar electrokinetic chromatography	MEKC
Micro synchrotron radiatio micro X-ray fluorescence spectrometry	μ-SR-XRF

Microparticle induced X-ray emission	μ-PIXE
Microwave	MW
Molecular weight cut-off	MWCO
Multiple-angle light scattering	MALS
Nanomaterial	NM(s)
Nanoparticle	NP(s)
Nanoparticle number concentration	N_{NP}
Nanoparticle tracking analysis	NTA
Nano-secondary ion mass spectrometry	Nano-SIMS
Natural organic matter	NOM
Near edge X-ray absorption fine structure	NEXAFS
Nebulisation efficiency	η_{neb}
Net photosynthetic rates	A
Non-photochemical quenching coefficient	NPQ
Octapole Reaction System	ORS
Organic matter content	OM
Organization for Economic Cooperation and Development	OECD
Photosynthetically active radiation	PAR
Point zero charge	PZC
Polyethyleneglycol	PEG
Polytetrafluoroethylene	PTFE
Polyvinylpyrrolidone	PVP
Quantum dots	QDs
Radio-frequency	RF
Reactive oxygen species	ROS
Reference material	RM
Registration, Evaluation, Authorisation and Restriction of Chemicals	REACH
Relative standard deviation	RSD
Reversed phase chromatography	RPC
Ribonucleic acid	RNA
Scanning electron microscopy	SEM
Scientific Committee on Emerging and Newly Identified Health Risks	SCENIHR
Scientific Committee on Consumer Safety	SCCS
Secondary ion mass spectrometry	SIMS
Selected-area electron diffraction	SAED
Silicon drift detectors	SDD
Silver nanoparticles	AgNP(s)
Single particle inductively coupled plasma mass spectrometry	SP-ICPMS
	SP-ICP-MS

Size exclusion chromatography	SEC
Solid-phase extraction	SPE
Standard deviation	sd
	SD
Stomatal conductance	g_s
Surface enhanced Raman	SERS
Surface plasmon resonance	SPR
Surface plasmon resonance band	SPRB
Synchrotron radiation X-ray absorption spectroscopy	SR-XAS
Total reflection X-ray fluorescence spectrometry	TXRF
Transmission electron microscopy	TEM
Transpiration rates	E
Triethanolamine	TEA
Ultracentrifugation	UC
Ultrafiltration	UF
Ultraviolet visible absorption spectroscopy	UV-Vis
Voltammetry of immobilized particles	VIP
Waste incineration plants	WIPs
Wastewater treatment plants	WWTPs
X-ray absorption near edge structure	XANES
X-ray absorption spectroscopy	XAS
X-ray diffraction	XRD
X-ray fluorescence	XRF
Zero-point charge pH	pH_{PZC}

List of figures

List of tables

Table of contents

ABSTRACT

The production of engineered nanomaterials (ENMs) has grown in recent years because of the different physicochemical properties that they present in respect to their bulk counterparts. Among the various types of ENMs, silver nanoparticles (AgNPs) are widely used in commercial products for their antibacterial properties. This fact enhances their intentional or unintentional release to the environment, where they can interact with natural components. These interactions can lead to transformation processes that may influence their behaviour, mobility and bioavailability. These phenomena can play an important role on their final toxic effects. Although nanosilver toxicology is still not clear, concern about the hazards it might pose for living organisms and human health has increased. To assess the risk of exposure to AgNPs and to further understand their effects, the characterisation and quantification of these emerging pollutants in environmental and biological samples by adequate analytical methodologies are necessary.

The research presented in this thesis focuses on the application and improvement of existing analytical methodologies, and on the development of new analytical procedures to acquire information about not only AgNPs mobility and bioavailability in soils, but also their accumulation, biotransformation and toxicity in edible plants.

Firstly, batch adsorption and leaching procedures (DIN 38414-S4 and DTPA) were applied to investigate the mobility and bioavailability of diverse types of AgNPs in soils with different physicochemical properties through inductively coupled plasma optic emission spectroscopy analysis (ICP-OES). The soil adsorption experiments demonstrated that nanosilver adsorption kinetics was fast (<6 h); while the leaching experiments indicated low mobility and bioavailability of these emerging contaminants in soils (recoveries of 0.4-7.8%). These experiments demonstrated that soil electrical conductivity, cation exchange capacity, organic matter content, clay minerals and nanosilver size and coating all play an important role in AgNPs soil adsorption/desorption processes. The single particle inductively coupled plasma mass spectrometry analysis (SP-ICPMS) of DIN 38414-S4 leachates indicated that during adsorption/desorption processes, AgNPs can maintain their nanoform or can be dissolved depending on the nanosilver and soil properties. With DTPA leachates, these emerging pollutants were completely dissolved.

As an alternative to common used spectrometric techniques in batch adsorption studies, a method based on the total reflection X-ray fluorescence spectrometry (TXRF) technique was developed to be

applied in this type of studies. The sample treatment procedure and TXRF parameters were optimised to quantify the total silver content (as AgNPs or ionic silver (Ag(I)) in aqueous and soil samples. Under the best conditions, the limit of detection (LOD) for silver in aqueous samples was around 37 μg L^{-1} and 1.7 mg kg^{-1} for directly analysed soils. The method was applied to soil adsorption kinetics, and showed that 75 nm of polyvinylpyrrolidone coated AgNPs were adsorbed in less than 6 h. The results were comparable with those ones obtained by ICP-OES, and demonstrated that TXRF can be employed to directly analyse solid suspensions, analyse low amounts of sample and to cost-effectively obtain information on other elements present in the sample.

As the presence of Ag(I) in natural systems can make the characterisation and quantification of AgNPs difficult, the combination of cloud point extraction (CPE) with TXRF and SP-ICPMS was investigated.

On the one hand, for the CPE-TXRF methodology, the experimental conditions for the separation and preconcentration of nanosilver in aqueous samples were optimised for different coated and sized AgNPs. LODs of 0.7-0.8 μg L^{-1} for all the studied NPs and acceptable extraction recoveries (73-105%) for the mixtures of different types of AgNPs were obtained. However for the mixtures of Ag(I)/AgNPs, extraction recoveries exceeded 100% with a Ag(I)/AgNPs ratio above 3. The developed methodology was applied to soil and consumer product aqueous extracts. The presence and concentration of AgNPs in these real samples were verified by SP-ICPMS analysis. A good agreement was observed between the nanosilver concentrations obtained by CPE-TXRF and SP-ICPMS in aqueous soil leachates. However for the consumer product water extracts, discrepancies were found between the nanosilver concentrations obtained by both analytical methods. These differences could be due to the presence of Ag(I) and a mixture of different sized AgNPs, as confirmed by SP-ICPMS and scanning electron microscopy coupled with electron dispersive spectroscopy analysis in the consumer product water extracts. Although more research is needed to analyse aqueous samples containing mixtures of nanosilver with different properties, CPE-TXRF can be a beneficial approach to quantify these emerging contaminants in complex aqueous samples.

On the other hand, in order to develop the CPE-SP-ICPMS methodology, critical CPE parameters for separating AgNPs from Ag(I) and for sample preparation were assessed by taking into account SP-ICPMS characteristics. The SP-ICPMS calculation methods to determine particle size and particle number concentration were examined and compared, and the particle size method proved to be better for AgNPs characterisation purposes than the particle frequency method. After verifying the absence of matrix effects, the developed methodology was applied to the determination of AgNPs size in three

weeks contaminated aqueous soil leachates. The application of CPE before SP-ICPMS proved to be a good approach to reduce the Ag(I) content, to facilitate the separation of AgNPs from Ag(I) signals and to improve the accuracy of particle size and particle number concentration determinations.

Finally, the accumulation, biotransformation and toxicity of AgNPs in *Lactuca sativa* (lettuce) (as a plant model) were evaluated. Lettuces were exposed to different coated and sized AgNPs for 9 days, and also at different nanosilver concentrations through a hydroponic growing medium. The uptake and accumulation of these emerging contaminants by lettuce roots were confirmed, depending on their concentration and size, but not on their coating. The translocation of nanosilver to lettuce shoots was influenced by the different studied parameters, being particle size one of the most important because it was observed that bigger NPs were more translocated than smaller ones. The SP-ICPMS and the X-ray absorption spectroscopy analysis with synchrotron radiation (Ag K-edge) indicated the dissolution of AgNPs inside lettuce tissues. Both techniques showed that AgNPs are more dissolved at low concentrations and in the case of small particles or coated with citrate or polyethylene glycol. The physiological parameters measured on lettuces after being exposed to nanosilver were lower than the controls, in particular transpiration and stomatal conductance, which indicated that NPs can exert toxicological effects on this edible plant type. Finally, the same tests performed with Ag(I) demonstrated that these silver species tended to accumulate more and can exert greater toxicity than AgNPs.

Resum

La producció de nanomaterials manufacturats (NMMs) ha incrementat en els darrers anys a causa de les diferents propietats fisicoquímiques que presenten respecte als seus metalls homòlegs. Dels diferents tipus de NMMs, les nanopartícules de plata (AgNPs) són àmpliament utilitzades en productes comercials per les seves propietats antibacterianes. Aquest fet propicia el seu alliberament intencionat o involuntari al medi ambient, on poden interaccionar amb els components naturals. Aquestes interaccions poden donar lloc a processos de transformació que poden influir en el seu comportament, la seva mobilitat i la seva biodisponibilitat. Aquests fenòmens poden jugar un paper important en els seus efectes tòxics finals. Tot i que la toxicologia de la nanoplata encara no està clara, ha augmentat la preocupació envers aquest material pels perills que pot representar pels organismes vius i la salut humana. Per avaluar el risc d'exposició a les AgNPs, i per entendre millor els seus efectes, és necessari caracteritzar i quantificar aquests contaminants emergents en mostres ambientals i biològiques mitjançant l'ús de metodologies analítiques adequades.

La recerca presentada en aquesta tesi es centra en l'aplicació i millora de metodologies analítiques existents i en el desenvolupament de nous procediments analítics per obtenir no només informació sobre la mobilitat i la biodisponibilitat de les AgNPs en els sòls, sinó també sobre la seva acumulació, biotransformació i toxicitat en plantes comestibles.

En primer lloc, es van dur a terme experiments d'adsorció i lixiviació (DIN 38414-S4 i DTPA) en "batch" per investigar la mobilitat i la biodisponibilitat de diversos tipus de AgNPs en sòls amb diferents propietats fisicoquímiques a través de l'anàlisi per espectrometria d'emissió òptica per plasma d'acoblament inductiu (ICP-OES). Els experiments d'adsorció en el sòl van demostrar que la cinètica d'adsorció de la nanoplata era ràpida (<6 h), mentre que els experiments de lixiviació van indicar una baixa mobilitat i biodisponibilitat d'aquests contaminants emergents una vegada adsorbits en els sòls (recuperacions de 0,4-7,8%). Aquests experiments van demostrar que la conductivitat elèctrica, la capacitat d'intercanvi catiònic, el contingut de matèria orgànica, els minerals argilosos i la mida i el recobriment de la nanoplata juguen tots un paper important en els processos d'adsorció/desorció de les AgNPs en el sòl. L'anàlisi dels lixiviats DIN 38414-S4 amb la detecció de partícules individuals mitjançant l'espectrometria de masses per plasma d'acoblament inductiu (SP-ICPMS) va indicar, que durant els processos d'adsorció/desorció, les AgNPs poden mantenir la seva nanoforma o poden dissoldre's en funció de les propietats de la nanoplata i del sòl. En els lixiviats DTPA, aquests contaminants emergents es van dissoldre

completament.

Com a alternativa a les tècniques espectromètriques més utilitzades en els estudis d'adsorció en "batch", es va desenvolupar un mètode basat en la tècnica d'espectrometria de fluorescència de raigs-X per reflexió total (TXRF) per ser aplicat en aquest tipus d'estudis. Es van optimitzar el procediment de tractament de mostra i els paràmetres de la TXRF per quantificar el contingut total de plata (com a AgNPs o plata iònica (Ag(I)) en mostres aquoses i en sòls. Usant les millors condicions, el límit de detecció (LOD) per la plata en mostres aquoses va ser del voltant de 37 μg L^{-1} i de 1,7 mg kg^{-1} pels sòls analitzats directament. El mètode desenvolupat es va aplicar a una cinètica d'adsorció en sòls i va mostrar que les AgNPs recobertes de polivinilpirrolidona de 75 nm eren adsorbides en menys de 6 h. Els resultats eren comparables amb els obtinguts per ICP-OES i van demostrar que la TXRF es pot emprar per analitzar directament les suspensions sòlides, analitzar petites quantitats de mostra i obtenir informació sobre altres elements presents a la mostra de manera econòmica.

Com que la presència de Ag(I) en sistemes naturals pot dificultar la caracterització i quantificació de les AgNPs, també es va investigar la combinació de l'extracció en punt de núvol (CPE) amb la TXRF i la SP-ICPMS.

D'una banda, per a la metodologia CPE-TXRF, es van optimitzar les condicions experimentals per la separació i preconcentració de la nanoplata en mostres aquoses per a diferents recobriments i mides. Es van obtenir LODs de 0,7-0,8 μg L^{-1} per a totes les NPs estudiades i recuperacions d'extracció acceptables (73-105%) per a les barreges de diferents tipus de AgNPs. No obstant això, per a les barreges Ag(I)/AgNPs amb una relació superior a 3, les recuperacions d'extracció van superar el 100%. La metodologia desenvolupada es va aplicar a extractes aquosos del sòl i de un producte de consum. La presència i concentració de AgNPs en aquestes mostres reals es van verificar mitjançant l'anàlisi per SP-ICPMS. Es va observar una bona concordança entre les concentracions de nanoplata obtingudes en els lixiviats aquosos del sòl per CPE-TXRF i SP-ICPMS. No obstant això, pels extractes aquosos del producte de consum, es van trobar discrepàncies entre les concentracions de nanoplata obtingudes amb ambdós mètodes analítics. Aquestes diferències podien ser degudes a la presència de Ag(I) i a una barreja de AgNPs amb diferents mides, tal i com es va confirmar en l'anàlisi de l'extracte del producte de consum mitjançant SP-ICPMS i microscòpia electrònica de rastreig acoblada a espectroscòpia d'energia dispersiva. Tot i que cal una investigació més exhaustiva per analitzar mostres aquoses que continguin barreges de nanoplata amb diferents propietats, el mètode CPE-TXRF pot ser beneficiós per a quantificar aquests contaminants emergents en mostres aquoses complexes.

D'altra banda, per tal de desenvolupar la metodologia CPE-SP-ICPMS, es van avaluar els paràmetres crítics de la CPE per separar les AgNPs de la Ag(I) i per a la preparació de mostra, tenint en compte les característiques de la SP-ICPMS. Els diferents mètodes de càlcul emprats en SP-ICPMS per determinar la mida de les partícules i la concentració en número de partícules es van examinar i comparar, i el mètode de la mida va demostrar ser millor que el mètode de la freqüència per a la caracterització de les NPs. Després de verificar l'absència d'efectes matriu, el mètode desenvolupat es va aplicar per determinar la mida de les AgNPs en lixiviats aquosos del sòl després d'estar contaminats durant 3 setmanes. L'aplicació de la CPE abans de la SP-ICPMS va resultar ser beneficiosa per reduir el contingut de Ag(I), facilitar la separació dels senyals de les AgNPs i la Ag(I) i millorar la precisió en la determinació de la mida de les NPs i la concentració en número de partícules.

Finalment, es va avaluar l'acumulació, la biotransformació i la toxicitat de les AgNPs a la *Lactuca sativa* (enciam) (com a model de planta). Els enciams es van exposar a AgNPs amb diferents recobriments i mides durant 9 dies, i també a diferents concentracions a través d'un medi de cultiu hidropònic. Es va confirmar que les arrels d'enciam capten i acumulen aquests contaminants emergents, en funció de la seva concentració i mida, però no del seu recobriment. La translocació de la nanoplata a les fulles d'enciam es va veure influenciada pels diferents paràmetres estudiats, sent la mida de la partícula un dels més importants perquè es va observar que les NPs més grans eren més translocades que les més petites. L'anàlisi per SP-ICPMS i per espectroscòpia d'absorció de raigs-X amb radiació de sincrotró (K-Ag) va indicar la dissolució de les AgNPs dins dels teixits d'enciam. Ambdues tècniques van mostrar que la dissolució de les AgNPs era més efectiva a baixes concentracions i en el cas de NPs petites o recobertes de citrat o polietilenglicol. Els paràmetres fisiològics mesurats en els enciams després de ser exposats a la nanoplata van ser pitjors que els controls, especialment pel que fa a la transpiració i a la conductància estomàtica, la qual cosa indicava que les NPs poden exercir efectes toxicològics sobre aquest tipus de planta comestible. Finalment, les mateixes proves realitzades amb Ag(I) van demostrar que aquesta espècie de plata tendeix a acumular-se més i pot exercir una major toxicitat que les AgNPs.

Resumen

La producción de nanomateriales manufacturados (NMMs) ha aumentado en los últimos años debido a las diferentes propiedades fisicoquímicas que presentan respecto a sus metales homólogos. Entre los distintos tipos de NMMs, las nanopartículas de plata (AgNPs) son ampliamente usadas en productos comerciales por sus propiedades antibacterianas. Este hecho propicia su liberación intencionada o involuntaria al medio ambiente, dónde pueden interaccionar con los componentes naturales. Estas interacciones pueden dar lugar a procesos de transformación que pueden influir en su comportamiento, su movilidad y su biodisponibilidad. Estos fenómenos pueden jugar un papel importante en sus efectos tóxicos finales. Aunque todavía no está clara la toxicología de la nanoplata, ha aumentado la preocupación por los peligros que este material puede representar para los organismos vivos y la salud humana. Para evaluar el riesgo de exposición a las AgNPs, y para comprender mejor sus efectos, es necesario caracterizar y cuantificar estos contaminantes emergentes en muestras ambientales y biológicas mediante el uso de metodologías analíticas adecuadas.

La investigación presentada en esta tesis se centra en la aplicación y la mejora de metodologías analíticas existentes y en el desarrollo de nuevos procedimientos analíticos para adquirir información no solo sobre la movilidad y la biodisponibilidad de las AgNPs en los suelos, sino también sobre su acumulación, biotransformación y toxicidad en las plantas comestibles.

En primer lugar, se llevaron a cabo experimentos de adsorción y lixiviación (DIN 38414-S4 y DTPA) en "batch" para investigar la movilidad y la biodisponibilidad de varios tipos de AgNPs en suelos con diferentes propiedades fisicoquímicas a través del análisis por espectrometría de emisión óptica por plasma de acoplamiento inductivo (ICP-OES). Los experimentos de adsorción en el suelo demostraron que la cinética de adsorción de la nanoplata era rápida (<6 h), mientras que los experimentos de lixiviación indicaron una baja movilidad y biodisponibilidad de estos contaminantes emergentes una vez adsorbidos en los suelos (recuperaciones de 0,4-7,8%). Estos experimentos demostraron que la conductividad eléctrica del suelo, la capacidad de intercambio catiónico, el contenido de materia orgánica, los minerales arcillosos y el tamaño y el recubrimiento de la nanoplata juegan todos un papel importante en los procesos de adsorción/desorción de las AgNPs en el suelo. El análisis de los lixiviados DIN 38414-S4 con la detección de partículas individuales mediante espectrometría de masas por plasma de acoplamiento inductivo (SP-ICPMS) indicó que durante los procesos de adsorción/desorción, las AgNPs pueden mantener su nanoforma o pueden disolverse dependiendo de las propiedades de la nanoplata y del suelo. En los lixiviados de DTPA, estos contaminantes emergentes se disolvieron

completamente.

Como alternativa a las técnicas espectrométricas más utilizadas en estudios de adsorción en "batch", se desarrolló un método basado en la técnica de espectrometría de fluorescencia de rayos-X por reflexión total (TXRF) para ser aplicado a este tipo de estudios. El procedimiento de tratamiento de muestra y los parámetros de la TXRF fueron optimizados para cuantificar el contenido total de plata (como AgNPs o plata iónica (Ag(I)) en muestras acuosas o en suelos. Usando las mejores condiciones, el límite de detección (LOD) para la plata en muestras acuosas fue de alrededor de 37 μg L^{-1} y de 1,7 mg kg^{-1} para los suelos analizados directamente. El método se aplicó a una cinética de adsorción en suelos y mostró que las AgNPs recubiertas de polivinilpirrolidona de 75 nm se adsorbieron en menos de 6 h. Los resultados fueron comparables con los obtenidos por ICP-OES y demostraron que se puede emplear la TXRF para analizar directamente las suspensiones sólidas, analizar pequeñas cantidades de muestra y obtener información sobre otros elementos presentes en la muestra de manera económica. Como la presencia de Ag(I) en sistemas naturales puede dificultar la caracterización y cuantificación de las AgNPs, también se investigó la combinación de la extracción en punto de nube (CPE) con la TXRF y la SP-ICPMS.

Por un lado, para la metodología CPE-TXRF, se optimizaron las condiciones experimentales para la separación y preconcentración de la nanoplata en muestras acuosas para distintos recubrimientos y tamaños. Se obtuvieron LODs de 0,7-0,8 μg L^{-1} para todas las NPs estudiadas y recuperaciones de extracción aceptables (73-105%) para las mezclas de diferentes tipos de AgNPs. Sin embargo, para las mezclas de Ag(I)/AgNPs con una proporción superior a 3, las recuperaciones de extracción superaron el 100%. La metodología desarrollada se aplicó a extractos acuosos del suelo y de un producto de consumo. La presencia y concentración de AgNPs en estas muestras reales se verificaron mediante el análisis por SP-ICPMS. Se observó una buena concordancia entre las concentraciones de nanoplata obtenidas en los lixiviados acuosos del suelo por CPE-TXRF y SP-ICPMS. Sin embargo, para los extractos acuosos del producto de consumo, se encontraron discrepancias entre las concentraciones de nanoplata obtenidas por ambos métodos analíticos. Estas diferencias podían ser debidas a la presencia de Ag(I) y a una mezcla de AgNPs con distintos tamaños, tal y como se confirmó en el análisis del extracto acuoso del producto de consumo mediante SP-ICPMS y microscopia electrónica de barrido acoplada a espectroscopia de energía dispersiva. Aunque se necesita una investigación más exhaustiva para analizar muestras acuosas que contengan mezclas de nanoplata con diferentes propiedades, el método CPE-TXRF puede ser beneficioso para cuantificar estos contaminantes

emergentes en muestras acuosas complejas.

Por otro lado, para desarrollar la metodología CPE-SP-ICPMS, se evaluaron los parámetros críticos de la CPE para separar las AgNPs de la Ag(I) y para la preparación de la muestra teniendo en cuenta las características de la SP-ICPMS. Los métodos de cálculo empleados en SP-ICPMS para determinar el tamaño de las partículas y la concentración en número de partículas se examinaron y compararon, y el método del tamaño demostró ser mejor que el de la frecuencia para la caracterización de las AgNPs. Después de verificar la ausencia de efectos matriz, el método desarrollado se aplicó para determinar el tamaño de las AgNPs en lixiviados acuosos de suelo después de estar contaminados durante 3 semanas. La aplicación de la CPE antes de la SP-ICPMS resultó ser beneficiosa para reducir el contenido de Ag(I), facilitar la separación de señales de las AgNPs y la Ag(I) y mejorar la precisión en la determinación del tamaño de las NPs y la concentración en número de partículas.

Finalmente, se evaluó la acumulación, la biotransformación y la toxicidad de las AgNPs a la *Lactuca sativa* (lechuga) (como modelo de planta). Las lechugas fueron expuestas a AgNPs con diferentes recubrimientos y tamaños durante 9 días, y también a diferentes concentraciones a través de un medio de cultivo hidropónico. Se confirmó que las raíces de lechuga captan y acumulan estos contaminantes emergentes, en función de su concentración y tamaño, pero no de su recubrimiento. La translocación de la nanoplata a las hojas de lechuga se vio influenciada por los diferentes parámetros estudiados, siendo el tamaño de partícula uno de los importantes porque se observó que las NPs más grandes eran más translocadas que las más pequeñas. El análisis por SP-ICPMS y por absorción de rayos-X con radiación de sincrotrón (Ag-K) indicaron la disolución de las AgNPs dentro de los tejidos de lechuga. Ambas técnicas mostraron que la disolución de las NPs era más efectiva a bajas concentraciones y en el caso de NPs pequeñas o recubiertas con citrato o polietilenglicol. Los parámetros fisiológicos medidos en las lechugas después de haber sido expuestas a la nanoplata fueron más negativos que los controles, en particular la transpiración y la conductancia estomática, lo que indicaba que las NPs pueden ejercer efectos toxicológicos en este tipo de plantas comestibles. Finalmente, las mismas pruebas realizadas con Ag(I) demostraron que esta especie de plata tiende a acumularse más y puede ejercer una mayor toxicidad que las AgNPs.

CHAPTER 1

General introduction

1.1 Silver nanoparticles in the environment

1.1.1 Nanoparticle definition, physicochemical properties and classification

Nanotechnology applications have rapidly grown in recent years in all areas of life (communication, health, manufacturing and materials) because engineered nanomaterials (ENMs) have emerged [1.1,1.2]. The definition of nanomaterial (NM) is still being discussed because scientific, regulatory and policy debates about these materials are ongoing [1.3]. International organisations and committees [1.4-1.6], industry [1.7-1.11] and governments [1.12-1.18] have proposed different NM definitions, most of which are based on European Commission (EC) Recommendation [1.19] and/or International Organization for Standardization (ISO) [1.2] definitions. According to the Recommendation of EC 2011/696/EU, NM is defined as a *natural, incidental or manufactured material containing particles, in an unbound state or as an aggregate or as an agglomerate and where, for 50% or more of the particles in the number size distribution, one or more external dimensions is in the size range 1 nm-100 nm*. In some cases, which are justified by concerns for the environment, health, safety or competitiveness, *the number size distribution threshold of 50% may be replaced by between 1-50%*. Additionally, the Recommendation specifies that (1) *fullerenes, graphene flakes and single wall carbon nanotubes with one or more external dimensions below 1 nm should be considered as NMs*; (2) *where technically feasible and requested in specific legislation, a material should be considered as falling under the definition when its specific surface area by volume is greater than 60 m^2/cm^3* [1.19]. In ISO/TS 80004:4-2011 "Nanotechnologies vocabulary-part 4: nanostructured materials", NM is defined as *a material having any external dimension in the nanoscale (size range from approximately 1 to 100 nm) or having internal structure or surface structure in the nanoscale*. This ISO standard also classifies NM as nano-object and nanostructured material, where the first term is described as *a discrete piece of material with one, two or three external dimensions in the nanoscale*. Nano-objects can be classified into three categories based on their dimensional characteristics: nanoparticle, nanofibre and nanoplate (see ***Fig. 1.1***). Therefore, according to the definition proposed by ISO, nanoparticle (NP) is a nano-object with three external dimensions within the nanoscale range (1-100 nm) [1.2,1.20].

The origin of these particles may be natural or they can be manufactured (engineered nanoparticles (ENPs)) [1.21]. NPs present characteristics that confer them unique physicochemical properties compared to their bulk counterparts. The principal factors responsible for their different behaviour are surface effects and quantum effects [1.22]. Surface effects are a consequence of

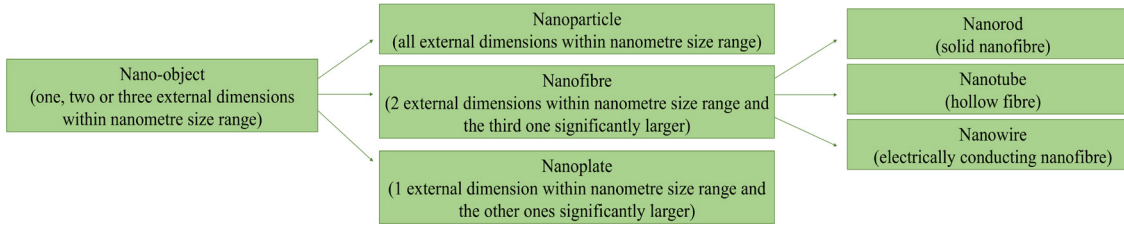

Fig. 1.1 *ISO/TS 80004:2-2015 definitions of nano-object, nanoparticle, nanofibre (nanorod, nanotube and nanowire) and nanoplate.*

their size and coating. Small size provides them a high surface area to volume ratio, and the fraction of surface atoms increases when particles become smaller. The presence of more surface atoms enhances their mechanical, thermal and catalytic properties [1.22-1.24]. Some NPs are functionalised with special coatings to improve certain physical or chemical particle properties (e.g. conductivity), or with stabilising agents (e.g. sodium citrate) to prevent them from aggregation by modifying their surface charge, their particle size and their steric stability [1.1,1.25]. Quantum effects are due to their small sizes that allow trapping electrons or electron holes to lead to special electrical, optical, magnetic and catalytic properties [1.22,1.24].

Given the multiple properties that NPs can present, diverse NPs are described that can be classified in different ways (e.g. origin, chemical composition, shape, *etc.*) [1.26]. The classification based on chemical composition divides NPs into the following five categories:

1.1.1.1 Carbon-based NPs

Carbon-based NPs are composed completely of carbon atoms. Depending on their structure, they can be fullerenes, carbon nanotubes, graphene, carbon nanofibres or carbon black, among others [1.27,1.28]. The bonding configuration of carbon nanostructures and the numerous surface atoms confer them unique adsorption, conductive, optical and thermal properties. Their main applications lie in environmental, energy, electronic, biological and medical fields [1.26,1.29].

1.1.1.2 Elemental metallic NPs

Elemental metallic NPs are inorganic nanoparticles made up of metals (silver (Ag), gold (Au), lead (Pb), cadmium (Cd), cobalt (Co), copper (Cu), zinc (Zn), iron (Fe) and aluminium (Al)) [1.27]. One important feature of these NPs is their surface plasmon resonance (SPR), caused by the interaction of conduction electrons (from the metal) with an incident light that provides them with special optoelectric, electric, magnetic and catalytic properties [1.30,1.31]. Metallic NPs are

useful for diverse applications like consumer products, biosensors, biomedical, detoxification of organic pollutants in the environment and catalysis [1.26,1.30,1.31].

1.1.1.3 Metal oxide NPs

Metal oxide NPs are metal-based nanoparticles with enhanced reactivity and efficiency as regards their elemental metallic NPs counterparts. Some existing metal oxide NPs are: copper oxide (CuO), cerium oxide (CeO_2), iron oxide (Fe_2O_3), silicon dioxide (SiO_2), titanium dioxide (TiO_2), zinc oxide (ZnO) and aluminium oxide (Al_2O_3) [1.27]. These nanoparticle oxides possess special optical, semiconducting and chemical sensing qualities due to their small size and the high density of edge surfaces. They are employed in areas like energy, electronics, biomedicine, pharmacy, medicine, cosmetics, textiles, food, construction and treatment of wastewaters, and groundwaters [1.26,1.30,1.32].

1.1.1.4 Organic NPs

Organic NPs are composed of organic compounds (polymeric (e.g. chitosan) or non-polymeric (e.g. liposome)) [1.33] and possess the particularity of being biodegradable and very stable in biological media. Some of these NPs have hollow cores (e.g. nanocapsules), which confer them the drug delivery capacity in biological systems [1.26,1.27]. Moreover, the optical and electronic properties of organic NPs differ from inorganic NPs because of their weaker quantisation effect and the joining mode of organic molecules [1.34]. The most important applications of organic NPs lie in biological and medical fields, but they can also be used for environmental monitoring, sensors or in agroindustry [1.26,1.27].

1.1.1.5 Quantum dots

Quantum dots (QDs) are semiconductor nanocrystals that fall within the diameter size range of 2-10 nm [1.35,1.36]. There are diverse types of quantum dots depending on their constituents: (1) QDs composed of binary metal complexes (e.g. cadmium selenide (CdSe) or cadmium tellurium (CdTe)); (2) core-shell QDs formed by the combination of two semiconductors (e.g. (CdSe) CdS); (3) carbon QDs that are small carbon NPs [1.26,1.37,1.38]. The quantum confinement of QDs due to their small size provides them with special optical, electrical, luminescence and chemical properties, such as a wide absorption spectra, a narrow emission spectra and high photostability [1.26,1.35,1.36]. Nanometre-scale semiconductor crystals are

used in optoelectronics, molecular biology, medicine, sensors and catalysis [1.30,1.37,1.38].

1.1.2 Occurrence and fate of silver nanoparticles in the environment

According to "The Project on Emerging Nanotechnologies" product database (Consumer Products Inventory (CPI)), created by the Woodrow Wilson International Centre for Scholars and PEW Charitable Trusts, the nanotechnology-based consumer products in the global market listed in the 2014 inventory contained predominantly metallic NPs (non-oxide and oxide) [1.39,1.40]. Allied Market Research declares that these NMs are the most manufactured, with an expected compound annual growth rate (CAGR) of 20.7% for 2016-2022 [1.41]. Among today's variety of metal-based NPs, silver nanoparticles (AgNPs) are popular in industry for their antibacterial properties. Silver bactericidal qualities in medicine have long since been known as silver was used as silver nitrite ($AgNO_2$) to treat ulcers or as silver sulfadiazine ($C_{10}H_9AgN_4O_2S$) for patients with burns, although long exposure to this metal provokes human skin or eye discoloration. This fact favoured the expansion of antibiotics (e.g. penicillin or cephalosporin) until the discovery of nanosilver [1.42]. AgNPs possess antibacterial activity against Gram-negative (e.g. *Escherichia coli*) and Gram-positive bacteria (e.g. *Staphylococcus aureus*) [1.43], antimicrobial properties against fungi (e.g. *Bipolaris sorokiniana*) [1.44] and antiviral activity against viruses (e.g. hepatitis B) [1.45]. Apart from this special quality, nanosilver presents good thermal and electrical conductivity, catalytic activity and chemical stability [1.42,1.46]. Thanks to these unique properties they have compared to their bulk counterparts, AgNPs are one of the most manufactured metallic NPs in industry with an estimated global annual production rate from 5.5-550 tons/year [1.22,1.47,1.48] and an expected growth with a CAGR of nearly 13% for 2016-2024 according to Global Market Insights Inc. [1.41]. Some commercialised products containing AgNPs in Europe and worldwide are listed in "The Nanodatabase" Inventory [1.49] and in "The Project of Emerging Nanotechnologies" CPI [1.50], respectively. Products in these inventories are classified into seven groups: appliances (e.g. washing machine, humidifier, *etc.*), automotive (e.g. car cleaning agent), electronics and computer (e.g. mobile phone and computer gadgets), food and beverage (e.g. food storage containers, kitchenware, *etc.*), health and fitness (e.g. sportswear, sanitary napkins, *etc.*), goods for children (e.g. pacifier, sleep suit, *etc.*) and home and garden (e.g. paint, floor cleaner, *etc.*). Of these categories, health and fitness is that with more nanosilver products and automotive has the fewest products containing these emerging contaminants as can be seen in ***Fig. 1.2***.

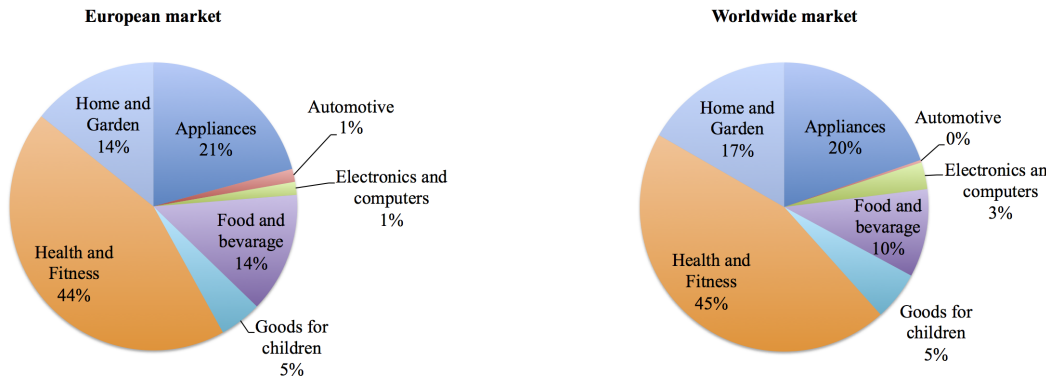

Fig. 1.2 *Graphical representation of the percentage of nanotechnology-based commercial products containing AgNPs listed in European [1.49] and worldwide [1.50] market inventories following their classification criteria.*

As a result of their wide production, inevitably these particles can intentionally or unintentionally reach the environment during their lifespan [1.51]. ***Fig. 1.3*** shows the life cycle of AgNPs, which begins during the synthesis and incorporation to nanoproducts, continues with transportation and usage, and ends with disposal [1.42,1.52].

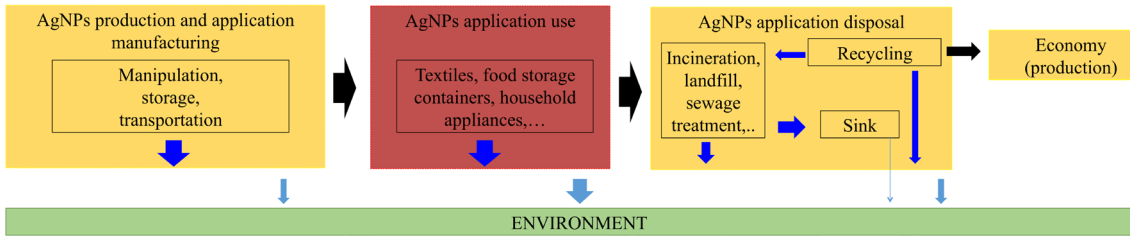

Fig. 1.3 *AgNPs life cycle diagram from their production to their final disposal. Electric blue arrows represent the release during nanosilver or nanoproducts manipulation. Light blue arrows represent the final transfer of these emerging contaminants to the environment. Arrow thickness denotes the potential of release, where thicker arrows indicate the most important release pathways [adapted from [1.52]].*

In the first cycle stage, nanosilver can be released to air, water or landfills from accidental spills while being manipulated as powder material, stored, transported or applied in manufactured products [1.52].

The second stage is considered the point at which more NPs are unintentionally released. Several studies have indicated the release of nanosilver from consumer products [1.42,1.52]. The release of AgNPs from textiles has been demonstrated after being exposed to distilled water [1.53], tap water [1.54], bleach [1.55], washing conditions [1.56] and artificial sweat [1.57]. Plastic food packaging embedded with nanosilver can also be a source of release of these emerging contaminants to food simulants, such as distilled water [1.58], aqueous ethanol [1.58,1.59], aqueous acetic acid [1.58,1.59], or to food like chicken breast [1.60]. Toothpaste, shampoo or toys exposed to tap water

can also release AgNPs [1.54]. These emerging pollutants can also migrate from medical devices, such as wound dressings, medical masks or catheters to water, saline or citrated human plasma [1.54,1.61]. One study has demonstrated the release of AgNPs from paints used on outdoor building façades under natural weather conditions [1.62]. What stems from these research works is that the potential release of nanosilver from these commercial products depends on the conditions of the medium where the nanoproduct is used [1.52]. Moreover, while they are released, they can undergo some transformation processes, such as dissolution or aggregation [1.59,1.61-1.64]. Although these NPs present in industrial products can pass directly to the environment, most end up in sewer systems and can, consequently, reach wastewater treatment plants (WWTPs) [1.65-1.67]. As several studies have reflected, these particles are efficiently removed by WWTPs (10->96%) [1.67-1.69]. During these treatments, AgNPs can undergo sulfidation processes, especially in anaerobic stages, to generate silver sulfide species (Ag_2S), and most accumulate in biosolids. Therefore, nanosilver being discharged to aquatic environments through treated effluents is low if the wastewater treatment process is adequate [1.65,1.68-1.70].

Finally, the release of AgNPs to the environment in the disposal phase at the end of their life cycle can be intentional or unintentional. One of the pathways of the intentional release of these emerging pollutants to the environment is when nanopesticides are applied to terrestrial crops for plant protection [1.71] and water treatment purposes [1.72]. Another way is by applying sewage sludge as a fertiliser to agricultural soils. However in some countries the use of biosolids is forbidden and, thus, the solid waste of WWTPs is incinerated or landfilled [1.54,1.73]. From these or other incineration activities, AgNPs unintentional emissions to the atmosphere can occur. Atmospheric particulate matter can be straightforwardly deposited on soils or in waters, while the nanosilver present in landfilled sewage sludge can leach into subsoil or groundwater. As previously mentioned, unintentional nanosilver delivery can also occur through wastewater effluent discharges to natural waters [1.65,1.74]. At the end of the cycle, a nanoproduct can be recycled and can, consequently, flow back to the production process [1.52]. In short, nanosilver can be present in different environmental compartments (air, water and soil).

Although most of the AgNPs present in the environment are of anthropogenic origin, they can also emerge spontaneously by the natural processes taking place in the environment. Several studies have reported the formation of these metallic NPs through the interaction of ionic silver (Ag(I)) with humic or fulvic acids functional groups (e.g. aldehydes, ketones, thiols, quinones,

carboxyls, phenols, *etc.*), which are natural organic matter (NOM). The interaction results in Ag(I) reduction to metallic silver (Ag(0)) [1.75,1.76]. The presence of iron species (Fe(II) or Fe(III)) or sulfide species also enhances the creation of AgNPs [1.77,1.78]. Nanosilver can also be generated through the sunlight reduction of Ag(I) by NOM [1.79]. These AgNPs formation processes are affected by diverse environmental factors (e.g. pH, temperature, light, *etc.*) [1.77-1.79]. Another way by which these emerging pollutants naturally appear is through the oxidative dissolution of Ag(0) from objects containing this metal and by the subsequent reduction of Ag(I) to Ag(0) under environmental conditions [1.80]. There are also reports that describe that living plants have the capacity to uptake Ag(I) and transform this metal species into nanosilver [1.81]. Thus, natural occurring NPs and ENPs coexist in different environmental compartments.

With existing analytical methodologies, the determination of AgNPs concentration levels to assess the environmental risk of these emerging pollutants is a difficult task given their low concentration and the coexistence of natural and anthropogenic nanosilver. For this reason, one of the possible tools to be used to gain information about the concentration levels of these emerging contaminants in the environment is prediction models. There are two different exposure models, as stated by Nowack (2017): material flow analysis (MFA) and environmental fate model (EFM). The first is based on tracking the materials flows in the entire NPs life cycle, while the second is based on describing the environmental fate and behaviour of AgNPs in environmental compartments (air, water or soil). Although the transfer factors of MFA models do not take into account physicochemical processes, this predicting model is an accepted approach to estimate nanosilver concentration levels in the environment because it is based on European Chemicals Agency (ECHA) guidance for chemical risk assessment [1.73]. ***Table 1.1*** shows the published works based on estimating AgNPs concentration levels in different environmental and technological compartments, using MFA models. The reported values indicated that the higher nanosilver concentration in technical compartments is found in sludge from WWTPs, waste incineration plants (WIPs) and solid waste. In environmental compartments (soil, surface water, sediments and air), the highest concentration of AgNPs is found in sediments and soils treated with sewage sludge, and the lowest concentration appears in air. Lower nanosilver values in the atmosphere could be due principally to it being well-extended, the short residence time or the low percentage of emissions from WIPs [1.82-1.84]. However, these predicted reported values are illustrative as experimental validation is lacking [1.85].

Table 1.1 *Silver nanoparticles environmental concentrations in different technical and environmental compartments in Europe shown as the mode (most frequently value) predicted by material flow analysis models (MFA).*

Environmental compartment	Material flow analysis models		
	Predicted environmental concentrations[a]	Probabilistic model flow analysis[b]	Dynamic probabilistic model flow analysis[c]
Air (ng m^{-3})	0.008	0.003	0.00
Solid waste to WIPs (µg kg^{-1})	-	60	10.6
Solid waste to landfill (µg kg^{-1})	-	-	35.4
WIPs bottom ash (µg kg^{-1})	-	230	111
WIPs fly ash (µg kg^{-1})	-	380	169
WWTPs effluent (ng L^{-1})	42.5	0.17	0.71
Surface water (ng L^{-1})	0.764	0.66	0.63
Sediment (µg kg^{-1})	0.952	2.3	23.8
Soil (µg kg^{-1})	0.0227	-	-
WWTPs sludge (µg kg^{-1})	1680	20	20.2
Natural and urban soil (µg kg^{-1})	-	0.0012	0.02
Sludge treated soil (µg kg^{-1})	1.581	0.11	0.73

[a] *Gottschlank et al., 2009 [1.82]. Estimated AgNPs concentrations in 2008 (black values) and annual concentration increase (red values).*

[b] *Sun et al., 2014 [1.83]. Estimated AgNPs concentrations in 2012 (black values) and annual concentration increase (red values).*

[c] *Sun et al., 2016 [1.84]. Estimated (accumulated) AgNPs concentrations in 2014 (interval from 1990 to 2020).*

1.1.3 Behaviour and transformation processes of silver nanoparticles in the environment

In the environment, nanosilver is susceptible to suffer interactions with environmental constituents, which that can induce transformation processes that modify their original characteristics and, consequently, their behaviour, fate, mobility and bioavailability can be affected (see ***Fig. 1.4***) [1.86,1.87]. These processes are governed mainly by particle properties (e.g. surface area, surface charge, particle size, chemical composition, solubility, shape, capping agent, aggregation ability and concentration) and the characteristics of the medium where these emerging contaminants are released (e.g. physiochemical properties of each environmental compartment) [1.86,1.88,1.89]. In the following sections, the possible transformation processes that AgNPs can undergo in different environmental compartments are described:

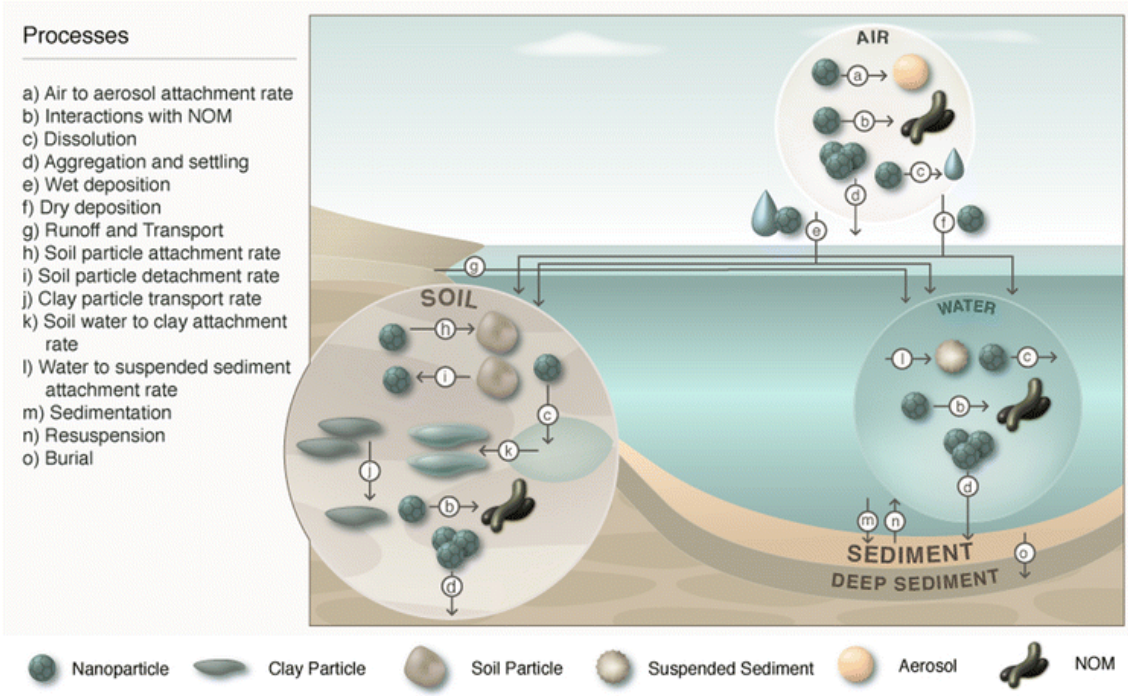

Fig. 1.4 *Diagram of how NPs are transported to different environmental compartments and the possible interactions they can undergo [Republished with permission of Journal of Nanoparticle Research, from [1.86]; permission conveyed through Copyright Clearance Center, Inc.].*

1.1.3.1 Atmosphere

Very little information about nanosilver transport in the air is available. Nevertheless, these emerging pollutants can remain suspended as individual particles or can undergo several interactions with the components of this medium before being deposited [1.86,1.90]. The phenomena that they can experience in this environmental compartment are the following:

a) Coagulation

Coagulation occurs with the collision of two or more AgNPs or a NP colliding with other particles present in the atmosphere due to their Brownian motion (random movement of particles in colloidal systems). This process is favoured between different sized particles because smaller particles have a large surface area and high Brownian diffusivity to collide with larger particles. As a result of collision, there is the formation of larger particles or agglomerates/aggregates through coalescence [1.91,1.92]. Agglomerates are the result of reversible weak physical interactions (e.g. Van der Waals forces) between particulate matter, while aggregation is caused by non-reversible strong chemical (e.g. covalent or ionic) or electrostatic interactions [1.89,1.93].

b) Coating process by organic and inorganic compounds

Silver nanoparticle size can be enlarged in the atmosphere due to organic and inorganic vapours condensating on the nucleus of pre-existing nanosilver to form a coating around the NPs. Yet not only can particle size be increased by condensation processes, but the formation of new nucleating particles can also take place [1.86,1.91].

c) Dissolution and chemical reactions

Dissolution of AgNPs into cloud or fog droplets by releasing Ag(I) can also occur if conditions are slightly acidic [1.90]. Apart from these phenomena, nanosilver in the atmosphere can react with other chemical compounds, such as atmospheric oxidants [1.94].

d) Deposition

Intact or transformed AgNPs are deposited in other environmental compartments (water and soil) by dry or wet deposition. The dry deposition process is governed mainly by Brownian diffusion and inertial impaction through particle transfer to air-surface interfaces. This form of transport is affected by particle size and density. Dry deposition through Brownian motion is favoured for smaller NPs given their higher diffusion coefficient compared to larger AgNPs. Conversely, dry deposition through impaction is better for larger NPs or aggregates because their gravitational sedimentation velocities are more efficient than smaller particles. Wet deposition particle transfer occurs by precipitation. This deposition can occur by nucleation scavenging (rainout) or aerosol-hydrometeor coagulation (washout). The first process consists in incorporating silver particles into aerosol by falling rain drops, while the second phenomenon consists in surrounding nanosilver with raindrops formed as condensation nuclei [1.86,1.91,1.95].

All these described processes that AgNPs can undergo in the atmosphere are also affected by environmental factors, such as temperature, humidity and atmospheric turbulence [1.86].

1.1.3.2 Water

In aquatic systems, AgNPs are exposed to various modification and transformation processes given the multiple natural existent components in this environmental compartment (e.g. colloids, NOM, cations, *etc.*) with which they can interact. These interactions are governed mainly by water chemistry (e.g. pH, ionic strength, dissolved oxygen, dissolved organic matter (DOM),

etc.), seasonal variations (e.g. temperature) and the aforementioned NPs physicochemical characteristics [1.86,1.89,1.96]. Transformation processes are classified as physical (dispersion, agglomeration/aggregation, adsorption/desorption and sedimentation), chemical (oxidation/dissolution, sulfidation, chlorination and photochemical) and biological (bio-transformation):

a) Dispersion

As previously mentioned, natural waters contain a wide variety of naturally occurring geo- and bio-colloids that are stabilised by electrostatic repulsion, steric hindrance, or by a combination of both [1.89,1.97]. Kinetic processes through Brownian motion are responsible for AgNPs stability and their dispersion in aquatic systems [1.89]. This phenomenon is favoured by low mono- and divalent cation concentrations in this environment (low ionic strength) [1.89,1.98,1.99]. NOM can enhance the stability of nanosilver in natural waters, but depends on the nature of organic molecules [1.98]. Smaller particles are less stable than larger particles because they are more prone to interact with natural water components given their large surface area [1.99]. Other factors that can contribute to dispersion efficiency are water pH and NPs characteristics, such as particle mass, density and surface properties [1.89].

b) Aggregation and agglomeration

In the absence of sufficient stability, AgNPs can undergo aggregation and agglomeration phenomena. As stated in Section 1.1.3.1, the difference between these two processes lies in agglomeration being a reversible process (weak interactions between particles), while aggregation is a non-reversible process (strong interactions between particles) [1.89]. Moreover, if aggregation occurs between similar particles, it is called homoaggregation, whereas if aggregation happens between different particles, it is called heteroaggregation, which is commoner in environmental systems [1.51]. The frequencies of particle collision to generate aggregates/agglomerates are driven by Brownian motion (perkinetic aggregation), fluid motion (othokinetic aggregation) and differential settling, of which the first is the most frequent [1.51,1.89]. Particle-particle collision can be controlled by electrostatic or steric interactions, the first of which is governed by the particle surface charge of the electrical double layer (EDL). The EDL comprises the surface-charged sites and a diffusive layer containing ions from the solution attracted by the particle's surface charge. The NPs

surface charge can be known by measuring the electrical potential at the interface of the diffusive layer and the bulk solution (zeta potential). When particle surface charges are repulsive (similar particle charges), the energy barrier between particles is high and NPs are maintained in dispersion. When particle surface charges are attractive (opposite particle charges), the kinetic energy of Brownian motion overcomes the energy barrier between NPs, which become aggregated/agglomerated [1.51,1.87,1.100]. The main factors that influence the stability of AgNPs are pH, ionic strength and particle coating. The pH value of the medium governs the particle surface charge, where the point zero charge (PZC) is the point at which a particle and a solution remain in a state of equilibrium. The net charge is positive when pH values are lower than the PZC, which occurs under acidic conditions because the addition of protons deteriorates the negative cloud of ions around silver particles and favours electrostatic attractive forces between the particles present in natural waters. In alkaline media, the net charge is negative (pH values over the PZC) as hydroxyl groups strengthen the negative cloud of ions around AgNPs and enhance the stability of particles in aqueous media [1.51,1.87]. The presence of anions and cations in natural waters also affects the surface charge by causing the following different phenomena: (1) the nanosilver surface charge is modified by the adsorption of ions (anions or cations) present in aqueous media onto the NPs surface even without varying ionic strength; (2) the AgNPs surface charge is altered by increased ionic strength, which reduces the EDL and, consequently, the destabilisation of particles takes place to favour their aggregation/agglomeration [1.51,1.101]. Particle coating impacts nanosilver behaviour because it can modify the surface charge of the core material, and its role is to maintain the particles in suspension stabilised. In natural waters the presence of NOM can also influence the surface charge, the surface potential and the structure of the NPs when it surrounds the AgNPs present in this environmental compartment. Aggregation/agglomeration can be disfavoured by NOM depending on the electrostatic (pH and ionic strength) and steric (NOM spatial arrangement) interaction mechanisms that take place in aqueous media [1.102]. Marine media are generally more alkaline, have great ionic strength, and there are more colloids and NOM present compared to freshwater. Thus aggregation/agglomeration is commoner in these aquatic compartments [1.103]. Dispersion and aggregation/agglomeration processes are described by the Derjaguin-Landau-Verwey Overweek (DLVO) theory, which takes into account

the attraction (Van der Waals) and repulsive (electrostatic) interaction energies that act between two particles. Other interaction processes (e.g. hydrophobic, steric repulsion, polymer bridging, *etc.*) are described by the non-DLVO processes [1.51,1.89].

c) Adsorption and desorption

A phenomenon related with aggregation/agglomeration is the adsorption of the substances present in natural waters onto nanosilver surfaces. As previously stated, NOM can be adsorbed onto AgNPs surfaces by changing their chemistry and can, consequently, affect attachment to the other particles present in aqueous media. The consequences that stem from NOM adsorption processes are difficult to be understood because the NOM family comprises a wide range of organic molecules and macromolecules. However, their presence can induce electrostatic repulsive interactions between NPs (low-molecular weight organic coatings) or steric repulsion (long-chain polymers) that hinder aggregation/agglomeration phenomena. The stabilisation of nanosilver by NOM, can affect the mobility of contaminants (e.g. organic or metallic) in aquatic environment. Apart from NOM, in groundwater common inorganic components (carbonates, phosphates, sulfates, chlorides and nitrates) can be adsorbed to AgNPs surfaces, which alters their chemical surface characteristics and affects their behaviour. Desorption can also occur due to forces exerted on particles (e.g. shear forces) that change their surface characteristics. These processes are influenced by NOM physicochemical properties (e.g. electric charge, size, *etc.*) and nanosilver surface charge [1.51,1.89,1.102].

d) Sedimentation

Another phenomenon that derives from aggregation/agglomeration processes in natural waters is sedimentation. The colloidal interactions that take place between particles increase their size and density and cause the settlement of the resulting aggregates by gravity, and larger particles more rapidly accumulate in water sediments than smaller ones [1.86,1.89].

e) Oxidation and dissolution

Oxidation and dissolution are relevant AgNPs transformation processes that take place in the presence of dissolved oxygen and protons [1.102,1.104]. In oxic natural waters, nanosilver can be oxidised by dissolved oxygen to generate Ag_2O that adheres to AgNPs surfaces

to form a core AgNP-shell structure. This oxidation process is slow, but Ag_2O quickly dissolves and, after being completely dissolved, nanosilver oxidation/dissolution continues [1.104]. AgNPs dissolution is influenced by their particle size and their concentration in aqueous media. At low concentration levels and with a small particle size, AgNPs are more prone to be dissolved than at high concentrations and with a large particle size because of the few quantity of atoms per volume in the surface area. pH also affects nanosilver dissolution, which is favoured by low pH values. However, the dissolution of these emerging contaminants can decrease due to several phenomena: (1) Ag(I) is adsorbed by AgNPs; (2) particle coating or organic matter coatings (NOM); (3) aggregation between particles; (4) certain environmental conditions (e.g. lowering dissolved oxygen concentration, lowering temperature, increasing pH, *etc.*) [1.51,1.101,1.102,1.104].

f) Sulfidation

Sulfidation is given by two possible ways, and mainly in anaerobic aquatic environments. Indirect sulfidation processes occur when the Ag(I) released by AgNPs through dissolution phenomena interact with sulfide species (e.g. HS^- or organic thiols) to form a silver sulfide precipitate (Ag_2S). Ag(I) species have a great affinity for thiol-containing ligands compared to other sulfide species. In direct sulfidation, AgNPs are transformed into a AgNP-shell (Ag_2S)-type structure. Nanosilver sulfidation is favoured at high HS^-/Ag ratios and for smaller NPs that are more reactive than larger ones. Nevertheless, the presence of NOM in natural water can inhibit the formation of silver sulfide species. For example, it can block the sulfidation process by surrounding the particle surface [1.101,1.104].

g) Chlorination

Chlorination phenomena occur after the dissolution of AgNPs, which is one of the sources of Ag(I) generation in oxic natural waters. Unlike the sulfidation process, the formation of core-shell structures (AgCl NP-type) or AgCl precipitates is favoured at low Cl^-/Ag ratios. At high Cl^-/Ag ratios, the creation of anionic Ag complexes (e.g. $AgCl_2^-$ $AgCl_3^{2-}$ $AgCl_4^{3-}$) is more likely. Given the high Cl^-/Ag ratio in seawater, the presence of anionic Ag complexes is frequent, but AgCl precipitates are commoner in freshwater due to the low Cl^-/Ag ratio [1.101,1.104].

h) Photochemical reduction and bio-transformation

In aquatic environments, the generation of AgNPs is also possible by the photochemical reduction of Ag(I), as mentioned in Section 1.1.2. The reduction mechanism process consists in superoxides production by sunlight irradiation to DOM functional groups. Subsequently these superoxides reduce the Ag(I) species present in aqueous media [1.104]. In this environmental compartment, different organisms can play a key role in the modification of AgNPs surface characteristics. For example, the material that they release can be attached to nanoparticle surfaces, or microbial organisms even have the ability to reduce Ag(I) to AgNPs [1.89].

1.1.3.3 Soils

Soil systems, including sediments, are the final biggest sink for the disposal of released AgNPs, both directly and indirectly. Soil matrices are relatively complex because they are constituted by two phases. One phase is the soil pore space, where NPs movement depends on soil solution characteristics and natural colloidal material. The other one is the soil solid phase, in which nanosilver retention is given by the interaction with organic matter and minerals [1.46,1.105]. The interactions that these emerging pollutants undergo in this environmental compartment can lead to the following processes:

a) Aggregation and agglomeration

As in water systems, AgNPs can be agglomerated or aggregated as a result of particle-particle collisions. As stated in Section 1.1.3.2, agglomerates and aggregates can be formed by electrostatic interactions. In soil pore space, the surface charge of NPs and soil colloids is one of the main factors responsible for the efficient attachment of particles by electrostatic interactions [1.100,1.106]. As in aquatic media, the particle surface charge is influenced mainly by the pH and ionic strength of the soil liquid phase. Repulsive forces reduce at great ionic strength and at pH values that come close or go below the PZC, which favours AgNPs agglomeration/aggregation with colloidal matter. The nanosilver surface charge can also be affected by changing the original surface properties as a result of the NPs coating or the adsorption of NOM. Soil organic matter can hinder the formation of agglomerates/aggregates by enhancing the mobility of these emerging contaminants in soil [1.86,1.100,1.105]. Particle size also influences these phenomena, and is favoured by small-sized particles given their large surface area [1.86].

b) Adsorption/retention and desorption

As in aquatic environments, an agglomeration/aggregation related phenomenon is the adsorption/retention of nanosilver to the soil solid phase. Nanosilver retention can occur by two ways in the soil solid phase: (1) surface interaction with clay minerals or organic matter; (2) pore straining. The first way retention is known as adsorption, and is governed by electrostatic interactions between AgNPs and soil surfaces. Therefore, retention on soil surfaces is favourable when nanosilver and soil have opposite surface charges (attractive forces), which reduces the mobility of these emerging pollutants [1.100,1.106,1.107]. The AgNPs characteristics (e.g. surface charge) and soil properties (e.g. pH, ionic strength, metal oxide content, organic fraction, texture, cation exchange capacity, *etc.*) play an important role in this process [1.105]. When ionic strength increases AgNPs mobility is reduced because they are less stable in soil solution under these conditions. So the attachment of these emerging pollutants to soil surfaces is more likely [1.46,1.107]. Moreover, soils with high pH and cation exchange capacity (related to soil clay mineralogy) favour the adsorption of positively charged AgNPs due to the presence of negatively charged sites and, consequently, more cation exchange reactions occur [1.46]. However, large amounts of organic matter in soil can enhance the mobility of negatively charged AgNPs in this medium because the presence of negative sites (e.g thiol groups) in the soil solid phase hampers access to positively charged surfaces [1.46]. Another factor that can hinder adsorption is an increase in NOM in the soil liquid phase by changing nanosilver surface properties through adsorption processes [1.46,1.86,1.106,1.107]. Particle size also influences nanosilver adsorption in the soil solid phase as small-sized particles are more reactive [1.86]. The second way, pore straining, is a physical retention mechanism that depends mainly on particle size and pore size distribution. AgNPs or aggregates are trapped in porous soils when particle size is larger than soil pore, which reduces their mobility. When they are smaller than soil pores, they can travel large distances, which enhances options to reach groundwater [1.86,1.106]. Therefore, small particles are more mobile and more likely to reach groundwater, while larger particles or aggregates are more prone to be blocked in upper soil layers. Apart from all these physicochemical processes that nanosilver can undergo in the soil compartment, the solution flow rate can also affect the mobility of these emerging pollutants, which is more favourable when the flow rate rises [1.100]. However, AgNPs can

be detached from the soil solid phase to the liquid soil phase by desorption processes. The presence of organic (herbicides/pesticides) and inorganic (heavy metals) pollutants in the soil liquid phase and the presence of biological excrements from living organisms can alter nanosilver mobility as they modify surface properties through their interactions [1.21,1.105].

c) Dissolution

Dissolution of AgNPs occurs when an ion detaches from the particle and migrates to the soil liquid solution. As mentioned in Section 1.1.3.2, this phenomenon is enhanced for small-sized nanosilver because of their large surface area. The resulting Ag(I) tends to bind to colloidal components or can be adsorbed by soil solid phases [1.46,1.100,1.101,1.104].

1.1.4 Potential toxicity risks and concerns to living beings and human health

Nanosilver is known for its antibacterial properties through the release of Ag(I), which is known to be toxic, and due to its specific effects [1.108]. As explained in Section 1.1.2, AgNPs are found in different environmental media at trace concentration levels. Despite these low concentration levels, living organisms present in air, water and soil can uptake nanosilver and can, consequently, accumulate these emerging pollutants. Bioaccumulation, which is related to the bioavailability of metallic NPs in media, is influenced by: (1) concentration of AgNPs; (2) NPs characteristics; (3) environmental conditions; (4) exposure route; (5) the biology and functional ecology of the involved organism. The quantity of nanosilver accumulated by an organism is determined by the balance struck between the uptake rate and loss rate, and *via* dilution by growth. Bioaccumulation is one of the main processes responsible for the chemical or physical toxic effects that these emerging contaminants can have on living organisms. Both the dose response effect and exposure pathway are important to understand the risk that AgNPs pose. The exposure pathway determines how NPs enter organisms. The various organisms that exist in different environmental media have distinct ways of uptaking nanosilver [1.46,1.85,1.86,1.109]. Once inside living organisms, AgNPs can be transported to target organs and can interact with membranes of cells to lead to endocytosis or diffusion processes. During the endocytosis process, the early endosomes located near the cell membrane uptake metallic NPs. Two internalisation pathways intervene in the diffusion process: AgNPs are diffused through the cell membrane (passive diffusion), or carrier proteins and channels can help to internalise them inside the cell (facilitated diffusion) [1.86,1.108,1.09].

Inside cells, and depending on the size and the surface chemistry of NPs, they are transported to target organelles, such as lysosomes, mitochondria or nucleus, where they can exert hazard effects (see ***Fig. 1.5***) [1.110]. The toxicity of these NPs is driven by different mechanisms that are not well-defined.

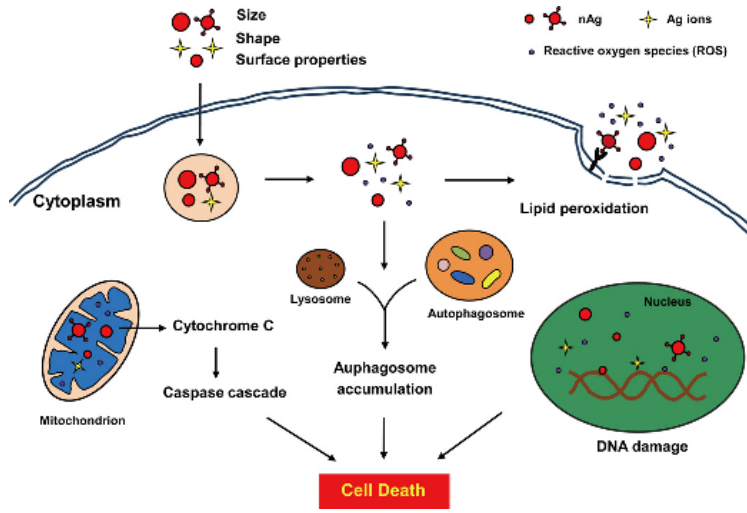

Fig. 1.5 *Schematic overview of silver NPs toxicity pathways in cells [Republished with permission of Nanoscale, from [1.111]; permission conveyed through Copyright Clearance Center, Inc.].*

1.1.4.1 Mechanisms of toxicity

Nanosilver toxicity is considered to be linked to Ag(I) (ion-related toxicity), AgNPs (particle-related toxicity) and the "Trojan-horse" effect (a combination of both) [1.104]. One way for toxicity to occur is the direct internalisation of Ag(I), derived from AgNPs dissolution processes in the environment, in the organism's circulatory system or in cells. Another possible mechanism is the attachment of AgNPs to the surface of cellular membranes and the release of Ag(I) within surface layers, which can disrupt plasma membrane activities. One of the main nanosilver toxicity hypotheses is the "Trojan-horse" effect mechanism, which consists in releasing silver ions from AgNPs to the cytoplasm [1.85,1.112,1.113]. The presence of these free silver ions causes some dysfunctions in the intracellular environment that provoke an increment in reactive oxygen species (ROS). ROS are oxygen species with an unpaired electron in their outer electron orbital, such as superoxide, hydrogen peroxide or hydroxyl radicals, among others [1.108,1.113]. Under normal physiological conditions, oxidant and antioxidant systems are balanced and achieve homeostasis inside the organism [1.114]. When the presence of ROS and the generation of other free radicals increase, the cellular enzymatic and non-enzymatic

antioxidant defence components involved in oxidative stress are activated to balance this increment [1.112]. An indication of cellular oxidative stress is increased malondialdehyde (MDA) production as a result of lipid peroxidation, or reduced glutathione (GSH), which is one of the important antioxidants for cell survival. An inflammatory response is generated once ROS amounts exceed the level at which antioxidants can neutralise. Apart from inflammatory responses, ROS species can also alter the activity of cellular organelles (e.g. depletion of ATP production by mitochondria), the autophagy defence function (e.g. degradation of damaged cellular components) and cause deoxyribonucleic acid (DNA) damage. All these cellular degenerations can induce cell death (apoptosis or necrosis) when defence mechanisms cannot respond to damage [1.108,1.111,1.115,1.116].

Despite claims that cellular alterations and toxicity effects of AgNPs are due to the release of Ag(I), nanosilver at sublethal doses can alter cellular functions in molecular terms, but without producing cytotoxicity and cell death. The cellular functions that nanosilver can affect include energy balances (e.g. metabolism energy related to gene expression and protein levels), transcription machinery by direct binding to ribonucleic acid (RNA) polymerase and gene cell expression propagation [1.111].

Toxic effects that AgNPs can exert on living organisms through the explained mechanisms are governed by the NPs potential reactivity in cells, which is dependent on nanosilver physicochemical properties. Particle size influences AgNPs sedimentation/deposition velocity, mass diffusivity and attachment efficiency on biological and solid surfaces. Smaller particles have a large surface area that favours their interactions with cellular proteins and organelles, and the release of Ag(I). The smaller the NPs are, the easier they pass through the cellular membrane. Therefore, smaller particles can exert stronger toxic effects than larger particles. Nanosilver shape can also affect their toxicity by influencing the cellular uptake mechanism. As mentioned in Section 1.1.3, the presence of capping agents modifies nanosilver characteristics (e.g. surface charge), the dissolution ratio, the agglomeration/aggregation possibility and, subsequently, their toxicity in cells. The surface coating can influence the uptake of these emerging contaminants by cells. Nanosilver aggregation/agglomeration and its concentration are other factors that can influence the toxicity level in living organisms. Aggregate/agglomerates formations are dependent on several interaction forces (e.g. diffusion, gravitation and convection forces) and on the composition of the biological medium (e.g. pH,

salt content and proteins). These phenomena mitigate nanosilver toxicity, but do not interfere with their internalisation by cells. Their localisation inside cells depends on the aggregate/agglomerate state of AgNPs. Apart from particle-particle and particle-cell interactions, AgNPs can also interact with proteins in biological media to produce protein corona by the adsorption of proteins on AgNPs surfaces. There are two types of protein corona: soft ones, which transport Ag(I) and are reversible NP-protein complexes; hard ones, which invade the cellular system and are irreversible NP-protein complexes. As in agglomeration/aggregation phenomena, adsorption of proteins by AgNPs depends on particle and protein properties (e.g. surface chemistry), interaction forces (e.g. Van der Waals) and biological conditions. Proteins corona affects the ability of AgNPs to dissolve to Ag(I) and NPs uptake. So the toxicity of these emerging contaminants is also controlled by this phenomenon. Regarding the adsorption phenomenon, nanosilver can interact with other pollutants (e.g. humic substances, surfactants and heavy metals) present in the environment, which can positively or negatively modify their bioavailability and toxicity. Although NPs characteristics are the main factors to influence the hazard level that these emerging pollutants can have on living beings, cell type can also contribute to final toxicological effects [1.110,1.112,1.115].

1.1.4.2 Toxicity to aquatic organisms

Aquatic organisms include microbes, algae and plants, invertebrates and vertebrates. The main ways that these organisms uptake nanosilver is through gill surfaces, olfactory organs, alimentary tracts and body walls [1.109,1.114]. Some studies done with Gram-negative bacteria have indicated that these organisms can undergo growth inhibition and cell membrane damage after being exposed to these emerging contaminants [1.117,1.118]. Very little research on toxicological effects on algae has been published, but existing studies reveal that nanosilver can reduce or inhibit algae cell growth, photosynthesis and chlorophyll production [1.85,1.119]. The literature demonstrates that invertebrates are also exposed to the hazard effects induced by AgNPs. For example, some studies performed with *Daphnia Magna* have shown that nanosilver produces abnormal swimming and alterations in protein metabolism and signal transduction [1.120,1.121]. *In vivo* studies with diverse fish species have demonstrated several phenomena induced by AgNPs toxicity, such as malformations (e.g. spinal cord, heart, embryonic and/or eye defects, *etc.*) and general toxicity (e.g. genetic alteration, cardiac arrhythmia, membrane integrity disruption, *etc.*) [1.42,1.85,1.122].

1.1.4.3 Toxicity to aerial and terrestrial organisms

The main routes by which AgNPs enter the microorganisms and vertebrates present in air-soil environments include inhalation, ingestion and dermatological uptake [1.109]. Although the literature contains very little information about the impact of these emerging pollutants on aerial and terrestrial microorganisms, some indicate that AgNPs are toxic to these living beings (e.g. growth inhibition, lower reproduction potential, reduced denitrification activity and/or enzymatic activity, *etc.*) [1.46,1.106,1.114,1.123]. Few studies have been also carried out about the impact of AgNPs on vertebrates. Most inhalation studies have been performed with *Rattus norvegicus domesticus* and indicate that the AgNPs taken by these animals are distributed in different organs, including the lung, and cause mainly physical changes (e.g. alveolar inflammation) and alterations to respiratory functions (e.g. tidal volume). Nanosilver dermal exposure research done with *Oryctolagus cuniculus* has demonstrated abnormalities in skin (e.g. hyperkeratosis), liver (e.g. pathological fatty changes) and brain (e.g. hyperaemic meninges). A study of the oral ingestion of AgNPs by *Gallus gallus domesticus* has shown histopathological changes in liver (e.g. fatty degeneration) [1.124-1.127]. The main ways of nanosilver uptake by plants are through roots or leaves. The toxicological impacts of these emerging contaminants on *Arabidopsis thaliana* are of the following kinds: morphology (e.g. inhibition of root elongation, stunted root hair development, *etc.*), physiology (e.g. diminished photosynthetic efficiency, lower chlorophyll content, *etc.*) and genetic (e.g. down-regulation of genes, modified transcription of antioxidant and aquaporin genes, *etc.*) [1.128-1.130].

1.1.4.4 Toxicity to humans

Humans are also exposed to nanosilver, thus the potential hazard that AgNPs can pose is an issue that causes growing concern. The main ways of human exposure are dermatological, inhalation and oral. Very little information is found in the literature about dermatological nanosilver exposure through consumer products or workplaces. However, a recent *in vitro* study indicates low dermal penetration of AgNPs [1.131,1.132]. *In vitro* studies have revealed that inhaled nanosilver can cause inflammation of respiratory and cardiovascular systems, known health illnesses (e.g. chronic bronchitis), and can alter the metabolic activities inside cells and damage DNA [1.90,1.133,1.134]. The oral ingestion of food supplements containing AgNPs can be absorbed by the digestive tract. Afterwards, some can be excreted (urine or faeces) or enter the liver, circulatory and lymphatic systems [1.131,1.135]. *In vitro* studies done with human liver

(HepG2) and intestinal cells (Caco-2) can be found in the literature for hazard assessments of nanosilver ingestion. For example, a study performed with Caco-2 cells has indicated changes in gene expression after being exposed to different sized AgNPs [1.131,1.136].

1.1.5 Regulations

As explained in Section 1.1.4, AgNPs can pose serious risks for organisms in the environment and for human health when they are released into the environment. However, no NPs mass-based thresholds have yet been established in environmental compartments because the different specific properties between the wide varieties of NPs entail difficulties for establishing a threshold for all existing NPs. For example, toxicological studies indicate that smaller NPs are more toxic than larger ones [1.137]. Notwithstanding, manufactured nanoparticles (MNPs) are included in the list of emerging contaminants [1.138]. Therefore, institutions and non-governmental organisations are working on setting and regulating the production and safe handling of NMs, including AgNPs [1.139]. The European Union (EU) approach for the safety and environmental regulation of NMs is described in the Second Regulatory Review of Nanomaterials. It states that all substances comprising NM forms have to be registered in the Registration, Evaluation, Authorisation and Restriction of Chemicals (REACH) tool of the ECHA, which is the most extensive legislative provision for chemicals in the EU. The registration procedure requires specific NM information, authorisation of NM for specific uses, and a safety assessment that contemplates NM properties [1.89,1.140-1.142]. Specific EU product regulations exist that provide similar information, but only for the consumer products involved in the regulation scope, such as medical devices [1.8], cosmetics [1.143], biocides [1.10], food [1.9,1.144,1.145], active and intelligent materials [1.146], and plastics [1.147]. Apart from REACH, the Scientific Committee on Emerging and Newly Identified Health Risks (SCENIHR), the Scientific Committee on Consumer Safety (SCCS), the European Food Safety Authority (EFSA), the European Medicines Agency (EMA) and the Organization for Economic Cooperation and Development (OECD) are also working to detect the possible hazards and risks that originate from NMs use by providing guidelines [1.140,1.141]. Other non-EU countries are working on regulatory frameworks to deal with NMs [1.139]. Despite these regulatory measures, some uncertainties as to the hazards of NMs for environment and human health still exist because their behaviour and fate are not completely understood. Therefore, more research on defining NMs, product labelling about the presence of NMs, and the development of analytical methods for the detection, characterisation and risk assessment of NMs, is needed to improve existing

regulations [1.89,1.141].

1.2 Analytical methodologies for the detection, characterisation and quanification of AgNPs in enviromental and biological samples

A wide range of methods and techniques to characterise and quantify nanosilver in simple matrices is available, but very few analytical approaches exist to determine these emerging contaminants in complex environmental compartments and biological samples. This lack of analytical tools is due to the unique physicochemical characteristics of these NPs compared to their bulk counterparts. For conventional analytes, the required information can be quantitative and/or qualitative. However for NPs (solid analytes), the demanded qualitative information can entail not only their detection, but also particle characteristics (e.g. core, size, shape, aggregation/agglomeration state, coating, *etc.*). Quantitative information can be required as mass or NP number concentration. Furthermore, as stated in Section 1.1.3, NPs can undergo transformations in different environmental compartments and living beings as a result of the interaction with other components, which makes their characterisation and quantification more difficult. Another challenge of analysing AgNPs in complex samples is the low concentration of these emerging pollutants and the coexistence of AgNPs with other chemical species (Ag(I)) or NPs of different origins (natural or manufactured) and with distinct characteristics (e.g. coating). For these reasons, the development or improvement of analytical metodologies is necessary to understand the fate and behaviour of nanosilver in the environment, as well as the hazards that they can exert on living beings. Knowledge of their behaviour will facilitate the improvement of existing guidelines, regulations and legislations [1.148,1.149,1.150].

1.2.1 Sample preparation

Taking into account the aforementioned problems with analysing AgNPs in environmental and biological samples, sample preparation methods are more frequently necessary in such samples than pure AgNPs suspensions. The sample treatment procedures shown in ***Fig. 1.6***, allow sample complexity to be reduced by removing the matrix, extracting/preconcentrating nanosilver (enables speciation analysis) and fractionating AgNPs by size. Depending on the selected analytical technique, sample requirements differ [1.148,1.151]. Hence several sample preparation methods can be found, and are described in the next points:

1.2.1.1 Sample preparation for total silver determination

Total silver determination in solid environmental and biological samples can be made by a

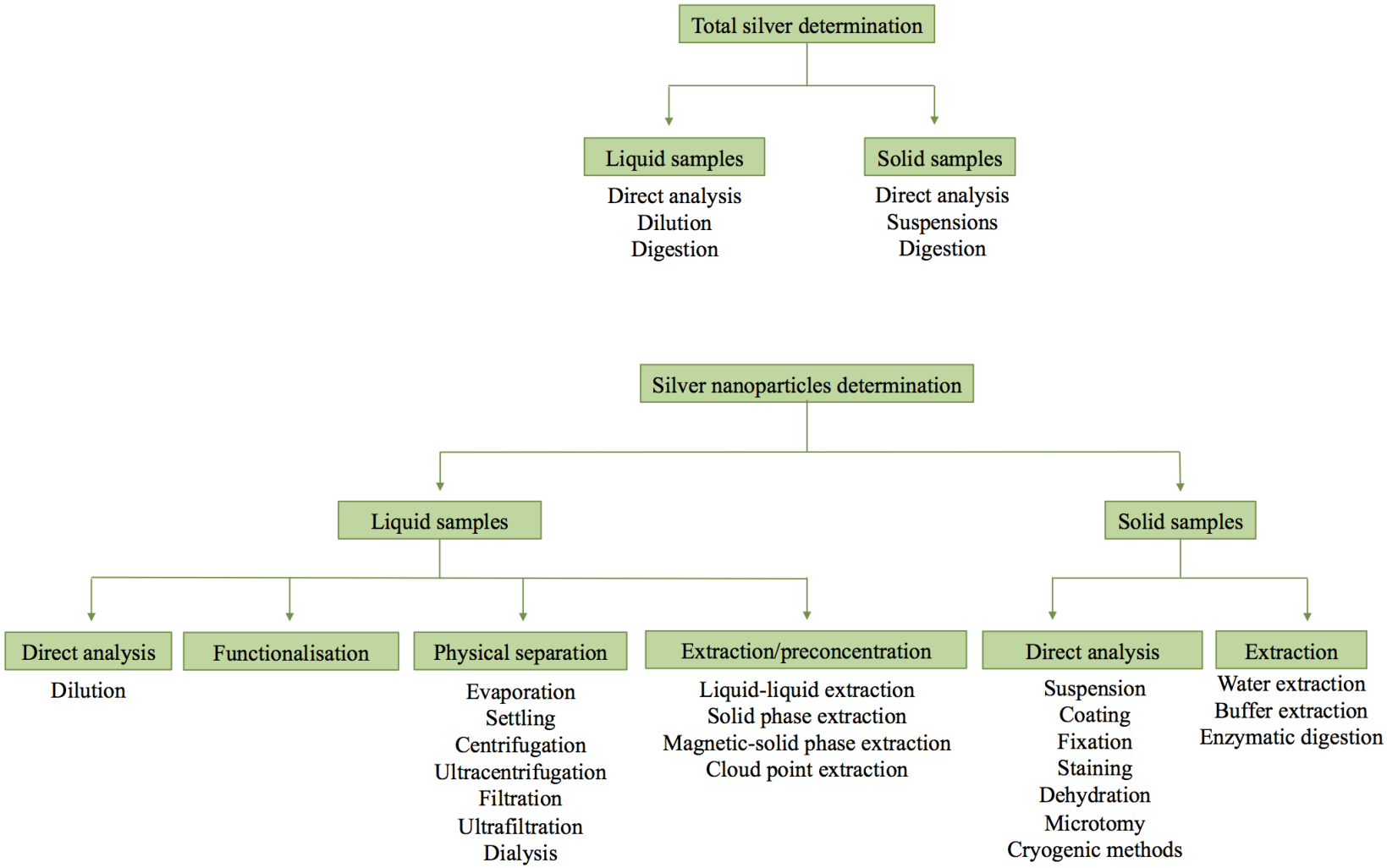

Fig. 1.6 *Main sample treatment procedures for determining total silver and AgNPs in liquid and solid samples.*

direct analysis with an adequate analytical technique (e.g. electrothermal atomic absorption spectrometry (ETAAS)) or by applying a sample treatment procedure, such as acid or basic digestion, prior to the analysis. Acid digestion of samples containing inorganic NPs is usually carried out with concentrated nitric acid either alone or combined with other strong acids and oxidants (e.g. hydrochloric acid, hydrogen peroxide, *etc.*) and by using conventional heating apparatus at atmospheric pressure or microwave ovens. Microwave digestion is the most widely used procedure thanks to its speed, reproducibility and efficiency. The amount of sample and the reagent volume required is normally 0.05-5g and a few µL-10 mL, respectively. Tetramethylamonium hydroxide is often employed in biological samples. The selection of reagents is important because they have to be able to completely degrade the sample matrix and to dissolve metallic NPs. Given the drastic conditions (concentrated acids/bases, high temperatures and pressures), this sample treatment procedure allows the total silver content to be determined, but not particle characteristics due to the dissolution of NPs [1.148,1.151-1.153]. Some analytical techniques entail the need to dilute liquid samples prior to the analysis. Dilution is commonly executed with ultrapure water but, depending on the technique and the sample matrix, other reagents can be employed (e.g. ethanol, buffer, *etc.*). For some analytical techniques, it is possible to analyse powdered samples by preparing homogeneous suspensions, in which the employment of an adequate surfactant helps the suspension to form. For both procedures, it is necessary to mix and homogenise the sample by vortex agitation, ultrasonic probe or bath sonication prior to the analysis to avoid aggregates [1.151].

1.2.1.2 Sample preparation to determine AgNPs

The determination of NPs characteristics (e.g. size or particle number concentration) in simple liquid samples (e.g. aqueous AgNPs standard) can be made by a direct analysis to avoid particle alterations. For complex matrices however, it is necessary to apply sample treatment procedures to simplify matrix complexity and/or to separate/preconcentrate the nanosilver [1.148,1.151]. Depending on the purpose of the analysis, the sample state (liquid or solid) and metal form (e.g. NP or ionic), different sample treatment procedures can be applied:

a) Dilution/suspension

As stated in Section 1.2.1.1, in some analytical techniques the dilution of liquid samples or the preparation of suspensions to analyse powdered samples is necessary [1.151].

b) Functionalisation

In some analytical techniques, the functionalisation of AgNPs before the analysis is necessary. For example, in field flow fractionation (FFF), nanosilver functionalisation sometimes enhances NPs stabilisation [1.151].

c) Coating

Coating samples before analysing them is usually required in electron microscopy (EM) techniques. Two different coating procedures are employed depending on the objective and the technique used. Conductive coating treatment is usually applied to non-conductive samples to improve image quality. For this purpose, the non-conducting or poor conducting target sample is covered with carbon or a conductive metal (e.g. Au, Pt, *etc.*). The other treatment consists in coating grids (sample holder) with carbon, metal or a polymer as a continuous thin layer to attach the sample to be analysed [1.151].

d) Fixation

Chemical fixation is a frequently used approach in the fixation of biological tissues prior to their analysis by imaging techniques (e.g. X-ray absorption spectroscopy (XAS)) to maintain the original internal tissue structure. During this sample preparation procedure, a fixative is required that is composed of a fixing agent and a vehicle. Fixing agents can be coagulants (e.g. acetone, ethanol, *etc.*), which change the conformation and solubility of protein molecules; or non-coagulants (e.g. aldehydes), which form inter- and intramolecular cross-links. Vehicles are normally buffer solutions that are used to maintain the desired pH during the fixation procedure [1.151,1.154].

e) Staining

Staining is employed to enhance the contrast for imaging techniques (e.g. EM) by facilitating the morphological studies of biological tissues. The more frequently reagents used for this sample preparation procedure are metallic salts of U (e.g. uranyl acetate), Pb (e.g. lead citrate) or Os (e.g. osmium tetroxide). There are two different contrasts depending on sample type. For thin sliced samples, "positive-staining" is used to make metals and metallic NPs react with the structure to be observed. In this case, the contrast has to be selective and any excess reagent has to be removed by running a rinse step. For organic fine particles, "negative-staining" is employed to create a black background in which the

sample is bright. Therefore, this procedure consists in adsorbing the contrast agent on the support film [1.151].

f) Dehydration

Dehydration consists of gradually substituting water for an organic solvent (e.g. alcohol). This procedure can cause coagulation and/or denaturation of proteins and dissolution of lipids if chemical fixation is not previously applied to the sample [1.151].

g) Microtomy

Microtomes are usually employed to prepare biological tissues (e.g. plant roots) to be analysed by imaging techniques (e.g. microparticle-induced X-ray emission (μ-PIXE)) because they enable the sample to be cut into thin slices by employing a special knife blade. Cryo-microtomes allow work to be done with frozen samples [1.151].

h) Cryogenic methods

Cryogenic methods (e.g. high-pressure freezing) are followed in imaging techniques (e.g. XAS), whose function is to fix the biological sample as in chemical fixation. The difference to chemical fixation lies in the fact that working with ideal conditions does practically not alter the sample during freezing treatment [1.151,1.154].

i) Physical separation

Physical separation methods allow NPs separation, purification and preconcentration. The possible physical separation procedures for samples containing AgNPs are as follows: (1) evaporation; (2) settling; (3) centrifugation and ultracentrifugation (UC); (4) filtration and ultrafiltration (UF); dialysis.

Evaporation consists of nanosilver preconcentration by submitting the sample to dryness and a subsequent redissolution [1.151].

Settling is useful for eliminating dense particulate matter, but can scavenge small particles due to differential sedimentation velocities [1.151].

Centrifugation and UC are performed with an easy handle apparatus that permits not only NPs to be isolated from an aqueous solution, but also nanosilver from their ionic species. However, long centrifugation times and high centrifugal forces sometimes do not suffice to separate AgNPs from aqueous media containing Ag(I) species. Furthermore, particle

aggregation/agglomeration is possible under these conditions by inducing the removal of undesired solids [1.148,1.151,1.155].

The conventional filtration of AgNPs suspensions is useful for removing interfering bulk particles, but should be avoided for the size fractionation of particles because large particles can be retained in the filter and are consequently discarded. Apart from traditional filtration, there are three other filtration methods: nanofiltration (100-1000 Da), microfiltration (0.2-10 µm) and ultrafiltration (1 kDa-100 mDa). UF is based on membranes with a molecular weight cut-off (MWCO), which enable species below this MWCO to pass thanks to a centrifugal force being applied. Therefore, the fractionation of particles and the separation of AgNPs and Ag(I) are possible. The disadvantages of this method are related to nanosilver recoveries, which can be affected by interactions with the ultrafiltration membrane, and poor size resolution [1.26,1.148,1.151,1.155].

Dialysis has the same function as UF, and allows NPs to be separated from their dissolved ions. This method is based on diffusing ionic species across a membrane due to a concentration gradient and osmotic pressure. However, it takes longer to achieve an equilibrium compared to UF [1.148,1.155].

j) Extraction/preconcentration

NPs can be extracted from liquid and solid samples by different methods and some of their properties are preserved [1.148]. The proposed nanosilver extraction procedures for liquid samples are the following: (1) liquid-liquid extraction (LLE); (2) solid-phase extraction (SPE); (3) magnetic solid-phase extraction (MSPE); (4) cloud point extraction (CPE).

LLE is a very well-known sample treatment procedure that consists of the extraction of hydrophobic NPs into an organic solvent and hydrophilic NPs into water or a mixture of solvents, depending on the partitioning of analytes. Extraction of NPs can be altered by the functionalisation of the particle surface [1.151,1.155].

SPE is also widely used for sample preparation and is based on retaining NPs in a solid phase for which, with AgNPs, anionic exchange resins have been proposed by coating NPs with mercaptosuccinic acid. This coating favours the electrostatic interaction between the ammonium group of the resin and the carboxylate groups of the mercaptosuccinic acid (coating), which enables efficient AgNPs separation preserving their size and shape [1.148,1.151,1.155].

MSPE employs supramagnetic particles (e.g. ferro-magnetic NPs) as sorbents to allow the preconcentration and separation of AgNPs from Ag(I) species [1.151].

CPE has been proposed for the separation and preconcentration of AgNPs in aqueous samples, and preserves the size and shape of the NPs [1.26,1.148,1.151]. As seen in ***Fig. 1.7***, the first step of this sample treatment procedure is pH adjustment. The second step consists in adding to the aqueous sample a neutrally charged surfactant (non-ionic), which is usually 1,1,3,3-(tetramethylbutyl)phenyl-polyethyleneglycol (Triton X-114), and at a concentration above the critical micellar concentration (cmc). In the nansoilver speciation analysis, addition of a complexing agent (e.g. thiosulphate) is necessary to complex Ag(I) species and to avoid the coextraction of AgNPs with their ionic species present in the sample. The third step involves incubating the sample at a temperature above the cloud point temperature, at which the surfactant becomes turbid, and micelles and aggregates form that encapsulate NPs. As micelles are denser than water, they settle after a time, and this process can be accelerated by centrifugation. At this point, the sample solution is separated into two

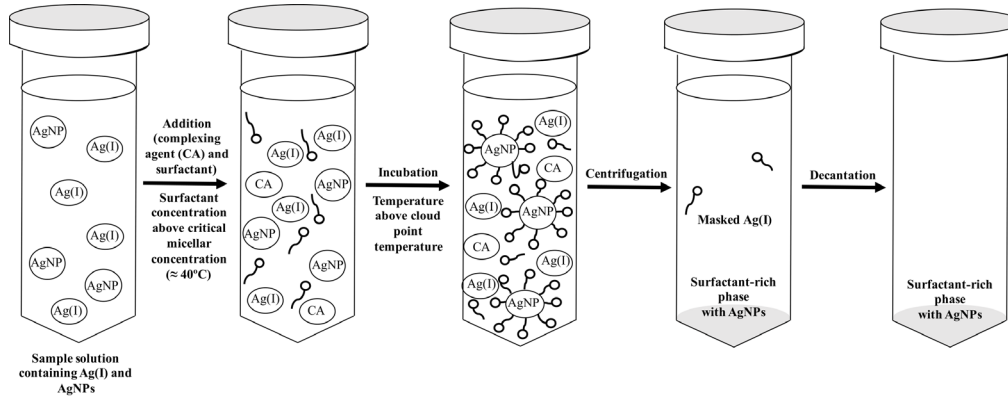

Fig. 1.7 *Schematic representation of the CPE procedure for the separation and/or preconcentration of AgNPs [adapted from [1.156]].*

isotropic phases: a small volume from the surfactant phase, which contains the analyte (AgNPs) trapped by micellar structures; and an aqueous phase containing the complexed silver ions. The last step involves the decantation of the aqueous phase. Some advantages of this sample treatment method are its high extraction efficiency and preconcentration, low cost and non-toxicity [1.26,1.148,1.151,1.156].

With solid samples, the proposed sample extraction procedures are as follows: (1) water extraction; (2) buffer extraction; (3) enzymatic digestion.

Water and buffer extractions are the simplest sample treatment methods for extracting NPs from samples. They consist in the sample containing AgNPs coming into contact with water or a buffer solution [1.151].

Similarly, enzymatic digestion is used for solubilising biological materials by degrading the matrix by enzymes and/or the extraction/isolation of AgNPs from biological tissues, preserving nanosilver form. Different enzymes are available for performing enzymatic digestion, depending on the analyte, sample type and the analytical technique used to analyse the resulting enzymatic digest. α-amylase allows carbohydrates to be degraded, while the collagenase+hyaluronidase mixture enables the separation of the extracellular matrix and the breakdown of proteins. Maceroenzym R-10 is composed of a mixture of cellulose, hemicellulose and pectinase, and is widely used to digest plant tissues. A buffer (e.g. ammonium bicarbonate, Tris-buffer saline or citrate) and a surfactant (e.g. sodium dodecyl sulfate or Triton X-100) are normally employed. In addition, agitation (e.g. vortex, sonication or magnetic) is applied to improve the digestion and solubilisation of proteins. The time required for this process is normally between 1 h and 24 h. The incubation temperature ranges from room temperature to 90 °C [1.148,1.151].

1.2.2 Analytical techniques

As previously mentioned, from an analytical point of view, the requested information of AgNPs is related to their characteristics, and to the quantity of these emerging pollutants in the analysed samples. Although a wide range of analytical tools are available, as seen in ***Table 1.2***, the combination of several techniques is necessary in most cases. The next section describes the possible analytical techniques that can be used to characterise and quantify AgNPs in environmental and biological samples:

1.2.2.1 Microscopy techniques

Microscopy techniques are the most widely used for NPs characterisation thanks to their potential for providing information about their size, structure, shape, aggregation state, dispersion and sorption through the surface images they generate (see the example in ***Fig.1.8***) [1.151].

In the literature, some of the microscoy techniques reported for NPs characterisation are the following:

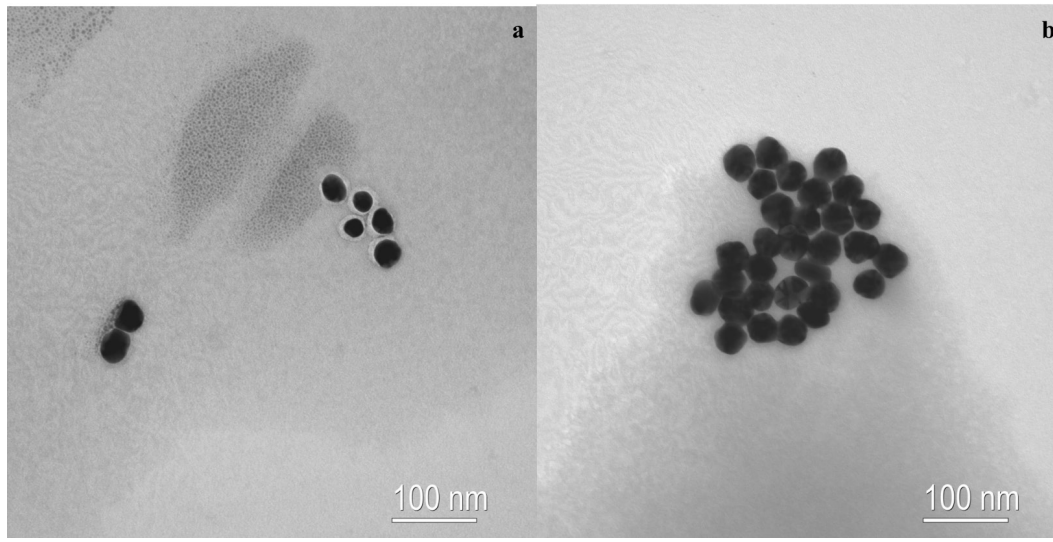

Fig. 1.8 *Transmission electron microscopy images of non-agglomerated/aggregated (**a**) and agglomerated/aggregated (**b**) 40 nm nanosilver standard.*

a) Optical microscopy techniques

Conventional optical microscopy-based techniques offer advantages over EM-based techniques, such as the direct observation of NPs in living specimens [1.157]. Although they are less employed than EM techniques, different studies have used laser-scanning confocal microscopy (LSCM) to investigate the uptake, transport and/or accumulation patterns of AgNPs in plants [1.157-1.159]. LSCM is a confocal microscopy (CM) technique in which images are obtained by scanning the sample in a raster pattern with a laser beam. Then the detector collects the fluorescence light emitted from each scan to create the image. This implies non-autofluorescence NPs having to be stained before exposing the studied samples for them to be detected in the LSCM analysis. LSCM includes a pinhole in the light detector pathway that allows the background resulting from the out-of-focus light of the sample fluorescence radiation to be reduced or eliminated. Therefore, this microscopy technique offers high optical resolution compared to EM techniques [1.157,1.160].

b) Electron microscopy techniques

Scanning electron microscopy (SEM) and transmission electron microscopy (TEM) are widely used for NPs characterisation. The image resulting from these techniques is obtained by the signals recorded in the detector that derive from the interaction of scanned (SEM) or transmitted (TEM) electrons with the analytes of the sample. SEM

Table 1.2 *Analytical techniques used for AgNPs determination in environmental and biological samples (n/a = not available).*

	Analytical information			Spatial resolution or limit of detection		References
Analytical technique	**Imaging**	**Characterisation**	**Quantification**	**Size**	**Concentration**	
Microscopy techniques						
Laser-scanning confocal microscopy	✓	X	X	n/a	n/a	[1.157,1.160]
Scanning electron microscopy	✓	✓	X	<10 nm	n/a	[1.161,1.162]
Transmission electron microscopy	✓	✓	X	<1 nm	n/a	[1.148]
Environmental scanning electron microscopy	✓	✓	X	30-50 nm	n/a	[1.148,1.162,1.163]
Atomic force microscopy	✓	✓	X	0.5-1 nm	n/a	[1.162,1.164]
Light-scattering techniques						
Dynamic light scattering	X	✓	X	3 nm-µm	n/a	[1.162,1.163]
Multi-angle light scattering	X	✓	X	50 nm-µm	n/a	[1.162]
Nanoparticle tracking analysis	X	✓	✓	20 nm	n/a	[1.148]
Spectrometric techniques						
Flame atomic absorption spectroscopy	X	X	✓	n/a	mg L^{-1}	[1.165]
Electrothermal atomic absorption spectrometry	X	X	✓	n/a	>µg L^{-1}	[1.165]
Inductively coupled plasma optic emission spectrometry	X	X	✓	n/a	µg L^{-1}	[1.148]
Inductively coupled plasma mass spectrometry	X	X	✓	n/a	ng L^{-1}	[1.148]
Single particle inductively coupled plasma mass spectrometry	X	✓	✓	10-20 nm	10^6 particles L^{-1}	[1.148]

Table 1.2 (continued) *Analytical techniques used for AgNPs determination in environmental and biological samples (n/a = not available).*

	Analytical information			Spatial resolution or limit of detection		References
Analytical technique	**Imaging**	**Characterisation**	**Quantification**	**Size**	**Concentration**	
Laser ablation inductively coupled plasma mass spectrometry	✓	X	✓	15-50 µm	0.01 µg g^{-1}	[1.109]
Total reflection X-ray fluorescence spectrometry	X	X	✓	n/a	µg L^{-1}	[1.166]
Microparticle induced X-ray emission	✓	X	✓	0.5 µm	1-20 µg g^{-1}	[1.109]
Synchrotron radiation X-ray absorption spectroscopy	✓	X	✓	>µm	mg kg^{-1}	[1.109,1.148,1.163]
Synchrotron radiation micro X-ray fluorescence spectrometry	✓	X	✓	>µm	ng g^{-1}	[1.109]
Surface-enhanced Raman spectroscopy	X	✓	X	Depending on the laser intensity	n/a	[1.167]
Fourier transformed infrared spectroscopy	✓	✓	X	10 µm	n/a	[1.168]
Ultraviolet visible spectroscopy	X	✓	✓	10-80 nm	>mg L^{-1}	[1.169,1.170]
Laser induced breakdown spectroscopy	X	✓	✓	>5 nm	ng L^{-1}	[1.162]
Darkfield spectroscopy	✓	✓	X	<200 nm	n/a	[1.109]
Nano-secondary ion mass spectrometry	✓	✓	X	>50 nm	n/a	[1.171]

Table 1.2 (continued) *Analytical techniques used for AgNPs determination in environmental and biological samples (n/a = not available).*

	Analytical information			Spatial resolution or limit of detection		References
Analytical technique	**Imaging**	**Characterisation**	**Quantification**	**Size**	**Concentration**	
Chromatographic/fractionation techniques						
Reversed phase chromatography	X	X	✓	n/a	RCP-ICPMS: ng L^{-1}	[1.172]
Size exclusion chromatography	X	✓	✓	0.5-10 nm	Depending on the detector	[1.148,1.162]
Hydrodynamic chromatography	X	✓	✓	5-1200 nm	Depending on the detector	[1.148,1.162, 1.163]
Field flow fractionation	X	✓	✓	Flow FFF: 1 -1000 nm Sed FFF: 50-1000 nm	Depending on the detector	[1.148,1.162, 1.163]
Electrophoretic techniques						
Capillary electrophoresis	X	✓	✓	5 nm	CE-ICPMS: µg L^{-1}	[1.148]
Electrochemical techniques						
Voltammetry of immobilized particles	X	✓	✓	10 nm	µg L^{-1}	[1.148]
Anodic particle coulometry	X	✓	✓	5 nm	10^{10} particles L^{-1}	[1.148]
Chemical sensors						
Ion selective electrode	X	X	✓	n/a	10^{-7} M	[1.173]
Surface plasmon resonance sensor	X	X	✓	n/a	µg L^{-1}	[1.174]

offers less resolution than TEM, and provides a view of AgNPs morphology, but sample composition can also be known if coupled with energy-dispersive X-ray spectroscopy (EDX) [1.149,1.175]. For example, SEM-EDX has been used to visualise the presence of AgNPs in root hair cells of a plant [1.158]. Conversely, TEM provides information about the NP structure, such as particle size [1.148,1.149]. Diverse works in the literature have employed this technique alone or coupled with EDX or electron-energy loss spectroscopy (EELS) to observe and provide information about AgNPs characteristics (e.g. morphology, particle size distribution or aggregation state) in complex environmental and biological samples [1.56,1.69,1.149,1.159,1.176]. One study has determined the crystallographic pattern of nanosilver inside algae by TEM coupled with selected-area electron diffraction (SAED) [1.149,1.177]. However, EM techniques cannot be used for quantitative purposes because many particles need to be considered to obtain representative results [1.148]. One of the major disadvantages of TEM and SEM is that liquid samples have to be submitted to a sample treatment procedure (e.g. chemical dehydration) because they operate under vacuum conditions. Consequently, artifacts in the sample can appear and can alter the results [1.151]. This problem in environmental scanning electron microscopy (ESEM) does not appear because samples are maintained in a gaseous environment instead of vacuum conditions while being analysed, which allows liquid samples to be imaged in their natural state with no prior preparation [1.151,1.178]. Although only a thin superficial layer of the sample can be analysed by this technique, it has been used to determine the physicochemical state of AgNPs in soils [1.148,1.179] or in washing wound dressing waters [1.180].

c) Atomic force microscopy technique

Atomic force microscopy (AFM) is less used than EM techniques for liquid or solid environmental analyses [1.164]. AFM relies on a scanning probe microscopy (SPM) technique that differs from other microscopy techniques because it is equipped with a physical tip (probe) that scans the surface of samples. This technique permits information on different NP properties to be acquired, such as physical (e.g. size, shape, surface texture and roughness), electronic or mechanical information with the topographic image of the sample surface, obtained from measuring atomic forces between the probe and the sample surface [1.26,1.163,1.181]. Although AFM enables liquid samples to be analysed and works under environmental conditions, sample treatment is also required to solidly

bind the sample to the substrate and consequently artifacts may appear [1.151,1.181]. For example, AFM has been used to evaluate the colloidal stability of AgNPs in different water types [1.98]. Despite the spatial resolution of AFM being below 1 nm, this technique can overestimate the dimension of AgNPs when the tip is larger than the NP size [1.163,1.164].

1.2.2.2 Light scattering techniques

Light-scattering techniques are used to make particle size determinations in aqueous suspensions. The different existing techniques include the following:

a) Dynamic light scattering

Dynamic light scattering (DLS) is the widest used technique of existing light-scattering techniques. It consists of measuring time-dependent fluctuations in scattering intensity, generated by the constructive and destructive interferences that result from the NPs Brownian motion of the analysed sample. Movement of NPs is directly related to an equivalent hydrodynamic diameter. One limitation of DLS is that sample viscosity and the refractory index, which are parameters that affect the Brownian motion of particles, are not easily determined in complex samples. Moreover, this analytical technique is unable to detect smaller particles among larger ones, so it is not suitable for analysing samples with a heterogeneous particle size distribution (e.g. environmental samples). This problem can be overcome by coupling DLS with fractionation techniques (e.g. FFF) [1.148,1.149,1.153]. Although using DLS is difficult for determining particle size in complex aqueous samples, it has been employed to establish the AgNPs hydrodynamic diameter and/or monitoring nanosilver aggregation processes in surface water, river water [1.182], wastewater [1.183] and seawater [1.184].

b) Multiple-angle light scattering

Multiple-angle light scattering (MALS) can provide information on different particle size parameters (e.g. gyration radius) by measuring the averaged intensities of the light scattered by the particles collected at several angles. This technique also presents difficulties with discriminating smaller NPs from bigger ones as DLS does. Its use is more limited than DLS because samples have to be cleaner and optical properties have to be well-known. However, combining MALS with DLS or FFF allows NPs shape to be determined [1.148,1.153]. Some works in the literature have employed MALS combined with FFF to determine the

AgNPs hydrodynamic diameter in wastewater, tap water and environmental water (e.g. river water) [1.185,1.186].

c) Nanoparticle tracking analysis

Nanoparticle tracking analysis (NTA) measures the movement of the NP under Brownian motion by using a video microscopy. The distance travelled by a NP after a certain time is related to its hydrodynamic diameter. By collecting information about different NPs, both particle number concentration and hydrodynamic size distributions can be obtained. The capacity of NTA to track individual particles exempts it from intensity limitations that DLS has for analysing samples with wide-ranging NP sizes. Additionally, it is able to measure a large number of particles in much less time compared to microscopy techniques [1.148,1.187]. The AgNPs size distributions and the changes in nanosilver physicochemical characteristics in natural freshwater and seawater have been evaluated by this analytical tool [1.188,1.189].

1.2.2.3 Spectrometric techniques

A large number of spectrometric techniques can be used for AgNPs characterisation and/or quantification in environmental and biological samples:

a) Flame and electrothermal atomic absorption spectrometry

Flame atomic absorption spectrometry (FAAS) and ETAAS are atomic absorption techniques in which free gaseous atoms of the analyte, generated in an atomiser, absorb electromagnetic radiation at a specific wavelength to produce a measurable signal. The absorption signal of free atoms is proportional to their concentration in the sample. The main difference between these analytical techniques lies in the heating sources used to produce atoms. In FAAS, fine droplets enter a flame where the following processes take place: desolvation of droplets, vaporisation of particles, dissociation of molecular species to form atoms and the possible ionisation of atoms. In ETAAS, sample vaporisation and atomisation occur in a tubular graphite tube that is electrically heated. Given its configuration, ETAAS offers the opportunity to directly analyse solid samples, but FAAS samples must be liquid. In addition, the limits of detection (LODs) are better in ETAAS (low $\mu g\ L^{-1}$) than in FAAS (low $mg\ L^{-1}$). The advantages of these analytical tools are their easy sample preparation, relatively low costs, and high selectivity, accuracy and sensitivity. Their principal limitations are that a few elements can be monitored per analytical run, plus the

presence of important matrix effects [1.109,1.155,1.165,1.190]. Moreover, these techniques are unable to distinguish AgNPs from their ionic species. Several studies in the literature have run a sample treatment procedure before the analysis to obtain quantitative information about nanosilver in environmental and biological samples. For example, dispersive liquid-liquid microextractions in river water and wastewater [1.191], and CPE in different water samples [1.192,1.193]. Nevertheless, a new ETAAS development, namely high-resolution continuum source ETAAS (HR-CS ETAAS), allows AgNPs to be discriminated from Ag(I) in solid biological samples by atomisation delay [1.26,1.194].

b) Inductively coupled plasma based techniques

Inductively coupled plasma (ICP)-based techniques are similar to FAAS and ETAAS, but sample dissociation occurs by an inductively coupled plasma source. The techniques that derive from ICP sources are inductively coupled plasma optic emission spectrometry (ICP-OES) and inductively coupled plasma mass spectrometry (ICPMS) [1.190,1.195,1.196].

In ICP-OES, the atomic or ionic excited species located in hot plasma return to their ground state by emitting the absorbed energy as photons at a characteristic wavelength of the analysed element. Lens or concave mirrors from an axial, radial, or a combination of both views, collect the photons emitted by the ICP source. A radial position implies viewing the side of plasma, and the potential background and spectral interferences are limited. In the axial mode, the view comes from the end of plasma by allowing the visualisation of the longer path available down the axis of plasma to obtain better LODs than with the radial mode. On the contrary, the probability of spectral and matrix induced interferences increases. From this viewing, the exiting wavelength from a selection device (e.g. monochromator) is converted into an electrical signal by a photodetector. Electrical signals, which are related to the emitted photons, are proportional to the concentration of the analyte that originates in the sample. Therefore with this analytical tool, quantitative information about an element or multiple elements can be obtained [1.197]. However, this technique has its drawbacks; e.g. only liquid samples can be analysed; information about physicochemical characteristics and the state of the metal (e.g. size, shape, aggregation) cannot be obtained. So this analytical technique only provides information about the total metal concentration. For this reason, several studies have applied sample treatment procedures to the samples of interest to separate AgNPs from other metal species (e.g.

Ag(I)) or to destroy the solid matrix. In the latter case, one study did an acid digestion of sand samples containing AgNPs before running the analysis by ICP-OES [1.148,1.198].

In ICPMS, the ions formed in the ICP source are collected with the help of a conical water-cooled sampler onto an interface. Immediately behind the sampler cone, a skimmer cone appears with a smaller orifice that focuses ions into the mass spectrometer (MS). Depending on the MS, after the sample ion beam has been collimated by the ion lens, it can enter a reaction cell (e.g. quadrupole or hexapole), where polyatomic molecular ions can be minimised from the beam before entering the mass analyser. Once inside the MS analyser (e.g. quadrupole, magnetic sector or time-of-flight), ions are separated according to their different mass-to-charge ratio (m/z). The isolated m/z ion beams arrive at the detector (e.g. electron multiplier), where their current is measured and the magnitude of the ion current is proportional to the concentration of the analyte ions in the sample. Despite the LODs of ICPMS being better than ICP-OES, it presents worst spectral interferences [1.190,1.195,1.199]. Furthermore, the limitation of discriminating AgNPs from other metal species (e.g. Ag(I)) in liquid samples can be solved by applying some of the sample treatment procedures explained in Section 1.2.1, such as CPE [1.200,1.201,1.202]. Alternatively to these strategies, fractionation techniques, such as FFF [1.203,1.204], capillary electrophoresis (CE) [1.205] or hydrodynamic chromatography (HDC) [1.176], can be coupled to ICPMS.

Apart from these alternatives, there is an emerging mode of ICPMS, called single particle inductively coupled plasma mass spectrometry (SP-ICPMS), that is becoming popular. This methodology consists of measuring very diluted NPs liquid suspensions in short dwell times (milliseconds or microseconds) so that only one particle arrives at the detector for each reading time. The total number of NP events detected (I_p) during the total acquisition time (t_i) is directly proportional to the NP number concentration (N_{NP}):

$$I_p = \eta_{neb} Q_{sample} N_{NP} t_i \qquad (1.1)$$

where η_{neb}= nebulisation efficiency and Q_{sample} = sample flow rate. The intensity of a NP detected in a single reading is related to the number of atoms included in this NP. For solid, spherical and pure NPs, particle size can be determined by relating the diameter with the total counts per reading of a NP (r_{NP}), as seen in the following equation:

$$r_{NP} = \eta_{neb} Q_{sample} \frac{AN_{Av}}{M_M} \frac{1}{6} X_{NP} \rho \Pi d^3 \quad (1.2)$$

where A = atomic abundance of the measured isotope, N_{Av} = Avogadro number, M_M = atomic mass of target element M, X_{NP} = mass fraction of the measured element, ρ = density of the NP and d = NP diameter. The mass of the analyte per NP can also be obtained by relating the r_{NP} to the mass of M per NP (m_{NP}) [1.206].

In order to link the frequency of NP events with the NP number concentration, and the signal intensity of a single NP with the size or the mass of the NP, two calibration strategies have been proposed in the literature. The first consists of performing a calibration curve by well-characterised NP standards. The second is based on determining the η_{neb} of the analyte by employing standard solutions. In the latter case, three different calculation methods can be employed to calculate η_{neb}: waste collection, particle frequency and particle size. Once η_{neb} is known, information about NPs size, NP number and mass concentration can be obtained [1.196]. Therefore, SP-ICPMS has the capability to characterise and provide quantitative information on AgNPs in complex samples at environmental concentrations. The presence of the analyte in an ionic form can be identified as a continuous signal together with the background [1.148]. If NPs coexist in a liquid sample with their ionic form, the discrimination of the corresponding signals of both species is sometimes a challenge. This problem occurs when a high ionic background of the target element is present in the sample, which difficult NPs from being detected and affects the LOD of NP size. To overcome this limitation, different iterative algorithms are reported in the literature to determine the threshold value from which an event corresponds to a NP. The estimation of the threshold value is critical because false positives will occur if it is set too low, or size LOD will increase if it is set too high [1.196]. Additional weaknesses that SP-ICPMS presents are: (1) inaccurate results can be obtained for the incomplete vaporisation of NPs; (2) detection of two NPs or the partial detection of a NP during a dwell time if the working conditions are inadequate; (3) limited or no multi-element capabilities using quadrupole-based ICPMS; (4) NP size LOD is still poor (10-20 nm); (5) only liquid samples can be analysed [1.148,1.196]. To overcome the last drawback, solid sample enzymatic digestion procedures that preserve the nanoform have been used in the literature [1.207].

Solid samples containing AgNPs can also be analysed by the laser ablation technique (LA) coupled to ICPMS, which enables the direct analysis of a solid sample by avoiding digestion procedures. Fewer mass spectral interferences are present in this coupling. LA consists of a focused laser beam that impacts the target sample in an argon atmosphere to generate an aerosol from the ablated sample. The ablated sample material is transported under atmospheric conditions with a carrier gas flow (argon or helium) to the ICP source [1.195,1.196]. Some critical aspects of this analytical tool are the spatial resolution, the ablation efficiency of the analytes from the solid surface, the transport efficiency of the target particles to the ICPMS, and the detection and quantification of NPs within the background of the sample's surface matrix [1.196]. LA-ICPMS has been used for the detection, visualisation and quantification of nanosilver in aquatic living organisms (*Danio rerio* and *Daphnia magna*) [1.208,1.209].

c) X-ray based techniques

Some of the X-ray techniques employed to detect, characterise and quantify NPs in environmental and biological samples are total reflection X-ray fluorescence spectrometry (TXRF), microparticle induced X-ray emission (μ-PIXE), micro synchrotron radiation X-ray fluorescence spectrometry (μ-SR-XRF) and synchrotron radiation X-ray absorption spectroscopy (SR-XAS).

TXRF is based on X-ray fluorescence (XRF) fundamentals. In XRF, an X-ray tube emits X-ray photons (primary beam), which impact the target sample. If the photon that impacts target atoms has more energy than the binding energy of a bound inner electron shell, this energy can be partially absorbed (photoelectric absorption) and the atomic electron is ejected from its atomic position (ionised atom). The inner shells of the atoms present in the sample are named K- (more internal), L- and M- (more external). The atom with an unstable state can return to its original state by two processes: (1) the rearrangement of the inner electrons provoking the emission of other photoelectrons (Auger effect); (2) an electron from an outer orbital is transferred to the vacancy position by emitting an X-ray photon (characteristic of XRF). In the latter case, depending on the electron that fills the vacancy, the frequency could be α, β, γ, η and 1 (from more intense to less intense). The resulting characteristic X-ray (secondary beam) is recorded in the detector system, which converts the X-ray photons into electrical pulses. These pulses are amplified and counted by a

multichannel analyser, which gives the intensity of the measured characteristic radiation photon that is the peak in the XRF spectrum [1.166,1.210].

Nowadays, the TXRF instruments available on the market are benchtop systems that operate under ambient conditions because they are equipped with air-cooled low-power X-ray tubes and Peltier cooled silicon drift detectors (SDD) [1.211]. This analytical tool has the capability to determine micro- and trace elements in a wide range of samples (e.g. liquid or powder). To perform an analysis, the samples have to be deposited on a reflective sample holder (e.g. quartz), which is selected depending on the reflector characteristics and the elements to be determined. Total reflection conditions are achieved by depositing the sample as a thin layer (<100 µm) on the sample holder, as well as a sample spot diameter within the X-ray beam size range. To obtain a thin layer, different sample preparation procedures can be applied to liquid and solid samples. Low-salinity liquid samples can be directly deposited (5-50 µL) on an adequate reflector, previously siliconised to avoid wide sample dispersion, and then drying them by heating or vacuum sources. For more complex samples, such as environmental samples, further sample treatment has to be performed. Dilutions, using ultrapure water or non-ionic surfactants (e.g. Triton X-114), can be carried out for concentrated samples, and a preconcentration procedure is useful (e.g. CPE) for low-element concentrations. The latter procedure allows the LODs of the target elements to improve and acquiring elemental speciation information. However, this additional step implies that very little multi-elemental information can be acquired. Moreover, a larger sample volume is required and the presence of systematic errors in the final results is likely as a result of sample losses or contamination by other elements [1.166]. Despite these drawbacks, the enrichment of AgNPs and gold nanoparticles (AuNPs) in complex aqueous matrices by CPE has been reported [1.212]. Solid samples can also be directly analysed or a previous sample preparation can be performed. The direct analysis of solid environmental samples (e.g. soils) is usually performed by preparing a suspension with an appropriate amount of a solid sample and with an adequate volume of solvent (ultrapure water or diluted non-ionic surfactant). It is important that sample thickness does not exceed 0.5 mm to prevent damage or contamination of the detector, and to also obtain a thin layer to accomplish the total reflection analysis conditions. Some complex solid samples cannot be directly analysed and sample treatment, such as acid digestion, is required to obtain a

liquid extract [1.166].

In TXRF, X-ray tubes are commonly supplied with a molybdenum (Mo) anode. Nonetheless, in some applications in which high atomic number elements have to be detected, the tungsten (W) anode is preferred as the excitation source. With Mo X-ray tubes, only Ag L-lines can be excited. Ag L-lines, particularly $L_{\alpha 1}$ peak (2.984 keV), are interfered by argon K_{α} (2.957 keV) and K_{β} (3.145 keV) when measurements are taken under air conditions. These interferences are overcome when using a W X-ray source because it is possible to use the K-lines of high Z elements [1.213]. The primary beam generated in the X-ray tube, which previously passes through the first reflector to eliminate possible interferences (e.g. K-lines of the anode material), hits the reflector containing the sample at a glancing angle of below 0.1°. As seen in ***Fig. 1.9***, in TXRF the incident beam angle is one of the main differences to conventional XRF techniques such as energy dispersive XRF (EDXRF; 40°). TXRF LODs (ng mL^{-1}) are better because the fluorescence signal intensity is enlarged since the reflected beam contributes to excitation and the detector is located perpendicularly and closer to the sample carrier, which minimises the scattered background.

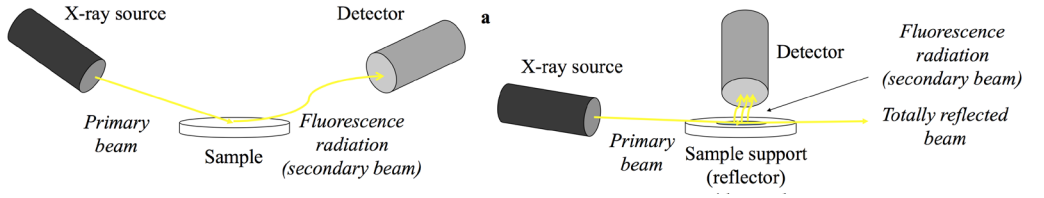

Fig. 1.9 *Schematic view of the EDXRF (**a**) and TXRF (**b**) systems.*

The TXRF spectrum shows the peaks corresponding to the different elements present in the target sample. Thus multi-elemental qualitative information about the sample can be acquired. As the intensity of the element characteristic peaks is proportional to their concentration in the analysed sample (matrix effects are negligible), quantitative information on the target elements can also be acquired. The most frequently used strategy for quantification purposes is internal standardisation, where a known amount of a mono-element standard is added to the sample and additionally it reduces sample deposition inaccuracies. The internal standard has to meet the following requirements: (1) not be present in the sample; (2) its fluorescence lines must not interfere with analytes; (3) its concentration has to fall within the range in the elements of interest. The concentration of elements is determined by the following equation:

$$C_i = \frac{C_{IS} N_i S_{IS}}{N_{IS} S_i} \quad (1.3)$$

where C_i = analyte concentration, C_{IS} = internal standard concentration, N_i = net signal of the analyte, S_{IS} = internal standard's relative sensitivity, N_{IS} = internal standard's net signal and S_i = analyte's relative sensitivity. Other adopted strategies include standardless quantification and external calibration [1.166,1.210].

μ-PIXE is based on the particle induced X-ray emission technique which, in turn, is based on XRF, but the excitation of the analytes contained in the analysed samples is produced by a beam of protons of sufficient energy instead of by electromagnetic radiation. The protons beam that emerges from a small electrostatic accelerator is injected into a beam line by an analysing magnet. Then this beam is led to the sample chamber by electrostatic or electromagnetic lenses without losing the beam intensity during this displacement. The impact of the beam of protons on the sample creates a vacancy in the atomic shell (atom ionisation). Subsequently, the vacancy is refilled by an outer electron shell that results in the emission of X-rays, which are measured by a detection system (usually an energy-dispersive one). In μ-PIXE, the protons beam focuses on small areal dimensions (as low as 1 μm) with the help of a microprobe that scans the sample surface and enables the distribution of the trace elements to be determined on a micrometer scale within a wide range of samples. It can be equipped with a scanning transmission ion microscope to allow the determination of element concentrations for the selected sample points [1.210,1.214]. This analytical tool offers lower LODs and higher sensitivity in comparison to tube-excited XRF systems. Despite that a particle accelerator is needed for producing the incident protons beam (1-4 MeV) this technique has been widely used in the biology field even for the determination of AgNPs distribution and quantification in animal cells [1.210,1.215,1.216].

μ-SR-XRF is based on the XRF fundamentals explained above, but the X-ray beam is produced by synchrotron radiation instead of by conventional X-ray tubes. Synchrotron radiation is generated from a source of electrons and positrons in a linear accelerator in which they are accelerated to produce a beam with energy at around 100 MeV. This beam of electrons or positrons is subsequently injected into a storage ring, where they are accelerated to energies within the giga electronvolt range by passing through diverse magnetic fields. As

a result, synchrotron radiation is produced. The main advantage of synchrotron is that the beam intensity is at least ten orders of magnitude higher than that of conventional X-ray tubes [1.210,1.217]. This analytical tool is non-destructive, the simultaneous imaging of a wide range of elements is possible, it has a high spatial resolution and sensitivity, and solid samples can be analysed [1.218]. In biological samples, sample preparation is often required before they are analysed (e.g. cryo-sectionning by microtome). Additionally, these samples are susceptible to suffer thermal disorder and radiation damage by synchrotron radiation so as to avoid alterations to their native state; data acquisition under cryogenic conditions is preferable [1.219]. For example, a study in the literature has frozen the sample leaves and cut them with a cryo-microtome before performing the SR-μ-XRF analysis [1.220]. One of the main disadvantages of this analytical technique is it requires synchrotron radiation facilities. Another synchrotron-based technique is SR-XAS, which is based on combining X-ray absorption spectroscopy and synchrotron radiation. XAS consists in scanning, by a monochromatic X-ray beam, the binding energy core shell of the element of interest to increase an absorption edge, where each edge represents a different core-electron binding energy. The X-ray absorbed by the core electron produces its excitation and the excess energy of the electronic binding energy leads to a photoelectron being ejected from the atom [1.210,1.217]. The resulting X-ray absorption spectrum is divided into: (1) pre-edge, where energy is limited to a few eV around the edge; (2) X-ray absorption near edge structure (XANES) or near edge X-ray absorption fine structure (NEXAFS), where energy falls within 50 eV of the edge; (3) an extended X-ray absorption fine structure (EXAFS), where energy goes from 50 eV to 1,000 eV or more above the edge [1.217]. XANES and EXAFS spectra provide complementary structural information. XANES allows information to be acquired about geometry and the oxidation state of the target metal atoms. EXAFS enables the determination of the distances to ligands and neighbouring atoms; and the coordination number from the absorbing target element [1.217,1.221]. Some advantages of SR-XAS are that it is element specific, a wide range of metals can be analysed and the sample state is not a limitation (powder, liquid or frozen). However, this analytical technique has its drawbacks, such as the sensitivity of the technique (mg kg^{-1} range), it requires synchrotron radiation facilities and it is difficult to interpret and deconvolute bulk data in complex samples [1.148,1.221]. Despite these limitations, this analytical tool is widely

used in biological systems because it provides information on the local structure of the elements at subatomic level, and on the oxidation state of the elements of interest that is related to their toxicity and chemical behaviour. As in μ-SR-XRF, sometimes in these type samples, the sample preparation procedures explained in Section 1.2.1.2 (e.g. cryogenic methods) are required [1.219]. For example, the literature includes a study that investigates nanosilver distribution, changes in their speciation and their accumulation in plant tissues after being exposed to coated/uncoated AgNPs and Ag(I) (as $AgNO_3$) using some of the sample treatments described in Section 1.2.1.2 before the μ-XANES analysis [1.220,1.222]. XAS has been employed to study the AgNPs distribution, behaviour and transformation in environmental samples such as wastewater effluents and sludge [1.66,1.69,1.223] .

d) Other techniques

Apart from the aforementioned techniques, there are other techniques that are capable of characterisation and provide quantitative information on NPs, including ultraviolet visible spectroscopy (UV-Vis), Raman spectroscopy, fourier-transformed infrared spectroscopy (FTIR), laser induced breakdown spectroscopy (LIBS), dark field spectroscopy and nano-secondary ion mass spectrometry (Nano-SIMS).

AgNPs surface electrons are able to absorb photons due to their characteristic surface plasmon resonance band (SPRB). From the changes that SPRB area undergo during UV-Vis measurements, it is possible to obtain information on both composition and concentration [1.169,1.224]. This analytical technique is widely used to characterise synthesised nanosilver, but the literature contains few studies that have employed UV-Vis in environmental samples. For example, one study employed this technique to evaluate the aggregation and dissolution of AgNPs upon their discharge to freshwater and seawater [1.224]. Another study quantified nanosilver in groundwater with this analytical tool [1.225].

Raman spectroscopy allows the characterisation of the NPs structure [1.149]. This technique relies on the inelastic light scattering produced by irradiating monochromatic laser light on the analysed sample. The resulting shifts of the scattered light frequency in comparison with original monochromatic frequency, which are a consequence of the change in the vibrational, rotational or electronic energy of the excited analyte, provides a molecular "fingerprint" of the sample [1.109,1.226,1.227]. Some advantages of Raman spectroscopy are minimum sample preparation and the possibility of analysing liquid and solid samples

[1.228]. However, the weak Raman scattering (inelastic) and fluorescence interferences (e.g. impurities or sample fluorescence) of this technique complicate the detection of analytes at low concentrations [1.167,1.228]. The surface-enhanced Raman spectroscopy (SERS) technique improves Raman signals by adsorbing the analyte molecule on a plasmonic metal surface, which is normally formed by metal colloids [1.102]. Despite most existing studies having utilised AgNPs as substrates of SERS to analyse chemical or biological analytes, one study has used a compound that binds the AgNPs present on the substrate and produces characteristic signals to indicate the presence of nanosilver in environmental (e.g. surface water) and biological (e.g. spinach leaves) samples [1.229]. Additionally, when it is combined with microscopy, it is possible to obtain maps of the biomolecule distribution in tissues [1.109].

FTIR is used mainly for determining structural changes of living beings after being exposed to NPs. This analytical technique has similar fundamentals to Raman spectroscopy, but the sample is irradiated with an infrared source and it measures the intensity of the light passing through the analysed sample at specific wavenumber. The main advantages of this analytical tool are that it requires minimum sample preparation, its analysis time is short, it is usually non-destructive, only a small portion of sample is needed, sample can be liquid or solid, and its high sensitivity, high accuracy and stability. However, one of its disadvantages is that multiple background scans and sample scans are needed to avoid artifacts and variations in spectra [1.227]. In the literature, FTIR does not come over as a widely used technique for analysing biological samples after being exposed to nanosilver. Some studies have employed transmittance FTIR to determine the conformational changes in the macromolecules of plants after being exposed to these emerging contaminants [1.230], or attenuated total reflectance FTIR (ATR-FTIR) to study the interactions of AgNPs with membrane biomolecules of bacteria [1.231].

LIBS has the potential to determine both particle size distribution and concentration. This technique is based on the fact that when a NP passes through the focal volume of a pulsed laser (energy correctly tuned), a plasma is formed and the resulting emitted light of the analyte is measured. This technique's main advantages are that all sample types can be analysed (liquid, solid or gaseous), it is a non-destructive technique, and offers high sensitivity for small-sized NPs. However, its main drawback is that it is unable to

discriminate different types of NPs (size and composition) [1.26,1.155,1.161]. Although very few studies that have used LIBS can be found in the literature, research has been done by this technique to quantify the AgNPs internalised in plant roots [1.232].

Dark field spectroscopy is the combination of dark field microscopy and a spectrometer (e.g. hyperspectral imaging spectrometer). This technique consists of analysing the collected scattered radiation from NPs, produced by an incident beam, which enables the detection and characterisation (e.g. size, shape, *etc.*) of nanostructures. The main advantage of dark field spectroscopy is that unstained samples can be imaged. However in some cases, it is necessary to stain the sample with an appropriate colour [1.152]. The potential of this technique for determining AgNPs transformations in wastewater effluents and biosolids [1.183], or for the detection, characterisation and semiquantification of nanosilver in complex waters (mesocosm water and secondary wastewater effluent) [1.233], has been reported.

Nano-SIMS is a new characterisation technique based on secondary ion mass spectrometry (SIMS), where the primary ion beam is generated by a nanoscale ion microprobe. This primary ion beam impacts the surface of the solid sample and analytes are sputtered from the sample as excited or secondary ions, which are subsequently collected and analysed by MS [1.234,1.235]. Its main advantage is its high resolution and surface specificity [1.171,1.234]. However, sample preparation is complex, high vacuum conditions are needed and NPs differentiation from ions proves difficult. The literature indicates one work that employed this analytical tool to analyse AgNPs morphology and distribution inside *Chlamydomonas reinhardtii* cells [1.177].

1.2.2.4 Chromatographic and fractionation techniques

Chromatography is a group of separation techniques in which components are separated into two phases; a stationary phase and the other moves in a definite direction (mobile phase) [1.236]. There are diverse types of chromatographic methods that allow NPs separation in liquid samples, including reversed phase chromatography (RPC), size exclusion chromatorgraphy (SEC) or HDC.

RPC is based on non-polar packing material columns, where the NP surface interacts and can be retained. Another approach is to use ionic exchange stationary phases. This method is able to separate NPs from other elements, such as Ag(I) (speciation analysis) [1.196,1.237]. The SEC and HDC methods are able to separate NPs based on their size and shape. SEC consists of a

porous stationary phase where particles larger than pores are retained to a lesser extent than smaller particles [1.26,1.162]. Conversely to the aforementioned chromatography methods, non-porous or very small pore packing materials constitute HDC columns that form flow capillary channels where separation takes place by a velocity gradient. Therefore, larger particles elute more quickly than smaller ones as they spend less time near capillaries [1.148,1.153].

Apart from chromatographic techniques, FFF also enables the fractionation of NPs. In FFF, different sized NPs are separated by the interaction of the analytes with an external field applied perpendicularly to the mobile phase flow, instead of a stationary phase. Depending on the applied field, there are different types of FFF, of which asymmetric flow FFF is frequently used to analyse complex samples [1.26,1.148].

Despite these analytical tools being capable of separating NPs according to their size, shape and composition, they present some drawbacks, such as a long analysis time and the possible adsorption of NPs on packaging material or membranes in FFF, which generates lower NPs recoveries. Thus optimising the working conditions is recommended to avoid these problems [1.148,1.153,1.162].

All the aforementioned fractionated techniques can be coupled with various detectors to determine some NPs characteristics (e.g. particle size distributions) and to quantify NPs, although the ICPMS detector is the most widely employed for analysing AgNPs in environmental and biological samples because of its selectivity and high sensitivity (LODs within the ng L^{-1} range) [1.148,1.176,1.238-1.240].

1.2.2.5 Electrophoretic techniques

Among the existing electrophoretic techniques, CE is the most frequently used for separating and determining NPs size, shape and surface chemistry. The separation of NPs is done by applying high voltage at the end of a thin capillary filled with an electrolyte, where NPs movement towards the electrode depends on NPs properties (e.g. charge, size, and shape) and the solvent medium [1.26,1.148,1.196]. In some cases, the presence of an electrolyte is not sufficient for non-charged NPs migration and the addition of ionic surfactants is required *via* two different phenomena: capillary zone electrophoresis, when a new coated NP forms as the result of strong NP-micelle interactions; micellar electrokinetic chromatography (MEKC), when NPs-micelles remain in equilibrium due to the weak interactions between them [1.196]. CE is a fast separation technique that also offers a high separation efficacy and is able to

discriminate AgNPs from Ag(I). Nevertheless, its LOD is high if it is coupled with UV-Vis or fluorescence spectrometry detectors, and its robustness is low to complex matrices of real samples [1.148,1.155,1.196]. As a result of these limitations, very few studies have employed this technique for AgNPs determination in environmental and biological samples. For example, one work in the literature employs CE-ICPMS to analyse the species generated *via* the interaction of AgNPs with metallothionein (protein) in rat liver extracts [1.205].

1.2.2.6 Electrochemical techniques

Electrochemical techniques are based on measuring an electrical property in an electrochemical cell that contains the analyte, which provides information on the analyte's characteristics and concentration. Therefore, these techniques enable NPs to be detected, characterised and quantified [1.241]. Voltammetry of immobilized particles (VIP) has been reported to detect and quantify AgNPs in seawater [1.242]. This technique consists of submerging an electrode, which contains the analyte or is chemically modified to retain the analyte, in an electrochemical cell in which it is voltammetrically scanned. During the electrochemical process, the total amount of oxidised or reduced NPs allows quantitative information to be acquired, and the resulting potentials of the peaks in the voltammograms can be related directly to particle size [1.148]. Anodic particle coulometry (APC) consists of the NP's impact on the surface of a microelectrode held at a fixed anodic potential, where the NP is oxidised/reduced and, consequently, a signal is recorded on the chronoamperogram. From this technique, particle size can be determined from the charge involved in the process, which is related to the mass of the electroactive species. The particle number concentration can also be obtained from the frequency of collisions with the microelectrode [1.148,1.243]. For example, in the literature one study determines the AgNPs size distribution in seawater [1.244].

1.2.2.7 Chemical sensors

Chemical sensors are devices that measure a physical or chemical property of the analyte in solution because they contain a specifically recognised zone for the target specimen. The signal produced by this measurement is normally proportional to the concentration of the analyte [1.245]. The literature reports that ion selective electrode (ISE) for silver can be employed to assess Ag(I) speciation and the adsorption processes of AgNPs in soils, which enables to determine the fraction of AgNPs that maintain their nanoform or that are attached

to colloids or soil solids [1.173]. Another application of a chemically modified ISE (fluorous-phase ionophore-doped ISE) has been employed to examine the release of Ag(I) from AgNPs, which is considered one of the main contributors of AgNPs toxicity, in water and bacterial growth media [1.246]. Apart from ISEs, one study has used an SPR sensor based on human metallothionein to detect AgNPs in river water samples [1.174]. Despite these analytical tools being cheap, sensitive, simple and portable, their application to environmental and biological samples to detect AgNPs is still scarce because very few devices have been developed and tested in these type of samples [1.148].

1.3 Laboratory studies to assess the behaviour of AgNPs in the environment

1.3.1 Study of the adsorption, mobility and desorption of AgNPs in soil samples

Experimental procedures to understand the transport and retention of AgNPs in terrestrial systems are scarce because effective analytical tools to detect, extract, characterise and quantify nanosilver from soils are lacking [1.247]. The existing experimental approaches used on a laboratory scale to study these phenomena are column tests and batch tests. Column tests consist of putting an amount of soil inside a rigid impermeable block through which a solution containing the analyte is percolated [1.248]. Some studies in the literature have conducted column experiments with well-defined model porous media, such as quartz sands, glass beads or sandstones. However, the relevance of these studies is slight because they cannot represent the complexity of natural soils, such as their variable composition. Therefore, more recent studies have performed column experiments with real soils [1.249,1.250]. Batch tests are easier and faster to perform than column experiments. This type of experiment is based on adding a AgNPs solution with a known concentration to an amount of soil, and the resulting mixture is shaken for a time period until the steady-state condition is achieved [1.251]. Although NPs dispersions can be kinetically stable over a time period, they are thermodynamically unstable and, consequently, the equilibrium state is never reached. Therefore, the equilibrium partitioning coefficients used in column and batch experiments for dissolved species cannot be used for NPs. Notwithstanding, the literature shows that valuable information can still be obtained about NPs attachment/detachment kinetics with these tests by using, for example, particle attachment efficiency (α), which has been contemplated by some authors as the most appropriate fate descriptor of NPs in aggregation or deposition experiments [1.254,1.255].

Table 1.3 *Different reported extracting methods for studying AgNPs desorption from soils.*

Analyte	Experiment	Extraction	Operational definition and extractant	Conditions	Reference
$AgNO_3$ Citrate coated AgNPs (5 nm) Uncoated AgNPs (19 nm)	Soils spiked with analytes during a long period of time (2 h to 10 weeks)	1 sequential extraction	1. Water soluble: 20 mL of deionized water 2. Exchangeable: 20 mL of 1 M CH_3COONH_4 (pH 7) 3. Weak acid dissolution: 20 mL of 1 M CH_3COONH_4 (adjusted to pH 5 with CH_3COOH) 4. Easily reducible: 20 mL of 0.04 M $NH_2OH{\cdot}HCl$ in 25% *v/v* CH_3COOH (pH 3) 5. Oxidizable: 15 mL of 30% H_2O_2(adjusted to pH 2 with HNO_3) then 5 mL of 3.2 M CH_3COOH in 20% *v/v* HNO_3 6. Acid digestible: 20 mL of 7 M HNO_3 7. Residual: Total activity (F1+F2+F3+F4+F4+F5+F6)	1. 1 h at 20 °C 2. 2 h at 20 °C 3. 2 h at 20 °C 4. 6 h at 80 °C 5. 5.5 h at 80°C then 30 min at 20 °C 6. 6 h at 80 °C	[1.252]
AgNM-300K	Soils incubated with AgNPs during a long period of time (3 days and 92 days)	1 single extraction	a) Disodium dihydrogen ethylenediaminetetraacetate (EDTA)	a) 24 h shaken at room temperature	[1.250]
AgNPs 60nm and 100 nm	Soils spiked with analytes during 24h	4 different single extractions	a) 10 mL Milli-Q water b) 10 mL Milli-Q water c) 10 mL of a 10 mM sodium dodecyl sulphate d) Pre-wetting (900 µL Milli-Q water) and 2 extractions with Milli-Q water	a) Centrifugation (8 min, 1,000 rpm) b) Sonication (15 min) Vortex (10 min, 1,500 rpm) Settling (3 h) c) Similar to b) d) Pre-wetting (24 h) Extractions similar to b)	[1.253]

Apart from adsorption processes occurring in the environment (attachment to particle surfaces), NPs can also undergo from desorption processes (detachment from particle surfaces). Desorption of AgNPs has been studied much less than adsorption, as seen in ***Table 1.3***. Different extracting methods can be employed to study the mobility and bioavailability of these NPs in polluted soils. Among them, single and sequential extraction procedures are widely used to evaluate the mobility and availability of contaminants in soils or for the partitioning of trace elements in environmental samples [1.252,1.256]. These extraction procedures use chemical extractants (e.g. water, EDTA, *etc.*) to displace metals from the soil matrix. The selection of the extracting agent is important to preserve AgNPs integrity by taking into account that their stability depends on the medium [1.250,1.253]. Although different tools are available to assess the mobility and transport of AgNPs in soil, most published studies have used soil samples spiked with well-characterised NPs suspensions. Furthermore, validated analytical tools for AgNPs characterisation in the soil matrix are still scarce. Therefore, the development and validation of advanced analytical methodologies to assess the behaviour of AgNPs in environmental matrices are required [1.247].

1.3.2 Bioaccumulation and biotransformation of AgNPs in vegetal samples

Plants remain constantly in contact with air, soil and water. As stated in Section 1.1.2, AgNPs are present in all these environmental compartments. Therefore, plants continuously interact with NPs, which favours their accumulation. As plants are the basis of the food chain, these emerging contaminants can be transferred to animals by their feed and can, consequently, pose a risk for human health. For this reason, it is important to perform experiments with plants to understand the mechanisms involved in AgNPs accumulation and the toxic effects that they can exert on these living organisms. However, lack of proper analytical tools to analyse AgNPs in environmental samples makes these studies difficult to carry out.

Despite this constraint, many studies in the bibliography have demonstrated that AgNPs can accumulate and can be biotransformed in different plant species. Among the studied plants, we find crops (e.g. *Zea mays*, *Hordeum vulgare*, *Oryza sativa*, *Vicia faba*, *Cucurbita pepo*, *Brassica oleracea*, *Solanaceae*, *Allium cepa*, *Lactuca sativa*, *Cucumis savitus*, *Raphanus sativus*, *Pisum sativum*, *Capsicum annuum*), wetland plants (e.g. *Carex lurida*, *Panicum virgatum*, *Lolium multiflorum*, *Phytolacca Americana*, *Eupatorium fistolum*), aquatic plants (e.g. *Spirodela polyrhiza*) and terrestrial plants (e.g. *Trigonella foenum-graecum*) [1.257,1.258]. From these studies, information

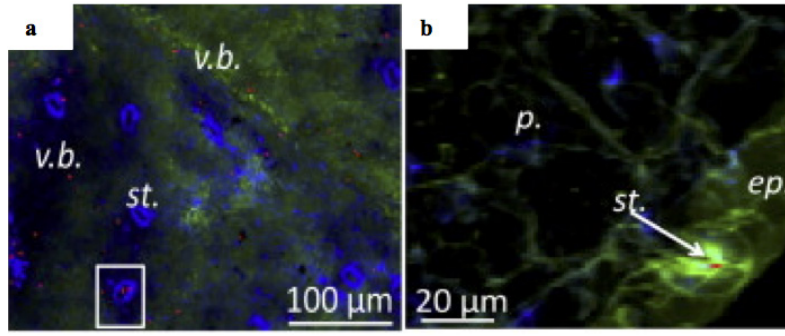

Fig. 1.10 *Elemental distribution lettuce leaves exposed to 100 µ g g^{-1} AgNPs analysed by µ-XRF being (**a**) plants cross sections and (**b**) plant surface. ep. epidermis, p. parenchyma, st. stomata, v.b. vascular bundle [Reprinted (adapted) from [1.220], Copyright (2019), with permission from Elsevier (or applicable society copyright owner)].*

about the accumulation and distribution of AgNPs in plant tissues can be obtained. For example, one study determines the distribution of AgNPs in lettuce shoots after foliar exposure (see ***Fig. 1.10***) [1.220]. Furthermore, the phytotoxicity, cytotoxicity and gentoxicicity of these emerging contaminants to plants can also be known (see ***Fig. 1.11***) [1.259].

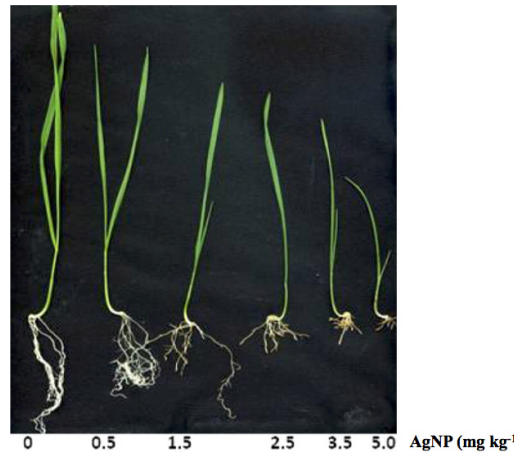

Fig. 1.11 *Growth shoots and roots response of wheat plants after being exposed 14 days to diferent AgNPs concentrations [Reprinted (adapted) from [1.258], Copyright (2019), American Chemical Society].*

However, running experiments with different plant species makes it difficult to generalise about the uptake mechanisms and distribution of the AgNPs inside plant tissues. To overcome this limitation, *Arabidopsis thaliana* has been used in many works as a model plant because of its short generation time, small size and excellent seed production, and because its genome sequence is known [1.257]. In the literature, different growing media have been employed to perform experiments, including hydroponic (e.g. Hoagland solution, Murashige and Skoog nutrient solution, *etc.*), soil, agar or sand [1.258]. In some studies, addition of fertilisers in soils is done [1.260] or nanosilver solution is sprayed instead of cultivating plants [1.220]. Seed germination

is normally carried out in Petri dishes [1.258]. Culture media composition can affect the uptake of AgNPs by plant roots, but growing conditions (e.g. temperature, humidity, concentration) and days of exposure to AgNPs also influence the final accumulation, biotransformation and toxicity of the studied plants. Therefore, as lots of variables can impact the evaluation of nanosilver risks for plants, it is necessary to make an effort to develop well-established protocols for assessing the nanotoxicity of these emerging pollutants to plants [1.257].

References

[1.1] P. Krystek, A. Ulrich, C.C. Garcia, S. Manohar, R. Ritsema, Application of plasma spectrometry for the analysis of engineered nanoparticles in suspensions and products, J. Anal. At. Spectrom. 26 (2011) 1701–1721.

[1.2] ISO/TS 80004-4:2011 Nanotechnologies vocabulary-part 4: nanostructured materials, International Organization for Standardization (ISO), Geneva, 2011.

[1.3] D.R. Boverhof, C.M. Bramante, J.H. Butala, S.F. Clancy, M. Lafranconi, J. West, *et al.*, Comparative assessment of nanomaterial definitions and safety evaluation considerations, Regul. Toxicol. Pharmacol. 73 (2015) 137–150.

[1.4] Opinion on the scientific basis for the definiton of the term "nanomaterial", Scientific Committee on Emerging and Newly Identified Health Risks (SCENIHR), Brussels, 2010.

[1.5] ICCA core elements of a regulatory definition of manufactured nanomaterials, International Council of Chemical Associations (ICCA), 2010.

[1.6] VCI position on the definition of the term "nanomaterial" for use in regulations laying down provisions on substances, German Chemical Industries Association (Verband der Chemischen Industrie), 2010.

[1.7] Report of the ICCR joint ad hoc working group on nanotechnology in cosmetic products: criteria and methods of detection, International Cooperation on Cosmetic Regulation (ICCR), Canada, 2010.

[1.8] Regulation (EU) 2017/745 of the European Parliament and of the Council of 5 April 2017 on medical devices, amending Directive 2001/83/EC, Regulation (EC) No 178/2002 and Regulation (EC) No 1223/2009 and repealing Council Directives 90/385/EEC and 93/42/EEC, Official Journal of the European Union, The European Parliament and the Council of the European Union, L117:1, Strasbourg, 2017.

[1.9] Regulation (EU) No 1169/2011 of the European Parliament and of the Council of 25 October 2011

on the provision of food information to consumers, amending Regulations (EC) No 1924/2006 and (EC) No 1925/2006 of the European Parliament and of the Council, and repealing Commission Directive 87/250/EEC, Council Directive 90/496/EEC, Commission Directive 1999/10/EC, Directive 2000/13/EC of the European Parliament and of the Council, Commission Directives 2002/67/EC and 2008/5/EC and Commission Regulation (EC) No 608/2004, Official Journal of the European Union, The European Parliament and the Council of the European Union, L304:18, Strasbourg, 2011.

[1.10] Regulation (EU) No 528/2012 of the European Parliament and of the Council of 22 May 2012 concerning the making available on the market and use of biocidal products, L167:1, Official Journal of the European Union, The European Parliament and the Council of the European Union, Strasbourg, 2012.

[1.11] Commission Delegated Regulation (EU) No 1363/2013 of 12 December 2013 amending Regulation (EU) No 1169/2011 of the European Parliament and of the Council on the provision of food information to consumers as regards the definition of "engineered nanomaterials", Official Journal of the European Union, The European Commission, L343/26, Brussels, 2013.

[1.12] Decree no. 2012-232 of February 2012 on the annual declaration on substances at nanoscale in application of article R. 523-4 of the environment code, Official Journal of the French Republic, Ministry of ecology, sustainable development, transport and housing, Text 4/44, 2012.

[1.13] Koninklijk besluit betreffende het op de markt brengen van stoffen geproduceerd in nanoparticulaire toestand op 27 Mei 2014, Federale overheidsdienst volksgezondheid veiligheid van de voedselketen en leefmilieu, Belgisch staatsbald, C-2014/24329:76184-76204, 2014.

[1.14] Bekendtgørelse om register over blandinger og varer, der indeholder nanomaterialer samt producenter og importørers indberetningspligt til registeret, Miljø-og Fødevareministeriet, Miljøstyrelsen, nr. 644, 2014.

[1.15] Safety data sheet (SDS): guidelines for synthetic nanomaterials, State Secretariat for Economic Affairs, Bern, 2016.

[1.16] Guidance for industry considering whether an FDA-regulated product involves the application of nanotechnology, U.S. Department of Helath and Human Services Food and Drug Administration of the Commissioner, FDA-2010-D-05302014, 2014..

[1.17] NICNAS working definition of industrial nanomaterial, Department of Helath, Australian Goverment. Available at: https://www.nicnas.gov.au/notify-your-chemical/data-requirements-for-new-chemical-notifications/data-requirements-for-notification-of-new-industrial-nanomaterials/

nicnas-working-definition-of-industrial-nanomaterial. Accesed: May 25, 2019.

[1.18] Policy statement on health canda's working definition for nanomaterial, Health Canada, Government of Canada. Available at: https://www.canada.ca/en/health-canada/services/science-research/reports-publications/nanomaterial/policy-statement-health-canada-working-definition.html. Accessed: May 25, 2019.

[1.19] Commission recommendation of 18 October 2011 on the definition of nanomaterial, Official Journal of the European Union, The European Comission, L275/38, Brussels, 2011.

[1.20] ISO/TS 80004-2:2015 Nanotechnologies vocabulary-part 2: nano-objects, International Organization for Standardization (ISO), Geneva, 2015.

[1.21] B. Pan, B. Xing, Applications and implications of manufactured nanoparticles in soils: a review, Eur. J. Soil Sci. 63 (2012) 437–456.

[1.22] J. Pulit-Prociak, M. Banach, Silver nanoparticles – a material of the future...?, Open Chem. 14 (2016) 76–91.

[1.23] V. Pareek, R. Gupta, J. Panwar, Do physico-chemical properties of silver nanoparticles decide their interaction with biological media and bactericidal action? A review, Mater. Sci. Eng. C 90 (2018) 739–749.

[1.24] T.C. Prathna, L. Mathew, N. Chandrasekaran, A.M. Raichur, A. Mukherjee, Biomimetic synthesis of nanoparticles: science, technology & applicability. In: Biomimetics learning from nature. London: Intech Open Access Publisher, 2010, pp. 1-20. Available at: https://www.intechopen.com/books/biomimetics-learning-from-nature/biomimetic-synthesis-of-nanoparticles-science-technology-amp-applicability. Accessed: April 3, 2019.

[1.25] T.M. Tolaymat, A.M. El Badawy, A. Genaidy, K.G. Scheckel, T.P. Luxton, M. Suidan, An evidence-based environmental perspective of manufactured silver nanoparticle in syntheses and applications: a systematic review and critical appraisal of peer-reviewed scientific papers, Sci. Total Environ. 408 (2010) 999–1006.

[1.26] A. López-Serrano, R.M. Olivas, J.S. Landaluze, C. Cámara, Nanoparticles: a global vision. Characterization, separation, and quantification methods. Potential environmental and health impact, Anal. Methods 6 (2014) 38–56.

[1.27] A.M. Ealias, M.P. Saravanakumar, A review on the classification, characterisation, synthesis of nanoparticles and their application, IOP Conf. Ser. Mater. Sci. Eng. 263 (2017) 032019.

[1.28] M. Sajid, M. Ilyas, C. Basheer, M. Tariq, M. Daud, N. Baig, *et al.*, Impact of nanoparticles on human

and environment: review of toxicity factors, exposures, control strategies, and future prospects, Environ. Sci. Pollut. Res. 22 (2015) 4122–4143.

[1.29] M.S. Mauter, M. Elimelech, Environmental applications of carbon-based nanomaterials, Environ. Sci. Technol. 42 (2008) 5843–5859.

[1.30] Y. Ju-Nam, J.R. Lead, Manufactured nanoparticles: an overview of their chemistry, interactions and potential environmental implications, Sci. Total Environ. 400 (2008) 396–414.

[1.31] T.Y. Olson, J.Z. Zhang, Structural and optical properties and emerging applications of metal nanomaterials, J. Mater. Sci. Technol. 24 (2008) 433–446.

[1.32] L. Escorihuela, B. Martorell, R. Rallo, A. Fernández, Toward computational and experimental characterisation for risk assessment of metal oxide nanoparticles, Environ. Sci. Nano 5 (2018) 2241–2251.

[1.33] P. Lai, W. Daear, R. Löbenberg, E.J. Prenner, Overview of the preparation of organic polymeric nanoparticles for drug delivery based on gelatine, chitosan, poly(D,L-lactide-co-glycolic acid) and polyalkylcyanoacrylate, Colloids Surf. B Biointerfaces 118 (2014) 154–163.

[1.34] P. Pramod, K.G. Thomas, M.V. George, Organic nanomaterials: morphological control for charge stabilization and charge transport, Chem. Asian J. 4 (2009) 806–823.

[1.35] A. Valizadeh, H. Mikaeili, M. Samiei, S.M. Farkhani, N. Zarghami, M. Kouhi, *et al.*, Quantum dots: synthesis, bioapplications, and toxicity, Nanoscale Res. Lett. 7 (2012) 480.

[1.36] V.G. Reshma, P.V. Mohanan, Quantum dots: applications and safety consequences, J. Lumin. 205 (2019) 287–298.

[1.37] D. Vasudevan, R.R. Gaddam, A. Trinchi, I. Cole, Core-shell quantum dots: properties and applications, J. Alloys Compd. 636 (2015) 395–404.

[1.38] R. Das, R. Bandyopadhyay, P. Pramanik, Carbon quantum dots from natural resource: a review, Mater. Today Chem. 8 (2018) 96–109.

[1.39] D. Rejeski, D. Lekas, Nanotechnology field observations: scouting the new industrial west, J. Clean. Prod. 16 (2008) 1014–1017.

[1.40] M.E. Vance, T. Kuiken, E.P. Vejerano, S.P. McGinnis, M.F. Hochella, D. Rejeski, *et al.*, Nanotechnology in the real world: redeveloping the nanomaterial consumer products inventory, Beilstein J. Nanotechnol. 6 (2015) 1769–1780.

[1.41] E. Inshakova, O. Inshakov, World market for nanomaterials: structure and trends, MATEC Web Conf. 129 (2017) 02013.

[1.42] S.-J. Yu, Y.-G. Yin, J.-F. Liu, Silver nanoparticles in the environment, Environ. Sci.: Processes Impacts 15 (2013) 78–92.

[1.43] M. Guzman, J. Dille, S. Godet, Synthesis and antibacterial activity of silver nanoparticles against gram-positive and gram-negative bacteria, Nanomedicine: NBM 8 (2012) 37–45.

[1.44] Y.-K. Jo, B.H. Kim, G. Jung, Antifungal activity of silver ions and nanoparticles on phytopathogenic fungi, Plant Dis. 93 (2009) 1037–1043.

[1.45] L. Lu, R.W.-Y. Sun, R. Chen, C.-K. Hui, C.-M. Ho, J.M. Luk, *et al.*, Silver nanoparticles inhibit hepatitis B virus replication, Antivir. Ther. 13 (2008) 253–262.

[1.46] N.A. Anjum, S.S. Gill, A.C. Duarte, E. Pereira, I. Ahmad, Silver nanoparticles in soil–plant systems, J. Nanopart. Res. 15 (2013) 1896.

[1.47] F. Piccinno, F. Gottschalk, S. Seeger, B. Nowack, Industrial production quantities and uses of ten engineered nanomaterials in Europe and the world, J. Nanopart. Res. 14 (2012) 1109.

[1.48] A.A. Keller, S. McFerran, A. Lazareva, S. Suh, Global life cycle releases of engineered nanomaterials, J. Nanopart. Res. 15 (2013) 1692.

[1.49] The Nanodatabase. Available at: http://nanodb.dk. Accessed: April 3, 2019.

[1.50] The Project on Emerging Nanotechnologies: consumer products inventory, Available at: http://www.nanotechproject.org/cpi/products. Accessed: April 3, 2019.

[1.51] S. Wagner, A. Gondikas, E. Neubauer, T. Hofmann, F. von der Kammer, Spot the difference: engineered and natural nanoparticles in the environment-release, behavior, and fate, Angew. Chemie - Int. Ed. 53 (2014) 12398–12419.

[1.52] A. Caballero-Guzman, B. Nowack, A critical review of engineered nanomaterial release data: are current data useful for material flow modeling?, Environ. Pollut. 213 (2016) 502–517.

[1.53] T.M. Benn, P. Westerhoff, Nanoparticle silver released into water from commercially available sock fabrics, Environ. Sci. Technol. 42 (2008) 4133–4139.

[1.54] T. Benn, B. Cavanagh, K. Hristovski, J.D. Posner, P. Westerhoff, The release of nanosilver from consumer products used in the home, J. Environ. Qual. 39 (2010) 1875–1882.

[1.55] L. Geranio, M. Heuberger, B. Nowack, The behavior of silver nanotextiles during washing, Environ. Sci. Technol. 43 (2009) 8113–8118.

[1.56] D.M. Mitrano, E. Rimmele, A. Wichser, R. Erni, M. Height, B. Nowack, Presence of nanoparticles in wash water from conventional silver and nano-silver textiles, ACS Nano 8 (2014) 7208–7219.

[1.57] K. Kulthong, S. Srisung, K. Boonpavanitchakul, W. Kangwansupamonkon, R. Maniratanachote,

Determination of silver nanoparticle release from antibacterial fabrics into artificial sweat, Part. Fibre Toxicol. 7 (2010) 8.

[1.58] G. Artiaga, K. Ramos, L. Ramos, C. Cámara, M. Gómez-Gómez, Migration and characterisation of nanosilver from food containers by AF4-ICP-MS, Food Chem. 166 (2015) 76–85.

[1.59] Y. Echegoyen, C. Nerín, Nanoparticle release from nano-silver antimicrobial food containers, Food Chem. Toxicol. 62 (2013) 16–22.

[1.60] M. Cushen, J. Kerry, M. Morris, M. Cruz-Romero, E. Cummins, Migration and exposure assessment of silver from a PVC nanocomposite, Food Chem. 139 (2013) 389–397.

[1.61] E.M. Sussman, P. Jayanti, B.J. Dair, B.J. Casey, Assessment of total silver and silver nanoparticle extraction from medical devices, Food Chem. Toxicol. 85 (2015) 10–19.

[1.62] R. Kaegi, B. Sinnet, S. Zuleeg, H. Hagendorfer, E. Mueller, R. Vonbank, *et al.*, Release of silver nanoparticles from outdoor facades, Environ. Pollut. 158 (2010) 2900–2905.

[1.63] C. Lorenz, L. Windler, N. von Goetz, R.P. Lehmann, M. Schuppler, K. Hungerbühler, *et al.*, Characterization of silver release from commercially available functional (nano)textiles, Chemosphere 89 (2012) 817–824.

[1.64] A. Mackevica, M.E. Olsson, S.F. Hansen, The release of silver nanoparticles from commercial toothbrushes, J. Hazard. Mater. 322 (2017) 270–275.

[1.65] B. Nowack, J.F. Ranville, S. Diamond, J.A. Gallego-Urrea, C. Metcalfe, J. Rose, *et al.*, Potential scenarios for nanomaterial release and subsequent alteration in the environment, Environ. Toxicol. Chem. 31 (2012) 50–59.

[1.66] R. Kaegi, A. Voegelin, C. Ort, B. Sinnet, B. Thalmann, J. Krismer, *et al.*, Fate and transformation of silver nanoparticles in urban wastewater systems, Water Res. 47 (2013) 3866–3877.

[1.67] L. Li, G. Hartmann, M. Döblinger, M. Schuster, Quantification of nanoscale silver particles removal and release from municipal wastewater treatment plants in Germany, Environ. Sci. Technol. 47 (2013) 7317–7323.

[1.68] A.C. Johnson, M.D. Jürgens, A.J. Lawlor, I. Cisowska, R.J. Williams, Particulate and colloidal silver in sewage effluent and sludge discharged from British wastewater treatment plants, Chemosphere 112 (2014) 49–55.

[1.69] R. Kaegi, A. Voegelin, B. Sinnet, S. Zuleeg, H. Hagendorfer, M. Burkhardt, *et al.*, Behavior of metallic silver nanoparticles in a pilot wastewater treatment plant, Environ. Sci. Technol. 45 (2011) 3902–3908.

[1.70] B. Kim, C.-S. Park, M. Murayama, M.F. Hochella, Discovery and characterization of silver sulfide nanoparticles in final sewage sludge products, Environ. Sci. Technol. 44 (2010) 7509–7514.

[1.71] M. Kah, T. Hofmann, Nanopesticide research: current trends and future priorities, Environ. Int. 63 (2014) 224–235.

[1.72] I. Gehrke, A. Geiser, A. Somborn-Schulz, Innovations in nanotechnology for water treatment, Nanotechnol. Sci. Appl. 8 (2015) 1–17.

[1.73] B. Nowack, Evaluation of environmental exposure models for engineered nanomaterials in a regulatory context, NanoImpact 8 (2017) 38–47.

[1.74] S.A. Blaser, M. Scheringer, M. MacLeod, K. Hungerbühler, Estimation of cumulative aquatic exposure and risk due to silver: contribution of nano-functionalized plastics and textiles, Sci. Total Environ. 390 (2008) 396–409.

[1.75] N. Akaighe, R.I. MacCuspie, D.A. Navarro, D.S. Aga, S. Banerjee, M. Sohn, *et al.*, Humic acid-induced silver nanoparticle formation under environmentally relevant conditions, Environ. Sci. Technol. 45 (2011) 3895–3901.

[1.76] N.F. Adegboyega, V.K. Sharma, K. Siskova, R. Zbořil, M. Sohn, B.J. Schultz, *et al.*, Interactions of aqueous Ag+ with fulvic acids: mechanisms of silver nanoparticle formation and investigation of stability, Environ. Sci. Technol. 47 (2013) 757–764.

[1.77] N.F. Adegboyega, V.K. Sharma, K.M. Siskova, R. Vecerova, M. Kolar, R. Zbořil, *et al.*, Enhanced formation of silver nanoparticles in Ag+-NOM-Iron(II, III) systems and antibacterial activity studies, Environ. Sci. Technol. 48 (2014) 3228–3235.

[1.78] A. Wimmer, A. Kalinnik, M. Schuster, New insights into the formation of silver-based nanoparticles under natural and semi-natural conditions, Water Res. 141 (2018) 227–234.

[1.79] Y. Yin, M. Shen, X. Zhou, S. Yu, J. Chao, J. Liu, *et al.*, Photoreduction and stabilization capability of molecular weight fractionated natural organic matter in transformation of silver ion to metallic nanoparticle, Environ. Sci. Technol. 48 (2014) 9366–9373.

[1.80] R.D. Glover, J.M. Miller, J.E. Hutchison, Generation of metal nanoparticles from silver and copper objects: nanoparticle dynamics on surfaces and potential sources of nanoparticles in the environment, ACS Nano 5 (2011) 8950–8957.

[1.81] L. Marchiol, A. Mattiello, F. Pošćić, C. Giordano, R. Musetti, *In vivo* synthesis of nanomaterials in plants: location of silver nanoparticles and plant metabolism, Nanoscale Res. Lett. 9 (2014) 101.

[1.82] F. Gottschalk, T. Sonderer, R.W. Scholz, B. Nowack, Modeled environmental concentrations of

engineered nanomaterials (TiO_2, ZnO, Ag, CNT, Fullerenes) for different regions, Environ. Sci. Technol. 43 (2009) 9216–9222.

[1.83] T.Y. Sun, F. Gottschalk, K. Hungerbühler, B. Nowack, Comprehensive probabilistic modelling of environmental emissions of engineered nanomaterials, Environ. Pollut. 185 (2014) 69–76.

[1.84] T.Y. Sun, N.A. Bornhöft, K. Hungerbühler, B. Nowack, Dynamic probabilistic modeling of environmental emissions of engineered nanomaterials, Environ. Sci. Technol. 50 (2016) 4701–4711.

[1.85] J. Fabrega, S.N. Luoma, C.R. Tyler, T.S. Galloway, J.R. Lead, Silver nanoparticles: behaviour and effects in the aquatic environment, Environ. Int. 37 (2011) 517–531.

[1.86] K.L. Garner, A.A. Keller, Emerging patterns for engineered nanomaterials in the environment: a review of fate and toxicity studies, J. Nanopart. Res. 16 (2014) 2503.

[1.87] I. Fernando, Y. Zhou, Impact of pH on the stability, dissolution and aggregation kinetics of silver nanoparticles, Chemosphere 216 (2019) 297–305.

[1.88] K. Afshinnia, B. Marrone, M. Baalousha, Potential impact of natural organic ligands on the colloidal stability of silver nanoparticles, Sci. Total Environ. 625 (2018) 1518–1526.

[1.89] D. Shevlin, N. O'Brien, E. Cummins, Silver engineered nanoparticles in freshwater systems – likely fate and behaviour through natural attenuation processes, Sci. Total Environ. 621 (2018) 1033–1046.

[1.90] M.E. Quadros, L.C. Marr, Environmental and human health risks of aerosolized silver nanoparticles, J. Air Waste Manag. Assoc. 60 (2010) 770–781.

[1.91] P. Kumar, M. Ketzel, S. Vardoulakis, L. Pirjola, R. Britter, Dynamics and dispersion modelling of nanoparticles from road traffic in the urban atmospheric environment-a review, J. Aerosol Sci. 42 (2011) 580–603.

[1.92] A.J. Tiwari, L.C. Marr, The role of atmospheric transformations in determining environmental impacts of carbonaceous nanoparticles, J. Environ. Qual. 39 (2010) 1883–1895.

[1.93] S.V. Sokolov, K. Tschulik, C. Batchelor-McAuley, K. Jurkschat, R.G. Compton, Reversible or not? Distinguishing agglomeration and aggregation at the nanoscale, Anal. Chem. 87 (2015) 10033–10039.

[1.94] B.J. Majestic, G.B. Erdakos, M. Lewandowski, K.D. Oliver, R.D. Willis, T.E. Kleindienst, *et al.*, A review of selected engineered nanoparticles in the atmosphere: sources, transformations, and techniques for sampling and analysis, Int. J. Occup. Environ. Health 16 (2010) 488–507.

[1.95] P. Kumar, A. Robins, S. Vardoulakis, R. Britter, A review of the characteristics of nanoparticles in the urban atmosphere and the prospects for developing regulatory controls, Atmos. Environ. 44 (2010) 5035–5052.

[1.96] P. Christian, F. Von der Kammer, M. Baalousha, Th. Hofmann, Nanoparticles: structure, properties, preparation and behaviour in environmental media, Ecotoxicology 17 (2008) 326–343.

[1.97] Tech Note: zeta/pH curves and isoelectric point data for standard nanocomposix silver citrate and PVP nanoparticle dispersions, (2012). Available at: https://cdn.shopify.com/s/files/1/0257/8237/files/Tech_Note_-_Zeta_and_pH_Curves_for_nanoComposix_Citrate_and_PVP_Capped_Silver_Nanoparticles.pdf. Accessed: August 18, 2017.

[1.98] S.L. Chinnapongse, R.I. MacCuspie, V.A. Hackley, Persistence of singly dispersed silver nanoparticles in natural freshwaters, synthetic seawater, and simulated estuarine waters, Sci. Total Environ. 409 (2011) 2443–2450.

[1.99] I. Römer, T.A. White, M. Baalousha, K. Chipman, M.R. Viant, J.R. Lead, Aggregation and dispersion of silver nanoparticles in exposure media for aquatic toxicity tests, J. Chromatogr. A 1218 (2011) 4226–4233.

[1.100] P.S. Tourinho, C.A.M. van Gestel, S. Lofts, C. Svendsen, A.M.V.M. Soares, S. Loureiro, Metal-based nanoparticles in soil: fate, behavior, and effects on soil invertebrates, Environ. Toxicol. Chem. 31 (2012) 1679–1692.

[1.101] C. Levard, E.M. Hotze, G.V. Lowry, G.E. Brown Jr., Environmental transformations of silver nanoparticles: impact on stability and toxicity, Environ. Sci. Technol. 46 (2012) 6900–6914.

[1.102] G.E. Schaumann, A. Philippe, M. Bundschuh, G. Metreveli, S. Klitzke, D. Rakcheev, *et al.*, Understanding the fate and biological effects of Ag- and TiO2-nanoparticles in the environment: the quest for advanced analytics and interdisciplinary concepts, Sci. Total Environ. 535 (2015) 3–19.

[1.103] S.J. Klaine, P.J.J. Alvarez, G.E. Batley, T.F. Fernandes, R.D. Handy, D.Y. Lyon, *et al.*, Nanomaterials in the environment: behaviour, fate, bioavailability, and effects, Environ. Toxicol. Chem. 27 (2008) 1825–1851.

[1.104] W. Zhang, B. Xiao, T. Fang, Chemical transformation of silver nanoparticles in aquatic environments: mechanism, morphology and toxicity, Chemosphere 191 (2018) 324–334.

[1.105] J.R. Peralta-Videa, L. Zhao, M.L. Lopez-Moreno, G. de la Rosa, J. Hong, J.L. Gardea-Torresdey, Nanomaterials and the environment: a review for the biennium 2008–2010, J. Hazard. Mater. 186 (2011) 1–15.

[1.106] V.L. Pachapur, A.D. Larios, M. Cledón, S.K. Brar, M. Verma, R.Y. Surampalli, Behavior and characterization of titanium dioxide and silver nanoparticles in soils, Sci. Total Environ. 563–564 (2016) 933–943.

[1.107] I. Dror, B. Yaron, B. Berkowitz, Abiotic soil changes induced by engineered nanomaterials: a critical review, J. Contam. Hydrol. 181 (2015) 3–16.

[1.108] S.J. Cameron, F. Hosseinian, W.G. Willmore, A current overview of the biological and cellular effects of nanosilver, Int. J. Mol. Sci. 19 (2018) 2030.

[1.109] C. Schultz, K. Powell, A. Crossley, K. Jurkschat, P. Kille, A.J. Morgan, *et al.*, Analytical approaches to support current understanding of exposure, uptake and distributions of engineered nanoparticles by aquatic and terrestrial organisms, Ecotoxicology 24 (2015) 239–261.

[1.110] K.B.R. Ahmed, A.M. Nagy, R.P. Brown, Q. Zhang, S.G. Malghan, P.L. Goering, Silver nanoparticles: significance of physicochemical properties and assay interference on the interpretation of *in vitro* cytotoxicity studies, Toxicol. in Vitro 38 (2017) 179–192.

[1.111] Z. Wang, T. Xia, S. Liu, Mechanisms of nanosilver-induced toxicological effects: more attention should be paid to its sublethal effects, Nanoscale 7 (2015) 7470–7481.

[1.112] J. Du, J. Tang, S. Xu, J. Ge, Y. Dong, H. Li, *et al.*, A review on silver nanoparticles-induced ecotoxicity and the underlying toxicity mechanisms, Regul. Toxicol. Pharmacol. 98 (2018) 231–239.

[1.113] T.A.J. de Souza, L.R.R. Souza, L.P. Franchi, Silver nanoparticles: an integrated view of green synthesis methods, transformation in the environment, and toxicity, Ecotoxicol. Environ. Saf. 171 (2019) 691–700.

[1.114] J. Zhang, W. Guo, Q. Li, Z. Wang, S. Liu, The effects and the potential mechanism of environmental transformation of metal nanoparticles on their toxicity in organisms, Environ. Sci. Nano 5 (2018) 2482–2499.

[1.115] M. Akter, T. Sikder, M. Rahman, A.K.M.A. Ullah, K.F.B. Hossain, S. Banik, *et al.*, A systematic review on silver nanoparticles-induced cytotoxicity: physicochemical properties and perspectives, J. Adv. Res. 9 (2018) 1–16.

[1.116] L.L. Maurer, J.N. Meyer, A systematic review of evidence for silver nanoparticle-induced mitochondrial toxicity, Environ. Sci. Nano 3 (2016) 311–322.

[1.117] M. Matzke, K. Jurkschat, T. Backhaus, Toxicity of differently sized and coated silver nanoparticles to the bacterium *Pseudomonas putida*: risks for the aquatic environment?, Ecotoxicology 23 (2014) 818–829.

[1.118] S. Pal, Y.K. Tak, J.M. Song, Does the antibacterial activity of silver nanoparticles depend on the shape of the nanoparticle? A study of the Gram-Negative bacterium *Escherichia coli*, Appl. Environ. Microbiol. 73 (2007) 1712–1720.

[1.119] A.-J. Miao, K.A. Schwehr, C. Xu, S.-J. Zhang, Z. Luo, A. Quigg, *et al.*, The algal toxicity of silver engineered nanoparticles and detoxification by exopolymeric substances, Environ. Pollut. 157 (2009) 3034–3041.

[1.120] S. Asghari, S.A. Johari, J.H. Lee, Y.S. Kim, Y.B. Jeon, H.J. Choi, *et al.*, Toxicity of various silver nanoparticles compared to silver ions in *Daphnia magna*, J. Nanobiotechnol. 10 (2012) 14.

[1.121] H.C. Poynton, J.M. Lazorchak, C.A. Impellitteri, B.J. Blalock, K. Rogers, H.J. Allen, *et al.*, Toxicogenomic responses of nanotoxicity in *Daphnia magna* exposed to silver nitrate and coated silver nanoparticles, Environ. Sci. Technol. 46 (2012) 6288–6296.

[1.122] Y. Wu, Q. Zhou, H. Li, W. Liu, T. Wang, G. Jiang, Effects of silver nanoparticles on the development and histopathology biomarkers of Japanese medaka (*Oryzias latipes*) using the partial-life test, Aquat. Toxicol. 100 (2010) 160–167.

[1.123] A.H. Jesmer, J.R. Velicogna, D.M. Schwertfeger, R.P. Scroggins, J.I. Princz, The toxicity of silver to soil organisms exposed to silver nanoparticles and silver nitrate in biosolids-amended field soil, Environ. Toxicol. Chem. 36 (2017) 2756–2765.

[1.124] J. Pulit-Prociak, K. Stokłosa, M. Banach, Nanosilver products and toxicity, Environ. Chem. Lett. 13 (2015) 59–68.

[1.125] J.H. Sung, J.H. Ji, J.U. Yoon, D.S. Kim, M.Y. Song, J. Jeong, *et al.*, Lung function changes in Sprague-Dawley rats after prolonged inhalation exposure to silver nanoparticles, Inhal. Toxicol. 20 (2008) 567–574.

[1.126] M.K. Koohi, M. Hejazy, F. Asadi, P. Asadian, Assessment of dermal exposure and histopathologic changes of different sized nano-silver in healthy adult rabbits, J. Phys. Conf. Ser. 304 (2011) 012028.

[1.127] A. Loghman, S.H. Iraj, D.A. Naghy, M. Pejman, Histopathologic and apoptotic effect of nanosilver in liver of broiler chickens, African J. Biotechnol. 11 (2012) 6207–6211.

[1.128] P.M.G. Nair, I.M. Chung, Assessment of silver nanoparticle-induced physiological and molecular changes in *Arabidopsis thaliana*, Environ. Sci. Pollut. Res. 21 (2014) 8858–8869.

[1.129] H. Qian, X. Peng, X. Han, J. Ren, L. Sun, Z. Fu, Comparison of the toxicity of silver nanoparticles and silver ions on the growth of terrestrial plant model *Arabidopsis thaliana*, J. Environ. Sci. 25 (2013) 1947–1956.

[1.130] R. Kaveh, Y.-S. Li, S. Ranjbar, R. Tehrani, C.L. Brueck, B. Van Aken, Changes in *Arabidopsis thaliana* gene expression in response to silver nanoparticles and silver ions, Environ. Sci. Technol. 47 (2013) 10637–10644.

[1.131] E. Fröhlich, E. Roblegg, Oral uptake of nanoparticles: human relevance and the role of in vitro systems, Arch. Toxicol. 90 (2016) 2297–2314.

[1.132] M.E.K. Kraeling, V.D. Topping, Z.M. Keltner, K.R. Belgrave, K.D. Bailey, X. Gao, *et al.*, *In vitro* percutaneous penetration of silver nanoparticles in pig and human skin, Regul. Toxicol. Pharmacol. 95 (2018) 314–322.

[1.133] K. Soto, K.M. Garza, L.E. Murr, Cytotoxic effects of aggregated nanomaterials, Acta Biomater. 3 (2007) 351–358.

[1.134] S. Park, Y.K. Lee, M. Jung, K.H. Kim, N. Chung, E.-K. Ahn, *et al.*, Cellular toxicity of various inhalable metal nanoparticles on human alveolar epithelial cells, Inhal. Toxicol. 19 (2007) 59–65.

[1.135] S. Gaillet, J.-M. Rouanet, Silver nanoparticles: their potential toxic effects after oral exposure and underlying mechanisms –a review, Food Chem. Toxicol. 77 (2015) 58–63.

[1.136] H. Bouwmeester, J. Poortman, R.J. Peters, E. Wijma, E. Kramer, S. Makama, *et al.*, Characterization of translocation of silver nanoparticles and effects on whole-genome gene expression using an *in vitro* intestinal epithelium coculture model, ACS Nano 5 (2011) 4091–4103.

[1.137] Review of environmental legislation for the regulatory of nanomaterials, Milieu Environmental Law&Policy and AMEC Environment&Infrastructure UK, 2011.

[1.138] S. Sauvé, M. Desrosiers, A review of what is an emerging contaminant, Chem. Cent. J. 8 (2014) 15.

[1.139] V. Amenta, K. Aschberger, M. Arena, H. Bouwmeester, F.B. Moniz, P. Brandhoff, *et al.*, Regulatory aspects of nanotechnology in the agri/feed/food sector in EU and non-EU countries, Regul. Toxicol. Pharmacol. 73 (2015) 463–476.

[1.140] Communication from the Comission to the European Parliment, the Council and the European Economic and Social Commite: Second Regulatory Review on Nanomaterials, European Comission, Brussels, 2012.

[1.141] H. Rauscher, K. Rasmussen, B. Sokull-Klüttgen, Regulatory aspects of nanomaterials in the EU, Chemie Ing. Tech. 89 (2017) 224–231.

[1.142] Commission Regulation (EU) 2018/1881 of 3 December 2018 amending Regulation (EC) No 1907/2006 of the European Parliament and of the Council on the Registration, Evaluation, Authorisation and Restriction of Chemicals (REACH) as regards Annexes I, III, VI, VII, VIII, IX, X, XI, and XII to address nanoforms of substances, Official Journal of the European Commision, The European Commission, L 308:1, Brussels, 2018.

[1.143] Regulation (EC) No 1223/2009 of the European Parliament and of the council of 30 November 2009 on cosmetic products, Official Journal of the European Commission, The European Parliment and the Council of the European Union, L342:59, Brussels, 2009.

[1.144] Regulation (EU) 2015/2283 of the European Parliament and the of the council of 25 November 2015 on novel foods, amending Regulation (EU) No 1169/2011 of the European Parliament and of the Council and repealing Regulation (EC) No 258/97 of the European Parliament and of the Council and Commission Regulation (EC) No 1852/2001, Official Journal of the European Union, The European Parliment and the Council of the European Union, L327:1, Strasbourg, 2015.

[1.145] Regulation (EC) No 1333/2008 of the European Parliment and of the Council of 16 December 2008 on food additives, Official Journal of the European Union, The European Parliment and the Council of the European Union, L354:16, Strasbourg, 2008.

[1.146] Comission Regulation (EC) No 450/2009 of 29 May 2009 on active and intelligent materials and articles intended to come into contact with food, Official Journal of the European Union, The Comission of the European Communities, L135:3, Brussels, 2009.

[1.147] Comission Regulation (EC) No 10/2011 of January 2011 on plastic materials and articles intended to come into contact with food, Official Journal of the European Union, The European Comission, L12:1, Brussels, 2011.

[1.148] F. Laborda, E. Bolea, G. Cepriá, M.T. Gómez, M.S. Jiménez, J. Pérez-Arantegui, *et al.*, Detection, characterization and quantification of inorganic engineered nanomaterials: a review of techniques and methodological approaches for the analysis of complex samples, Anal. Chim. Acta. 904 (2016) 10–32.

[1.149] M. Farré, J. Sanchís, D. Barceló, Analysis and assessment of the occurrence, the fate and the behavior of nanomaterials in the environment, Trends Anal. Chem. 30 (2011) 517–527.

[1.150] G. Hartmann, T. Baumgartner, M. Schuster, Influence of particle coating and matrix constituents on the cloud point extraction efficiency of silver nanoparticles (Ag-NPs) and application for monitoring the formation of Ag-NPs from Ag^+, Anal. Chem. 86 (2014) 790–796.

[1.151] I. De la Calle, M. Menta, F. Séby, Current trends and challenges in sample preparation for metallic nanoparticles analysis in daily products and environmental samples: a review, Spectrochim. Acta - Part B At. Spectrosc. 125 (2016) 66–96.

[1.152] F.A. Monikh, L. Chupani, M.G. Vijver, M. Vancová, W.J.G.M. Peijnenburg, Analytical approaches for characterizing and quantifying engineered nanoparticles in biological matrices from an (eco)

toxicological perspective: old challenges, new methods and techniques, Sci. Total Environ. 660 (2019) 1283–1293.

[1.153] Z. Gajdosechova, Z. Mester, Recent trends in analysis of nanoparticles in biological matrices, Anal. Bioanal. Chem. 411 (2019) 4277-4292.

[1.154] E.C.T. Yeung, C. Stasolla, M.J. Sumner, B.Q. Huang, Plant microtechniques and protocols, Springer International, pp. 23-43, 2015.

[1.155] S.M. Majedi, H.K. Lee, Recent advances in the separation and quantification of metallic nanoparticles and ions in the environment, Trends Anal. Chem. 75 (2016) 183–196.

[1.156] I. Hagarová, Separation and quantification of metallic nanoparticles using cloud point extraction and spectrometric methods: a brief review of latest applications, Anal. Methods 9 (2017) 3594–3601.

[1.157] C. Kole, D.S. Kumar, M. V. Khodakovskaya, Plant nanotechnology: principles and practices, Springer International, Switzerland, 2016.

[1.158] J. Geisler-Lee, M. Brooks, J.R. Gerfen, Q. Wang, C. Fotis, A. Sparer, *et al.*, Reproductive toxicity and life history study of silver nanoparticle effect, uptake and transport in *Arabidopsis thaliana*, Nanomaterials 4 (2014) 301–318.

[1.159] J. Geisler-Lee, Q. Wang, Y. Yao, W. Zhang, M. Geisler, K. Li, *et al.*, Phytotoxicity, accumulation and transport of silver nanoparticles by *Arabidopsis thaliana*, Nanotoxicology 7 (2013) 323–337.

[1.160] F. Adams, C. Barbante, Chemical imaging analysis, Volume 69, 1st edition, Elsevier, Netherlands, 2015.

[1.161] S. Bandyopadhyay, J.R. Peralta-Videa, J.A. Hernandez-Viezcas, M.O. Montes, A.A. Keller, J.L. Gardea-Torresdey, Microscopic and spectroscopic methods applied to the measurements of nanoparticles in the environment, Appl. Spectrosc. Rev. 47 (2012) 180–206.

[1.162] M. Hassellöv, J.W. Readman, J.F. Ranville, K. Tiede, Nanoparticle analysis and characterization methodologies in environmental risk assessment of engineered nanoparticles, Ecotoxicology 17 (2008) 344–361.

[1.163] K. Tiede, A.B.A. Boxall, S.P. Tear, J. Lewis, H. David, M. Hassellöv, Detection and characterization of engineered nanoparticles in food and the environment, Food Addit. Contam. Part A Chem. Anal. Control. Expo. Risk Assess. 25 (2008) 795–821.

[1.164] F. Part, G. Zecha, T. Causon, E.-K. Sinner, M. Huber-Humer, Current limitations and challenges in nanowaste detection, characterisation and monitoring, Waste Manag. 43 (2015) 407–420.

[1.165] P. Worsfold, C. Poole, A. Townshend, M. Miró , Encyclopedia of analytical science, 3rd edition,

Elsevier, Netherlands, 2019.

[1.166] R. Klockenkämper, Total-reflection X-ray fluorescence analysis, Wiley&Sons, United States of America, 1996.

[1.167] H. Guo, L. He, B. Xing, Applications of surface-enhanced Raman spectroscopy in the analysis of nanoparticles in the environment, Environ. Sci. Nano 4 (2017) 2093–2107.

[1.168] P. Ducheyne, K.E. Healy, D.W. Hutmacher, D.W. Grainger, C.J. Kirkpatrick, Comprehensive biomaterials II: metallic, ceramic and polymeric biomaterials, Elsevier, Netherlands, 2017.

[1.169] E. Tomaszewska, K. Soliwoda, K. Kadziola, B. Tkacz-Szczesna, G. Celichowski, M. Cichomski, *et al.*, Detection limits of DLS and UV-Vis spectroscopy in characterization of polydisperse nanoparticles colloids, J. Nanomaterials, 2013(2013)1-10.

[1.170] P. Lodeiro, E.P. Achterberg, M.S. El-Shahawi, Detection of silver nanoparticles in seawater at ppb levels using UV-Visible spectrophotometry with long path cells, Talanta 164 (2017) 257–260.

[1.171] R. Sekine, K.L. Moore, M. Matzke, P. Vallotton, H. Jiang, G.M. Hughes, *et al.*, Complementary imaging of silver nanoparticle interactions with green algae: dark-field microscopy, electron microscopy, and nanoscale secondary ion mass spectrometry, ACS Nano 11 (2017) 10894–10902.

[1.172] J. Soto-Alvaredo, M. Montes-Bayón, J. Bettmer, Speciation of silver nanoparticles and silver(I) by reversed-phase liquid chromatography coupled to ICPMS, Anal. Chem. 85 (2013) 1316–1321.

[1.173] R. Benoit, K.J. Wilkinson, S. Sauvé, Partitioning of silver and chemical speciation of free Ag in soils amended with nanoparticles, Chem. Cent. J. 7 (2013) 75.

[1.174] S.R. Raz, M. Leontaridou, M.G.E.G. Bremer, R. Peters, S. Weigel, Development of surface plasmon resonance-based sensor for detection of silver nanoparticles in food and the environment, Anal. Bioanal. Chem. 403 (2012) 2843–2850.

[1.175] K.D. Vernon-Parry, Scanning electron microscopy: an introduction, III-Vs Rev. 13 (2000) 40–44.

[1.176] K. Tiede, A.B.A. Boxall, X. Wang, D. Gore, D. Tiede, M. Baxter, *et al.*, Application of hydrodynamic chromatography-ICP-MS to investigate the fate of silver nanoparticles in activated sludge, J. Anal. At. Spectrom. 25 (2010) 1149–1154.

[1.177] S. Wang, J. Lv, J. Ma, S. Zhang, Cellular internalization and intracellular biotransformation of silver nanoparticles in *Chlamydomonas reinhardtii*, Nanotoxicology 10 (2016) 1129–1135.

[1.178] A.M. Donald, The use of environmental scanning electron microscopy for imaging wet and insulating materials, Nat. Mater. 2 (2003) 511–516.

[1.179] J. Tuoriniemi, S. Gustafsson, E. Olsson, M. Hassellöv, In situ characterisation of physicochemical

state and concentration of nanoparticles in soil ecotoxicity studies using environmental scanning electron microscopy, Environ. Chem. 11 (2014) 367–376.

[1.180] R.D. Holbrook, K. Rykaczewski, M.E. Staymates, Dynamics of silver nanoparticle release from wound dressings revealed via in situ nanoscale imaging, J. Mater. Sci. Mater. Med. 25 (2014) 2481–2489.

[1.181] V.V. Tsukruk, S. Singamaneni, Scanning probe microscopy of soft matter: fundamentals and practices, Wiley-VCH, Weinheim, 2012.

[1.182] Y. Yin, X. Yang, X. Zhou, W. Wang, S. Yu, J. Liu, *et al.*, Water chemistry controlled aggregation and photo-transformation of silver nanoparticles in environmental waters, J. Environ. Sci. 34 (2015) 116–125.

[1.183] T. Théoret, K.J. Wilkinson, Evaluation of enhanced darkfield microscopy and hyperspectral analysis to analyse the fate of silver nanoparticles in wastewaters, Anal. Methods 9 (2017) 3920–3928.

[1.184] D. António, C. Cascio, Ž. Jakšić, D. Jurašin, D. Lyons, A.J.A. Nogueira, *et al.*, Assessing silver nanoparticles behaviour in artificial seawater by mean of AF4 and spICP-MS, Mar. Environ. Res. 111 (2015) 162–169.

[1.185] W.-C. Lee, B.-T. Lee, S. Lee, Y.S. Hwang, E. Jo, I.-C. Eom, *et al.*, Optimisation, evaluation and application of asymmetrical flow field-flow fractionation with single particle inductively coupled plasma mass spectrometry (SP-ICP-MS) to characterise silver nanoparticles in environmental media, Microchem. J. 129 (2016) 219–230.

[1.186] Y.-J. Chang, Y.-H. Shih, C.-H. Su, H.-C. Ho, Comparison of three analytical methods to measure the size of silver nanoparticles in real environmental water and wastewater samples, J. Hazard. Mater. 322 (2017) 95–104.

[1.187] J.A. Gallego-Urrea, J. Tuoriniemi, M. Hassellöv, Applications of particle-tracking analysis to the determination of size distributions and concentrations of nanoparticles in environmental, biological and food samples, Trends Anal. Chem. 30 (2011) 473–483.

[1.188] F. Piccapietra, L. Sigg, R. Behra, Colloidal stability of carbonate-coated silver nanoparticles in synthetic and natural freshwater, Environ. Sci. Technol. 46 (2012) 818–825.

[1.189] A. Turner, D. Brice, M.T. Brown, Interactions of silver nanoparticles with the marine macroalga, *Ulva lactuca*, Ecotoxicology 21 (2012) 148–154.

[1.190] J.A.C. Broekaert, Analytical atomic spectrometry with flames and plasmas, 2nd ed., Wiley-VCH, Weinheim, 2005.

[1.191] H.Z. Wu, L. F Meng, Flame atomic absorption spectrometry determination of silver nanoparticles in environmental waters using dispersive liquid-liquid microextraction, Appl. Ecol. Environ. Res. 16 (2018) 5705-5714.

[1.192] G. Hartmann, C. Hutterer, M. Schuster, Ultra-trace determination of silver nanoparticles in water samples using cloud point extraction and ETAAS, J. Anal. At. Spectrom. 28 (2013) 567-572.

[1.193] I. López-García, Y. Vicente-Martínez, M. Hernández-Córdoba, Speciation of silver nanoparticles and Ag(I) species using cloud point extraction followed by electrothermal atomic absorption spectrometry, Spectrochim. Acta Part B At. Spectrosc. 101 (2014) 93-97.

[1.194] N.S. Feichtmeier, K. Leopold, Detection of silver nanoparticles in parsley by solid sampling high-resolution-continuum source atomic absorption spectrometry, Anal. Bioanal. Chem. 406 (2014) 3887-3894.

[1.195] J.S. Becker, Inorganic mass spectrometry: principles and applications, John Wiley & Sons, England, 2007.

[1.196] B. Meermann, V. Nischwitz, ICP-MS for the analysis at the nanoscale-a tutorial review, J. Anal. At. Spectrom. 33 (2018) 1432-1468.

[1.197] X. Hou, R.S. Amais, B.T. Jones, G.L. Donati, Inductively coupled plasma optical emission spectrometry, Encyclopedia of analytical chemistry, Wiley&Sons, United States of America, 2016.

[1.198] I.L. Molnar, J.I. Gerhard, C.S. Willson, D.M. O'Carroll, The impact of immobile zones on the transport and retention of nanoparticles in porous media, Water Resour. Res. 51 (2015) 8973-8994.

[1.199] H.E. Taylor, Inductively coupled plasma-mass spectrometry: practices and techniques, Academic Press, United States of America, 2001.

[1.200] J.-F. Liu, J.-B. Chao, R. Liu, Z.-Q. Tan, Y.-G. Yin, Y. Wu, *et al.*, Cloud point extraction as an advantageous preconcentration approach for analysis of trace silver nanoparticles in environmental waters, Anal. Chem. 81 (2009) 6496-6502.

[1.201] J.-B. Chao, J.-F. Liu, S.-J. Yu, Y.-D. Feng, Z.-Q. Tan, R. Liu, *et al.*, Speciation analysis of silver nanoparticles and silver ions in antibacterial products and environmental waters via cloud point extraction-based separation, Anal. Chem. 83 (2011) 6875-6882.

[1.202] S.-J. Yu, J.-B. Chao, J. Sun, Y.-G. Yin, J.-F. Liu, G.-B. Jiang, Quantification of the uptake of silver nanoparticles and ions to HepG2 cells, Environ. Sci. Technol. 47 (2013) 3268-3274.

[1.203] W. Liu, I.A.M. Worms, N. Herlin-Boime, D. Truffier-Boutry, I. Michaud-Soret, E. Mintz, *et al.*, Interaction of silver nanoparticles with metallothionein and ceruloplasmin: impact on metal

substitution by Ag(I), corona formation and enzymatic activity, Nanoscale 9 (2017) 6581–6594.

[1.204] T.K. Mudalige, H. Qu, S.W. Linder, Asymmetric flow-field flow fractionation hyphenated ICP-MS as an alternative to cloud point extraction for quantification of silver nanoparticles and silver speciation: application for nanoparticles with a protein corona, Anal. Chem. 87 (2015) 7395–7401.

[1.205] B. Michalke, I. Vinković-Vrček, Speciation of nano and ionic form of silver with capillary electrophoresis-inductively coupled plasma mass spectrometry, J. Chromatogr. A 1572 (2018) 162–171.

[1.206] F. Laborda, J. Jiménez-Lamana, E. Bolea, J.R. Castillo, Critical considerations for the determination of nanoparticle number concentrations, size and number size distributions by single particle ICP-MS, J. Anal. At. Spectrom. 28 (2013) 1220–1232.

[1.207] D. Bao, Z.G. Oh, Z. Chen, Characterization of silver nanoparticles internalized by *Arabidopsis* plants using single particle ICP-MS analysis, Front. Plant Sci. 7 (2016) 32.

[1.208] S. Böhme, H.-J. Stärk, D. Kühnel, T. Reemtsma, Exploring LA-ICP-MS as a quantitative imaging technique to study nanoparticle uptake in *Daphnia magna* and zebrafish (*Danio rerio*) embryos, Anal. Bioanal. Chem. 407 (2015) 5477–5485.

[1.209] S. Böhme, M. Baccaro, M. Schmidt, A. Potthoff, H.-J. Stärk, T. Reemtsma, *et al.*, Metal uptake and distribution in the zebrafish (*Danio rerio*) embryo: differences between nanoparticles and metal ions, Environ. Sci. Nano 4 (2017) 1005–1015.

[1.210] E. Marguí, R. van Grieken, X-ray fluorescence spectrometry and related techniques: an introduction, Momentum Press, United States, 2013.

[1.211] E. Marguí, J.C. Tapias, A. Casas, M. Hidalgo, I. Queralt, Analysis of inlet and outlet industrial wastewater effluents by means of benchtop total reflection X-ray fluorescence spectrometry, Chemosphere 80 (2010) 263–270.

[1.212] Z. Bahadir, L. Torrent, M. Hidalgo, E. Marguí, Simultaneous determination of silver and gold nanoparticles by cloud point extraction and total reflection X-ray fluorescence analysis, Spectrochim. Acta - Part B At. Spectrosc. 149 (2018) 22–29.

[1.213] M. Menzel, U.E.A. Fittschen, Total reflection X-ray fluorescence analysis of airborne silver nanoparticles from fabrics, Anal. Chem. 86 (2014) 3053–3059.

[1.214] B. Gonsior, Particle induced X-Ray emission (PIXE), Tech. Instrum. Anal. Chem. 8 (1988) 123–179.

[1.215] S. Novak, T. Romih, B. Drašler, G. Birarda, L. Vaccari, P. Ferraris, *et al.*, The *in vivo* effects of silver nanoparticles on terrestrial isopods, *Porcellio scaber*, depend on a dynamic interplay between

shape, size and nanoparticle dissolution properties, Analyst 144 (2019) 488–497.

[1.216] Ž.P. Tkalec, D. Drobne, K. Vogel-Mikuš, P. Pongrac, M. Regvar, J. Štrus, *et al.*, Micro-PIXE study of Ag in digestive glands of a nano-Ag fed arthropod (*Porcellio scaber*, *Isopoda*, Crustacea), Nucl. Instruments Methods Phys. Res. Sect. B Beam Interact. with Mater. Atoms. 269 (2011) 2286–2291.

[1.217] J.E. Penner-Hahn, X-ray absorption spectroscopy, in: Encycl. Life Sci., John Wiley & Sons, United States, 2005.

[1.218] S. Majumdar, J.R. Peralta-Videa, H. Castillo-Michel, J. Hong, C.M. Rico, J.L. Gardea-Torresdey, Applications of synchrotron μ-XRF to study the distribution of biologically important elements in different environmental matrices: a review, Anal. Chim. Acta 755 (2012) 1–16.

[1.219] H.A. Castillo-Michel, C. Larue, A.E.P. del Real, M. Cotte, G. Sarret, Practical review on the use of synchrotron based micro- and nano-X-ray fluorescence mapping and X-ray absorption spectroscopy to investigate the interactions between plants and engineered nanomaterials, Plant Physiol. Biochem. 110 (2017) 13–32.

[1.220] C. Larue, H. Castillo-Michel, S. Sobanska, L. Cécillon, S. Bureau, V. Barthès, *et al.*, Foliar exposure of the crop *Lactuca sativa* to silver nanoparticles: evidence for internalization and changes in Ag speciation, J. Hazard. Mater. 264 (2014) 98–106.

[1.221] J. Yano, V.K. Yachandra, X-ray absorption spectroscopy, Photosynth. Res. 102 (2009) 241–254.

[1.222] L. Yin, Y. Cheng, B. Espinasse, B.P. Colman, M. Auffan, M. Wiesner, *et al.*, More than the ions: the effects of silver nanoparticles on *Lolium multiflorum*, Environ. Sci. Technol. 45 (2011) 2360–2367.

[1.223] E. Lombi, E. Donner, S. Taheri, E. Tavakkoli, Å.K. Jämting, S. McClure, *et al.*, Transformation of four silver/silver chloride nanoparticles during anaerobic treatment of wastewater and post-processing of sewage sludge, Environ. Pollut. 176 (2013) 193–197.

[1.224] P. Lodeiro, E.P. Achterberg, J. Pampín, A. Affatati, M.S. El-Shahawi, Silver nanoparticles coated with natural polysaccharides as models to study AgNP aggregation kinetics using UV-Visible spectrophotometry upon discharge in complex environments, Sci. Total Environ. 539 (2016) 7–16.

[1.225] R. Sahraei, S. Abbasi, R. Hushmandfar, H. Noorizadeh, A. Farmany, Sensitive quantification of silver nanoparticles by kinetic-spectrophotometry method in groundwater samples, Water. Air Soil Pollut. 223 (2012) 3393–3398.

[1.226] C.S.S.R. Kumar, Raman spectroscopy for nanomaterials characterization, Springer Science&Busniess Media, Berlin, 2012.

[1.227] F. Faghihzadeh, N.M. Anaya, L.A. Schifman, V. Oyanedel-Craver, Fourier transform infrared

spectroscopy to assess molecular-level changes in microorganisms exposed to nanoparticles, Nanotechnol. Environ. Eng. 1 (2016) 1.

[1.228] R.E. Whan, ASM Handbook. Materials Chracterization. Volume 10, ASM International, United States of America, 1986.

[1.229] H. Guo, B. Xing, L.C. Hamlet, A. Chica, L. He, Surface-enhanced Raman scattering detection of silver nanoparticles in environmental and biological samples, Sci. Total Environ. 554–555 (2016) 246–252.

[1.230] N. Zuverza-Mena, R. Armendariz, J.R. Peralta-Videa, J.L. Gardea-Torresdey, Effects of silver nanoparticles on Radish Sprouts: root growth reduction and modifications in the nutritional value, Front. Plant Sci. 7 (2016) 90.

[1.231] M.A. Ansari, H.M. Khan, A.A. Khan, M.K. Ahmad, A.A. Mahdi, R. Pal, *et al.*, Interaction of silver nanoparticles with *Escherichia coli* and their cell envelope biomolecules, J. Basic Microbiol. 54 (2013) 905-915.

[1.232] M.D. Scherer, J.C.V. Sposito, W.F. Falco, A.B. Grisolia, L.H.C. Andrade, S.M. Lima, *et al.*, Cytotoxic and genotoxic effects of silver nanoparticles on meristematic cells of *Allium cepa* roots : a close analysis of particle size dependence, Sci. Total Environ. 660 (2019) 459–467.

[1.233] A.R. Badireddy, M. Wiesner, J. Liu, Detection, characterization, and abundance of engineered nanoparticles in complex waters by hyperspectral imagery with enhanced darkfield microscopy, Env. Sci. Technol. 46 (2012) 10081–10088.

[1.234] S.J. Fonash, M.H. Van de Voorde, Engineering, medicine, and science at the nano-scale, Wiley-VCH, United States of America, 2018.

[1.235] J. Lv, P. Christie, S. Zhang, Uptake, translocation, and transformation of metal-based nanoparticles in plants: recent advances and methodological challenges, Environ. Sci. Nano 6 (2019) 41–59.

[1.236] C.F. Poole, The Essence of Chromatography, Elsevier, Netherlands, 2003.

[1.237] T.A. Hanley, R. Saadawi, P. Zhang, J.A. Caruso, J. Landero-Figueroa, Separation of silver ions and starch modified silver nanoparticles using high performance liquid chromatography with ultraviolet and inductively coupled mass spectrometric detection, Spectrochim. Acta Part B At. Spectrosc. 100 (2014) 173–179.

[1.238] X.-X. Zhou, R. Liu, J.-F. Liu, Rapid chromatographic separation of dissoluble Ag(I) and silver-containing nanoparticles of 1-100 nanometer in antibacterial products and environmental waters, Environ. Sci. Technol. 48 (2014) 14516–14524.

[1.239] C.A. Sötebier, S.M. Weidner, N. Jakubowski, U. Panne, J. Bettmer, Separation and quantification of silver nanoparticles and silver ions using reversed phase high performance liquid chromatography coupled to inductively coupled plasma mass spectrometry in combination with isotope dilution analysis, J. Chromatogr. A 1468 (2016) 102–108.

[1.240] A.R. Poda, A.J. Bednar, A.J. Kennedy, A. Harmon, M. Hull, D.M. Mitrano, *et al.*, Characterization of silver nanoparticles using flow-field flow fractionation interfaced to inductively coupled plasma mass spectrometry, J. Chromatogr. A 1218 (2011) 4219–4225.

[1.241] D. Harvey, Book: analytical chemistry 2.0, Chapter 11: Electrochem. methods. (2018). Available at: https://chem.libretexts.org/Bookshelves/Analytical_Chemistry/Book%3A_Analytical_Chemistry_2.0_(Harvey). Accesed: April 5, 2019.

[1.242] E.J.E. Stuart, K. Tschulik, D. Lowinsohn, J.T. Cullen, R.G. Compton, Gold electrodes from recordable CDs for the sensitive, semi-quantitative detection of commercial silver nanoparticles in seawater media, Sensors Actuators B Chem. 195 (2014) 223–229.

[1.243] K. Tschulik, B. Haddou, D. Omanović, N.V. Rees, R.G. Compton, Coulometric sizing of nanoparticles: cathodic and anodic impact experiments open two independent routes to electrochemical sizing of Fe3O4 nanoparticles, Nano Res. 6 (2013) 836–841.

[1.244] E.J.E. Stuart, N.V. Rees, J.T. Cullen, R.G. Compton, Direct electrochemical detection and sizing of silver nanoparticles in seawater media, Nanoscale 5 (2013) 174–177.

[1.245] L. Dai, Carbon nanotechnology: recent developments in chemistry, physics, materials science and device applications, Elsevier, Netherlands, 2006.

[1.246] M.A. Maurer-Jones, M.P.S. Mousavi, L.D. Chen, P. Bühlmann, C.L. Haynes, Characterization of silver ion dissolution from silver nanoparticles using fluorous-phase ion-selective electrodes and assessment of resultant toxicity to *Shewanella oneidensis*, Chem. Sci. 4 (2013) 2564–2572.

[1.247] S.M. Rodrigues, T. Trindade, A.C. Duarte, E. Pereira, G.F. Koopmans, P.F.A.M. Römkens, A framework to measure the availability of engineered nanoparticles in soils: trends in soil tests and analytical tools, Trends Anal. Chem. 75 (2016) 129–140.

[1.248] J. Lewis, J. Sjöstrom, Optimizing the experimental design of soil columns in saturated and unsaturated transport experiments, J. Contam. Hydrol. 115 (2010) 1–13.

[1.249] D. Wang, L. Ge, J. He, W. Zhang, D.P. Jaisi, D. Zhou, Hyperexponential and nonmonotonic retention of polyvinylpyrrolidone-coated silver nanoparticles in an Ultisol, J. Contam. Hydrol. 164 (2014) 35–48.

[1.250] M. Hoppe, R. Mikutta, J. Utermann, W. Duijnisveld, S. Kaufhold, C.F. Stange, *et al.*, Remobilization of sterically stabilized silver nanoparticles from farmland soils determined by column leaching, Eur. J. Soil Sci. 66 (2015) 898–909.

[1.251] S. Treumann, S. Torkzaban, S.A. Bradford, R.M. Visalakshan, D. Page, An explanation for differences in the process of colloid adsorption in batch and column studies, J. Contam. Hydrol. 164 (2014) 219–229.

[1.252] C. Coutris, E.J. Joner, D.H. Oughton, Aging and soil organic matter content affect the fate of silver nanoparticles in soil, Sci. Total Environ. 420 (2012) 327–333.

[1.253] K.N.M. Mahdi, R.J.B. Peters, E. Klumpp, S. Bohme, M. van der Ploeg, C. Ritsema, *et al.*, Silver nanoparticles in soil: aqueous extraction combined with single-particle ICP-MS for detection and characterization, Environ. Nanotechnol., Monit. Manag. 7 (2017) 24–33.

[1.254] A. Praetorius, N. Tufenkji, K.-U. Goss, M. Scheringer, F. von der Kammer, M. Elimelech, The road to nowhere: equilibrium partition coefficients for nanoparticles, Environ. Sci. Nano 1 (2014) 317–323.

[1.255] G. Cornelis, Fate descriptors for engineered nanoparticles: the good, the bad, and the ugly, Environ. Sci. Nano 2 (2015) 19–26.

[1.256] G. Rauret, Extraction procedures for the determination of heavy metals in contaminated soil and sediment, Talanta 46 (1998) 449–455.

[1.257] A. Montes, M.A. Bisson, J.A. Gardella Jr., D.S. Aga, Uptake and transformations of engineered nanomaterials: critical responses observed in terrestrial plants and the model plant *Arabidopsis thaliana*, Sci. Total Environ. 607–608 (2017) 1497–1516.

[1.258] A. Rastogi, M. Zivcak, O. Sytar, H.M. Kalaji, X. He, S. Mbarki, *et al.*, Impact of metal and metal oxide nanoparticles on plant: a critical review, Front. Chem. 5 (2017) 78.

[1.259] C.O. Dimkpa, J.E. McLean, N. Martineau, D.W. Britt, R. Haverkamp, A.J. Anderson, Silver nanoparticles disrupt wheat (*Triticum aestivum* L.) growth in a sand matrix, Environ. Sci. Technol. 47 (2013) 1082–1090.

[1.260] C.L. Doolette, M.J. McLaughlin, J.K. Kirby, D.A. Navarro, Bioavailability of silver and silver sulfide nanoparticles to lettuce (*Lactuca sativa*): effect of agricultural amendments on plant uptake, J. Hazard. Mater. 300 (2015) 788–795.

CHAPTER 2

Objectives

As illustrated in the General Introduction, the presence of AgNPs in different environmental systems is a cause of concern about the potential hazards that they can pose to living organisms and human health. The toxicological effects that these emerging contaminants may have for living beings are influenced by their physicochemical characteristics, which can change in the environment. Therefore, it is necessary to understand their behaviour, mobility and bioavailability in the environment because these phenomena can impact final NPs toxic effects. Furthermore, their possible transfer to living organisms and their toxicological effects must also be understood. Many analytical methodologies have been employed for the detection, characterisation and quantification of nanosilver in simple matrices, but their use in environmental and biological samples still requires sample treatment methods and analytical procedures being developed and improved due to the complexity of these matrices. Given these difficulties, the overall aim of this study is to assess AgNPs mobility and bioavailability in terrestrial environments, and their accumulation, biotransformation and toxicity in edible plants with existing analytical methodologies or by developing new analytical approaches for this purpose. This goal will be accomplished by achieving the specific objectives, which are divided into the following points:

- Study the adsorption and desorption processes of diverse coated and sized AgNPs in soils with different characteristics and their possible transformation in this environmental matrix with time.
- Evaluate TXRF for the detection and quantification of AgNPs in soil adsorption studies as a cheap effective alternative to commonly used ICP-based atomic spectrometric techniques.
- Study the combination of CPE and TXRF for the separation and preconcentration of AgNPs in complex aqueous samples.
- Evaluate the capabilities of CPE as a sample treatment procedure to be used in combination with SP-ICPMS for the accurate determination of nanosilver size and concentration in complex aqueous samples that contain large amounts of Ag(I).
- Study different calculation methods in the SP-ICPMS analysis to obtain nanosilver nebulisation efficiencies and assess diverse iterative algorithms for the subsequent calculation of their sizes and number concentrations in unknown samples.
- Evaluate the uptake of various coated and sized AgNPs by *Lactuca Sativa* (lettuce) roots at different concentration levels and their translocation to aerial plant parts.
- Assess the toxicological effects induced by these emerging pollutants and their potential biotransformation inside the plant *Lactuca Sativa*.

CHAPTER 3

Interaction of silver nanoparticles with mediterranean agricultural soils: lab-controlled adsorption and desorption studies

This chapter corresponds to the following publication:

L. Torrent, E. Marguí, I. Queralt, M. Hidalgo, M. Iglesias, *Interaction of silver nanoparticles with mediterranean agricultural soils: Lab-controlled adsorption and desorption studies*. J. Environ. Sci. 83 (2019) 205-216

Abstract

The production of silver nanoparticles (AgNPs) has increased tremendously during recent years due to their antibacterial and physicochemical properties. As a consequence, these particles are released inevitably into the environment, with soil being the main sink of disposal. Soil interactions have an effect on AgNP mobility, transport and bioavailability. To understand AgNP adsorption processes, lab-controlled kinetic studies were performed. Batch tests performed with five different Mediterranean agricultural soils showed that cation exchange capacity and electrical conductivity are the main parameters controlling the adsorption processes. The adsorption kinetics of different sized (40, 75, 100 and 200 nm) and coated (citrate, polyvinylpyrrolidone and polyethyleneglycol (PEG)) AgNPs indicated that these nanoparticle properties have also an effect on the adsorption processes. To assess the mobility and bioavailability of AgNPs and to determine if their form is maintained during adsorption/desorption processes, loaded soils were submitted to leaching tests three weeks after batch adsorption studies. The DIN 38414-S4 extraction method indicated that AgNPs were strongly retained on soils, and single-particle inductively coupled plasma mass spectrometry confirmed that silver particles maintained their nanoform, except for 100 nm PEG-AgNPs and 40 nm citrate-coated AgNPs. The DTPA (diethylenetriaminepentaacetic acid) leaching test was more effective in extracting silver, but there was no presence of AgNPs in almost all of these leachates.

Keywords: Silver nanoparticles, Agricutural soils, Sorption kinetics, Leaching tests, Single-particle inductively coupled plasma mass spectrometry

3.1 Introduction

During recent years, the use of manufactured nanoparticles (MNPs) for domestic and industrial purposes has grown tremendously [3.1,3.2]. The fraction of atoms at the nanoparticle surface is high because of its nanosize (1–100 nm), thus promoting both the specific surface area and adsorption capacity. Consequently, the physicochemical characteristics (electrical conductivity, mechanical strength, optical or magnetic properties) of nanoparticles are unique, and differ from those of their bulk counterparts. Among different types of nanoparticles, metallic MNPs have experienced substantial growth in the industry, with silver nanoparticles (AgNPs) being one of the most produced NPs due to their effective biocidal activity. Their applications are spread across a variety of commercial goods such as foods, textiles, construction, medicines, cosmetics, power, pharmacy, biomedicine, household goods and agriculture [3.1,3.3,3.4]. As a consequence of the widespread production of AgNPs, these particles are inevitably released through different pathways into the environment (air, water and soil). Soil is the biggest sink of disposal for most of the released MNPs. The main source of entry of these emerging contaminants to soils is through the application of sewage sludge from wastewater treatment plants (WWTPs) to agricultural lands. In WWTPs, AgNPs can undergo different transformations (e.g. dissolution, oxidation or sulfidation), with transformation to silver sulfide in sewage sludge being the main pathway. However, anthropogenic silver nanoparticles can also enter agricultural land directly *via* unintentional emissions, accidental spills or application of nanopesticides [3.3,3.5,3.6]. Soil matrices are relatively complex because they present a solid phase, consisting of organic matter and minerals, and an aqueous phase that contains various amounts of natural colloidal/particulate materials [3.7,3.8]. Consequently, AgNP interactions with soils are difficult to interpret. These interactions lead to processes, such as aggregation/agglomeration, dissolution to metal ions or sorption onto surfaces, which are responsible for their mobility, transport and bioavailability in the environment [3.8]. Aggregation and agglomeration are associations of particles due to physicochemical processes including Van der Waals forces, electrostatic interactions or Brownian motion. Dissolution of AgNPs into their constituent atoms is governed by diverse phenomena, such as chemical reactions that take place due to the presence of oxygen, chlorine and enzymes [3.3]. Deposition occurs when particles are retained on a solid surface or when aggregation (both homo- and hetero-aggregation)/agglomeration takes place. Adsorption of nanoparticles onto the solid components of soils is influenced by particle properties (size, shape, surface charge, surface and core chemistry, capping agent, agglomeration state, crystallinity, redox

potential, catalytic activity and porosity) as well as soil features (pH, organic matter content, ionic strength, zeta potential and texture) [3.4,3.9]. The capping agent is one of the main determinant characteristics since it affects the surface charge, which governs attraction/repulsion interactions among particles, and the steric hindrance [3.8,3.10-3.13]. Additionally, particle size is another property that strongly influences immobilisation on soil surfaces, especially when there is aggregate formation [3.9,3.14,3.15].

Batch experiments are commonly used in order to understand the retention and transport of contaminants in soils. This approach allows one to examine the retention under well-defined conditions in an easier and faster way compared to column experiments [3.16,3.17]. However, as stated in different reports, nanoparticle dispersions are thermodynamically unstable and their behaviour cannot be described as an equilibrium process. Despite this fact, batch tests can still provide valuable information on nanoparticle attachment/detachment kinetics [3.18,3.19]. For example, Cornelis *et al.* (2012) concluded from batch tests that adsorption of polyvinylpyrrolidone (PVP) coated AgNPs (negatively charged) on iron and aluminum oxides and mineral clay edges may be important in retention processes in soils [3.20]. An additional batch retention experiment using sterically stabilised AgNPs determined that immobilisation of nanosilver depends on soil properties such as clay content, pH and calcium content [3.14]. Furthermore, organic matter content is also relevant in adsorption of AgNPs onto silt particles, as stated by Klitzke *et al.* (2015) [3.21].

Scarce information on the desorption of AgNPs from soil particles to the liquid phase exists in the published literature [3.22,3.23]. To evaluate the potential mobility and bioavailability of metals in polluted soils, leaching tests are frequently used [3.24], which gives information related to soil–plant transfer of pollutants and their migration in a soil profile that is connected with groundwater [3.25]. More recently, some leaching tests have been used to evaluate the bioaccessibility of AgNPs from soils in the human gastrointestinal tract [3.26].

Common analytical tools for quantitative determination of AgNPs in liquid extracts are inductively coupled plasma optical emission spectrometry (ICP-OES) and inductively coupled plasma mass spectrometry (ICP-MS). These analytical techniques allow the determination of total metal content, hindering the ability to distinguish the metallic AgNPs from other silver (Ag) species present in the solution [3.27]. However, in recent years the use of single-particle ICP-MS (SP-ICP-MS) to detect and characterise MNPs at trace levels in environmental samples has increased [3.28,3.29]. Analysis with SP-ICP-MS requires nanoparticle suspensions that have been sufficiently diluted and a short

dwell time to ensure that a maximum of one particle is measured in each integration time. Once injected into the plasma, the discrete particle is vaporised, atomised and ionised, producing a burst of ions that can be measured as a single pulse [3.30-3.32]. This analytical technique allows differentiation between nanosilver and soluble silver species and also can give information about the size distribution [3.33].

In this work, batch experiments and leaching tests were carried out in order to understand the adsorption and desorption processes of AgNPs with soils. The goal of this study was to determine the adsorption kinetics of AgNPs with different soils, using different particle sizes and coatings, and assessing the desorption of these particles by leaching tests. Furthermore, the possible AgNP transformations during the studied interaction processes were evaluated by analysing the samples by the SP-ICP-MS technique. To our knowledge, few research papers exist involving the adsorption and desorption of AgNPs from soils that test nanoparticles with different physicochemical properties. In addition, none of them employ SP-ICP-MS for AgNP detection after the adsorption and desorption processes.

3.2 Materials and methods

3.2.1 Chemicals, materials, apparatus and instrumentation

ICP-OES standard solutions were prepared from a silver stock solution (silver nitrate ($AgNO_3$) in nitric acid (HNO_3)) of 1,000 ± 2 mg L^{-1} from Merck (Germany). High purity water from a Milli-Q purification system (Millipore Corp., Bedford, MA) was employed for the leaching experiments (DIN 38414-S4 extraction method). It was also used to dilute stock solutions and soil leachates (supernatants). Triethanolamine (TEA) (Sigma–Aldrich, Germany), diethylenetriaminepentaacetic acid (DTPA) (Panreac, Spain) and calcium chloride dehydrate ($CaCl_2{\cdot}2H_2O$, Panreac, Spain) were utilised to prepare the extracting solution for the DTPA leaching test.

Batch adsorption experiments and leaching tests were performed employing LD-76 rotary mixers (Dinko, Spain). In order to break down the possible agglomerates of AgNPs, an ultrasonic bath (J.P. Selecta, Spain) was used. A Rotofix 32A centrifuge (Hettich-Zentrifugen, Germany) was utilised to separate the soil and the soil extract after kinetic adsorption tests and leaching tests. Total silver content in aqueous suspensions from adsorption and leaching experiments was determined using an ICP-OES Vertical Dual View 5100 system (Agilent Technologies, Japan), with calibration curves ranging between 5 and 350 µg kg^{-1} silver concentration. SP-ICP-MS for

silver nanoparticle detection in aqueous leachates was performed using a quadrupole-based ICP-MS Agilent 7500c system (Agilent Technologies, Japan) equipped with Octapole Reaction System (ORS) technology. The instrumental characteristics and measurement conditions of the two instruments are summarised in the Supporting information of this chapter ***Table S3.1***. Histograms of the results were summarised and plotted using Microsoft Excel software.

3.2.2 Nanoparticles

Silver nanoparticles of different sizes and coatings were tested in this work. Two suspensions of silver nanoparticles stabilised with sodium citrate (citrate-AgNPs) of 40 and 100 nm were obtained from Sigma–Aldrich (USA) and one of 200 nm from NanoComposix (USA). Polyvinylpyrrolidone-coated silver nanoparticles (PVP-AgNPs) of 75 and 100 nm and polyethyleneglycol-coated silver nanoparticles (PEG-AgNPs) of 100 nm were purchased from NanoComposix (USA). The principal difference between these nanoparticles was the zeta potential, which depends on the capping agent and is related to the surface charge. The most negative zeta potential at pH 7 was found for citrate-AgNPs and the least negative for PEG-AgNPs, which was almost neutral [3.34]. Detailed information about the characteristics of the studied AgNPs can be found on the manufacturers' webpages.

3.2.3 Soils studied

Five Mediterranean agricultural soils with different physicochemical properties were tested in order to evaluate their influence in AgNP adsorption processes. The five studied soils were sampled at different locations from Barcelona and Girona provinces (NE Spain): Soil 1 and Soil 2 (Vallcebre), Soil 3 (Castellbisbal), Soil 4 (Gavà) and Soil 5 (La Tallada d'Empordà). These soils were selected to cover the variety of soils along this Mediterranean region. Composite and representative surface soil samples were obtained by combining several subsamples per location. They were collected using a polypropylene shovel and subsequently transferred to clean polypropylene bags. In the laboratory, soil samples were dried at room temperature, sieved (2 mm) and stored in polypropylene containers.

The particle size distribution (Supporting information of this chapter ***Table S3.2***) revealed strong differences regarding the smallest sizes, <0.125 mm, ranging from near 4% for Soil 3 to around 50% for Soil 4. Soil mineralogy was determined by X-ray diffraction (XRD), following randomly oriented powder methodology for bulk composition and the oriented aggregate method for

the identification of clay minerals. From the results, (Supporting information of this chapter ***Table S3.3***) studied soils could be classified as marly soils, characterised by the prevalence of carbonates (mainly calcite, $CaCO_3$) and quartz. Soils from the Vallcebre area (Soil 1 and Soil 2) differed in the type of carbonate, dolomite ($MgCaCO_3$) for Soil 1 and a noticeable content of gypsum for Soil 2. Dealing with the content of clay minerals, Soils 1 and 2 were characterised by the presence of swelling clays of the smectite group, with a minor amount of kaolinite, whereas the rest of the soils exhibited different clay assemblages, illite-kaolinite for Soil 3 and chlorite-illite for Soils 4 and 5. Clay mineralogy is the key factor in the cation exchange capacity (CEC) of soils. Pure smectite has a CEC from 80 to 150 mEq 100 g^{-1}, with illite and chlorite ranging from 10 to 40 mEq 100 g^{-1} and kaolinite from 3 to 15 mEq 100 g^{-1}. Minor quantities of feldspars and hematite were also detected in the XRD runs.

The physicochemical properties of these studied soils are shown in ***Table 3.1***. As can be expected from the mineralogy, the pH of the soil samples was neutral to slightly basic. The cation exchange capacity, around three times higher in Soils 1 and 2, was directly related to the presence of smectite. The electrical conductivity was very high in Soil 2 due to the presence of gypsum, exhibiting a wide variety for the rest of the soils, and the organic matter was nearly constant (5%–6%), except for Soil 5 that had the lowest content.

Table 3.1 *Physicochemical characteristics of studied soils.*

	pH (in H_2O)	**Moisture (%)**	**O.M. (%)**	**CEC (meq 100 g^{-1})**	**EC (µS cm^{-1})**
Soil 1	8.0	13.3	6.5	20.1	105.1
Soil 2	7.4	13.05	5	18.9	2,460
Soil 3	7.6	9.3	5.7	6.5	276.5
Soil 4	7.4	3.7	6.1	7	427.3
Soil 5	7.1	0.5	1.8	5.3	87.3

O.M.: organic matter content. CEC: cation exchange capacity. EC: electrical conductivity.

3.2.4 Adsorption studies

Batch adsorption experiments were performed in order to investigate the interaction between AgNPs and soil in lab-controlled conditions. For this purpose, 0.5 g of soil was weighed into polystyrene tubes. Then, 20 mL of a 1 or 10 mg L^{-1} aqueous suspension of AgNPs was added followed by agitation with a rotary mixer at 35 r min^{-1}.

Afterwards, samples were removed in duplicate at specific times (10 min, 20 min, 30 min, 1 hr, 2 hr, 4 hr or 6 hr) and centrifuged at 3500 r min^{-1} for 8 min. Finally, the supernatant was transferred

to a new polystyrene tube and stored overnight at 4 °C until analysis.

Prior to analysis by ICP-OES, liquid samples were ultrasonicated for 5 min to break down the possible agglomerates of silver nanoparticles present in the aqueous suspension. Then, samples were shaken vigorously for 1 min and filtered through a 0.45 µm cellulose acetate filter (Whatman, Filterlab, Spain) to remove suspended soil particles. Finally, the samples were analysed by ICP-OES and the total silver content was quantified using an ionic silver (Ag^+) calibration curve. All experiments were carried out in duplicate.

3.2.5 Leaching studies: DIN 38424-S4 and DTPA

In order to study the possible release of AgNPs from soils, two leaching tests named DIN 38414-S4 [3.35] and DTPA [3.36] were performed. These leaching tests were selected to allow the evaluation of the mobility and bioavailability of metals in the environment. The DIN 38414-S4 leaching test gives information about the more mobilised metals and the DTPA leaching method predicts the bioavailability of metals to plants [3.25,3.37]. To this aim, soils containing known amounts of adsorbed AgNPs were tested 21 days after the adsorption experiment.

For the DIN 38414-S4 extraction procedure, 5 mL of Milli-Q water was added to 0.5 g of loaded soil and the mixture was submitted to rotation with a rotary mixer (35 r min^{-1}) for 24 hr at room temperature (22 °C). In the case of the DTPA extraction test, 5 mL of DTPA solution (0.005 mol L^{-1} DTPA, 0.01 mol L^{-1} TEA, 0.5 mol L^{-1} $CaCl_2{\cdot}2H_2O$ adjusted to pH 7.3) was agitated (35 r min^{-1}) with 0.5 g of loaded soil for 2 hr at room temperature (22 °C).

After these contact times, samples were centrifuged for 8 min at 3500 r min^{-1}, after which the supernatants were transferred to new polystyrene tubes and stored overnight at 4 °C until analysis by ICP-OES and SP-ICP-MS techniques.

3.2.6 Evaluation of the presence of Ag as AgNPs by SP-ICP-MS analysis

SP-ICP-MS was used to confirm the presence of AgNPs in the stripping solutions. To obtain good results in SP-ICP-MS, the Ag concentration in the form of AgNPs should be very low to afford a solution that has at maximum one particle in the volume aspirated during the dwell time (10 msec). For this reason, the Ag concentration of the samples was determined by the ICP-OES technique before SP-ICP-MS analysis to determine which dilution was needed to obtain a final solution of approximately 0.8 µg L^{-1}. Previous to the ICP-OES analysis, in order to remove the suspended soil particles, samples were filtered through a cellulose acetate filter of 0.45 µm after being

ultrasonicated for 5 min and shaken for 1 min to avoid the possibility of agglomerates. Finally, the samples were analysed by SP-ICP-MS to determine if silver was present in the leachate solution (supernatant) in nanosilver form. In the case of DTPA solutions, the stability of AgNPs had been previously verified. The presence of nanoparticles was confirmed in this media for 100 nm AgNPs with the three different coatings after 2 hr of agitation.

3.3 Results and discussion

3.3.1 Stability and storage of AgNPs solutions

Some recent publications have highlighted the potential alteration of the dispersion state of nanoparticles by laboratory procedures [3.38]. For this reason, previous to the soil adsorption studies, some experiments were carried out in order to evaluate the stability of silver nanoparticle suspensions submitted to different treatments and storage conditions. Specifically, various times of storage (<6 hr and 6 days) at different temperatures (around 4 °C and around –20 °C) were evaluated. Moreover, the effect of filtration of these suspensions was also tested. Results can be observed in the Supporting information of this chapter ***Fig. S3.1***.

Good recoveries of fresh suspensions (95%–100%) assessed using an ICP-OES system and silver standard solutions for quantification purposes confirmed the good performance of the analytical procedure.

It can be seen that the storage of aqueous silver nanoparticles suspensions during 6 days caused a 40% decrease in their recovery with respect to the ones stored for <6 hr for all types of AgNPs tested (significant statistical differences by Student's t-test, $t_{critical} < t_{experimental}$). Nevertheless, a recovery of (104.6% ± 1.2%) was obtained from an aqueous suspension of citrate-coated silver nanoparticles (100 nm) after being stored 24 hr at 4 °C (data not shown in the bar chart). No significant statistical differences were observed (Student's t-test, $t_{critical} > t_{experimental}$) between storing the samples at 4 or at -20 °C. Finally, it was shown that the filtration of fresh samples does not cause any effect on the recovery of AgNPs (no significant statistical differences by Student's t-test, $t_{critical} > t_{experimental}$). Moreover, the supernatant solution had no effect on silver recovery (94.6% ± 1.3%) of 100 nm PVP-AgNPs after filtration. However, the filtration process caused an important decrease in the AgNP concentration when silver nanoparticles aqueous suspensions had been stored at -20 °C (significant statistical differences by Student's t-test, $t_{critical} < t_{experimental}$). Some aggregation processes have been reported for nanoparticles suspension

under these low temperatures [3.39]. These aggregations can produce a loss of particles when they are subjected to filtration afterwards. Taking into account all these results, the adsorption studies could be carried out analysing the samples after storage for a maximum of 24 hr at 4 °C and subjecting the samples to a filtration process if necessary.

3.3.2 Adsorption of AgNPs in agricultural soils: Kinetic studies

Some preliminary experiments were performed in order to determine the appropriate amount of soil and the volume and concentration of silver nanoparticle suspensions. The aim of these experiments was to establish the conditions that permitted the evaluation of the adsorption of AgNPs onto soil surfaces. For this purpose, 2, 1 and 0.5 g of soil were put in contact with 20 mL of a 1 mg L^{-1} citrate-AgNPs (100 nm) suspension (Supporting information of this chapter ***Fig. S3.2***). Likewise, 10, 15 and 20 mL of 75 nm PVP-AgNP suspensions (1, 5 and 10 mg L^{-1} concentrations) were mixed with 0.5 g of soil (Supporting information of this chapter ***Fig. S3.3***). In both cases the soil and nanoparticle suspensions were stirred under rotary agitation conditions (35 r min^{-1}) for 2 hr. Afterwards, the silver concentration in the supernatant was determined by ICP-OES analysis. Results showed that a smaller amount of soil (0.5 g) and greater volume of solution (20 mL) gave higher Ag concentrations in the supernatant suspensions, indicating slower kinetics in comparison with that obtained using high soil amounts. This is favourable for detection of the differences in adsorption kinetics of different types of AgNPs. Therefore, it was decided to use 0.5 g of soil and 20 mL of a 10 mg L^{-1} silver nanoparticle suspension (PVP-AgNPs 75 nm) only for testing the influence of soil properties on AgNP adsorption. For the other tests (coating and size effects), 0.5 g of soil and 20 mL of 1 mg L^{-1} AgNP suspensions were used due to the low concentration of the stock solutions available (20 mg L^{-1}). Using these conditions, a kinetic study was undertaken.

The study was conducted with all the soils described in Section 3.2.3 (for details of soil characteristics see Supporting information of this chapter ***Tables S3.2*** and ***S3.3***). The results obtained using AgNPs of 75 nm coated with PVP are shown in ***Fig. 3.1a***. As can be seen, the adsorption rates obtained for all tested soils after 4 hr of rotation were high (80% of adsorption). Soil 2 showed the fastest adsorption rate, reaching almost 100% adsorption in less than 10 min. The main characteristics of this soil are its high electrical conductivity and cation exchange capacity. This fact agrees with different works that point out the increase of AgNP adsorption on soils with increasing ionic strength [3.40]. Thus, both homo- and hetero-aggregation processes

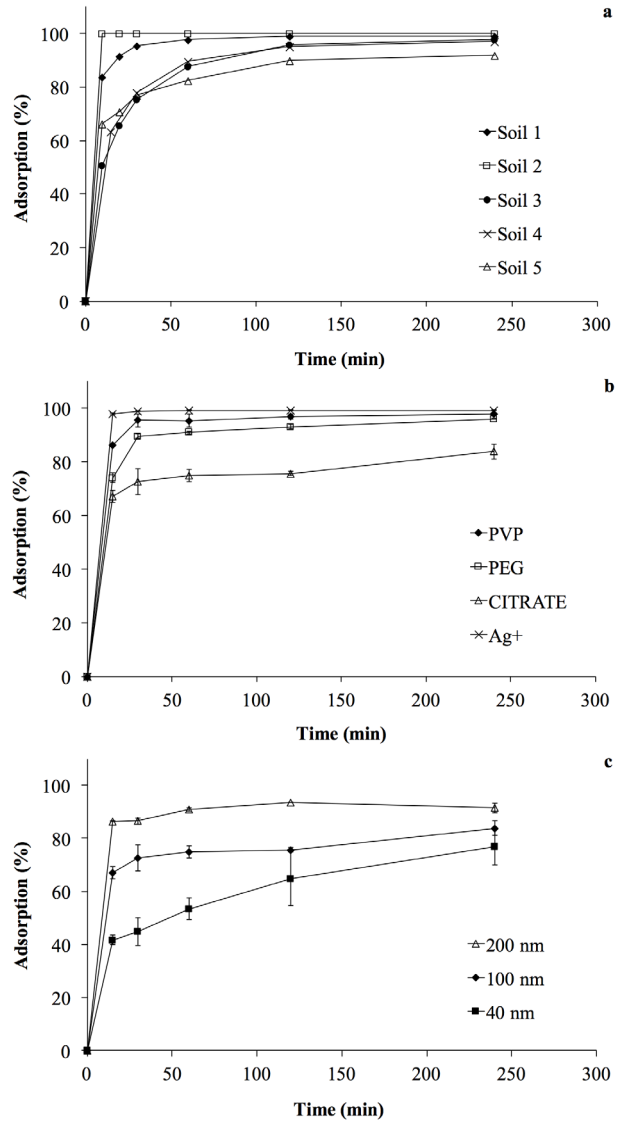

Fig. 3.1 *Percentage of adsorption of different silver nanoparticles in agricultural soils (0.5 g of soil and 20 mL of nanoparticle suspension). (**a**) Comparison of agricultural soils with different physicochemical properties using a suspension of 10 mg L^{-1} of 75 nm ϕ polyvinylpyrrolidone (PVP) coated AgNPs. (**b**) Comparison of different coatings (PVP, polyethyleneglycol (PEG), citrate) of 100 nm ϕ nanoparticles using Soil 3 and a solution of 1 mg L^{-1} of total silver. (**c**) Comparison of different sizes of citrate silver nanoparticles using Soil 3 and a solution of 1 mg L^{-1} total silver concentration.*

could be responsible of this adsorption. On the other hand, Soil 3 after half an hour of the kinetic adsorption study presented the slowest adsorption rate (75%). This soil had one of the lowest cation exchange capacity values; however, its electrical conductivity was higher than that of Soil 1, which shows a higher rate of adsorption. After 4 hr of the kinetic study, the slowest adsorption rate was obtained for Soil 5, which had the lowest cation exchange capacity and electrical conductivity. The size distribution of soil particles seems not to have a great influence

in the adsorption rate, although the soils with a lower adsorption rate (Soils 3, 4 and 5) were those with greater amounts of small soil particles. Cornelis *et al.* (2013) determined a correlation between clay content and AgNP retention by natural soils [3.41]. This correlation seems to be explained by the hetereocoagulation of AgNPs with colloids naturally present in soils.

Using these results, an approximate value for the affinity coefficient, α, could be calculated following the methodology developed by Barton *et al.* (2014) [3.42]. For removal of AgNP suspensions at time *t*, *r(t)* was calculated as $r(t) = (C_o - C_t)/C_o$, with C_o (μg L^{-1}) being the initial AgNP mass concentration and C_t (μg L^{-1}) the AgNP mass concentration in the supernatant suspension at time *t* (min). Afterwards, $ln\ (rC_o/C_t + 1)$ *vs* time was plotted and a linear portion was obtained for these plots (between 10 and 60 min) except for Soil 2, which showed very fast adsorption (Supporting information of this chapter ***Fig. S3.4***). The values of the slope of this linear portion correspond to the product $\alpha\beta B$, which is a measure of the relative affinity of the nanoparticles for soil. β and *B* are the collision frequency and the concentration of soil particles respectively, which in this case were constant. From these calculations the values of $\alpha\beta B$ determined were 6.42×10^{-4}, 4.88×10^{-4}, 3.21×10^{-4} and 2.16×10^{-4} for soils 1, 3, 4 and 5 respectively. These affinity coefficients thus obtained are in agreement with the soil adsorption kinetics, because Soil 1 is one of the soils with the fastest AgNP adsorption kinetics and its affinity coefficient is the highest, meanwhile Soil 5 shows the slowest AgNP adsorption kinetics and its affinity coefficient is the lowest.

3.3.3 Effect of the coating and size of AgNPs in soil adsorption

Soil 3 was chosen to study the adsorption behaviour of different types of nanoparticles (surface and size) because, as observed previously, this soil had an intermediate affinity toward AgNPs among all the studied soils.

First of all, the adsorption kinetics of different coated silver nanoparticles (PVP, PEG and citrate) onto Soil 3 was compared using AgNPs of ϕ 100 nm. For comparison purposes, the adsorption kinetics of silver ions (added as $AgNO_3$) was also examined. Results are depicted in ***Fig. 3.1b***.

As can be observed, Ag^+ showed a faster adsorption rate than silver nanoparticles, reaching 100% of adsorption in 15 min. In fact, different works underline the high capacity of Ag^+ to be adsorbed by soils, either by thiol groups or to colloidal particles [3.40]. The different types of AgNPs showed quite fast and similar adsorption rates, achieving a steady-state concentration in less than 60 min. Nevertheless, AgNPs with a citrate surface coating were less adsorbed (80%) than PEG- and PVP-coated nanoparticles, which reached almost 100% adsorption under the

present conditions. For citrate particles an additional value was determined at 6 hr (data not shown), which was very similar to the adsorption value obtained at 4 hr. The lower adsorption rate of citrate-AgNPs respect to PEG-AgNPs and PVP-AgNPs could be due to their zeta potential, which is controlled by the pH of the solution. Zeta potential, which is the charge at the surface of the electrical double layer, is a key indicator of the stability of colloidal dispersions. Usually, capping of the particles with highly negative zeta potential indicates the increase of particle stabilisation. As detailed by the manufacturer, citrate-AgNPs present a highly negative zeta potential (negatively charged) in comparison to PVP-AgNPs and PEG-AgNPs. Thus, citrate-AgNPs are more stable and their aggregation tendency is lower due to higher repulsion with negatively charged soil surfaces in comparison to other tested AgNPs [3.24,3.43,3.44].

Adsorption rates of AgNPs with different sizes should also be compared. To this aim, citrate-coated AgNPs of 40, 100 and 200 nm diameters were used. From the results (***Fig. 3.1c***) it can be observed that silver nanoparticles with a size of 200 nm were adsorbed faster in comparison to 40 nm AgNPs. In addition, the largest AgNPs were almost totally adsorbed (90%) in 1 hr of contact time; meanwhile, the smallest AgNPs (40 nm) reached a value of 50%, achieving a 75% after 4 hr. It must be taken into account that in this work, we compared suspensions with the same Ag mass concentration but different particle number concentrations. The smaller the nanoparticle size, the higher the particle number concentration for the same Ag mass concentration. So, there were more particles able to be adsorbed in the 40 nm AgNP solution than in 100 nm or in 200 nm ones. These results agree with those obtained by He *et al.* (2019) and seem to indicate that no dissolution process is taking place for AgNPs [3.15]. On one hand, smaller nanoparticles are reported to dissolve more quickly. On the other hand, silver ions are more quickly retained in soils. Both facts point in the opposite direction as the behaviour observed.

Finally, the adsorption rates of all types of nanoparticles using the five soils considered in this study were compared. In all cases the concentration of silver in the supernatant solution was determined after two hours of rotation (35 r min^{-1}) at 22 °C. Higher concentrations of silver in the supernatant indicated lower adsorption degree on the soil. Results are depicted in ***Fig. 3.2***.

As can be seen in this figure, the lowest adsorption was obtained for 100 nm citrate-coated nanoparticles in comparison to 100 nm PVP-AgNPs and PEG-AgNPs, observing significant statistical differences, except for Soil 2 (Student's t-test, $t_{critical} < t_{experimental}$). AgNPs with PVP and PEG surfaces (100 nm) showed similar results and higher adsorption than citrate-coated

nanoparticles (no significant statistical differences by Student's t-test, $t_{critical}>t_{experimental}$), except for Soil 5, where significant statistical differences were observed (Student's t-test, $t_{critical}<t_{experimental}$). This different behaviour of Soil 5 could be due to its lower organic matter content. Hoppe *et al.* (2014) stated that citrate-stabilised AgNP adsorption processes in soils are related to the soil organic matter content, which tends to be negatively charged and may hamper access to positively charged groups [3.14,3.45]. Thus, the low organic matter content of Soil 5, in comparison to other studied soils, indicates that the particles of this soil may contain less negative charges, favouring the adsorption of citrate-AgNPs (highly negatively charged).

Significant statistical differences were also observed between small citrate nanoparticles (40 nm) and the big ones (100 nm) in all the tested soils (Student's t-test, $t_{critical}<t_{experimental}$) except for Soil 1 (Student's t-test, $t_{critical}>t_{experimental}$), showing a lower adsorption than the small ones. As stated above, the reason for this phenomenon can be the presence of more particles in the 40 nm AgNP solution than in the 100 nm one.

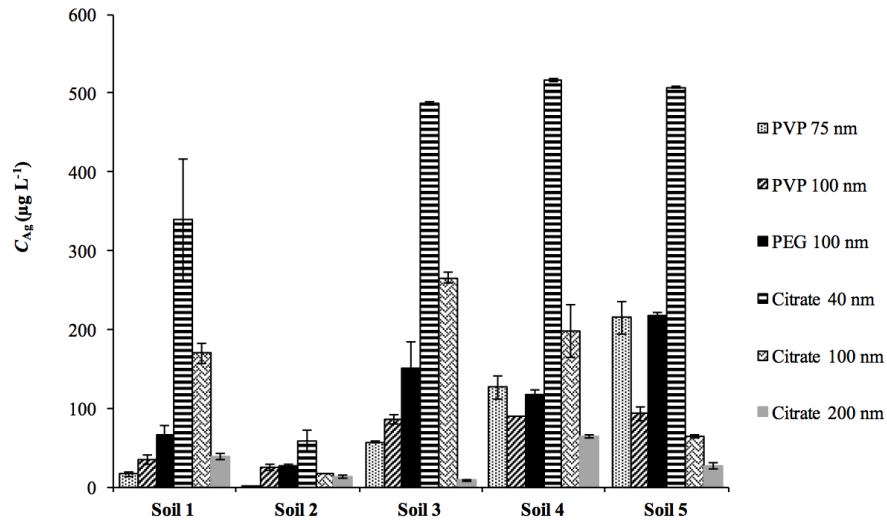

Fig. 3.2 *Silver supernatant concentration after 2 hr adsorption in different soils (0.5 g of soil and 20 mL of nanoparticle suspension with 1,000 µg L^{-1} total silver concentration).*

When comparing the behaviours of the soils, again Soil 2 showed a higher adsorption degree for all types of AgNPs in comparison to the other studied soils in this work (significant statistical differences by Student's t-test, $t_{critical}<t_{experimental}$). As stated above, the most important difference of this soil compared to the others is its high electrical conductivity derived from the presence of gypsum, which is related with the ionic strength [3.46], and also the synergic presence of smectite clays, acting as an additional AgNP trapping agent due to its surface properties and CEC features

[3.47]. Several authors have pointed out that high ionic strength favours nanoparticle adsorption when electrostatic repulsion is present [3.48].

3.3.4 Recovery of AgNPs from soils using DIN 38414-S4 and DTPA leaching procedures

To evaluate the mobility and bioavailability of different sized and coated AgNPs retained in agricultural soils, two leaching procedures were carried out after 3 weeks of being adsorbed. DIN 38414-S4 and DTPA leaching procedures were applied to Soil 3 to gain information on the potential risks associated with these pollutants. Results can be observed in ***Table 3.2***. In this table, μg $Ag_{initial}$ is the total silver amount in the initial suspension, which was put in contact with Soil 3 under rotary agitation (35 r min^{-1}) for 2 hr and after this time, the suspension was centrifuged and the supernatant was separated, filtered and analysed. The μg $Ag_{supernatant}$ is the total silver amount in the supernatant. After the separation from the supernatant, the soil was dried and kept at room temperature for 3 weeks. Finally, a DIN 38414-S4 or a DTPA leaching procedure was carried out and the silver concentration of this leachate was determined. From these values the total amount of silver in each case was determined (μg $Ag_{leached}$).

As can be seen, the DIN 38414-S4 procedure gave very low recovery values for total silver, with ionic silver being the most retained silver form together with 100 nm PVP-AgNPs (no significant statistical differences by Student's t-test, $t_{critical}>t_{experimental}$). From the results of PVP and citrate coatings, it can be concluded that small nanoparticles show a lower tendency to be adsorbed and a higher trend toward desorption than larger ones, especially 40 nm citrate-AgNPs with respect to 100 and 200 nm, because significant statistical differences were observed (Student's t-test, $t_{critical}<t_{experimental}$). Significant statistical differences (one-way ANOVA test, $F_{critical}<F_{experimental}$) on leaching recoveries for the differently coated AgNPs tested can be also observed. In the leaching tests, fewer 100 nm PVP-AgNPs were leached, observing statistical differences (Student's t-test, $t_{critical}<t_{experimental}$), in comparison to citrate-AgNPs and PEG-AgNPs. Therefore, PVP-AgNPs were more strongly retained than the other types of AgNPs tested in Soil 3. The DTPA leaching procedure gave higher recovery values than the DIN 38414-S4 extraction method, except for the smaller particles (40 and 75 nm). Surprisingly, the tendencies were completely opposite to those observed using the DIN 38414-S4 procedure: smaller AgNPs gave lower recovery values than bigger ones and ionic silver was the most leached silver form, showing significant statistical differences with respect to tested AgNPs (one-way ANOVA test, $F_{critical}<F_{experimental}$). Similarly, for different coated AgNPs, opposite trends were observed. Significant statistical differences

(Student's t-test, $t_{critical}<t_{experimental}$) were observed between citrate-AgNPs and PVP-AgNPs and PEG-AgNPs, indicating that citrate-AgNPs were the least leached. The complexing capacity of DTPA for Ag^+ could partially explain these results [3.49]. As well, organic matter content could have played a role in the stabilisation of some of the AgNPs [3.21,3.50]. Some differences in the leaching capability of these extraction procedures were also observed for samples with different characteristics [3.51].

Table 3.2 *DIN 38414-S4 and DTPA leaching tests of Soil 3 after adsorption of AgNPs.*

Leaching method	AgNPs	µg $Ag_{initial}$	µg $Ag_{supernatant}$	µg $Ag_{leached}$	Recovery (%)
DIN 38414-S4	PVP 75 nm	19.7	0.6 (0.1)	0.16 (0.02)	0.8 (0.1)
	PVP 100 nm	20.0	0.4 (0.2)	0.08 (0.02)	0.4 (0.1)
	PEG 100 nm	18.6	1.1 (0.5)	0.21 (0.02)	1.2 (0.2)
	Citrate 40 nm	20.3	9.8	0.5	4.6
	Citrate 100 nm	20.2	5 (2)	0.165 (0.003)	1.1 (0.1)
	Citrate 200 nm	20.3	1.6 (0.5)	0.14 (0.03)	0.8 (0.2)
	Ag^+	20.6	0.160 (0.008)	0.09 (0.01)	0.4 (0.1)
DTPA	PVP 75 nm	19.7	0.6 (0.2)	0.10 (0.02)	0.5 (0.1)
	PVP 100 nm	20.0	0.6 (0.2)	0.8 (0.1)	3.9 (0.5)
	PEG 100 nm	18.6	1.0 (0.3)	0.47 (0.04)	2.7 (0.2)
	Citrate 40 nm	20.3	9.6	0.05	0.5
	Citrate 100 nm	20.2	5 (1)	0.11 (0.09)	0.7 (0.6)
	Citrate 200 nm	20.3	1.4 (0.1)	0.28 (0.06)	1.5 (0.3)
	Ag^+	20.6	0.135 (0.003)	1.60 (0.02)	7.8 (0.1)

DTPA: diethylenetriaminepentaacetic acid.

Values expressed as mean, $n = 2$ (standard deviation), except for nanoparticles of 40 nm with citrate surface ($n = 1$).

3.3.5 AgNP presence in leaching solutions by SP-ICP-MS

The interaction of nanoparticles with soils can lead to transformations that alter their form and consequently their behaviour in the environment [3.48]. In order to determine if silver nanoparticles maintain their nanoform after the adsorption and desorption processes onto soils, leachates from DIN 38414-S4 and DTPA tests were also analysed with SP-ICP-MS. As mentioned above, this analytical technique allows differentiating between nanoparticulate silver and dissolved silver.

As can be seen in the time-resolved signal plot obtained from SP-ICP-MS analysis of PEG-AgNPs DIN 38414-S4 leachates (***Fig. 3.3b***), the baseline counts were shifted to higher values (around 400 counts) and the signal was practically constant, indicating the presence of dissolved silver [3.52]. Although the presence of some peaks above the baseline was observed, they were not enough to confirm the presence of nanosilver. Therefore, during the adsorption or desorption

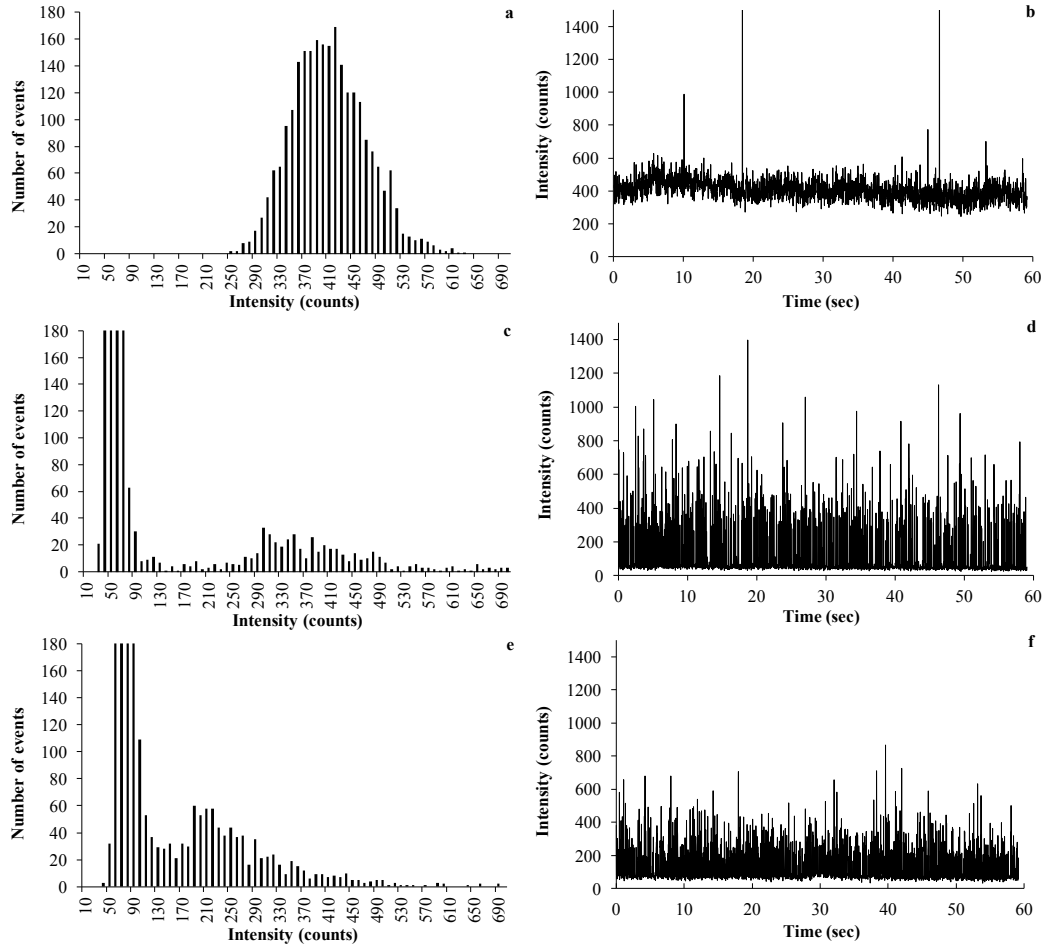

Fig 3.3 *SP-ICP-MS histograms and time-resolved signal plots of polyetyleneglycol silver nanoparticles 100 nm (**a,b**), citrate silver nanoparticles 100 nm (**c, d**), polyvinylpyrrolidone silver nanoparticles 100 nm (**e**, **f**) from Soil 3 DIN 38414-S4 leachates.*

processes, PEG-AgNPs were mainly dissolved. However, the presence of citrate-AgNPs in DIN 38414-S4 leachates was confirmed due to the large number of peaks present above the baseline, which is around 40 counts, indicating that there was also a small amount of dissolved silver (***Fig. 3.3d***). In addition, the histogram obtained from this measurement confirmed the presence of AgNPs, because two distributions could be observed (***Fig. 3.3c***). The distribution at low pulse

intensity represents the dissolved silver, and that at higher pulse intensity values represents the nanoparticles. So, citrate-AgNPs maintained their nanoform after adsorption and desorption processes. Similarly, PVP-AgNPs of 100 nm size also maintained their form after the DIN 38414-S4 leaching procedure (***Fig. 3.3e–f***).

In the DIN 38414-S4 leachates of 200 nm citrate-AgNPs, the presence of nanosized particles was also confirmed, as shown in ***Fig. 3.4c–d***. However, for citrate-AgNPs with dimension of 40 nm, no nanoparticles were present (***Fig. 3.4a–b***). Therefore, it seems that smaller sized AgNPs are more prone to dissolution in soil adsorption and desorption processes in comparison with larger sized nanoparticles. These results agree with some other results found in the literature [3.48], which mentioned a higher rate of dissolution for smaller nanoparticles than for bigger ones due to the larger fraction of surface atoms or the lower redox potentials of smaller AgNPs.

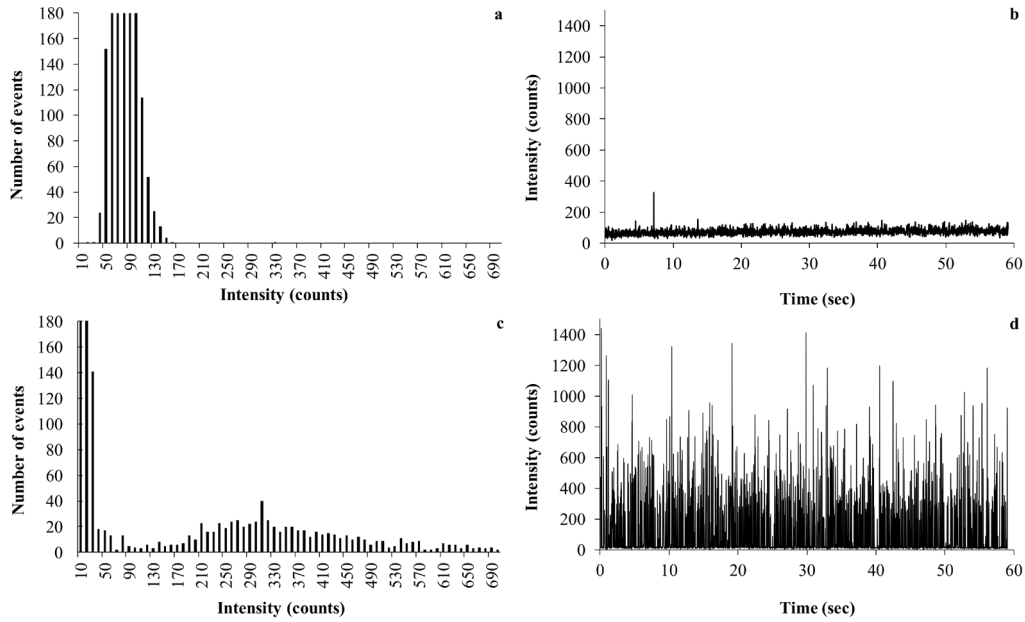

Fig 3.4 *SP-ICP-MS histograms and time-resolved signal plots of citrate silver nanoparticles 40 nm (**a, b**) and 200 nm citrate silver nanoparticles (**c, d**) from Soil 3 DIN 38414-S4 leachates.*

The leachates of 200 nm citrate-AgNPs for the five soils studied were also analysed in order to determine if there were some differences in the AgNP forms caused by the physicochemical properties of the soils. In ***Fig. 3.5***, it can be seen that for Soils 1, 3 and 4, the silver nanoparticles maintain their form after adsorption and desorption experiments. However, for Soils 2 and 5, the presence of nanoparticles cannot be confirmed (***Fig. 3.5b*** and **e**). These two soils have a

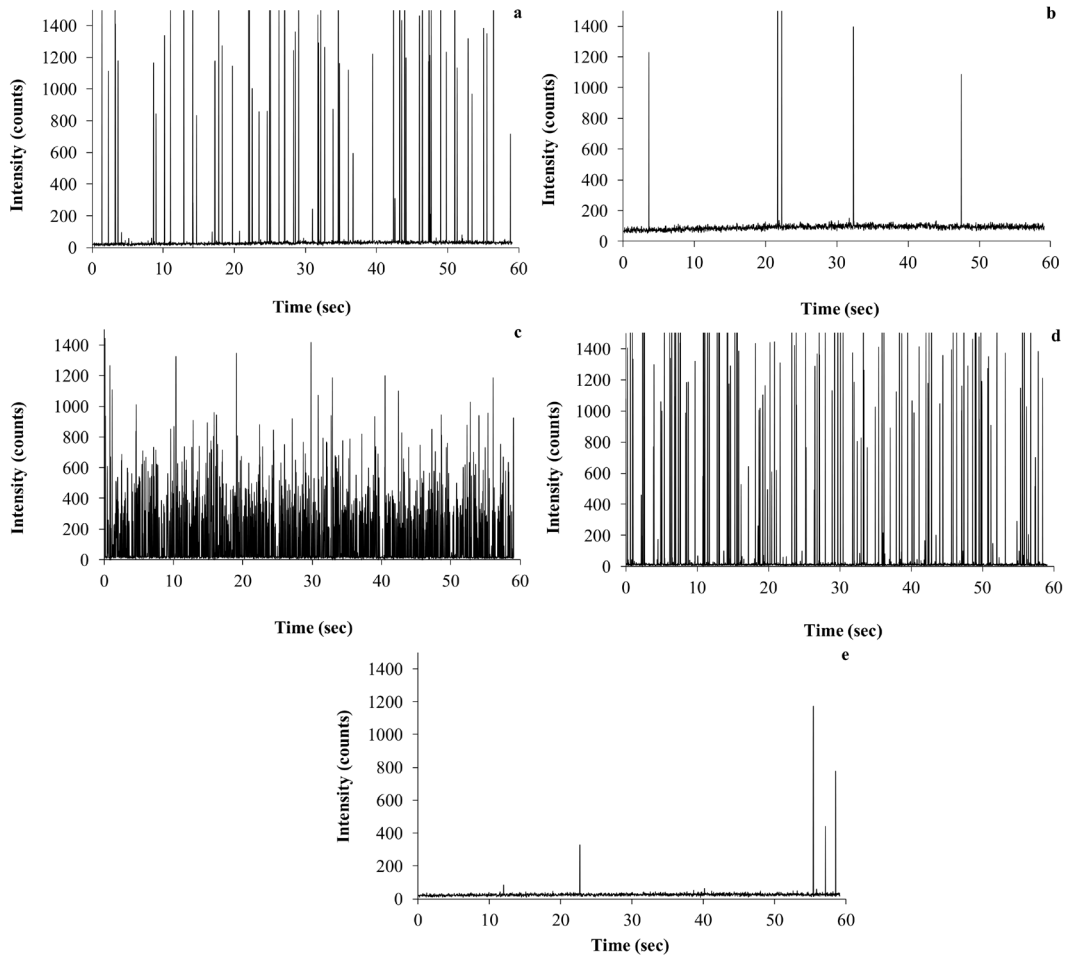

Fig 3.5 *SP-ICP-MS time-resolved signal plots for 200 nm citrate silver nanoparticles obtained from DIN 38414-S4 leaching experiments using Soil 1 (**a**), Soil 2 (**b**), Soil 3 (**c**), Soil 4 (**d**) and Soil 5 (**e**).*

lower amount of organic matter than the rest. Some studies have related the presence of organic matter to the colloidal stability of NPs due to electrostatic and steric interactions [3.3,3.48].

For the DTPA leaching procedure, the results obtained by SP-ICP-MS analysis of leachates of different types of coated AgNPs, different AgNPs sizes and different tested soils indicated that silver was dissolved in all cases, except for 75 nm PVP-AgNPs and 100 nm PEG-AgNPs leachates that seem to contain some nanoparticles, due to the presence of some peak pulses above the baseline (Supporting information of this chapter ***Fig. S3.5***). Even in these two the cases, number of particles is very small, as can be observed in the histograms (Supporting information of this chapter ***Fig. S3.6***). The presence of mainly dissolved silver in all the DTPA leachates could be due to the complexation capacity of DTPA, which could leach silver ions (Ag^+) strongly attached

to soils, as was already observed (***Table 3.2***).

3.4 Conclusions

The interaction of AgNPs with soils and their transformations depend on several factors, including the physicochemical characteristics of the soil, the clay mineralogy, as well as the size and coating of the nanoparticles. The goal of the present work was to study the parameters that control the kinetic adsorption processes of AgNPs, including both those related to soil features and those affected by nanoparticle characteristics. The results showed that cation exchange capacity and electrical conductivity, which are related to soil clay mineralogy, are the main soil features affecting these processes. On the other hand, highly negatively charged citrate-coated AgNPs were retained less than almost neutral polyethyleneglycol-coated AgNPs and negatively charged polyvinylpyrrolidone-coated AgNPs for most of the soils, organic matter content being one of the factors that hampers their adsorption. Citrate-coated AgNPs of different sizes showed slower retention of smaller nanoparticles (40nm) than bigger ones (100 and 200nm) in one of the soils.

Soils were submitted to the leaching procedures 3 weeks after the adsorption process. The results derived from the analysis of the leachates confirmed the low mobility and bioavailability of AgNPs. Only a small fraction of the nanoparticles (<5%) was leached from soils. The smallest nanoparticles used in this work (40 nm) were more easily eluted than larger ones (100 and 200 nm) with DIN 38414-S4, being transformed to soluble forms. It is also interesting to remark that both the capping agent of the nanoparticle and soil physicochemical characteristics seemed to have an effect on the dissolution process of AgNPs. PEG-coated nanoparticles were more easily dissolved than citrate- or PVP-coated ones, and organic matter seemed to stabilise the nanoparticles, avoiding their dissolution. Although this work clarifies some aspects of AgNP adsorption and desorption behaviour in soils, more work is needed in order to completely understand these processes.

Acknowledgments

The Spanish Ministry of Economy and Competitiveness financed this work through the project CGL2013-48802-C3-2-R (Program 2014) and L. Torrent gratefully acknowledges a FPI grant (Ref. BES-2014-070625). The authors are also thankful to Andreu Llort and Albert Salado for their contribution on the performance of this work and the University of Girona for financial support (MPCUdG2016/103).

References

[3.1] J. Pulit-Prociak, M. Banach, Silver nanoparticles – a material of the future...?, Open Chem. 14 (2016) 76–91.

[3.2] M. Sajid, M. Ilyas, C. Basheer, M. Tariq, M. Daud, N. Baig, *et al.*, Impact of nanoparticles on human and environment: review of toxicity factors, exposures, control strategies, and future prospects, Environ. Sci. Pollut. Res. 22 (2015) 4122–4143.

[3.3] V.L. Pachapur, A.D. Larios, M. Cledón, S.K. Brar, M. Verma, R.Y. Surampalli, Behavior and characterization of titanium dioxide and silver nanoparticles in soils, Sci. Total Environ. 563–564 (2016) 933–943.

[3.4] F. Van Koetsem, T.T. Geremew, E. Wallaert, K. Verbeken, P. Van der Meeren, G. Du Laing, Fate of engineered nanomaterials in surface water: factors affecting interactions of Ag and CeO_2 nanoparticles with (re)suspended sediments, Ecol. Eng. 80 (2015) 140–150.

[3.5] M. Li, P. Wang, F. Dang, D.-M. Zhou, The transformation and fate of silver nanoparticles in paddy soil: effects of soil organic matter and redox conditions, Environ. Sci. Nano. 4 (2017) 919–928.

[3.6] A. Azimzada, N. Tufenkji, K.J. Wilkinson, Transformations of silver nanoparticles in wastewater effluents: links to Ag bioavailability, Environ. Sci. Nano. 4 (2017) 1339–1349.

[3.7] J.R. Peralta-Videa, L. Zhao, M.L. Lopez-Moreno, G. de la Rosa, J. Hong, J.L. Gardea-Torresdey, Nanomaterials and the environment : a review for the biennium 2008–2010, J. Hazard. Mater. 186 (2011) 1–15.

[3.8] P.S. Tourinho, C.A.M. Van Gestel, S. Lofts, C. Svendsen, A.M.V.M. Soares, S. Loureiro, Metal-based nanoparticles in soil: fate, behavior, and effects on soil invertebrates, Environ. Toxicol. Chem. 31 (2012) 1679–1692.

[3.9] T.K. Darlington, A.M. Neigh, M.T. Spencer, O.T. Nguyen, S.J. Oldenburg, Nanoparticle characteristics affecting environmental fate and transport through soil, Environ. Toxicol. Chem. 28 (2009) 1191–1199.

[3.10] P. Christian, F. Von der Kammer, M. Baalousha, Th. Hofmann, Nanoparticles: structure, properties, preparation and behaviour in environmental media, Ecotoxicology 17 (2008) 326–343.

[3.11] S. Lin, Y. Cheng, J. Liu, M.R. Wiesner, Polymeric coatings on silver nanoparticles hinder autoaggregation but enhance attachment to uncoated surfaces, Langmuir 28 (2012) 4178–4186.

[3.12] E. McGillicuddy, I. Murray, S. Kavanagh, L. Morrison, A. Fogarty, M. Cormican, *et al.*, Silver nanoparticles in the environment: sources, detection and ecotoxicology, Sci. Total Environ. 575 (2017) 231–246.

[3.13] C. Schultz, K. Powell, A. Crossley, K. Jurkschat, P. Kille, A.J. Morgan, *et al.*, Analytical approaches to support current understanding of exposure, uptake and distributions of engineered nanoparticles by aquatic and terrestrial organisms, Ecotoxicology 24 (2015) 239–261.

[3.14] M. Hoppe, R. Mikutta, J. Utermann, W. Duijnisveld, G. Guggenberger, Retention of sterically and electrosterically stabilized silver nanoparticles in soils, Environ. Sci. Technol. 48 (2014) 12628–12635.

[3.15] J. He, D. Wang, D. Zhou, Transport and retention of silver nanoparticles in soil: effects of input concentration, particle size and surface coating, Sci. Total Environ. 648 (2019) 102–108.

[3.16] S. Treumann, S. Torkzaban, S.A. Bradford, R.M. Visalakshan, D. Page, An explanation for differences in the process of colloid adsorption in batch and column studies, J. Contam. Hydrol. 164 (2014) 219–229.

[3.17] F. Plassard, T. Winiarski, M. Petit-Ramel, Retention and distribution of three heavy metals in a carbonated soil: comparison between batch and unsaturated column studies, J. Contam. Hydrol. 42 (2000) 99–111.

[3.18] A. Praetorius, N. Tufenkji, K.-U. Goss, M. Scheringer, F. Von der Kammer, M. Elimelech, The road to nowhere: equilibrium partition coefficients for nanoparticles, Environ. Sci. Nano. 1 (2014) 317–323.

[3.19] G. Cornelis, Fate descriptors for engineered nanoparticles: the good, the bad, and the ugly, Environ. Sci. Nano. 2 (2015) 19–26.

[3.20] G. Cornelis, C. Doolette, M. Thomas, M.J. McLaughlin, J.K. Kirby, D.G. Beak, D. Chittleborough, Retention and dissolution of engineered silver nanoparticles in natural soils, Soil Sci. Soc. Am. J. 76 (2012) 891–902.

[3. 21] S. Klitzke, G. Metreveli, A. Peters, G.E. Schaumann, F. Lang, The fate of silver nanoparticles in soil solution—sorption of solutes and aggregation, Sci. Total Environ. 535 (2015) 54–60.

[3.22] C. Coutris, E.J. Joner, D.H. Oughton, Aging and soil organic matter content affect the fate of silver nanoparticles in soil, Sci. Total Environ. 420 (2012) 327–333.

[3.23] D.A. Navarro, J.K. Kirby, M.J. McLaughlin, L. Waddington, R.S. Kookana, Remobilisation of silver and silver sulphide nanoparticles in soils, Environ. Pollut. 193 (2014) 102–110.

[3.24] M. Hoppe, R. Mikutta, J. Utermann, W. Duijnisveld, S. Kaufhold, C.F. Stange, *et al.*, Remobilization of sterically stabilized silver nanoparticles from farmland soils determined by column leaching, Eur. J. Soil Sci. 66 (2015) 898–909.

[3.25] G. Rauret, Extraction procedures for the determination of heavy metals in contaminated soil

and sediment, Talanta 46 (1998) 449–455.

[3.26] F. Dang, Y. Jiang, M. Li, H. Zhong, W.G.M. Peijnenburg, W. Shi, *et al.*, Oral bioaccessibility of silver nanoparticles and ions in natural soils: importance of soil properties, Environ. Pollut. 243 (2018) 364–373.

[3.27] G.F. Koopmans, T. Hiemstra, I.C. Regelink, B. Molleman, R.N.J. Comans, Asymmetric flow field-flow fractionation of manufactured silver nanoparticles spiked into soil solution, J. Chromatogr. A 1392 (2015) 100–109.

[3.28] D.M. Mitrano, J.F. Ranville, A. Bednar, K. Kazor, A.S. Hering, C.P. Higgins, Tracking dissolution of silver nanoparticles at environmentally relevant concentrations in laboratory, natural, and processed waters using single particle ICP-MS (spICP-MS), Environ. Sci. Nano. 1 (2014) 248-259.

[3.29] M.D. Montaño, H.R. Badiei, S. Bazargan, J.F. Ranville, Improvements in the detection and characterization of engineered nanoparticles using spICP-MS with microsecond dwell times, Environ. Sci. Nano. 1 (2014) 338-346.

[3.30] F. Laborda, J. Jiménez-Lamana, E. Bolea, J.R. Castillo, Critical considerations for the determination of nanoparticle number concentrations, size and number size distributions by single particle ICP-MS, J. Anal. At. Spectrom. 28 (2013) 1220–1232.

[3.31] J. Tuoriniemi, G. Cornelis, M. Hassellöv, Size discrimination and detection capabilities of single-particle ICPMS for environmental analysis of silver nanoparticles, Anal. Chem. 84 (2012) 3965–3972.

[3.32] Y. Yang, C.-L. Long, Z.-G. Yang, H.-P. Li, Q. Wang, Characterization and determination of silver nanoparticle using single particle-inductively coupled plasma-mass spectrometry, Chin. J. Anal. Chem. 42 (2014) 1553–1560.

[3.33] S.M. Majedi, H.K. Lee, Recent advances in the separation and quantification of metallic nanoparticles and ions in the environment, Trends Anal. Chem. 75 (2016) 183–196.

[3.34] Nanocomposix. Standard Capping Agents, 2018. Available at: http://cdn.shopify.com/s/files/1/0257/8237/files/Standard_Capping_Agents.pdf. Accessed date: 6 February 2018.

[3.35] German Standard legislation, DIN 38414-S4 German Standards Methods for Examination of Water, Waste Water and Sludge; Group S (Sludge and Sediments); Determination of Leachability by Water (S4), Deutsches Institut für Normung E.V. (DIN), Berlin, 1984.

[3.36] P. Quevauviller, Operationally defined extraction procedures for soil and sediment analysis I. Standardization, Trends Anal. Chem. 17 (1998) 289–298.

[3.37] D.S. Kosson, H.A. Van der Sloot, T.T. Eighmy, An approach for estimation of contaminant release during utilization and disposal of municipal waste combustion residues, J. Hazard. Mater. 47 (1996) 43–75.

[3.38] B.M. Simonet, M. Valcárcel, Monitoring nanoparticles in the environment, Anal. Bioanal. Chem. 393 (2009) 17–21.

[3.39] K. Sigfridsson, A. Lundqvist, M. Strimfors, Evaluation of exposure properties after injection of nanosuspensions and microsuspenions into the intraperitoneal space in rats, Drug Dev. Ind. Pharm. 39 (2013) 1832–1839.

[3.40] N.A. Anjum, S.S. Gill, A.C. Duarte, E. Pereira, I. Ahmad, Silver nanoparticles in soil–plant systems, J. Nanopart. Res. 15 (2013) 1896.

[3.41] G. Cornelis, L. Pang, C. Doolette, J.K. Kirby, M.J. McLaughlin, Transport of silver nanoparticles in saturated columns of natural soils, Sci. Total Environ. 463–464 (2013) 120–130.

[3.42] L.E. Barton, M. Therezien, M. Auffan, J.-Y. Bottero, M.R. Wiesner, Theory and methodology for determining nanoparticle affinity for heteroaggregation in environmental matrices using batch measurements, Environ. Eng. Sci. 31 (2014) 421–427.

[3.43] Tech Note: Zeta/pH Curves and Isoelectric Point Data for Standard Nanocomposix Silver Citrate and PVP Nanoparticle Dispersions, 2012. Available at: https://cdn.shopify.com/s/files/1/0257/8237/files/Tech_Note_-_Zeta_and_pH_Curves_for_nanoComposix_Citrate_and_PVP_Capped_Silver_Nanoparticles.pdf. Accessed date: 18 August 2017.

[3.44] T.C. Prathna, N. Chandrasekaran, A. Mukherjee, Studies on aggregation behaviour of silver nanoparticles in aqueous matrices: effect of surface functionalization and matrix composition, Colloids Surf. A Physicochem. Eng. Asp. 390 (2011) 216–224.

[3.45] Q. Ketterings, S. Reid, R. Rao, Cation Exchange Capacity (CEC), Agron. Fact Sheet Ser. 22 (2007) 1–2.

[3.46] L. Torrent, M. Iglesias, M. Hidalgo, E. Marguí, Analytical capabilities of total reflection X-ray fluorescence spectrometry for silver nanoparticles determination in soil adsorption studies, Spectrochim. Acta Part B At. Spectrosc. 126 (2016) 71-78.

[3.47] A. Solé, F. Plana, F. Gallart, R. Josa, G. Pardini, R. Aringhieri, , How mudrock and soil physical properties influence badland formation at Vallcebre (pre-pyrenees, NE Spain), Catena 19 (1992) 287–300.

[3.48] A.D. Dwivedi, S.P. Dubey, M. Sillanpää, Y.-N. Kwon, C. Lee, R.S. Varma, Fate of engineered

nanoparticles: implications in the environment, Coord. Chem. Rev. 287 (2015) 64–78.

[3.49] G. Anderegg, F. Arnaud-Neu, R. Delgado, J. Felcman, K. Popov, Critical evaluation of stability constants of metal complexes of complexones for biomedical and environmental applications (IUPAC Technical Report), Pure Appl. Chem. 77 (2005) 1445–1495.

[3.50] Y. Liang, S.A. Bradford, J. Simunek, H. Vereecken, E. Klumpp, Sensitivity of the transport and retention of stabilized silver nanoparticles to physicochemical factors, Water Res. 47 (2013) 2572–2582.

[3.51] E. Marguí, V. Salvadó, I. Queralt, M. Hidalgo, Comparison of three-stage sequential extraction and toxicity characteristic leaching tests to evaluate metal mobility in mining wastes, Anal. Chim. Acta 524 (2004) 151–159.

[3.52] F. Laborda, E. Bolea, J. Jiménez-Lamana, Single particle inductively coupled plasma mass spectrometry: a powerful tool for nanoanalysis, Anal. Chem. 86 (2014) 2270–2278.

Supplementary information

Table S3.1 *Instrumental specifications and operating conditions.*

Agilent 5100 Vertical Dual View ICP-OES spectrometer	
Ag wavelength	328.068 nm
Wavelength selector	Echelle polychromator
RF power	1200 W
Pump speed	12 r min^{-1}
Plasma configuration	Axial (double vision)
Plasma gas flow rate	12 L min^{-1}
Spray chamber	Double pass glass cyclonic
Nebuliser	Concentric glass
Nebuliser flow rate	0.7 L min^{-1}
Detector	Charge-coupled device (CCD)
Reading time	1 sec
Readings per replicate	3
Agilent 7500c ICP-MS spectrometer	
RF power	1500 W
Plasma gas flow rate	15 L min^{-1}
Nebuliser	Babington
Nebuliser chamber	Double pass scott
Nebuliser gas flow rate	1.1 L min^{-1}
Pump speed	12 r min^{-1}
Sampling cone	Ni, 1 mm aperture diameter
Skimmer cone	Ni, 0.4 mm aperture diameter
Analyser	Quadrupole
Detector	Electron multiplier
Integration time for each isotope	10 msec
Reading time	60 sec
Isotopes monitored	^{107}Ag

Table S3.2 *Particle size distribution of studied soils (determined by granolometry).*

	>2 mm	2-1 mm	1-0.5 mm	0.5-0.25 mm	0.25-0.125 mm	<0.125 mm
Soil 1	5.7	11.2	29.3	21.7	10.3	21.2
Soil 2	14.6	8.1	11.6	19.4	18.2	28.2
Soil 3	4.7	2.5	3.0	39.6	46.4	3.8
Soil 4	3.1	1.6	4.6	10.2	28.4	52.2
Soil 5	-	7.4	19.2	23.6	17.4	31.8

Table S3.3 *Mineral composition of studied soils obtained by X-ray diffraction analysis powder & oriented aggregates.*

	Soil 1	Soil 2	Soil 3	Soil 4	Soil 5
Albite	-	-	-	-	++
Calcite	+	+++	+++	+++	++
Chlorite	-	-	-	+	++
Dolomite	+++	+	+	++	+
Feldspar	-	-	+	-	-
Gypsum	-	+++	-	-	-
Hematite	+	+	+	-	-
Illite	-	-	+	+	++
Kaolinite	+	+	+	-	-
Quartz	+++	++	+++	+++	+++
Smectite	+	+	-	-	-
Sanidine	-	-	-	++	++

- absent, + trace, ++ minor, +++ major.

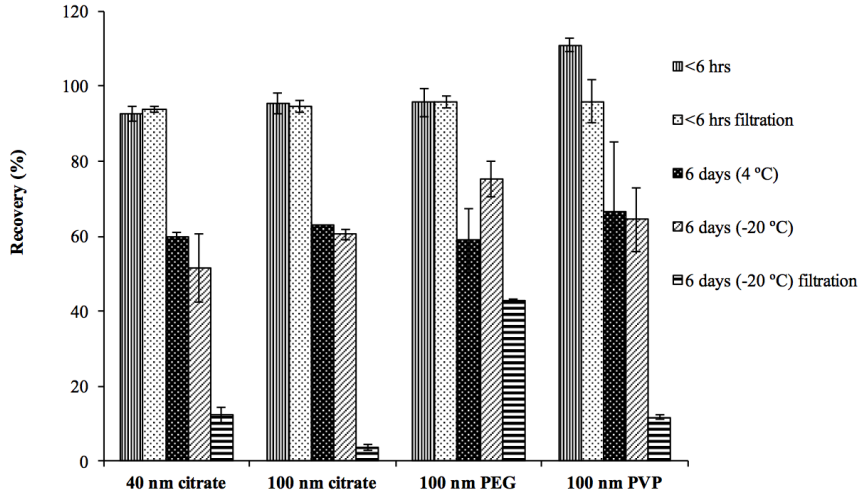

Fig. S3.1 *Silver nanoparticles recovery (%) from stability and storage studies.*

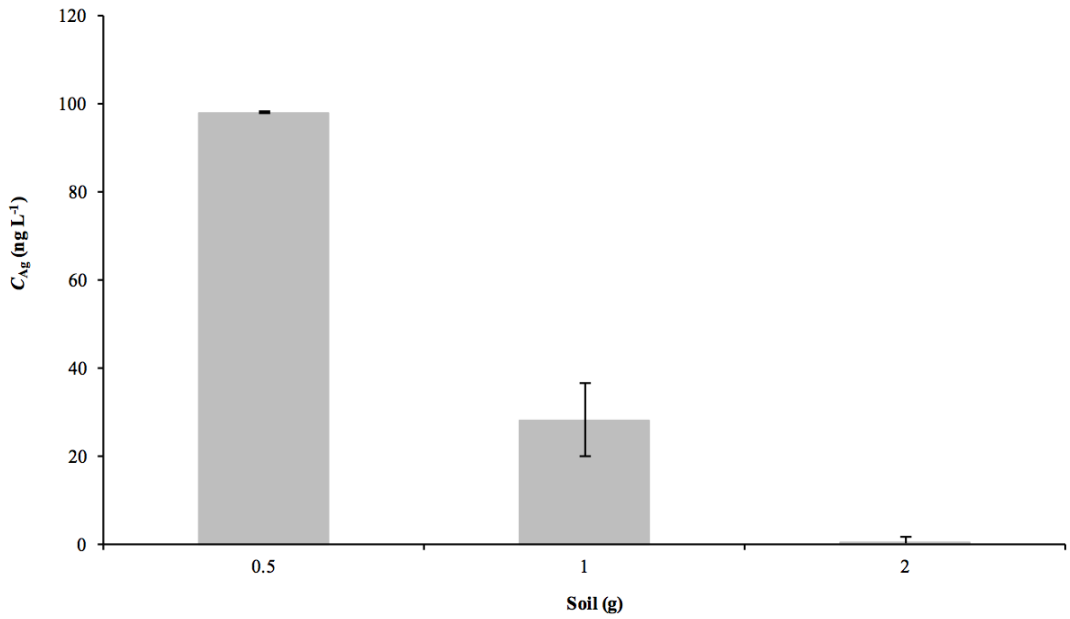

Fig. S3.2 *Silver nanoparticles concentration in the supernatant after 2 hr of soil-silver nanoparticles solution contact using different amounts of Soil 3 (20 mL of 1 mg L^{-1} citrate-AgNPs (100 nm) suspension).*

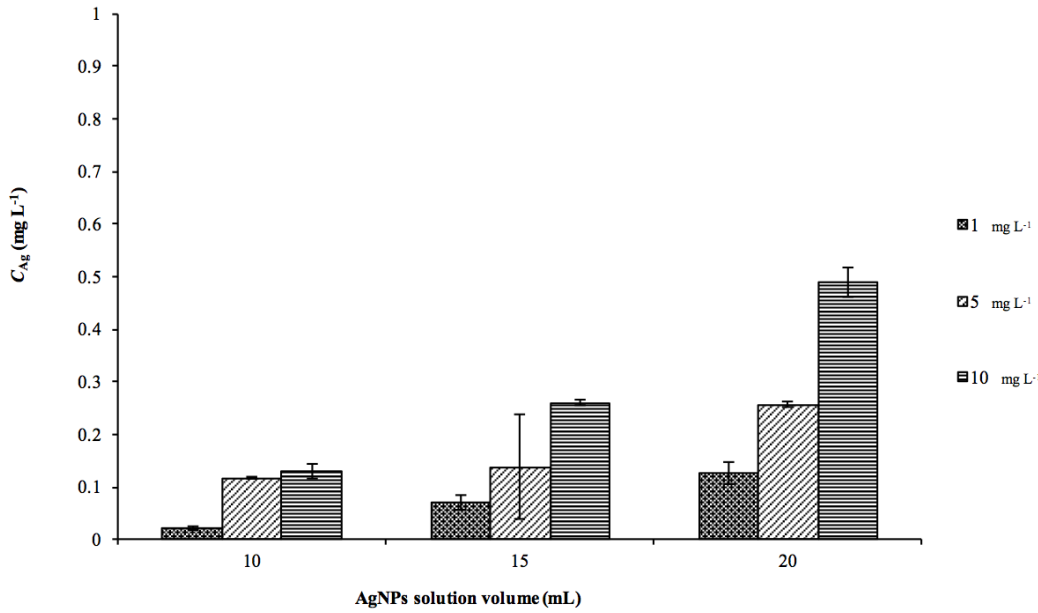

Fig. S3.3 *Silver nanoparticles (AgNPs) concentration in the supernatant after batch adsorption experiments (2 hr) using different AgNPs suspensions volumes and concentrations (0.5 g of Soil 3 and polyvinylpyrrolidone-AgNPs (75 nm) suspension).*

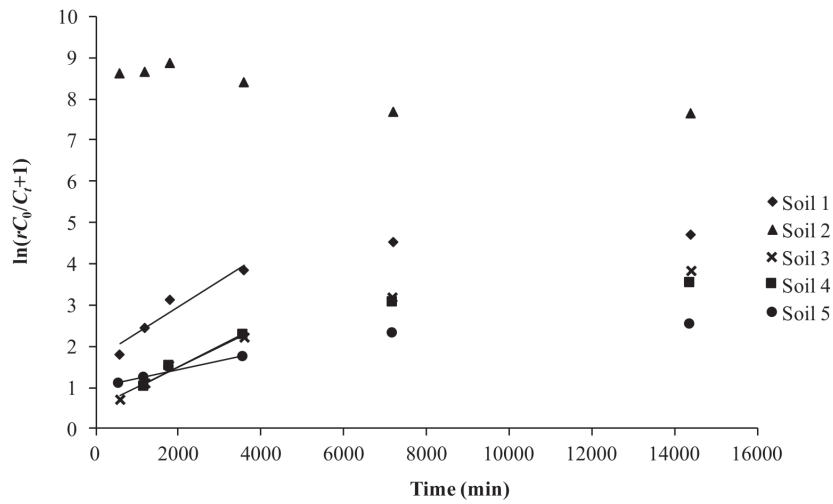

Fig. S3.4 *Representation of ln(rC_o/C_t+1) versus time to determine soil affinity coefficients.*

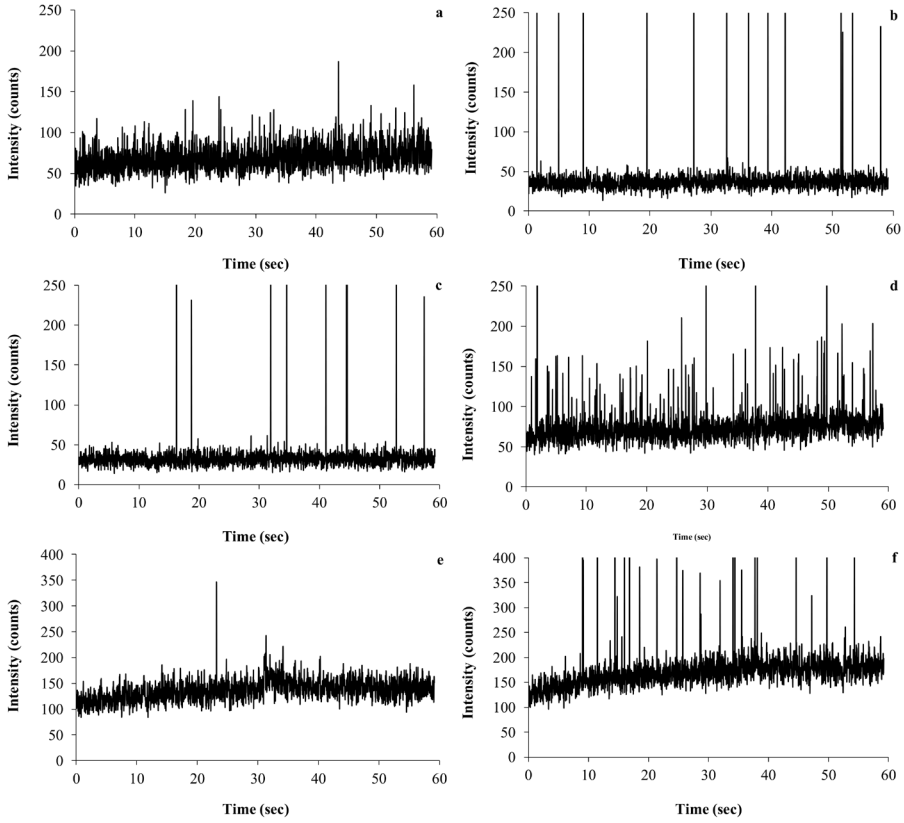

Fig S3.5 *SP-ICP-MS time-resolved signal plots of DTPA (diethylenetriaminepentaacetic acid) leachates for Soil 3 using different types of silver nanoparticles (**a**: citrate 40 nm; **b**: citrate 100 nm; **c**: citrate 200 nm; **d**: polyvinylpyrrolidone 75 nm; **e**: polyvinylpyrrolidone 100 nm; **f**: polyethyleneglycol 100 nm).*

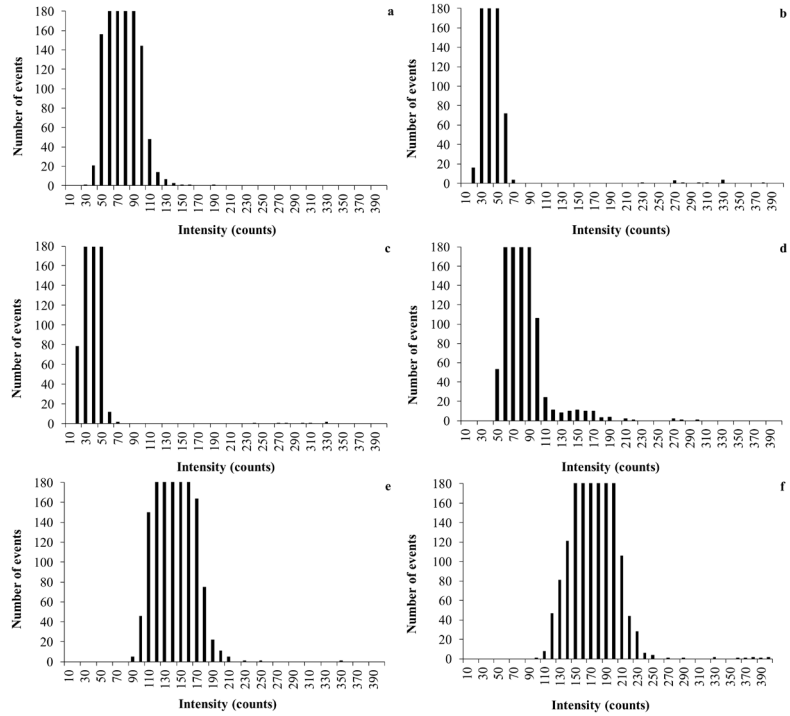

Fig S3.6 *SP-ICP-MS histograms of DTPA leachates of Soil 3 using different types of silver nanoparticles (**a**: citrate 40 nm; **b**: citrate 100 nm; **c**: citrate 200 nm; **d**: polyvinylpyrrolidone 75 nm; **e**: polyvinylpyrrolidone 100 nm; **f**: polyethylenglycol 100 nm).*

CHAPTER 4

Analytical capabilities of total reflection X-ray fluorescence spectrometry for silver nanoparticles determination in soil adsorption studies

This chapter corresponds to the following publication:

L. Torrent, M. Iglesias, M. Hidalgo, E. Marguí, *Analytical capabilities of total reflection X-ray fluorescence spectrometry for silver nanoparticles determination in soil adsorption studies*. Spectrochim. Acta Part B, Atomic spectroscopy 126 (2016) 71-78

Abstract

In recent years, the production of silver nanoparticles (AgNPs) has grown due to their antibacterial properties. This fact enhances the release of these particles into the environment, especially in soils that are the major sink. To better understand adsorption processes in soils, usually batch kinetic studies are carried out. In this context, we tested the possibilities of using total reflection X-ray fluorescence spectrometry (TXRF) to monitor the silver content in soil adsorption kinetic studies. It was found that the lower limit of detection for Ag (through Ag-Kα detection) in aqueous solutions was around 37 μg L^{-1}, which was suitable to carry out this kind of studies. Moreover, the direct analysis of Ag adsorbed onto soil after the kinetic studies was investigated. In this case, the limit of detection for Ag was around 1.7 mg kg^{-1}. All TXRF results were compared with those obtained by inductively coupled plasma optic emission spectrometry and good agreement was found. The batch adsorption tests performed showed that 98% of polyvinylpyrrolidone coated AgNPs were retained on the tested soils in <6 h.

Keywords: Silver nanoparticles, Soils, Sorption study, Total reflection X-ray fluorescence spectrometry, Suspension

4.1 Introduction

Nanoparticles are nanomaterials with three dimensions with a size range below 100 nm. Particles of this size are present in environmental compartments, however in recent years the production and use of engineered nanomaterials (ENMs) for several industrial applications has grown [4.1,4.2]. Among the different types of ENMs, metallic nanoparticles have been increasingly used in many products with different purposes. One of the most utilised metallic nanoparticles are silver nanoparticles (AgNPs) which are added as antibacterial agents in commercial products like clothes, domestic appliances, paints, food storage containers, varnish, medical products, cosmetic products and children's toys [4.2,4.3].

Despite the many existing sources of release, the major sink of AgNPs deposition into the environment is currently in soils through the application of treated effluents and sewage sludge from wastewater treatment plants [4.4]. Soils are complex matrices, because they consist of a solid phase that contains minerals and organic matter, as well as a liquid phase, which contains appreciable amounts of natural colloids and particulate materials. AgNPs can easily interact with all these components. These interactions can lead to processes such as aggregation/agglomeration, sorption to surfaces and dissolution to ionic metals affecting the mobility, transport and bioavailability of these pollutants [4.5]. Sorption is one of the main processes that regulate the mobility of these emerging contaminants. In this process, the substances are attached to solid surfaces by Van der Waals attraction forces (physisorption), electrostatic interactions (cation exchange) or chemical bounding (chemisorption) [4.6]. These interactions occur depending on soil properties (ionic strength, pH, Z-potential, cation exchange capacity and texture) and the physicochemical properties of pollutants (dispersion, agglomeration/aggregation, dissolution rate, size, surface area and charge, and surface chemistry). These features are unique for AgNPs due to their small size. Moreover, coating greatly affects AgNPs behaviour in the environment. As a consequence of the different characteristics that present these emerging pollutants in comparison to bulk silver (Ag), it is believed that their behaviour in the environment may be different from their homologous metals in solution [4.2,4.7]. For this reason, it is important to evaluate the presence of these particles through the environment.

To assess the transport and retention of AgNPs in terrestrial environments, several studies based on column experiments have been published. Some of them were performed using inert porous media with glass beads, quartz or sand [4.8-4.11]. In these tests, the complexity of soils cannot be completely represented because these artificial soils do not contain the same components as natural

soils. Consequently, the approach of the mobility of AgNPs cannot be totally reflected. However, in recent studies the AgNPs dispersions were percolated through real soils in column tests [4.12-4.16], addressing to the real transport of the pollutants in natural matrices. Another approach for investigating the interactions between the pollutants and the natural components of soils are batch adsorption studies, which are designed to examine the thermodynamic equilibrium. Despite the differences between the two methodologies for the evaluation of pollutants mobility, both can be used to study the adsorption of AgNPs on soil [4.12,4.16-4.22].

Usual analytical techniques for the quantitative detection of AgNPs in solid (soil) and liquid (aqueous) phase from batch adsorption studies include inductively coupled plasma optical emission spectrometry (ICP-OES) and inductively coupled plasma mass spectrometry (ICP-MS), which allow the determination of total silver concentration [4.23]. However, one of the main disadvantages of these instruments is that samples can only be analysed in liquid phase, and therefore soil samples have to be treated by means of an acidic digestion before being analysed [4.24]. This means that solid samples treatment is time-consuming in comparison with liquid samples that can be directly analysed. Furthermore, the use of corrosive and harmful reagents for the digestion process and the large consumption of argon gas for ICP measurements make these techniques expensive. Hence, the development of rapid and low cost analytical techniques combined with minimum sample treatment is needed.

Total reflection X-ray fluorescence spectrometry (TXRF) is a powerful microanalytical technique for trace element determination in several types of samples, especially liquid samples or fine powdered materials, among others [4.25,4.26]. This spectrometric technique is a variant of energy dispersive X-ray fluorescence (EDXRF) where the main difference to conventional EDXRF is that the monochromatic X-ray beam is directed onto the sample at an angle that is smaller than the critical angle (usually <0.1°). As a result, the beam interacts minimally with the sample holder leading to a total reflection of the beam's photons. Characteristic X-rays emitted from the sample enter into a solid-state energy dispersive detector that is very close to the sample (~0.5 mm). Due to the total reflection of the beam and the proximity of the detector to the sample, an improvement of the sensitivity is achieved in comparison to conventional EDXRF systems. To perform analysis under total reflection conditions, samples must be provided as thin films. For liquid samples, this is done by depositing 5-50 µL of sample on a reflective carrier with a subsequent drying by applying heat or vacuum. Preparation of samples as thin layers exclude matrix effects, like absorption and secondary

excitation and thus, the quantification in TXRF analysis can be done directly by the addition of an internal standard to the sample.

Last decades, most of the published TXRF analyses were performed using instruments based on high-power X-ray tubes that required water-cooling systems and liquid-nitrogen cooled detectors. But nowadays, the commercially TXRF instruments available are benchtop systems equipped with air-cooled low-power X-ray tubes and Peltier cooled silicon drift detectors (SDD), making this technique simpler, cheaper and more available in many fields [4.27-4.32].

The aim of this research is to evaluate the TXRF capabilities for the determination of silver nanoparticles in soils and aqueous matrices as a cost-effective alternative to commonly used atomic spectrometric techniques. As a study case, the TXRF developed method was tested to study AgNPs adsorption in soils through batch adsorption experiments. To our knowledge, very few papers about TXRF determination of AgNPs exist, and there are none for AgNPs determination in soil and aqueous solutions.

First, an evaluation of the best sample preparation and TXRF measurement conditions for Ag determination in soils and soil supernatants was made. The analytical figures of merit (limits of detection (LODs), accuracy and precision of results) for both methodologies were evaluated and the obtained results were compared with those obtained by means of ICP-OES.

4.2 Experimental

4.2.1 Reagents, materials and apparatus

A commercial solution of AgNPs stabilised with sodium citrate (100 nm) was purchased from Sigma Aldrich (St. Louis, USA). Polyethyleneglycol coated AgNPs of 100 nm (AgNPs-PEG) and polyvinylpyrrolidone coated AgNPs (AgNPs-PVP) of 75 nm and 100 nm were from NanoComposix (San Diego, USA). A silver stock solution of 1,000 ± 2 mg L^{-1} (Merck KGaA, Darmstadt, Germany) was used to determine the limit of detection of this element in TXRF analysis and for preparing the ICP-OES standard solutions. To dilute stock solutions and samples, high purity water obtained from a Milli-Q purification system (Millipore Corp., Bedford, MA) was employed. The non-ionic surfactant Triton X-100 (polyethyleneglycol tert-octylphenyl ether) was purchased from Sigma Aldrich (St. Louis, USA) and a stock solution of palladium (Pd, 1,016 mg L^{-1}) used as an internal standard (IS) was acquired from Aldrich Chemical Company (Milwaukee, USA). For microwave sample digestion, analytical grade hiperpur quality nitric acid (HNO_3 69%, Ag 0.1 ng g^{-1}, Panreac,

Barcelona, Spain) and hydrochloric acid (HCl 35%, Panreac, Barcelona, Spain) were used.

Batch adsorption experiment was performed using a rotary mixer Dinko (Barcelona, Spain). The separation of soil and soil extracts after batch adsorption experiment was done with a Rotofix 32A centrifuge (Hettich-Zentrifugen, Lauenau, Germany). An ultrasonic bath J.P. Selecta (Barcelona, Spain) was used in order to break down the possible aggregated AgNPs.

The acid digestion of soil samples was performed with an ETHOS PLUS Milestone microwave digestion system (Sorisole, Bergamo, Italy) equipped with HPR-1000/10S high pressure segmented rotor and a temperature sensor.

Finally, in TXRF analysis, quartz glass discs with a diameter of 30 mm and a thickness of 3 ± 0.1 mm were used as sample holders. The sample carriers were siliconised before sample deposition by silicone from Serva Electrophoresis GmbH (Heidelberg, Germany). GXR1 (Drum Mountains soil, [Ag] = 32.6 ± 0.9 mg kg^{-1}, U.S. Geological Survey Geochemical Reference Materials and Certificates, Virginia, USA), GXR2 (Park City soil, [Ag] = 17.4 ± 0.6 mg kg^{-1}, U.S. Geological Survey Geochemical Reference Materials and Certificates, Virginia, USA), SLUDGE 2 (sewage sludge, [Ag] = 70.40 ± 4.36 mg kg^{-1}, Resource Technology Corporation, Laramie, USA), SLUDGE 3 (sewage sludge, [Ag] = 100.00 ± 9.96 mg kg^{-1}, Resource Technology Corporation, Laramie, USA) certified reference materials (CRM) were used to evaluate limits of detection and accuracy for Ag determination in soils by TXRF.

4.2.2 Soil samples

To study the applicability of the developed methodology for the intended purpose, two farmland soil samples were studied (SOIL 1 and SOIL 2). These soils were selected due to their different physicochemical characteristics. As it is shown in ***Table S4.1*** (Supporting information of this chapter), SOIL 1 (Gavà, Barcelona, Spain) contained mainly particles of 0.25–0.1 mm in comparison with SOIL 2 (Castellbisbal, Barcelona, Spain) that contain a larger proportion of particles <0.1 mm. Conductivity was also quite different between both soils with values of 427.33 µS cm^{-1} for SOIL 1 and 276.5 µS cm^{-1} for SOIL 2, respectively (see ***Table S4.2*** from the Supporting information of this chapter). Other characteristics of these soils are shown in the Supporting information of this chapter (***Table S4.2***).

4.2.3 AgNPs batch adsorption experiments

In this work, batch adsorption experiments were done to study the interaction between AgNPs

and soil in laboratory conditions. With this purpose, 1.0 g of SOIL 1 and 0.5 g of SOIL 2 were weighted into polystyrene tubes of 25 mL. Then, 20 mL of a 10 mg L^{-1} aqueous solution of AgNPs-PVP with a diameter of 75 nm were added and they were submitted to rotation with a rotary mixer at 35 rpm.

Afterwards, each sample (7 samples in duplicate) submitted to rotation was removed at a specific time (10 min, 20 min, 30 min, 60 min, 120 min, 240 min, 360 min) and they were centrifuged at 3500 rpm for 8 min. Next, the supernatant was pipetted to a new polystyrene tube and was stored overnight at 4 °C until its analysis.

4.2.3.1 Analysis of aqueous solutions

Prior to the analysis by ICP-OES and TXRF, the liquid samples obtained by batch adsorption experiments were subjected to ultrasonication for 5 min to break down the possible aggregated silver nanoparticles present in the aqueous solution. Next, the samples were shaken vigorously for 1 min and were then filtered through a 0.45 µm cellulose acetate filter (Whatman, Filterlab, Barcelona) to avoid suspended soil particles. After this procedure, soil extracts were analysed directly by ICP-OES with a calibration curve of ionic silver standards that ranged between 0.01 and 1.5 mg L^{-1}.

For the quantification of silver in TXRF analysis, 50 µL of Pd used as IS (final concentration 13 mg L^{-1}) were added to 0.5 mL of soil extract. Then, the aliquots were sonicated again for 5 min and homogenized with a vortex device for 1 min. After that, the sample carriers were siliconised with 10 µL of silicone and then dried using infrared radiation. Finally, an aliquot of 10 µL was deposited onto a quartz sample holder and was left to dry using infrared radiation. In a previous work we demonstrated that this was the optimum volume to carry out soil extract analysis by TXRF [4.31].

4.2.3.2 Analysis of soil samples

Before preparing soil suspensions, soil samples from batch adsorption experiments were dried overnight at 65–70 °C. Afterwards 50 mg of dried soil were suspended with 1 mL of a 1% Triton X-100 (non-ionic surfactant) solution. Then, 75 µL of Pd (200 mg L^{-1}) used for internal standardisation were added to the soil suspension. The resulting solution was homogenised with a vortex device and was stored at 4 °C until its analysis. For the TXRF analysis, suspension samples were sonicated for 5 min and homogenised for 1 min with a vortex device. Lastly

aliquots of 5 µL were deposited onto a siliconised quartz glass sample reflectors and dried with infrared radiation.

Table 4.1 *Instrumental characteristics and measurement conditions.*

S2 PICOFOX TXRF benchtop spectrometer	
Anode X-ray tube	Tungsten (W)
Voltage (kV)	50
Current intensity (µA)	1,000
Monochromator	Multilayer (Ni/C), 17.5 keV, 80% reflectivity
Silicon drift detector X-Flash®	<160 eV resolution Mn-K_α, 10 mm^2 active area
Working environment	Air
Live time (s)	2,000
Sample station	Automatic cassette changer for 25 samples
Size, weight	600 x 300 x 450 mm, 37 kg
Agilent 5100 Vertical Dual View ICP-OES spectrometer	
Ag wavelength	328.068 nm
Wavelength selector	Echelle polychromator
RF power	1,200 W
Pump speed	12 rpm
Plasma configuration	Axial (double vision)
Plasma gas flow rate	12 L min^{-1}
Spray chamber	Double pass glass cyclonic
Nebuliser	Concentric glass
Nebuliser flow rate	0.7 L min^{-1}
Detector	Charge-coupled device (CCD)
Reading time (s)	1
Stabilisation time (s)	25
Readings per replicate	3

To compare silver concentrations obtained using the TXRF method with those resulting from ICP-OES analysis it was necessary to perform a microwave acidic digestion of soil samples from batch adsorption experiments according to the EPA Method 3051A [4.33] (Method 3051A, US Environmental Protection Agency 2007). Following this method, 0.5 g of soil sample were placed in a polytetrafluoroethylene (PTFE) reactor with 3 mL of HNO_3 (69%) and 9 mL of HCl (35%). After capping the vessels, the samples were digested into the microwave following a digestion program consisting on a first step of 10 min to reach 200 °C, a second step of 15 min at 200 °C and a third step of 15 min of cooling to room temperature. Once at room

temperature, soil digests were filtered into polystyrene tubes and were diluted to 25 mL with Milli-Q water. These sample digests were analysed directly by ICP-OES.

For TXRF analysis, 75 µL of a Pd 200 mg L^{-1} Pd internal standard solution were added to 1 mL of soil digest. Afterwards, the mixture was homogenised with a vortex device for 1 min and an aliquot of 10 µL was deposited onto a pre-siliconised quartz sample carrier and it was dried with infrared radiation before TXRF analysis.

4.2.4 Instrumental conditions

The analysis of silver in soil extracts, soil suspensions and soil digests was done with a "S2 PICOFOX" benchtop TXRF spectrometer (Bruker AXS Microanalysis GmbH, Berlin, Germany). To verify TXRF results of total silver analysis in soil extracts and soil digests, an ICP-OES system (Agilent 5100 Vertical Dual View, Agilent Technologies, California, USA) was employed. The instrumental specifications and operating conditions for both systems are summarised in ***Table 4.1***.

4.3 Results and discussion

4.3.1 QA/QC

4.3.1.1 Aqueous samples

Firstly to check TXRF capabilities for silver nanoparticles determination in aqueous samples, LODs for ionic silver (Ag^+) and AgNPs with different coatings and sizes were evaluated. In all cases, experimental tests were carried out using a standard solution containing 1,000 µg L^{-1} of AgNPs or Ag^+. LODs calculation for each type of AgNPs and Ag^+ was based on the 3σ definition of the LOD [3.34].

As it is shown in ***Table 4.2***, no relevant differences were obtained between different types of silver nanoparticles and Ag^+ (LODs: 34-40 µg L^{-1} corresponding to 3.4-4 ng of Ag). Despite the fact that the obtained LODs were quite high taking into account AgNPs concentration in environmental waters [4.35], they are suitable to monitor AgNPs in soil adsorption studies. In addition, these values are lower than the existing bibliographic LODs obtained with molybdenum (Mo) X-ray tube measurements in ambient air conditions (50 ng of Ag), but slightly higher from the LODs obtained measuring with Mo X-ray tube in nitrogen atmosphere conditions (0.2 ng of Ag) [4.36]. The standards used for LODs calculation were also analysed

with ICP-OES and the values obtained were lower than the limits of detection of TXRF (see in ***Table 4.2***).

Table 4.2 *Limits of detection and quantitative results for the analysis of different Ag nanoparticles and ionic silver solutions (1,000 µg L^{-1}) by TXRF and ICP-OES.*

	TXRF					ICP-OES		
		Quantification mode-1[a]		Quantification mode-2[b]				
Standard	LOD (µg L^{-1})	Recovery (%)	RSD (%)[c]	Recovery (%)	RSD (%)[c]	LOD (µg L^{-1})	Recovery (%)	RSD (%)[c]
Citrate 100 nm	35	90	4	102	14	2	76.0	0.3
PVP 100 nm	34	108	6	113	14	2	113	1
PVP 75 nm	40	92	12	92	5	2	112.5	0.9
PEG 100nm	35	87	59	103	11	2	105	3
Ag^+	40	84	8	95	7	2	105.6	0.1

[a] *Quantification mode-1: internal standardisation (using Pd).*
[b] *Quantification mode-2: external calibration (using Ag area).*
[c] *RSD(%): relative standard deviation of duplicate analysis.*

As stated in the Introduction section, internal standardisation is usually employed as quantification strategy by TXRF. In the present contribution we compare the results obtained with this quantitative approach with the results obtained by external calibration.

The choice of the IS is certainly important; because it must not interfere with the analyte signal. Yttrium (Y) or gallium (Ga) are commonly used in TXRF water analysis as internal standards but these elements can be present in soil extracts. For example, in a previous study, considerable amounts of Ga (15 mg kg^{-1}) and Y (38 mg kg^{-1}) were found in the analysis of a soil CRM [4.30]. Therefore, in the present work, Pd was selected as internal standard for quantification purposes.

To evaluate the quantification mode, the same samples prepared for LODs determination were mixed with 50 µL of 100 mg L^{-1} Pd (final concentration 5 mg L^{-1}). Then the silver content of the samples was quantified by internal standardisation and by external calibration (AgNPs standards ranging from 200 to 2,000 µg L^{-1}).

As it can be seen in ***Table 4.2***, the accuracy values obtained for the different types of AgNPs and Ag^+ were between 84 and 108% with internal standardisation quantification mode and

92–113% with external calibration quantification mode. Relative standard deviation (RSD) for both quantification modes were under 15% in most cases. According to the obtained results, external calibration was chosen to quantify the silver content in aqueous solutions equilibrated with soil. Furthermore, the recoveries obtained by TXRF were similar with those obtained with ICP-OES (see in ***Table 4.2***).

4.3.1.2 Solid samples

An interesting advantage of TXRF technique is the possibility of direct quantitative analysis of metal content in solid samples without previous chemical treatment such as microwave digestion. This analytical alternative can be reached by a suspension of the solid sample with an adequate solvent followed by internal standardisation.

Therefore, in this study, the capabilities of TXRF to determine silver nanoparticles content in soil samples from batch adsorption experiments through suspensions were also tested. With this purpose, limits of detection for Ag in solid samples were evaluated using GXR1 and GXR2 soil certified reference materials. Furthermore, LODs for Ag in sewage sludge CRMs (SLUDGE 2 and SLUDGE 3) were additionally examined because one of the main AgNPs entries into the environment is through the application of sewage sludge in agricultural lands as fertiliser [4.37]. For that, 50 mg of CRM were mixed with 1 g of 1% Triton X-100 (non-ionic surfactant) solution and 75 µL of Pd 200 mg L^{-1} (IS). As mentioned above, Pd was selected as internal standard because of its low possibilities to be present in soils (Section 4.3.1.1). Afterwards, an aliquot of 5 µL was deposited onto sample carriers and was analysed by TXRF. LODs obtained for Ag were 1.9 mg kg^{-1} for GXR1 and 1.5 mg kg^{-1} for GXR2. And the limits of

Table 4.3 *Silver concentration (mg kg^{-1}) and limits of detection of solid certified reference materials suspensions by TXRF analysis (n = 2 (± SD)).*

Certified reference material	Ag concentration certified value (mg kg^{-1})	LOD (mg kg^{-1})	Ag concentration determined (mg kg^{-1})	Ag concentration determined corrected (mg kg^{-1})
GXR 1	32.6 ± 0.9	1.9 ± 0.1	19 ± 4	33 ± 7
GXR 2	17.4 ± 0.6	1.5 ± 0.2	10.0 ± 0.2	-[a]
SLUDGE 2	70.40 ± 4.36	1.83 ± 0.01	28 ± 1	65 ± 3
SLUDGE 3	100.00 ± 9.96	1.66 ± 0.02	42 ± 8	-[a]

[a] *Certified reference material used to estimate the correction factor.*

detection for SLUDGE 2 and SLUDGE 3 were 1.83 mg kg^{-1} and 1.66 mg kg^{-1}, respectively (***Table 4.3***). The LOD values obtained were satisfactory for the aim of this study.

With the same samples prepared for LODs evaluation, internal standardisation quantification mode was tested to directly quantify silver nanoparticles in solid sample suspensions. The obtained results of total silver content were lower than the certified value of reference materials, as can be seen in ***Table 4.3***. These diminished responses of the X-ray fluorescence signal is because the particles analysed in this study are one order of magnitude higher than the critical thickness and this provokes the presence of absorption effects. The correction of this absorption effects is possible using a factor estimated from the analysis of a CRM [4.34,4.38]. The correction factor was based on the proportional ratio between the silver content certified values of the CRM with the silver concentration determined by TXRF. The correction factors applied in the different CRM silver concentration determined values by TXRF were 1.74 for soils and 2.38 for sewage sludge samples. As consequence, the Ag concentration corrected values obtained were really close to silver certified values of CRM, especially for soil CRM (see in ***Table 4.3***). Additionally, in order to assess the suitability of TXRF system for direct soil suspension analysis, two CRM were digested and analysed with ICP-OES. The results obtained for SLUDGE 2 (79 ± 8) and SLUDGE 3 (89 ± 3) were in close agreement with the certified values. Therefore, the application of direct quantitative analysis in TXRF was possible and in this research was evaluated the possibility to employ it in batch adsorption studies.

However, the direct quantification of silver in solid sample suspensions without previous sample digestion is not the only advantage of TXRF analytical technique. The TXRF system gives information of all the elements present in the sample. For example, the calculated concentration of zinc (Zn) in GXR1 certified reference material, obtained with the application of a correction factor described above, was 653 ± 93 mg kg^{-1} and the certified value was 675 ± 8 mg kg^{-1}. Hence, TXRF allows obtaining an approximation of concentration values of all the elements present in the sample.

4.3.2 Application of TXRF to AgNPs batch adsorption studies

4.3.2.1 Analysis of aqueous solutions

Adsorption is one of the main interaction processes that regulate the mobility of emerging

pollutants when they interact with soil [4.6]. For this reason, batch adsorption experiments between soil and aqueous silver nanoparticles solution were performed as is described in Section 4.2.3. In this work, two soil samples (SOIL 1 and SOIL 2) with different physicochemical characteristics (see Section 4.2.2) were studied. The soil supernatants obtained from the adsorption experiments were directly analysed by TXRF. The quantification of silver content in the analysed samples was done by external calibration, as it is mentioned in Section 4.3.1.1. Then, the percentage (%) of adsorption was calculated with Eq. (4.1):

$$\%adsorption = \frac{Initial\ concentration\ in\ soil\ extract - Final\ concentration\ in\ soil\ extract}{Initial\ concentration\ in\ soil\ extract} \cdot 100 \quad (4.1)$$

In ***Fig. 4.1*** the graphical representation of the % adsorption of the two soil samples and the concentration of AgNPs-PVP in the supernatants as a function of time is shown. As can be seen, 90% of AgNPs adsorption on SOIL 1 was reached during the first 10 min, the same adsorption value was achieved after 6 h of sample rotation for SOIL 2. The adsorption differences could be mainly due to the electrical conductivity values of soils; SOIL 2 had a lower electrical conductivity (276.5 μS cm^{-1}) compared to SOIL 1 (427.33 μS cm^{-1}). This agrees with the assumption that high ionic strength favors the adsorption process [4.37,4.39].

Samples were also analysed with ICP-OES, which is the technique most often used, in order to compare our TXRF results from AgNPs quantification in batch adsorption studies. Silver quantification was also done by external calibration and the % of adsorption was also calculated with Eq. (4.1). The results obtained for both soil samples by ICP-OES do not deviate much from those obtained by TXRF analysis, especially in SOIL 1, where during the first 10 min the silver nanoparticles were practically adsorbed and the differences were barely noticeable (see in ***Fig. 4.1a***). Slight differences could be observed on AgNPs % adsorption results between the two techniques in the first 30 min for SOIL 2 (see ***Table S4.3*** in the Supporting information of this chapter). Also, the graphical plot of silver concentration in the supernatant (***Fig.4.1b*** and ***d***) shows the same trend using both analytical techniques as the results obtained of AgNPs% adsorption on soil. So, it can be concluded that the TXRF system can be used as an analytical tool for silver determination in batch adsorption studies of silver nanoparticles.

TXRF is a microanalytical technique requiring only minute amounts of sample. Therefore the possibility to use fewer tubes to perform batch adsorption studies was evaluated. Minute amounts of sample lead to a reduction of the AgNPs solution volume to carry out the kinetic experiments.

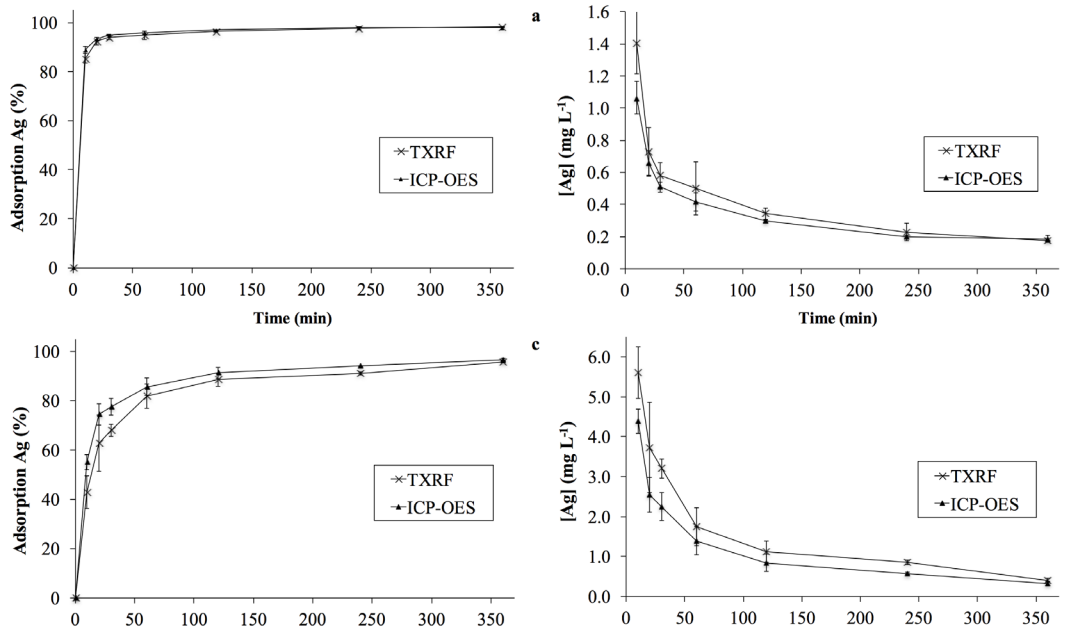

Fig. 4.1 *Comparison between the kinetics of silver nanoparticles adsorption on SOIL 1 (**a**,**b**) and SOIL 2 (**c**,**d**) using TXRF and ICP-OES.*

For this test, only one tube (n = 2) instead of 7 tubes (n = 14) were used to carry out the batch adsorption study. The soil used for this test was SOIL 1. The experimental procedure was the same as is described in Section 4.2.3 but the sample collection was done removing 50 µL of supernatant of the tube that was submitted to rotation at the corresponding studied times (10 min, 30 min, 60 min, 120 min, 240 min), after a centrifugation step (8 min). When the aliquot was taken, the tube was rotated until the next sample collection. Due to the small amount of sample withdrawn each time, the supernatant was not filtered prior to the TXRF analysis.

The same study was done centrifuging the sample only 1 min instead of 8 min in order to test if it was possible to decrease the analysis time. As can be seen in ***Table 4.4***, the AgNPs adsorption values obtained centrifuging the sample 1 min were significantly lower compared with those obtained centrifuging the sample 8 min. This could be explained taking into account that a short time of centrifugation hinders the total separation of the two phases and solid particles remain suspended in the liquid phase. Consequently, AgNPs present in the liquid phase as well as in the solids suspended are quantified in the liquid analysis. Taking into account these results, the use of 1 min as centrifugation time in batch adsorption experiments was discarded.

Table 4.4 *Silver nanoparticles adsorption percentage of SOIL 1 obtained varying the centrifugation time and the number of sample tubes used for batch adsorption experiments (n = 2 (± SD)).*

Time (min)	1 sample tube[a]	1 sample tube[b]	7 sample tubes	
	% adsorption TXRF	% adsorption TXRF	% adsorption TXRF	% adsorption ICP-OES
10	47.8 ± 0.2	85.1 ± 0.7	85 ± 2	89 ± 1
30	67 ± 5	89.40 ± 0.06	94.0 ± 0.8	95.0 ± 0.3
60	72 ± 2	93 ± 3	95 ± 2	95.9 ± 0.6
120	65 ± 8	93 ± 3	96.4 ± 0.4	97.02 ± 0.09
240	65.1 ± 0.4	91 ± 1	97.6 ± 0.6	98.0 ± 0.1

[a] *1 min of centrifugation*
[b] *8 min of centrifugation*

As it is also shown in ***Table 4.4***, AgNPs adsorption percentages obtained using only 1 sample were similar but slightly lower in comparison with those obtained in the prior study where 7 samples were used, especially for the last aliquot. This fact can be explained taking into account that the agitation was paused at certain times for centrifuging and collecting the sample. Nevertheless, the use of only one sample can be a good choice to carry out kinetic studies when a small amount of sample is available.

4.3.2.2 Analysis of loaded soil samples

In this study, TXRF analysis of soil samples from kinetic studies was performed preparing a soil suspension (minimum sample treatment) and also submitting the sample to an acid microwave digestion in order to verify the results. The soil digests were also analysed with ICP-OES to compare the obtained results between both techniques.

AgNPs concentrations obtained using the different sample treatments and techniques are shown in ***Table 4.5***. Silver concentration values in soil digests were calculated on the basis of duplicate samples. As it is shown, concentrations obtained by the digestion process were really similar with both studied techniques (TXRF and ICP-OES). In addition, the relative standard deviation (n = 2) was acceptable for both techniques with RSD values in most cases lower than 15%.

The results obtained for the direct soil suspension analysis by TXRF were comparable with the silver concentrations obtained by soil digests.

As mentioned previously, the direct solid analysis by TXRF not only allows the quantification of the analyte of interest but also allows obtaining multi-elemental information. As an example,

in ***Fig. 4.2***, the overlapped spectrums of a soil sample obtained before and after the AgNPs adsorption study are shown. As it can be seen, a peak of silver can be observed in the spectrum of the soil only after performing the kinetic study. This indicates that prior to the adsorption study, the soil sample was not contaminated with silver.

Table 4.5 *AgNPs content (mg kg^{-1}) in SOIL 1 obtained using different analytical approaches (n = 2 ((± SD)).*

Time (min)	TXRF		ICP-OES
	Suspension (mg kg^{-1})	Digestion (mg kg^{-1})	Digestion (mg kg^{-1})
10	143 ± 7	148 ± 3	123 ± 1
20	173 ± 15	151 ± 1	145 ± 9
30	154 ± 14	171 ± 23	159 ± 5
60	188 ± 4	146 ± 1	142 ± 5
120	179 ± 17	155 ± 16	144 ± 14
240	195 ± 40	148 ± 7	152 ± 3
360	204 ± 10	131 ± 24	137 ± 27

To complete the study, a mass balance was calculated in order to determine if there was a loose of the analyte during the experimental procedures. This calculation was done with the silver content values obtained from the analysis of supernatants and soils, and the silver nanoparticles content at the beginning of the kinetic study. The following Eq. (4.2) was used for this calculation:

$$\textit{Mass balance} \rightarrow \textit{mg AgNPs (supernatant)} + \textit{mg AgNPs (soil)} = \textit{mg AgNPs} \qquad (4.2)$$

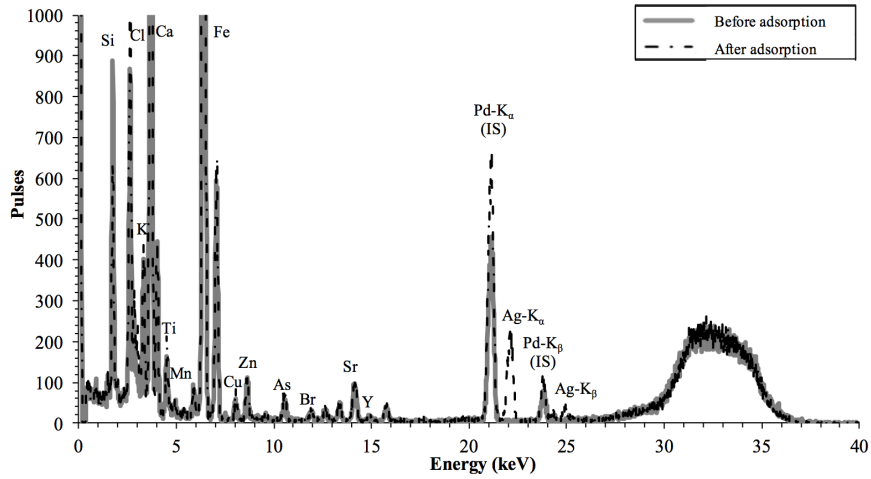

Fig. 4.2 *TXRF spectra obtained from a SOIL 1 suspension before and after the kinetic batch adsorption experiment.*

Table 4.6 *Data for the mass balance calculation (n = 2 ((± SD)).*

Sample	mg AgNPs (supernatant)		mg AgNPs (soil)			mg AgNPs (total)		
	TXRF	ICP-OES	TXRF digestion	TXRF suspension	ICP-OES digestion	TXRF digestion	TXRF suspension	ICP-OES digestion
10 min	0.028 ± 0.004	0.021 ± 0.002	0.149 ± 0.003	0.145 ± 0.007	0.124 ± 0.002	0.177 ± 0.007	0.17 ± 0.01	0.145 ± 0.001
20 min	0.014 ± 0.003	0.013 ± 0.002	0.152 ± 0.002	0.17 ± 0.01	0.145 ± 0.008	0.166 ± 0.005	0.18 ± 0.01	0.158 ± 0.007
30 min	0.012 ± 0.002	0.0101 ± 0.0006	0.17 ± 0.02	0.15 ± 0.01	0.159 ± 0.005	0.18 ± 0.02	0.16 ± 0.01	0.169 ± 0.004
60 min	0.010 ± 0.003	0.008 ± 0.001	0.1464 ± 0.0006	0.190 ± 0.003	0.143 ± 0.005	0.156 ± 0.004	0.2 ± 0.006	0.151 ± 0.004
120 min	0.007 ± 0.001	0.0059 ± 0.0002	0.16 ± 0.02	0.18 ± 0.02	0.15 ± 0.01	0.17 ± 0.02	0.19 ± 0.02	0.16 ± 0.01
240 min	0.005 ± 0.001	0.0040 ± 0.0002	0.149 ± 0.007	0.20 ± 0.04	0.152 ± 0.0034	0.154 ± 0.008	0.20 ± 0.04	0.156 ± 0.003
360 min	0.0032 ± 0.0001	0.0034 ± 0.0003	0.13 ± 0.024	0.21 ± 0.01	0.14 ± 0.03	0.13 ± 0.02	0.21 ± 0.01	0.14 ± 0.03

Initial concentration of 10 mg L^{-1} silver nanoparticles solution that corresponds to 0.2 mg AgNPs.

The results obtained show that the difference between the sum of silver content present in the analysed samples with the initial silver content was in most cases <20% using the digestion procedure for soil samples analysis (both by TXRF and ICP-OES) (see the results in ***Table 4.6***). Despite the fact that slightly differences on the mass balance are found for TXRF soil suspension analysis in comparison with digested soil values, the benefits of this fast and less time-consuming analytical approach make it desired for this type of environmental studies.

4.4 Conclusions

In this paper, we have demonstrated the analytical possibilities of TXRF spectrometry for AgNPs determination in batch adsorption studies. Although LODs obtained were high for both aqueous AgNPs solutions and solid CRM suspensions compared to other spectrometric techniques, they were low enough for the application of TXRF methodology to soil adsorption experiments.

The TXRF developed method was applied in batch adsorption studies to enhance the understanding of AgNPs sorption processes in agricultural soils. The simulation of the interaction between the AgNPs and soils showed that soil physicochemical properties, such as electrical conductivity, can play a key role in the sorption of these particles onto soils. Despite the differences of the AgNPs adsorption process between the two soils tested in this study, the results obtained for soil extracts and loaded soil samples by TXRF were in close agreement to those obtained by ICP-OES technique. However, for direct analysis of soil samples by TXRF, a factor to correct absorption effects is needed to obtain quantitative results. In addition, it can be concluded that AgNPs are easily adsorbed on soils because the total sorption of these pollutants in the soils tested was reached in <6 h.

With the possibility to analyse soil suspensions by TXRF, sample manipulation is reduced, less amount of reagents are needed and sample preparation is faster in comparison with other more common spectrometric techniques. Furthermore, an approximation of the multi-elemental composition of the soil can be obtained.

The developed methodology can be successfully applied for the determination of AgNPs content in soil samples when a small quantity of sample is available consuming less AgNPs solution.

An additional advantage of the developed TXRF method includes low operating costs because the TXRF system used does not require cooling media for function.

All these advantages make the proposed method a fast and economic alternative to popular spectrometric techniques like ICP-OES and ICP-MS.

Acknowledgments

The Spanish Ministry of Economy and Competitiveness financed this work through the project CGL2013-48802-C3-2-R (Program 2014). L. Torrent gratefully acknowledges a FPI grant from the Spanish Ministry of Economy and Competitiveness (Ref. BES-2014-070625). The authors are also thankful to chemistry degree students, Lourdes Fernández and Andreu Llort, for their contribution on the performance of this work.

References

[4.1] P. Krystek, A. Ulrich, C.C. Garcia, S. Manohar, R. Ritsema, Application of plasma spectrometry for the analysis of engineered nanoparticles in suspensions and products, J. Anal. At. Spectrom. 26 (2011) 1701–1721.

[4.2] N.A. Anjum, S.S. Gill, A.C. Duarte, E. Pereira, I. Ahmad, Silver nanoparticles in soil-plant systems, J. Nanopart. Res. 15 (2013) 1896.

[4.3] G.E. Schaumann, A. Philippe, M. Bundschuh, G. Metreveli, S. Klitzke, D. Rakcheev, *et al.*, Understanding the fate and biological effects of Ag- and TiO2-nanoparticles in the environment: the quest for advanced analytics and interdisciplinary concepts, Sci. Total Environ. 535 (2015) 3–19.

[4.4] S.A. Blaser, M. Scheringer, M. MacLeod, K. Hungerbühler, Estimation of cumulative aquatic exposure and risk due to silver: Contribution of nano-functionalized plastics and textiles, Sci. Total Environ. 390 (2008) 396–409.

[4.5] S. Wagner, A. Gondikas, E. Neubauer, T. Hofmann, F. Von Der Kammer, Spot the difference: engineered and natural nanoparticles in the environment-release, behavior, and fate, Angew. Chem. Int. Ed. 53 (2014) 12398–12419.

[4.6] B. Nowack, J.F. Ranville, S. Diamond, J.A. Gallego-Urrea, C. Metcalfe, J. Rose, *et al.*, Potential scenarios for nanomaterial release and subsequent alteration in the environment, Environ. Toxicol. Chem. 31 (2012) 50–59.

[4.7] J.R. Peralta-Videa, L. Zhao, M.L. Lopez-Moreno, G. de la Rosa, J. Hong, J.L. Gardea-Torresdey, Nanomaterials and the environment: a review for the biennium 2008 – 2010, J. Hazard. Mater. 186 (2011) 1–15.

[4.8] A.R. Petosa, D.P. Jaisi, I.R. Quevedo, M. Elimelech, N. Tufenkji, Aggregation and deposition of engineered nanomaterials in aquatic environments: role of physicochemical interactions, Environ. Sci. Technol. 44 (2010) 6532–6549.

[4.9] Y. Tian, B. Gao, C. Silvera-Batista, K.J. Ziegler, Transport of engineered nanoparticles in saturated porous media, J. Nanopart. Res. 12 (2010) 2371–2380.

[4.10] S. Lin, Y. Cheng, Y. Bobcombe, K.L. Jones, J. Liu, M.R. Wiesner, Deposition of silver nanoparticles in geochemically heterogeneous porous media: predicting affinity from surface composition analysis, Environ. Sci. Technol. 45 (2011) 5209–5215.

[4.11] Y. Liang, S.A. Bradford, J. Simunek, H. Vereecken, E. Klumpp, Sensitivity of the transport and retention of stabilized silver nanoparticles to physicochemical factors, Water Res. 47 (2013) 2572–2582.

[4.12] O. Sagee, I. Dror, B. Berkowitz, Transport of silver nanoparticles (AgNPs) in soil, Chemosphere 88 (2012) 670–675.

[4.13] Y. Liang, S.A. Bradford, J. Simunek, M. Heggen, H. Vereecken, E. Klumpp, Retention and remobilization of stabilized silver nanoparticles in an undisturbed loamy sand soil, Environ. Sci. Technol. 47 (2013) 12229–12237.

[4.14] G. Cornelis, L. Pang, C. Doolette, J.K. Kirby, M.J. McLaughlin, Transport of silver nanoparticles in saturated columns of natural soils, Sci. Total Environ. 463–464 (2013) 120–130.

[4.15] D. Wang, C. Su, W. Zhang, X. Hao, L. Cang, Y. Wang, *et al.*, Laboratory assessment of the mobility of water-dispersed engineered nanoparticles in a red soil (Ultisol), J. Hydrol. 519 (2014) 1677–1687.

[4.16] M. Hoppe, R. Mikutta, J. Utermann, W. Duijnisveld, S. Kaufhold, C.F. Stange, *et al.*, Remobilization of sterically stabilized silver nanoparticles from farmland soils determined by column leaching, Eur. J. Soil Sci. 66 (2015) 898–909.

[4.17] G. Cornelis, J.K. Kirby, D. Beak, D. Chittleborough, M.J. McLaughlin, A method for determination of retention of silver and cerium oxide manufactured nanoparticles in soils, Environ. Chem. 7 (2010) 298–308.

[4.18] G. Cornelis, C. Doolette, M. Thomas, M.J. McLaughlin, J.K. Kirby, D.G. Beak, D. Chittleborough, Retention and dissolution of engineered silver nanoparticles in natural soils, Soil Sci. Soc. Am. J. 76 (2012) 891–902.

[4.19] M. Hoppe, R. Mikutta, J. Utermann, W. Duijnisveld, G. Guggenberger, Retention of sterically and electrosterically stabilized silver nanoparticles in soils, Environ. Sci. Technol. 48 (2014) 12628–12635.

[4.20] S. Klitzke, G. Metreveli, A. Peters, G.E. Schaumann, F. Lang, The fate of silver nanoparticles in soil solution - sorption of solutes and aggregation, Sci. Total Environ. 535 (2015) 54–60.

[4.21] F. Plassard, T. Winiarski, M. Petit-Ramel, Retention and distribution of three heavy metals in a carbonated soil: comparison between batch and unsaturated column studies, J. Contam. Hydrol. 42 (2000) 99–111.

[4.22] D.L. Wise, Remediation engineering of contaminated soils, CRC Press, 2000.

[4.23] A. López-Serrano, R.M. Olivas, J.S. Landaluze, C. Cámara, Nanoparticles: a global vision. Characterization, separation, and quantification methods. Potential environmental and health impact, Anal. Methods. 6 (2014) 38–56.

[4.24] F. Laborda, E. Bolea, G. Cepriá, M.T. Gómez, M.S. Jiménez, J. Pérez-Arantegui, *et al.*, Detection, characterization and quantification of inorganic engineered nanomaterials: a review of techniques and methodological approaches for the analysis of complex samples, Anal. Chim. Acta. 904 (2016) 10–32.

[4.25] N.V. Alov, Total reflection X-ray fluorescence analysis: physical foundations and analytical application (a review), Inorg. Mater. 47 (2011) 1487–1499.

[4.26] P. Wobrauschek, Total reflection X-ray fluorescence analysis—a review, X-Ray Spectrom. 36 (2007) 289–300.

[4.27] E.K. Towett, K.D. Shepherd, G. Cadisch, Quantification of total element concentrations in soils using total X-ray fluorescence spectroscopy (TXRF), Sci. Total Environ. 463–464 (2013) 374–388.

[4.28] N.L. Misra, K.D. Singh Mudher, Total reflection X-ray fluorescence: a technique for trace element analysis in materials, Prog. Cryst. Growth Charact. Mater. 45 (2002) 65–74.

[4.29] E. Marguí, J.C. Tapias, A. Casas, M. Hidalgo, I. Queralt, Analysis of inlet and outlet industrial wastewater effluents by means of benchtop total reflection X-ray fluorescence spectrometry, Chemosphere 80 (2010) 263–270.

[4.30] E. Marguí, G.H. Floor, M. Hidalgo, P. Kregsamer, G. Román-Ross, C. Streli, *et al.*, Analytical possibilities of total reflection X-ray spectrometry (TXRF) for trace selenium determination in soils, Anal. Chem. 82 (2010) 7744–7751.

[4.31] G.H. Floor, E. Marguí, M. Hidalgo, I. Queralt, P. Kregsamer, C. Streli, *et al.*, Study of selenium sorption processes in volcanic ash using total reflection X-Ray fluoresence (TXRF), Chem. Geol. 352 (2013) 19–26. doi:10.1016/j.chemgeo.2013.05.034.

[4.32] H. Stosnach, Environmental trace-element analysis using a benchtop total reflection X-ray fluorescence spectrometer, Anal. Sci. 21 (2005) 873–876.

[4.33] M. US EPA, OSWER,ORCR, SW-846 test method 3051A: microwave assisted acid digestion of sediments, sludges, soils, and oils, (n.d.). Available at: https://www.epa.gov/hw-sw846/sw-846-test-method-3051a-microwave-assisted-acid-digestion-sediments-sludges-soils-and-oils. Accessed August 31, 2016.

[4.34] R. Klockenkämper, Total-reflection X-ray fluorescence analysis, Wiley, 1997.

[4.35] G. Hartmann, T. Baumgartner, M. Schuster, Influence of particle coating and matrix constituents on the cloud point extraction efficiency of silver nanoparticles (Ag-NPs) and application for monitoring the formation of Ag-NPs from Ag+, Anal. Chem. 86 (2014) 790–796.

[4.36] M. Menzel, U.E.A. Fittschen, Total reflection X-ray fluorescence analysis of airborne silver nanoparticles from fabrics, Anal. Chem. 86 (2014) 3053–3059.

[4.37] P.S. Tourinho, C.A.M. van Gestel, S. Lofts, C. Svendsen, A.M.V.M. Soares, S. Loureiro, Metal-based nanoparticles in soil: fate, behavior and effects on soil invertebrates, Environ. Toxicol. Chem. 31 (2012) 1679–1692.

[4.38] A. von Bohlen, M. Krämer, C. Sternemann, M. Paulus, The influence of X-ray coherence length on TXRF and XSW and the characterization of nanoparticles observed under grazing incidence of X-rays, J. Anal. At. Spectrom. 24 (2009) 792–800.

[4.39] A.M. El Badawy, T.P. Luxton, R.G. Silva, K.G. Scheckel, M.T. Suidan, T.M. Tolaymat, Impact of environmental conditions (pH, ionic strength, and electrolyte type) on the surface charge and aggregation of silver nanoparticles suspensions, Environ. Sci. Technol. 44 (2010) 1260–1266.

Supplementary information

Table S4.1 *Particle size distribution of SOIL 1 and SOIL 2.*

	>4	4-2 mm	2-1 mm	1- 0.5 mm	0.5-0.32 mm	0.32-0.25 mm	0.25-0.1 mm	< 0.1 mm
[a]**SOIL 1**	1.7	2.9	2.5	3.01	12.5	27.05	46.4	3.8
[b]**SOIL 2**		3.1	1.6	4.6		10.2	28.4	52.2

[a]*SOIL 1: Gavà, Barcelona, Spain;* [b]*SOIL 2: Castellbisbal, Barcelona, Spain.*

Table S4.2 *Physicochemical properties of SOIL 1 and SOIL 2.*

	pH water	pH KCl 0.1N	[c]EC (μS cm^{-1})	[d]Moisture (%)	[e]LOI (%)	[f]OM (%)	[g]CEC (meq 100g^{-1})
[a]**SOIL 1**	7.4	7.1	427.3	3.7	13.3	6.08	7.0
[b]**SOIL 2**	7.6	7.2	276.5	9.3	22.04	5.7	6.5

[a]*SOIL 1: Gavà, Barcelona, Spain;* [b]*SOIL 2: Castellbisbal, Barcelona, Spain;* [c]*EC: electrical conductivity at 25°C;* [d]*Moisture at 60°C,* [e]*LOI: loss on ignition at 1050 °C, 4h;* [f]*OM: organic matter content at 560 °C, 3h;* [g]*CEC: cation exchange capacity.*

Table S4.3 *Percentage of adsorption of silver nanoparticles onto SOIL 1 and SOIL 2 obtained from the TXRF and ICP-OES analysis of the supernatants (n = 2 (± SD)).*

Sample	% adsorption SOIL1[a]		% adsorption SOIL 2[b]	
	TXRF	ICP-OES	TXRF	ICP-OES
10 min	85 ± 2	89 ± 1	43 ± 7	55 ± 3
20 min	93 ± 2	93.3 ± 0.8	63 ± 11	75 ± 4
30 min	94.0 ± 0.8	95.0 ± 0.3	68 ± 2	78 ± 3
60 min	95 ± 2	95.9 ± 0.6	82 ± 5	86 ± 4
120 min	96.4 ± 0.4	97.02 ± 0.08	88 ± 3	91 ± 2
240 min	97.6 ± 0.6	98.00 ± 0.09	91.1 ± 0.6	94.0 ± 0.2
360 min	98.224 ± 0.002	98.2 ± 0.2	95.8 ± 0.5	96.6 ± 0.6

[a]*SOIL 1: Gavà, Barcelona, Spain;* [b]*SOIL 2: Castellbisbal, Barcelona, Spain*

CHAPTER 5

Determination of silver nanoparticles in complex aqueous matrices by total reflection X-ray fluorescence spectrometry combined with cloud point extraction

This chapter corresponds to the following publication:

L. Torrent, M. Iglesias, M. Hidalgo, E. Marguí, *Determination of silver nanoparticles in complex aqueous matrices by total reflection X-ray spectrometry combined with cloud point extraction.* J. Anal. At. Spectrom. 33 (2018) 383-394

Abstract

The development of methods for the analysis of silver nanoparticles (AgNPs) is of special relevance to achieve detailed insights into the fate, transport and exposure of these emerging pollutants in the environment. In the present contribution, for the first time, the possibilities and drawbacks of cloud point extraction (CPE) in combination with total reflection X-ray fluorescence spectrometry (TXRF) have been evaluated for the determination of AgNPs content in soil and consumer product water extracts. The experimental conditions for the separation and preconcentration of AgNPs with different coatings (PVP, PEG and citrate) and sizes (40–100 nm) were evaluated, paying attention to possible modifications required by the characteristics of the TXRF technique. Single particle inductively coupled plasma mass spectrometry (SP-ICPMS) analysis of the same aqueous extracts was also carried out in order to confirm the presence and percentage of AgNPs. Good agreement with respect to AgNPs concentrations in the analysed soil extracts was obtained between CPE-TXRF and SP-ICPMS, confirming the absence of matrix effects for this type of sample by CPE. On the contrary, large discrepancies were found between both analytical approaches for the studied consumer product water extracts. SP-ICPMS analysis evidenced the presence of ionic silver with a heterogeneous mixture of different sizes including relatively large Ag particles (>100 nm). This fact was also verified by SEM-EDS analysis. The results from this study highlight the necessity to study in more detail the effectiveness of existing methodologies (including CPE-based methods and SP-ICPMS) for the monitoring of AgNPs in complex aqueous matrices involving mixtures of different NPs sizes and coatings.

5.1 Introduction

Silver nanoparticles (AgNPs) are well-known for their excellent antibacterial ability and are widely used in a growing number of applications ranging from home disinfectants and medical devices to water purifiers [5.1]. In fact, according to a 2011 report from "The project on emerging methodologies", there are more than 300 consumer products containing nano-Ag [5.2]. Once present in the environment, the normally useful antibacterial properties may instead become a potential hazard for both humans and the environment [5.3]. For instance, the toxicity of AgNPs to aquatic organisms at micrograms per litre levels has already been demonstrated [5.4]. Therefore, although AgNPs are not yet regulated, they are already included in the list of emerging pollutants [5.5].

In order to fully investigate the fate and transport of AgNPs in the environment, the development of analytical tools for the characterisation and detection of AgNPs in complicated environmental samples is urgently needed. Compared to classical and other emerging contaminants, the determination of nanoparticles is posing previously unknown challenges mostly due to the lack of information about the size, shape and capping agent used in AgNPs containing products [5.1].

Several analytical approaches have been developed in the last few years for the characterisation and determination of AgNPs [5.6,5.7]. Electron microscopy techniques are a popular option in visualisation and characterisation of NPs. However, since very small proportions of samples are analysed, to get a representative result, hundreds and thousands of particles have to be counted, which is laborious and time consuming [5.6]. The discrimination of Ag^{+} and AgNPs is still one of the greatest challenges due to their common occurrence in the environment. In this sense, hyphenated techniques such as field flow fractionation (FFF) or capillary electrophoresis (CE) coupled with inductively coupled plasma mass spectrometry (ICPMS) are emerging as one of the most promising tools for AgNPs determination [5.8-5.13]. However, these techniques are expensive and present also some drawbacks including the membrane fouling effect in FFF-ICPMS or the cumbersome interpretation of migration times in CE-ICPMS [5.8,5.10]. In 2011, Laborda and co-workers highlighted the possibilities of single particle ICPMS (SP-ICPMS) for identification, characterisation and determination of the mass and number concentration of dissolved silver and AgNPs at the ng L^{-1} level [5.14]. Despite the advantages of SP-ICPMS, it demands well-educated and trained operators and its application for the analysis of complicated environmental samples is still scarce [5.15]. In addition to the sophisticated methods aforementioned, other simpler and cost-effective methodologies for AgNPs determination and speciation have been developed. Most of them are based on the

combination of a preconcentration/separation step followed by an atomic spectroscopic technique [5.16,5.17]. In this category it is important to emphasise the recent use of cloud point extraction (CPE) as a promising environment-friendly alternative for the extraction and preconcentration of AgNPs [5.18]. In this method, NPs are encapsulated in the micelles after the addition of a surfactant (mostly 1,1,3,3-tetramethylbutyl)phenyl-polyethyleneglycol, (Triton™ X-114) and concentrated to a small volume with the assistance of centrifugation [5.19]. Fractionation analysis of AgNPs and Ag^+ can be carried out by adding a suitable complexing agent to the aqueous sample before extraction. CPE exhibits many advantages in comparison with other developed preconcentration procedures including high extraction efficiency, low cost, easy handling and compliance with the green analytical chemistry rules. As shown in ***Table 5.1***, CPE has been applied in combination with several detection analytical techniques for the determination and/or fractionation of AgNPs in different types of samples. For quantification, after the extraction and phase separation, the Triton™ X-114 rich phase containing the nanoparticles is analysed. The first study published in 2009 about the potential use of CPE for AgNPs determination in aqueous samples was in combination with ICP-MS [5.18]. Limits of detection at the ng L^{-1} level were obtained, but due to the blocking or clogging of the sample tips within the spray chamber caused by the NPs, sample digestion was needed before ICPMS analysis [5.20,5.21]. More recent studies have used CPE in combination with electrothermal atomic absorption spectroscopy (ETAAS). Using this approach, sample digestion is not needed and thus the analysis time and limits of detection are improved [5.16, 5.22-5.24]. Although less used, other detection systems such as UV spectroscopy and flow injection analysis coupled with chemiluminescence have also been employed in CPE systems. As can be seen in ***Table 5.1***, most of the published contributions dealing with the use of CPE are focused on the analysis of water (e.g. tap, river, and waste waters) but a few deal with the analysis of more complex environmental samples. In fact, a recent study has pointed out a reduction of recovery factors in more complex water matrices and variations in extraction efficiency with AgNPs size [5.27]. Another relevant point is that quantitative AgNPs results in most studies are obtained by spiking tests using one kind of lab-made AgNPs. However, in most real samples, AgNPs of different compositions and coatings are present [5.1]. This fact can have an important influence not only on the ecotoxicological effects of the particles in the environment, but also on the extraction efficiency and subsequent determination. Recently, Hartmann *et al.* demonstrated a significant reduction of extraction efficiency for hydrophilic protein-coated AgNPs by CPE [5.23].

In the present contribution, for the first time, the possibilities and drawbacks of CPE in combination

with total reflection X-ray fluorescence spectrometry (TXRF) have been evaluated for the determination of AgNPs in complex aqueous samples such as soil and antibacterial product water extracts. The experimental conditions for the separation and preconcentration of mixtures of AgNPs with different coatings (citrate, PVP, and PEG) and sizes (40–100 nm) have been evaluated, paying attention to possible modifications required by the characteristics of TXRF [5.28]. Few papers report about Ag determination by TXRF due to the lack of sensitivity and overlapping problems associated with Ag-L_α line analysis with TXRF systems equipped with Mo X-ray tubes [5.29]. In the present study, the TXRF instrument used is equipped with a W X-ray tube that allows performing analysis using Ag-K_α lines [5.30]. The quantitative AgNPs results by the proposed method were compared with the ones by SP-ICPMS.

5.2 Experimental section

5.2.1 Chemicals, materials and apparatus

Sodium citrate stabilised (2 mM) silver nanoparticle commercial solutions (citrate-AgNPs) of 40 nm and 100 nm were purchased from Sigma Aldrich (St. Louis, Missouri, USA). Polyvinylpyrrolidone coated AgNPs (PVP-AgNPs) of 100 nm stabilised with sodium citrate (2 mM) and polyethyleneglycol coated AgNPs (PEG-AgNPs) of 100 nm diluted in water were obtained from NanoComposix (San Diego, USA). These AgNPs stock solutions were used to prepare different standards and spiked samples for the evaluation of the cloud point extraction methodology. An ionic silver stock solution of 1,000 ± 2 mg L^{-1} (Merck KGaA, Darmstadt, Germany) was employed to study the effects of dissolved silver on AgNPs extraction by CPE and for preparing the inductively coupled plasma optical emission spectrometry (ICP-OES) standards. High purity water obtained from a Milli-Q purification system (Millipore Corp., Bedford, USA) was used throughout the work.

For the cloud point extraction procedure, sodium thiosulfate pentahydrate ($Na_2S_2O_3{\cdot}5H_2O$) from Panreac (Barcelona, Spain) and non-ionic surfactant Triton X-114® ((1,1,3,3-tetramethylbutyl)phenyl-polyethyleneglycol) from Sigma Aldrich (St. Louis, USA) were used. In addition, the pH of the samples was adjusted with 0.05 M nitric acid (prepared with the same nitric acid used for the sample acidic digestion). The reconstitution of CPE organic extracts for their analysis by total reflection X-ray fluorescence spectrometry (TXRF) was done by testing the following solvents: carbon tetrachloride (CCl_4), tetrahydrofuran (THF), a mixture of methanol (CH_3OH): nitric acid (HNO_3) and chloroform ($CHCl_3$) from Panreac (Barcelona, Spain).

Table 5.1 *Cloud point extraction based analytical procedures published last few years for AgNPs quantification.*

Detection technique	Sample treatment (preconcentrated sample)	LOD (μg L^{-1})	Application			Recovery (%)	Additional information	Ref.
			Analyte	Sample	Range (μg L^{-1})			
ICPMS	MW digestion	0.006	AgNPs	Spiked lake, river and WWTP waters	0.1-146	64-116	AgNPs with PVP capping agent	5.18
		0.13 (AgNPs)[a] 0.07 (Ag^+)[a]	AgNPs/Ag^+	Antibacterial products (liquids and gels)	0.025-99.4[a]	75-108	Ag^+ is evaluated by difference between total silver and AgNPs	5.20
		2.94 (AgNPs) 2.40 (Ag^+)	AgNPs/Ag^+	Spiked cell lysates	μg L^{-1} level	92-94	AgNPs and Ag^+ are evaluated after MW digestion of the 2 phases	5.21
ETAAS	Dissolution with ethanol	0.0007	AgNPs	Spiked river, WWTP waters	0.02-0.3	88-117	AgNPs stabilised with citrate	5.22
		0.0007	AgNPs	Synthetic aqueous solutions	0.1-0.4	n.a.	AgNPs with different capping agents	5.23
		0.0007	AgNPs	Municipal WWTP waters	ng L^{-1} level	n.a.		5.16
	None	0.002	AgNPs/Ag^+	Tap, bottled and seawater, water extracts	0.005-10	96-105	AgNPs stabilised with citrate AgNPs and Ag^+ are evaluated using two extraction procedures	5.24
FIA-CL	Backextraction and dissolution to precursor ions	0.0002	AgNPs	River, lake and WWTP waters	0.0003-0.0009	74-95	Determination of Ag, Au and Fe_3O_4NPs	5.25
UV spectroscopy	Oxidation and tween 20-AuNPs addition	1	AgNPs	Tap and seawater	17-425	n.a.	Small-sized AgNPs (10 nm)	5.26
TXRF	Evaporation and dissolution	0.7	AgNPs	Antibacterial products and soil water extracts	5-1000	73-114	AgNPs with different capping agents[c] (PVP, PEG, stabilised with citrate) AgNPs sizes (40-100-200 nm)	This work

[a]Units expressed as μg g^{-1}, [b]Evaluation of extraction efficiency at only one concentration level (1-3 μg g^{-1}), [c]Evaluation of extraction efficiency in the range of concentration levels (5, 25, 200 μg g^{-1}).

Table 5.2 *Study of the effect of AgNPs surface, size and presence of ionic silver (Ag^+) on the determination of AgNPs content using the developed CPE-TXRF system. Quantitative results were obtained using AgNPs with citrate surface calibration curve.*

Studied effect	**Aqueous standard composition**	**AgNPs total added ($\mu g\ L^{-1}$)**	**AgNPs total CPE+TXRF ($\mu g\ L^{-1}$)**	**Recovery (%)**
Effect of AgNPs surface[a]	5 $\mu g\ L^{-1}$ citrate-AgNPs + 5 $\mu g\ L^{-1}$ PVP-AgNPs + 5 $\mu g\ L^{-1}$ PEG-AgNPs	15	11 (SD = 2)	73
	25 $\mu g\ L^{-1}$ citrate-AgNPs + 25 $\mu g\ L^{-1}$ PVP-AgNPs + 25 $\mu g\ L^{-1}$ PEG-AgNPs	76	80 (SD = 20)	105
	200 $\mu g\ L^{-1}$ citrate-AgNPs + 200 $\mu g\ L^{-1}$ PVP-AgNPs + 200 $\mu g\ L^{-1}$ PEG-AgNPs	598	440 (SD = 40)	74
Effect of AgNPs size	25 $\mu g\ L^{-1}$ citrate-AgNPs 40 nm + 25 $\mu g\ L^{-1}$ citrate-AgNPs 100 nm	51	54 (SD = 8)	106
Effect of Ag^+ presence[b]	75 $\mu g\ L^{-1}$ citrate-AgNPs + 75 $\mu g\ L^{-1}$ Ag^+ (ratio Ag^+/AgNPs: 1)	76	87 (SD = 6)	114
	75 $\mu g\ L^{-1}$ citrate-AgNPs + 200 $\mu g\ L^{-1}$ Ag^+ (ratio Ag^+/AgNPs: 2.7)	75	130 (SD = 10)	173
	75 $\mu g\ L^{-1}$ citrate-AgNPs + 500 $\mu g\ L^{-1}$ Ag^+ (ratio Ag^+/AgNPs: 6.7)	75	210 (SD = 20)	280

[a] *NPs sizes: citrate-AgNPs: 100 nm, PVP-AgNPs: 75 nm, PEG-AgNPs: 100nm.* [b] *NPs sizes: citrate-AgNPs: 100nm.*

Quartz glass discs with a diameter of 30 mm and a thickness of 3 ± 0.1 mm were used as sample holders for TXRF analysis. Silicone from Serva Electrophoresis GmbH (Heidelberg, Germany) was employed for siliconising the sample carriers before sample deposition.

5.2.2 AgNPs standard solutions and samples

5.2.2.1 AgNPs standard solutions

In order to evaluate the effect of the AgNPs surface, the AgNPs size and the presence of ionic silver on the recoveries of AgNPs using the developed method, several aqueous standards containing mixtures of different AgNPs and ionic silver were prepared (see ***Table 5.2*** for details). In all cases, dilutions of the commercial AgNPs stock solutions were used.

5.2.2.2 Samples

To test the applicability of the developed CPE-TXRF methodology for the isolation and preconcentration of AgNPs, two different types of samples were considered: consumer product and soil water extracts.

5.2.2.2.1 Consumer product water extracts

As stated in the Introduction section, AgNPs are widely used in commercial products for antibacterial purposes. In this research, Hansaplast Universal Antibacterial Plasters from Beiersdorf AG (Hamburg, Germany) were selected as a study case. According to the product packaging, the sanitary towel of the band aid contains silver nanoparticles that are progressively released during the healing process. To study the release of nanosilver and/or ionic silver, the band aid was submitted to a leaching procedure using Milli-Q water as an extracting agent. In brief: an aliquot of 1.25 g of the band aid (cut into 1 cm x 1 cm pieces) was put in contact with 25 mL of Milli-Q water. The mixture was submitted to rotation with a rotary agitator (35 rpm) at room temperature for a period of 24 hours. After the leaching period, the water extract was filtered with a cellulose acetate membrane filter of 0.45 µm pore size to separate the particulate solids in suspension. Finally, the water extract was analysed by using the developed CPE-TXRF methodology and the presence of AgNPs was confirmed by SP-ICPMS and SEM-EDS analysis.

5.2.2.2.2 Soil water extracts

As a consequence of the fabrication and use of AgNPs, these nanomaterials are released

inevitably into the environment with soil being the main sink of disposal [5.31]. Once in the soil, AgNPs can be adsorbed and/or desorbed from solid components affecting their mobility, transport and bioavailability. To better understand these processes, lab-controlled experiments are usually performed. For this purpose, 0.5 g of soil was mixed with 20 mL of a solution containing 1 mg L^{-1} of 100 nm AgNPs with the citrate surface or 5 mg L^{-1} of 75 nm AgNPs with the PVP surface with a rotary agitator (35 rpm) at room temperature for a period of 2 hours (at this time more than 90% of the AgNPs are retained in the soil) [5.30]. Then, soil samples were dried at 65–70 °C in an oven overnight and they were put in contact with 15 mL of Milli-Q water for 24 hours to assess the leaching and mobility of AgNPs. This extraction method was based on the German Standard Method DIN38414-S4. Soil water extracts were then filtered using an acetate cellulose membrane filter of 0.45 µm pore size to separate the particulate solids in suspension. In order to determine the presence of AgNPs in the resulting extract, the CPE-TXRF methodology was applied. SP-ICPMS analysis was also carried out to confirm the presence of silver nanoparticles.

5.2.3 CPE procedure and sample preparation for TXRF analysis

In this study, the CPE methodology was used to preconcentrate and isolate silver nanoparticles in aqueous extracts containing dissolved silver previous to TXRF determination. The CPE methodology was based on the method described by Liu *et al.* with modifications to allow the combination of CPE with TXRF analysis (see ***Fig. 5.1*** for details) [5.18]. In brief: 9.5 mL of an aqueous AgNPs solution or an aqueous sample was placed in a 15 mL long tapered polypropylene tube. Then, the pH of the aqueous solution was adjusted with 0.05 M nitric acid at pH 3.7 (see details in Section 5.3.1). Afterwards, 0.1 mL of 1 M $Na_2S_2O_3$ and 0.2 mL of 5% Triton X-114® surfactant were added to the sample solution. The mixture was vigorously shaken and was incubated at 40 °C in a water bath for 30 min. After 30 min, the sample was centrifuged at 2,000 rpm for 5 min and cooled down in a freezer for 15 min to increase the viscosity of the surfactant-rich phase at the bottom of the vial and facilitate phase separation.

The viscous, micelle-rich phase obtained is usually digested or diluted with an adequate solvent to enable injection into the analytical instrument (see ***Table 5.1***). In the present research, two chemical strategies were tested for Ag quantification by TXRF analysis.

5.2.3.1 Sample treatment-1 (direct measurements by TXRF)

An aliquot of 5 µL of the surfactant-rich phase was directly pipetted onto a siliconised quartz

reflector and dried using an infrared lamp for 15 min for the later TXRF analysis.

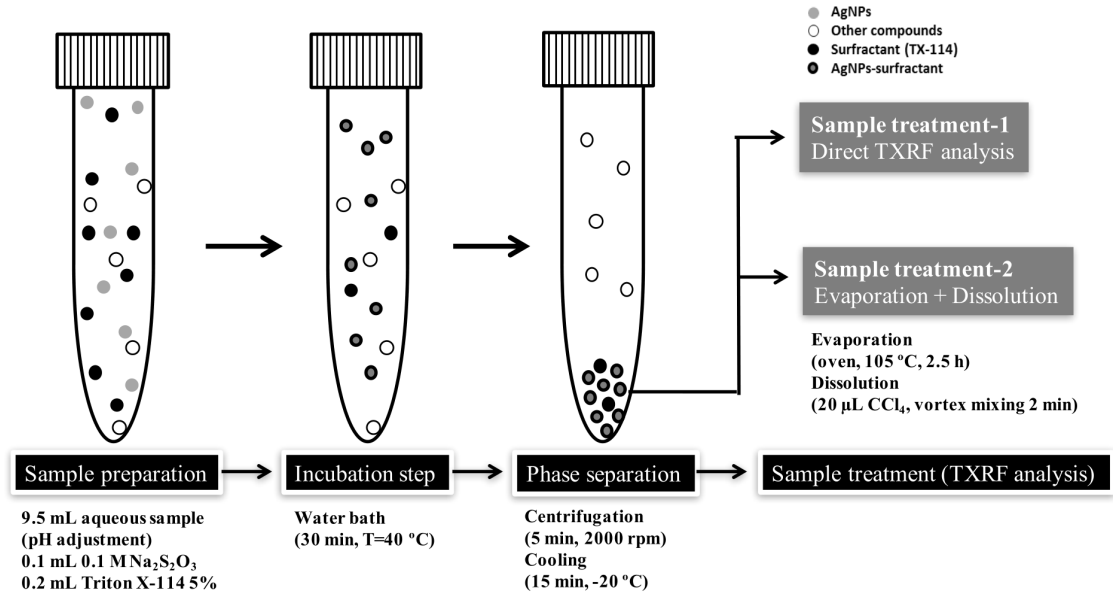

Fig. 5.1 *Schematic and analytical conditions for the CPE-TXRF system.*

5.2.3.2 Sample treatment-2 (evaporation + dissolution)

The remaining surfactant phase containing the AgNPs was put in an oven at 100–105 ºC for 2.5 hours in order to completely evaporate the sample. Then, the extract was reconstituted with 20 µL of CCl_4 and mixed with a vortex device for 2 min. Finally, 5 µL of the organic phase was pipetted onto a siliconised quartz reflector and dried using an infrared lamp for 10 min for the later TXRF analysis.

5.2.4 Instrumentation

The silver content after the CPE procedure was determined using an "S2 PICOFOX" benchtop TXRF spectrometer (Bruker AXS Microanalysis GmbH, Berlin, Germany). This instrument is equipped with a 50 W X-ray tube with a tungsten (W) anode and a multilayer monochromator (35.0 keV), which allows the analysis of high number atomic element K-lines such as silver and cadmium [5.30,5.32]. The characteristic radiation emitted by the elements present in the sample is detected by a silicon drift detector with an active area of 10 mm^2 and a resolution of 160 eV (Mn-K_a). The measurements were performed in an air atmosphere using a measurement time of 2,000 s.

In order to determine the presence of silver nanoparticles in water extracts, single-particle

ICPMS analysis was performed with an ICPMS Agilent 7500 c (Agilent Technologies, Tokyo, Japan). Measurement parameters were: 1500 W RF power, 15 L min^{-1} plasma gas flow rate, 10 ms dwell time and ^{107}Ag the isotope monitored.

Prior to the SP-ICPMS analysis, the total silver content was determined using an ICP-OES system (Agilent 5100 Vertical Dual View, Agilent Technologies, Tokyo, Japan) in order to adjust the silver concentration in water extracts at the ~1 µg L^{-1} level. The plasma was operated with a 12 L min^{-1} plasma gas flow rate. The type of detector was a silicon based multichannel array CCD (charge coupled device). Other measurement parameters were: 1200 W RF power, axial plasma configuration, concentric nebuliser type, double pass glass cyclonic spray chamber and echelle polychromatic wavelength selector. The silver wavelength (nm) used was 328.068 nm.

A stereoscopic optical microscope (NIKON SMZ-1000) was used for the morphological study of the deposited surfactant-rich phase containing the extracted AgNPs on quartz reflectors. Finally, a scanning electron microscope (SEM) (Zeiss DSM 960 Germany) coupled with an EDX (Oxford, UK) was employed for AgNPs identification in water leachates. SEM samples were prepared by loading 5 µL of water extract onto a carbon support.

5.3 Results and discussion

5.3.1 AgNPs stability tests

Some recent publications have highlighted the potential alteration of the dispersion state of nanoparticles by laboratory procedures [5.33]. For this reason, some essential issues such as the adsorption of AgNPs to laboratory containers and storing conditions of AgNPs solutions were first evaluated. Tests were performed using 200 µg L^{-1} standard solutions of the target 100 nm AgNPs (AgNPs-citrate, AgNPs-PVP and AgNPs-PEG) prepared by dilution of the commercial stock standards. The results obtained by monitoring the total silver content by ICP-OES in the solutions showed a significant adsorption process of the AgNPs on the container walls over time regardless of the type of container used (glass, polypropylene and polystyrene). Only quantitative recoveries were obtained (92–112%) when keeping the samples at 4 °C up to 24 h. A significant reduction of 40–50% of the initial silver content was found when storing AgNPs solutions at 4 °C for longer times (6 days) or after using freezing as the storing procedure. Taking into account these results, AgNPs solutions were prepared in polypropylene containers just before their use.

5.3.2 Evaluation of the CPE procedure and TXRF analysis

Liu and co-workers highlight the significance of pH in the CPE of nanomaterials, with the highest extraction efficiency at the zero-point charge pH (pH_{PZC}) [5.18]. According to the AgNPs manufacture characteristics, pH_{PZC} is not found for the studied AgNPs in the pH range 2–10. As a result, a study of the influence of pH on the extraction of the target 100 nm AgNPs (citrate-AgNPs, PVP-AgNPs, and PEG-AgNPs) was carried out (see ***Fig. 5.2***). pH values lower than 3 were discarded due to the possible dissolution of AgNPs. The results showed that the highest silver analytical signal was obtained at about pH 3.7 for AgNPs with citrate or PVP capping agents and at about pH 3 for AgNPs with a PEG surface. Taking into account that one of the aims of the present research was the isolation and preconcentration of different types of AgNPs at the same time, a pH value of 3.7 was selected for further CPE experiments.

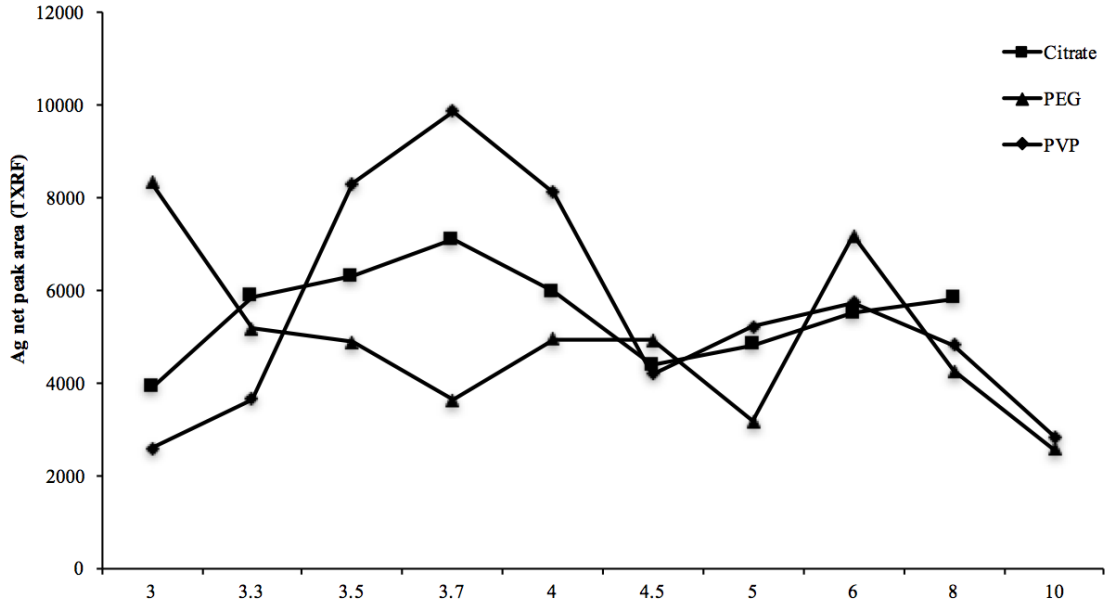

Fig. 5.2 *pH effect on the silver analytical response for AgNPs with different capping agents (AgNPs standard concentration: 50 μg L^{-1}).*

As stated in the Experimental section, the CPE methodology was based on the method previously described by Liu *et al.* [5.18]. In that contribution, after the CPE procedure, the micelle-rich phase obtained was treated by means of microwave digestion to enable the subsequent total Ag determination by the ICPMS technique. In the present research, for the first time, the TXRF technique is proposed as the detection technique after the CPE procedure. To perform analysis under total reflection conditions, samples must be provided as thin films. For liquid samples, this is done by depositing 5–50 μL of sample on a reflective carrier with subsequent drying of the

drop [5.34]. Therefore, TXRF analysis is not limited by an injection process into the analytical instrument and other simpler and low-cost sample treatments in addition to digestion can be tested for the analysis of the preconcentrated sample. In the present research, in an attempt to avoid the digestion procedure, two additional sample treatment approaches were applied to the surfactant-rich phase containing the extracted AgNPs, including direct measurements *via* TXRF without further preparation and evaporation of the preconcentrated phase with subsequent dissolution using an alternative solvent (see ***Fig. 5.1*** and Section 5.2.3 for details). It is interesting to remark that for all the experiments in this Section we used citrate-coated AgNPs as the study case because they are very likely the most frequently used type of AgNPs [5.35]. In particular, experimental tests were performed using preconcentrated aqueous standard solutions containing 100 nm citrate-coated AgNPs at the level of 100 μg L^{-1}.

5.3.2.1 Sample treatment-1 (direct measurements by TXRF)

Taking into account that the use of surfactants (e.g. Triton X-114® and Triton X-100®) is a common practice to prepare homogeneous solid suspensions for TXRF analysis [5.36,5.37], the possibility to analyse directly the surfactant-rich phase after the CPE procedure was studied. However, an unacceptable dispersion in terms of RSD was obtained for the analysis of the aforementioned preconcentrated AgNPs standard (RSD >30%, n = 5). It seems that after exceeding the cloud point temperature (40 °C), the surfactant (Triton X-114®) is too viscous and a proper deposition of the organic drop on the quartz reflector surface was really critical. Another drawback was the drying of the drop before TXRF analysis. For this reason, different drying modes were tested in order to ensure the achievement of a centered-thin film on the reflector including (i) drying under an IR-lamp after deposition, (ii) the deposition of the drop on a preheated quartz reflector (it has been proved to be a good approach for the drying of organic drops on TXRF sample carriers) [5.38], (iii) drying in an oven at ~80°C after deposition and (iv) drying under a vacuum chamber. However, complete drying of the drop on the reflector surface was not possible. As an example, in ***Fig. 5.3***, an optical microscope image in transmitted light for the direct analysis of a 5 μL sample spot on a quartz glass reflector is shown. For this reason, it was decided that the direct TXRF analysis of the resulting CPE phase was not suitable for obtaining quantitative results.

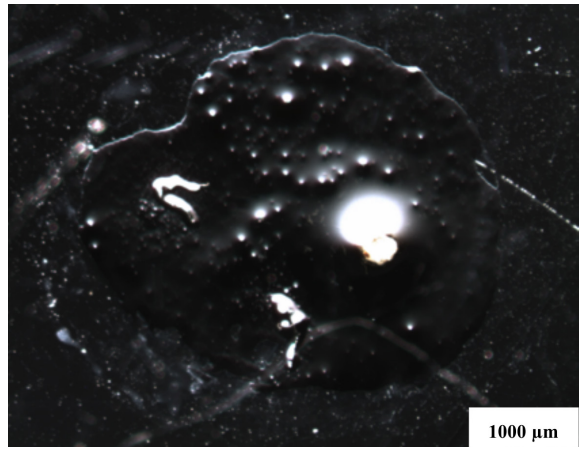

Fig. 5.3 *Optical microscope image in transmitted light for a 5 µL sample spot (preconcentrated 100 µg L^{-1} AgNPs-citrate standard) on a quartz glass reflector using sample treatment-1 (see the manuscript text for details, Section 5.2.3).*

5.3.2.2 Sample treatment-2 (evaporation + dissolution)

Chlorine-containing organic solvents have been proved to be appropriate solvents to be measured with TXRF due to their high volatility that facilitates the drying step of the organic drop for subsequent analysis [5.39]. For this reason, a test based on the evaporation of the CPE organic phase (at 60 ºC in an oven overnight) and redissolution of the residue using an alternative solvent (200 µL) was carried out for the TXRF analysis of the aforementioned AgNPs standard. Several solvents were tested for such a purpose including chloroform, carbon tetrachloride, and a mixture of MeOH/HNO_3 and tetrahydrofuran. Both carbon tetrachloride and tetrahydrofuran could dissolve the evaporated CPE residue but the use of carbon tetrachloride leads to a higher Ag response (data not shown). For this reason, carbon tetrachloride was selected for further experiments. Taking into account the toxicity of this solvent and the green analytical chemistry trend, an additional test was performed using lower amounts of solvent (60 and 20 µL). As can be seen in ***Fig. 5.4a***, with only 20 µL of carbon tetrachloride, the residue could be quantitatively dissolved and moreover a higher analytical response was obtained in comparison with the use of higher volumes of solvent. Finally, the effect of the evaporation temperature of the CPE phase on the Ag TXRF responses was also evaluated. The results obtained (***Fig. 5.4b***) showed that there were no significant differences when evaporating the CPE phase at 60 ºC or at 100 ºC. A final temperature of 100 ºC was selected because the time required to evaporate the organic phase was considerably shorter (2.5 hours in comparison with 5 hours). Using the best sample preparation-2 conditions (evaporation at 100 ºC and dissolution with 20 µL of carbon tetrachloride) an acceptable RSD

~12% (n = 3) was obtained. For this reason, sample preparation-2 was finally selected as the sample treatment procedure for the later TXRF analysis.

Once established the best conditions to prepare CPE samples for TXRF analysis, it was considered appropriate to study the possibility to increase the method sensitivity by decreasing the amount of surfactant used in the CPE procedure.

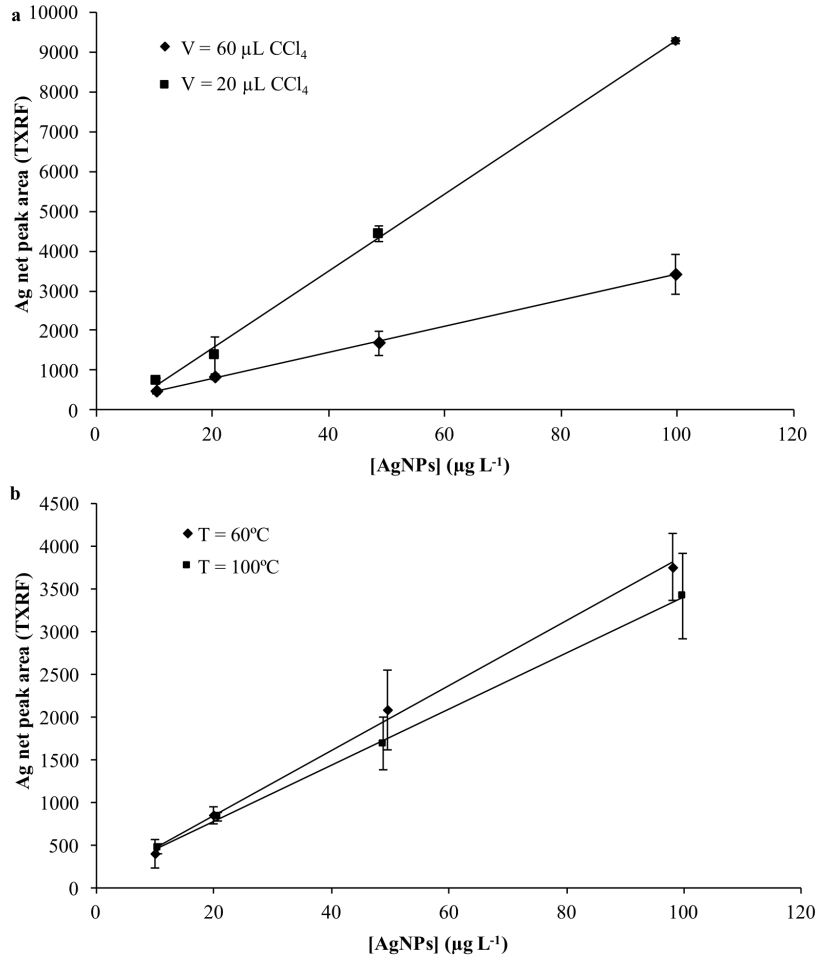

Fig. 5.4. *Effect of organic solvent volume (**a**) and evaporation temperature (**b**) for the evaporation-dissolution of the CPE extract (sample treatment-2). Error bars corresponds to the standard deviation of triplicate analysis.*

For this reason, a 50 µg L^{-1} citrate coated AgNPs standard was analysed in triplicate by using the developed CPE-TXRF procedure but decreasing the volume of Triton X-114 (5% in water). As seen in ***Fig. 5.5***, a significant increase of the Ag peak area was found when reducing the volume of the surfactant from 0.4 to 0.2 mL. The employment of lower volumes (0.1 mL) did not imply a rise of the method sensitivity but increased the uncertainty of the obtained

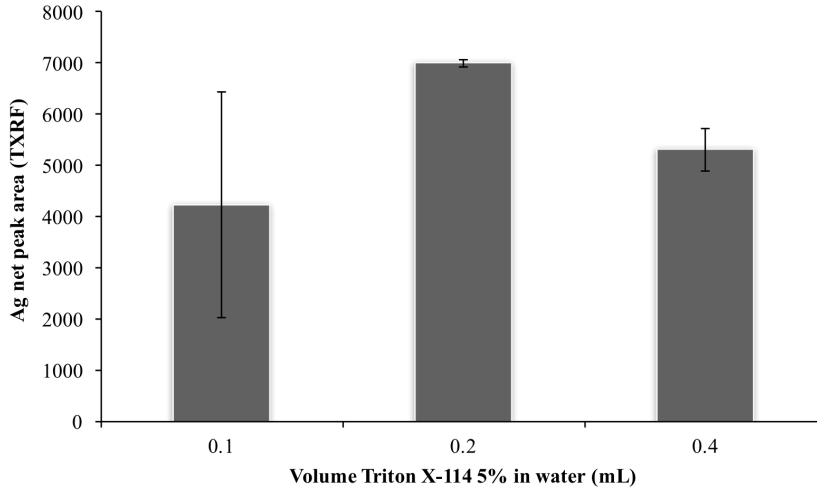

Fig. 5.5 *Influence of Triton X-114 (5% in water) volume used in the CPE procedure on silver analytical response for AgNPs. Error bars corresponds to the standard deviation of triplicate analysis.*

results. For this reason, a volume of 0.2 mL of Triton X-114 (5% in water) was established for further experiments.

5.3.2.3 TXRF analysis

Finally, operating conditions for TXRF measurements were also evaluated to obtain the best instrumental sensitivity for Ag determination. Taking into account the type of matrix and the concentration of the studied element, the rate of kV mA^{-1} of the X-ray tube was selected to work under conditions of maximum efficiency of excitation (50 kV, 1 mA, max. power 50 W). Concerning the measurement time, it was selected as a trade-off between an acceptable instrumental sensitivity, repeatability of measurements (RSD <2%, n = 5, 50 mg L^{-1} of 100 nm citrate coated AgNPs standard) and total analysis time and it was established as 2,000 s.

5.3.3 Analytical figures of merit (CPE-TXRF system)

5.3.3.1 Limits of detection

In order to check the CPE-TXRF capability for AgNPs determination in aqueous samples, limits of detection (LODs) for AgNPs with different coatings (citrate, PVP, and PEG) were evaluated. In all cases, experimental tests were carried out by preconcentrating a standard solution containing 15 µg L^{-1} of AgNPs. LODs were theoretically estimated from the Ag net intensity and background values obtained in the TXRF analysis of the aforementioned solutions [5.34]. LODs calculated were lower than 1 µg L^{-1} and no relevant differences were obtained between

the different capping agents tested (LODs: 0.7–0.8 μg L^{-1}). Despite the fact that the obtained LODs are higher than those associated with the combination of CPE with other popular spectrometric techniques such as ICP-MS or ETAAS (see ***Table 5.1***) and are not adequate to monitor AgNPs in most water samples (AgNPs concentrations usually below 1.5 μg L^{-1}) [5.16], they are suitable for the determination of AgNPs in other types of interesting aqueous solutions including antibacterial products or soil water extracts. Moreover, the low operating and maintenance costs of the TXRF benchtop system (cooling media and gas consumption are not needed for function) make this analytical technique an interesting analytical tool combined with CPE strategies for the cost-effective analysis of aqueous solutions containing AgNPs at μg L^{-1} levels.

5.3.3.2 Linearity

Since the aim of the CPE method is to determine the total amount of nanosized silver in aqueous samples, it is of outmost importance that all AgNPs can be extracted at the same rate. As mentioned in the Introduction Section, few contributions have been published with respect to the influence of different AgNPs coatings on nanosized silver extraction and most of them evaluate the extraction efficiencies of different coated AgNPs at a single and fixed initial AgNPs concentration (1–3 μg L^{-1}) [5.23]. In the present contribution, the effect of AgNPs coating (citrate, PVP and PEG) on the Ag signal has been evaluated at different initial concentration levels in the range of 10 to 100 μg L^{-1}. The results obtained are displayed in ***Fig. 5.6***. As shown, a good linearity (R^2 ≥0.99) between the Ag signal and the initial AgNPs concentration in the solution was obtained in the studied concentration range for all the tested AgNPs coverings. Taking into account that citrate coated-AgNPs are the most frequently used in many commercial products, the linearity for this type of AgNPs was expanded up to 1,000 μg L^{-1} and a good linearity was also obtained (data not shown). As seen in ***Fig. 5.6***, slight differences in the Ag response were identified between the different AgNPs, above all at high concentration levels. For instance, at 100 μg L^{-1}, the analytical response for the AgNPs with the citrate capping agent was 24% higher than that obtained for PVP-AgNPs and 45% higher than that associated with PEG-AgNPs. In general, citrate- and PVP-AgNPs TXRF responses were more similar than those obtained for PEG-AgNPs. This fact can be related to the different zeta potential estimated at pH 7 for the target AgNPs. As detailed by the manufacturer, citrate-AgNPs and PVP-AgNPs present a negative zeta potential whereas PEG-AgNPs are

characterised by a neutral zeta potential [5.40]. The zeta potential is a key indicator of the

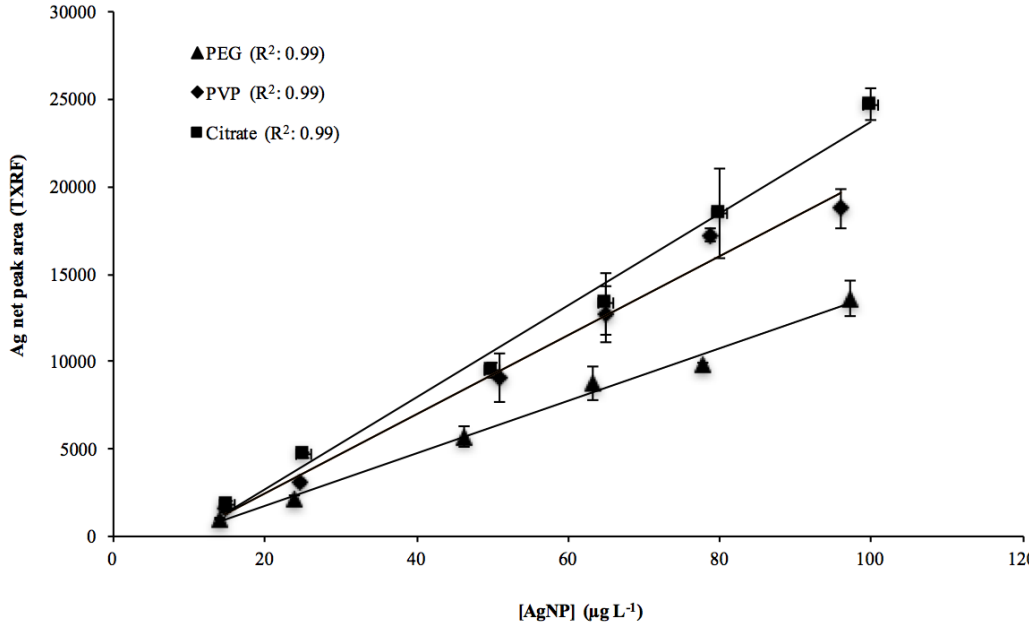

Fig. 5.6 *Calibration curves for different AgNPs surfaces using the developed CPE-TXRF method. Error bars corresponds to the standard deviation of triplicate analysis.*

stability of colloidal dispersions. Usually, colloids with high zeta potential (negative or positive) are electrically stabilised while colloids with low zeta potentials tend to aggregate [5.40]. Therefore, in the case of PEG-AgNPs, the possible agglomeration of the AgNPs might affect the extraction of such particles by CPE.

5.3.3.3 Accuracy of the results

5.3.3.3.1 Effect of AgNPs surface

Taking into account the slightly different Ag responses with respect to the type of AgNPs coating (***Fig. 5.6***), several solutions containing mixtures of the target AgNPs at different initial concentration levels were prepared and analysed by the CPE-TXRF method. In all the experiments, for quantification purposes, the AgNPs with citrate surface calibration curve was used. As shown in the first row of ***Table 5.2***, for all the mixtures considered, recovery values range from 73 to 105%. These values are in agreement with other reported recoveries for AgNPs determination using the CPE method (see ***Table 5.1***). Therefore, it seems that there is not a significant impact of the variation of the analytical responses of the different types of AgNPs coatings on the final quantitative results.

5.3.3.3.2 Effect of AgNPs size

The effect of AgNPs size on the quality of the quantitative results was also tested by analysing an aqueous solution containing a mixture of both 40 nm AgNPs and 100 nm AgNPs at 25 μg L^{-1}. As shown in the results displayed in ***Table 5.2***, a recovery value of 106% was obtained indicating that mixtures of AgNPs with sizes in the range of 40–100 nm can be successfully extracted and determined using the proposed methodology.

5.3.3.3.3 Effect of ionic silver presence

Finally, a study was conducted to evaluate the effect of the presence of ionic silver on AgNPs determination. For this, several solutions containing increasing Ag^+/AgNPs ratios were analysed using the CPE-TXRF method. Acceptable recovery values were obtained for Ag^+/AgNPs ratio values lower than 3.0. For higher Ag^+ proportions, it seems that the use of $Na_2S_2O_3$ is no longer effective to reduce the adsorption of Ag^+ on AgNPs surfaces and ionic silver is extracted into the surfactant-rich phase leading to overestimated recovery values (see ***Table 5.2***). However, for most of the environmental water samples (wastewater effluents, surface and pore waters) [5.41], the concentration of dissolved silver is in the same range as that of AgNPs and thus the contribution of ionic silver to the quantification of AgNPs using the CPE-TXRF method can be neglected. Taking into account that the Ag^+/AgNPs ratios identified in the target soil and consumer product water extracts (for details see the next Section and ***Table 5.3***) were in all cases significantly lower than 1, it can be concluded that the coexisting Ag^+ has negligible effects also for the extraction and quantification of AgNPs in this type of aqueous sample.

5.3.3.4 Precision of the results

The total uncertainty of the results obtained by the CPE-TXRF method consists of many errors associated with the CPE, sample deposition on the reflector and the TXRF measurements (counting statistics). In order to evaluate the total uncertainty for the determination of the target AgNPs, six aqueous standards containing 15 μg L^{-1} of each of the studied AgNPs were analysed with the developed methodology and the relative standard deviations of the obtained results were in all cases in the range of 10–15%. Taking into account that the estimated TXRF measurement error using time of 2,000 s is around 2% it can be concluded that the contribution of sample treatment involving both the CPE extraction and the sample

deposition on the reflector is the major source of error.

5.3.4 Application to complex aqueous samples

The developed CPE-TXRF methodology was applied to determine the AgNPs content in soil and consumer product water extracts (for details see Section 5.2.2.2). For comparison purposes, the same water extracts were also analysed by ICP-OES to estimate the total silver content and by SP-ICPMS to determine the presence of AgNPs and to obtain information regarding the content of AgNPs and Ag^+/AgNPs ratio in the target water extracts. As stated in the Introduction Section, SP-ICPMS is an emerging analytical method that has great potential for monitoring the size and concentration of NPs [5.14]. For the determination of AgNPs percentage, first the raw data obtained by SP-ICPMS were plotted as pulse intensity (counts) *versus* the number of events using a histogram representation. To distinguish the AgNPs against Ag^+, values of the histogram below the first minimum were considered to be related to background or dissolved silver, and values higher than the first minimum were considered to be related to AgNPs [5.42]. After the discrimination between Ag^+ and AgNPs, the percentage of AgNPs was calculated by summing up the number of counts corresponding to AgNPs divided by the total sum of counts recorded (AgNPs + Ag^+) [5.14]. To carry out the aforementioned ICP-OES and SP-ICPMS measurements, it was necessary to filter the water extracts. For this, an experiment was conducted to test the influence of the filtration step on AgNPs recoveries. An aqueous standard solution containing 200 μg L^{-1} of the target 100 nm AgNPs (citrate-AgNPs, PVP-AgNPs, and PEG-AgNPs) was filtered (using a 0.45 μm acetate cellulose filter) and analysed by ICP-OES. A recovery value of 95% was calculated indicating that the filtration step has no influence on AgNPs determination.

5.3.4.1 Soil water extracts

The presence of matrix effects in the CPE procedure has been pointed out in the literature for the AgNPs determination in some environmental samples such as lake water [5.27]. For this reason, recovery values for the determination of AgNPs in soil extracts by the CPE-TXRF method were evaluated by analysing spiked soil water extracts with PVP- and citrate-AgNPs at the 75 μg L^{-1} level. Recoveries obtained in both cases were around 70%. These values were similar to the ones obtained in the determination of AgNPs in distilled water (see ***Table 5.2***) and thus it was concluded that matrix effects for this type of water extract were negligible. In ***Fig. 5.7***, TXRF spectra (CPE-TXRF system), Ag time scans and related signal distribution

histograms (SP-ICPMS) for the studied soil extracts are displayed. As shown, appreciable Ag peaks were obtained in the TXRF spectra after the CPE procedure leading to the conclusion of the presence of AgNPs in both soil extracts. The presence of AgNPs was also confirmed by the results obtained by SP-ICPMS analysis. ***Fig. 5.7*** shows typical signals recorded as a function of time for AgNPs. As described by Laborda *et al.*, a large number of spikes above the baseline in Ag time scans are characteristic of solutions containing AgNPs [5.14]. Moreover, for both soil extracts, the signal distribution histograms show two components: at low counts, a Poisson contribution due to the background or dissolved silver signals, and at higher counts, the contribution of the nanoparticles. This is also the typical profile when AgNPs are present in the analysed solution.

Table 5.3 *AgNPs and total silver concentration in soil and consumer product water extracts.*

[a]Sample type	[a]Total Ag (ICP-OES) (μg L^{-1})	[b]AgNPs (CPE + TXRF) (μg L^{-1})	[c]AgNPs (SP-ICPMS) (%)
Soil Extract-1	120 ± 20	119 ± 5	97
Soil Extract-2	254 ±4	220 ± 10	97
Consumer product extract	250 ± 20	60 ± 5	91

[a] *Results obtained by external calibration using ionic silver stock solution (mean ± SD, n = 3, in μg L^{-1}).*

[b] *Results obtained by external calibration using 100 nm citrate AgNPs standards (mean ± SD, n = 3, in μg L^{-1}).*

[c] *Percentage of AgNPs vs total silver content*

Good agreement with respect to AgNPs concentrations in the analysed soil extracts was obtained between CPE-TXRF and SP-ICPMS (see ***Table 5.3***). As shown, a significant part of the Ag determined in both soil extracts was present in nanosilver form (97%). This fact indicated that the studied AgNPs (citrate 100 nm AgNPs and PVP 75 nm AgNPs) maintain their form after being desorbed from the loaded soil. Despite the fact that additional studies are needed (using other types of AgNPs and soils) the results obtained in this study can contribute to the understanding of mobility and bioavailability of these compounds in the environment. Moreover, it seems that the system CPE-TXRF could be a good analytical approach for this purpose.

5.3.4.2 Consumer product water extract

As shown in ***Fig. 5.7***, Ag characteristic X-ray lines were also detected in the TXRF spectrum obtained by analysing the band aid water extract (see Section 5.2.2.2 for additional details) by

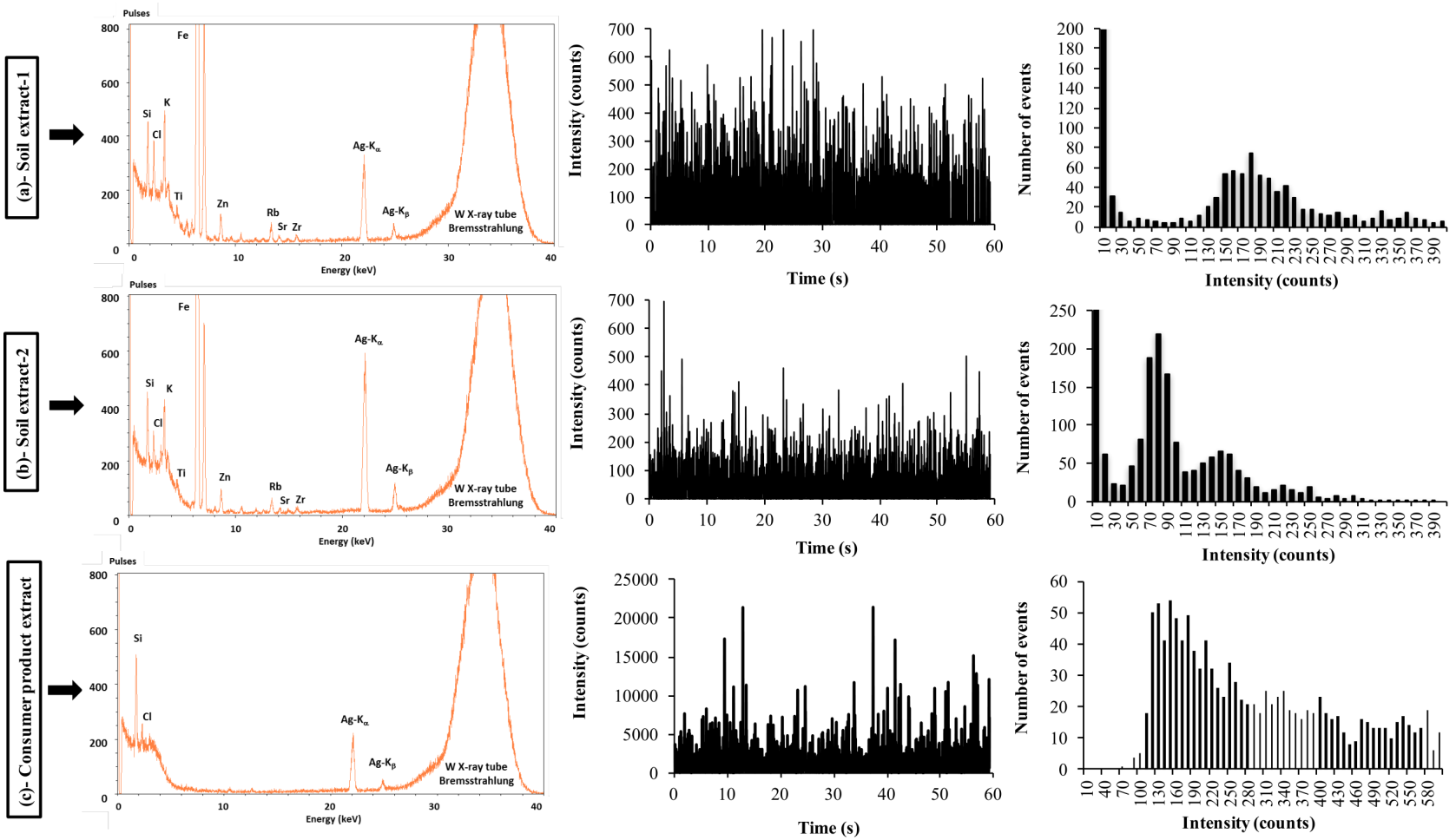

Fig. 5.7 *From left to right: TXRF spectra (CPE-TXRF system), ^{107}Ag time scans and related signal distribution histograms (SP-ICPMS) for: (**a**) soil extract-1 (100 nm citrate-AgNPs), (**b**) soil extract-2 (75 nm PVP-AgNPs), (**c**) consumer product extract (band aid).*

the CPE-TXRF method, indicating the presence of AgNPs. SP-ICPMS results confirmed the presence of Ag in nanosilver form but also a higher proportion of Ag^+ (~10%) in comparison with the aforementioned soil extracts. Moreover, from the obtained Ag time scans and signal distribution histograms, it was evidenced that the AgNPs were a heterogeneous mixture of different sizes including relatively large Ag particles (>100 nm). This fact was also verified by SEM and EDS analysis (***Fig. 5.8***). In contrast to the results obtained in the analysis of the soil extracts, large discrepancies were obtained between the results obtained for the analysis of the band aid water extract by using both methods. As shown in ***Table 5.3***, concentration values obtained by the CPE-TXRF were significantly lower (~76%) than those estimated by

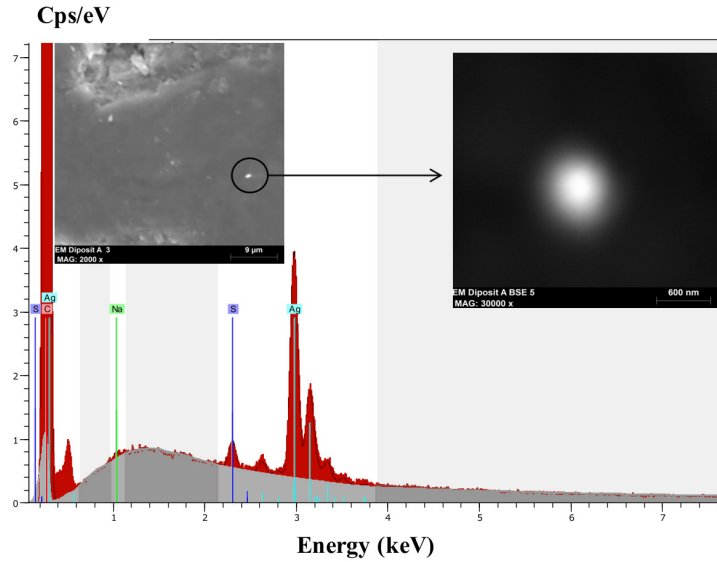

Fig. 5.8 *Identification of AgNPs in the water extract of the studied consumer product (band aid) by SEM and EDS.*

SP-ICPMS. These differences may be probably due to a decrease in the CPE efficiency for AgNPs with a considerable size. In fact, Duester *et al.* pointed out that the extraction efficiency could be dependent on the particle size. Using similar noble metal nanoparticles (AuNPs) it was found that the extraction efficiency decreases from 101% to 52% with an increase of nanoparticle size from 2 to 150 nm [5.43].

Moreover, it has to be kept in mind that the presence of a large mixture of different AgNPs sizes in the water extract also hampers the estimation of the AgNPs/Ag^+ ratio by SP-ICPMS as well as the fact that the peak of ionic silver in the histogram is not well separated from the distribution due to the presence of nanoparticles. Thus, the uncertainty of both reported results could be significant. This fact highlights the necessity to study in more detail the effectiveness

of existing methodologies (including CPE-TXRF and SP-ICPMS) for the monitoring of AgNPs in complex matrices involving mixtures of different NPs coatings and particle sizes.

5.4 Conclusions

In the present contribution, the analytical capabilities of CPE in combination with TXRF have been evaluated for the quantification of AgNPs in complex aqueous samples including soil and consumer product water extracts. The best way to prepare the preconcentrated sample after the CPE was found to be the evaporation of the organic rich phase and its redissolution using 20 μg L^{-1} of carbon tetrachloride. Using this analytical approach, detection limits lower than 1 μg L^{-1} were achieved with a relative standard deviation of around 10–15% (n = 5).

Good agreement with respect to AgNPs concentrations in the analysed soil extracts was obtained between CPE-TXRF and SP-ICPMS, confirming the absence of matrix effects for this type of sample by CPE. Although the variations of the analytical responses depending on the AgNPs coating (citrate, PVP and PEG) and size (40–100 nm) were almost negligible when considering the analysis of AgNPs aqueous standards, appreciable discrepancies with SP-ICPMS results were obtained for the analysis of consumer product water extracts containing mixtures of different sizes (including Ag particles >100 nm). This fact highlights the necessity to increase our understanding on size-resolved extraction efficiencies by CPE in order to increase the reliability of CPE-based methods for the analysis of real aqueous samples containing mixtures of different NPs particle sizes and coatings. The benefit of complementary use of CPE-based methods and SP-ICPMS for the analysis of complex samples is also remarkable.

Acknowledgments

The Spanish Ministry of Economy and Competitiveness financed this work through the project CGL2013-48802-C3-2-R (Program 2014). L. Torrent gratefully acknowledges a FPI grant from the Spanish Ministry of Economy and Competitiveness (Ref. BES- 2014-070625). The authors are also thankful to Lourdes Fernández for her contribution on the performance of this work.

References

[5.1] S.-H. Yu, Y.G. Yin, J.-F. Liu, Silver nanoparticles in the environment, Environ. Sci. Process Impacts 15 (2013) 78–92.

[5.2] Woodrow Wilson International Center for Scholars. Project on Emerging Nanotechnology, 2011.

Available at: www.nanotechproject.org. Accessed October, 2017.

[5.3] O. Geiss, C. Cascio, D. Gilliland, F. Franchini, J. Barrero-Moreno, Size and mass determination of silver nanoparticles in an aqueous matrix using asymmetric flow field flow fractionation coupled to inductively coupled plasma mass spectrometer and ultraviolet–visible detectors, J. Chromatogr. A 1321 (2013) 100–108.

[5.4] F. Gottschalk, T. Sun, B. Nowack, Environmental concentrations of engineered nanomaterials: review of modeling and analytical studies, Environ. Pollut. 181 (2013) 287–300.

[5.5] S.D. Richardson, Water analysis: emerging contaminants and current issues, Anal. Chem. 81 (2009) 4645–4677.

[5.6] J.-F. Liu, S.-J. Yu, Y.-G. Yin, J.-B. Chao, Methods for separation, identification, characterization and quantification of silver nanoparticles, Trends Anal. Chem. 33 (2012) 95–106.

[5.7] B. Ferreira da Silva, S. Pérez, P. Gardinalli, R.K. Singhal, A.A. Mozeto, Analytical chemistry of metallic nanoparticles in natural environments, Trends Anal. Chem. 30 (2011) 528–540.

[5.8] H. Qu, T.K. Mudalige, S.W. Linder, Capillary electrophoresis coupled with inductively coupled mass spectrometry as an alternative to cloud point extraction based methods for rapid quantification of silver ions and surface coated silver nanoparticles, J. Chromatogr. A 1429 (2016) 348–353.

[5.9] T.K. Mudalige, H. Qu, S.W. Linder, Asymmetric flow-field flow fractionation hyphenated ICP-MS as an alternative to cloud point extraction for quantification of silver nanoparticles and silver speciation: application for nanoparticles with a protein corona, Anal. Chem. 87 (2015) 7395–7401.

[5.10] M.E. Hoque, K. Khosravi, K. Newman, C.D. Metcalfe, Detection and characterization of silver nanoparticles in aqueous matrices using asymmetric-flow field flow fractionation with inductively coupled plasma mass spectrometry, J. Chromatogr. A 1233 (2012) 109–115.

[5.11] Z.-Q. Tan, J.-F. Liu, X.-R. Guo, Y.-G. Yin, S.K. Byeon, M.H. Moon, *et al.*, Toward full spectrum speciation of silver nanoparticles and ionic silver by on-line coupling of hollow fiber flow field-flow fractionation and minicolumn concentration with multiple detectors, Anal. Chem. 87 (2015) 8441–8447.

[5.12] X.-X. Zhou, J.-F. Liu, G.-B. Jiang, Elemental mass size distribution for characterization, quantification and identification of trace nanoparticles in serum and environmental waters, Environ. Sci. Technol. 51 (2017) 3892–3901.

[5.13] B. Franze, C. Engelhard, Fast separation, characterization, and speciation of gold and silver nanoparticles and their ionic counterparts with micellar electrokinetic chromatography coupled

to ICP-MS, Anal. Chem. 86 (2014) 5713–5720.

[5.14] F. Laborda, J. Jiménez-Lamana, E. Bolea, J.R. Castillo, Selective identification, characterization and determination of dissolved silver(I) and silver nanoparticles based on single particle detection by inductively coupled plasma mass spectrometry, J. Anal. At. Spectrom. 26 (2011) 1362.

[5.15] A.-L. Fabricius, L. Duester, B. Meermann, T.A. Ternes, ICP-MS-based characterization of inorganic nanoparticles—sample preparation and off-line fractionation strategies, Anal. Bioanal. Chem. 406 (2014) 467–479.

[5.16] L. Li, G. Hartmann, M. Döblinger, M. Schuster, Quantification of nanoscale silver particles removal and release from municipal wastewater treatment plants in germany, Environ. Sci. Technol. 47 (2013) 7317–7323.

[5.17] S.M. Majedi, B.C. Kelly, H.K. Lee, Efficient hydrophobization and solvent microextraction for determination of trace nano-sized silver and titanium dioxide in natural waters, Anal. Chim. Acta 789 (2013) 47–57.

[5.18] J.-F. Liu, J.-B. Chao, R. Liu, Z.-Q. Tan, Y.-G. Yin, Y. Wu, *et al.*, Cloud point extraction as an advantageous preconcentration approach for analysis of trace silver nanoparticles in environmental waters, Anal. Chem. 81 (2009) 6496–6502.

[5.19] A. Melnyk, J. Namieśnik, L. Wolska, Theory and recent applications of coacervate-based extraction techniques, Trends Anal. Chem. 71 (2015) 282–292.

[5. 20] J.-B. Chao, J. -F. Liu, S. -J. Yu, Y. -D. Feng, Z. -Q. Tan, R. Liu, *et al.*, Speciation analysis of silver nanoparticles and silver ions in antibacterial products and environmental waters via cloud point extraction-based separation, Anal. Chem. 83 (2011) 6875–6882.

[5.21] S.-J. Yu, J.-B. Chao, J. Sun, Y.-G. Yin, J.-F. Liu, G.-B. Jiang, Quantification of the uptake of silver nanoparticles and ions to HepG2 cells, Environ. Sci. Technol. 47 (2013) 3268–3274.

[5.22] G. Hartmann, C. Hutterer, M. Schuster, Ultra-trace determination of silver nanoparticles in water samples using cloud point extraction and ETAAS, J. Anal. At. Spectrom. 28 (2013) 567.

[5.23] G. Hartmann, T. Baumgartner, M. Schuster, Influence of particle coating and matrix constituents on the cloud point extraction efficiency of silver nanoparticles (Ag-NPs) and application for monitoring the formation of Ag-NPs from Ag+, Anal. Chem. 86 (2014) 790–796.

[5.24] I. López-García, Y. Vicente-Martínez, M. Hernández-Córdoba, Speciation of silver nanoparticles and Ag(I) species using cloud point extraction followed by electrothermal atomic absorption spectrometry, Spectrochim. Acta Part B At. Spectrosc. 101 (2014) 93–97.

[5.25] G.Z. Tsogas, D.L. Giokas, A.G. Vlessidis, Ultratrace determination of silver, gold, and iron oxide nanoparticles by micelle mediated preconcentration/selective back-extraction coupled with flow injection chemiluminescence detection, Anal. Chem. 86 (2014) 3484–3492.

[5.26] Z.-H. Wu, W.-L. Tseng, Combined cloud point extraction and Tween 20-stabilized gold nanoparticles for colorimetric assay of silver nanoparticles in environmental water, Anal. Methods 3 (2011) 2915–2920.

[5.27] L.M. Furtado, M.E. Hoque, D.M. Mitrano, J.F. Ranville, B. Cheever, P.C. Frost, *et al.*, The persistence and transformation of silver nanoparticles in littoral lake mesocosms monitored using various analytical techniques, Environ. Chem. 11 (2014) 419–430.

[5.28] C. Streli, Recent advances in TXRF, Appl. Spectrosc. Rev. 41 (2006) 473–489.

[5.29] M. Menzel, U.E.A. Fittschen, Total reflection X-ray fluorescence analysis of airborne silver nanoparticles from fabrics, Anal. Chem. 86 (2014) 3053–3059.

[5.30] L. Torrent, M. Iglesias, M. Hidalgo, E. Marguí, Analytical capabilities of total reflection X-ray fluorescence spectrometry for silver nanoparticles determination in soil adsorption studies, Spectrochim. Acta Part B At. Spectrosc. 126 (2016) 71–78.

[5.31] S.A. Blaser, M. Scheringer, M. MacLeod, K. Hungerbühler, Estimation of cumulative aquatic exposure and risk due to silver: Contribution of nano-functionalized plastics and textiles, Sci. Total Environ. 390 (2008) 396–409.

[5.32] E. Marguí, I. Queralt, M. Hidalgo, Determination of cadmium at ultratrace levels in environmental water samples by means of total reflection X-ray spectrometry after dispersive liquid–liquid microextraction, J. Anal. At. Spectrom. 28 (2013) 266–273.

[5.33] B.M. Simonet, M. Valcárcel, Monitoring nanoparticles in the environment, Anal. Bioanal. Chem. 393 (2009) 17–21.

[5.34] R. Klockenkämper, Total-reflection X-ray fluorescence analysis, Wiley, New York, 1st edn, 1997.

[5.35] T.M. Tolaymat, A.M. El Badawy, A. Genaidy, K.G. Scheckel, T.P. Luxton, M. Suidan, An evidence-based environmental perspective of manufactured silver nanoparticle in syntheses and applications: A systematic review and critical appraisal of peer-reviewed scientific papers, Sci. Total Environ. 408 (2010) 999–1006.

[5.36] R. Dalipi, E. Marguí, L. Borgese, L.E. Depero, Multi-element analysis of vegetal foodstuff by means of low power total reflection X-ray fluorescence (TXRF) spectrometry, Food Chem. 218 (2017) 348–355.

[5.37] H. Gallardo, I. Queralt, J. Tapias, L. Candela, E. Marguí, Bromine and bromide content in soils: analytical approach from total reflection X-ray fluorescence spectrometry, Chemosphere 156 (2016) 294–301.

[5.38] E. Marguí, M. Sagué, I. Queralt, M. Hidalgo, Liquid phase microextraction strategies combined with total reflection X-ray spectrometry for the determination of low amounts of inorganic antimony species in waters, Anal. Chim. Acta 786 (2013) 8–15.

[5.39] E. Marguí, B. Zawisza, R. Sitko, Trace and ultratrace analysis of liquid samples by X-ray fluorescence spectrometry, Trends Anal. Chem. 53 (2014) 73–83.

[5.40] Nanocomposix. Standard Capping Agents. Available at: http://cdn.shopify.com/s/files/1/0257/8237/files/Standard_Capping_Agents.pdf. Accessed: October 6, 2017.

[5.41] N.W.H. Adams, J.R. Kramer, Silver speciation in wastewater effluent, surface waters, and pore waters, Environ. Toxicol. Chem. 18 (1999) 2667–2673.

[5.42] D.M. Mitrano, A. Barber, A. Bednar, P. Westerhoff, C.P. Higgins, J.F. Ranville, Silver nanoparticle characterization using single particle ICP-MS (SP-ICP-MS) and asymmetrical flow field flow fractionation ICP-MS (AF4-ICP-MS), J. Anal. At. Spectrom. 27 (2012) 1131–1142.

[5.43] L. Duester, A.-L. Fabricius, S. Jakobtorweihen, A. Philippe, F. Weigl, A. Wimmer, *et al.*, Can cloud point-based enrichment, preservation, and detection methods help to bridge gaps in aquatic nanometrology?, Anal. Bioanal. Chem. 408 (2016) 7551–7557.

CHAPTER 6

Combination of cloud point extraction with single particle inductively coupled plasma mass spectrometry to characterize silver nanoparticles in soil leachates

This chapter corresponds to the following publication:

L. Torrent, F. Laborda, E. Marguí, M. Hidalgo, M. Iglesias, *Combination of cloud point extraction with single particle inductively coupled plasma mass spectrometry to characterize silver nanoparticles in soil leachates*. Anal. Bioanal. Chem. 411 (2019) 5317-5329

Abstract

The expansion of silver nanoparticle (AgNP) applications in industry as antibacterial agents has generated an increment of their presence in the environment. Once there, their behaviour is not clear because they can undergo different transformation processes that affect their transport, mobility, bioavailability, and toxicity. Therefore, the characterisation and quantification of these emerging contaminants are important to understand their behaviour and the toxicity effects that can be exerted on living beings. Single particle inductively coupled plasma mass spectrometry (SP-ICPMS) has demonstrated its ability to characterise and give quantitative information on AgNPs in aqueous samples. However, sometimes, the discrimination of the signal corresponding to AgNPs from the signal of dissolved species (Ag(I)) is a challenge. In the present contribution, it is shown that the presence of high amounts of Ag(I) hamper silver nanoparticle size and nanoparticle concentration determination in aqueous samples by SP-ICPMS. To facilitate signal discrimination of both chemical forms, the combination of cloud point extraction (CPE) with SP-ICPMS was studied. CPE experimental conditions to separate AgNPs from Ag(I) were assessed and adapted taking into account the characteristics of the SP-ICPMS technique. CPE and soil matrix effects on particle size were evaluated, showing that particle size was not modified after being in contact with soil matrix and after being separated by CPE. Additionally, frequently used calculation methods for SP-ICPMS data treatment were assessed. Finally, the potential of the developed methodology CPE-SP-ICPMS was evaluated in aqueous soil leachates contaminated with mixtures of AgNPs/Ag(I).

Keywords: Silver nanoparticles, Dissolved silver species, Single particle inductively coupled plasma mass spectrometry, Cloud point extraction, Soils, Aqueous leachates

6.1 Introduction

In the last decades, the production of engineered nanoparticles (ENPs) has increased gradually, forecasting by the end of 2020 a global market value of about 30 billion USD. This expansion is related to their special reactivity, strength, and electrical properties given by the unique physicochemical characteristics (e.g. small particle size (1–100 nm), surface area, surface reactivity, charge, and shape) that they present in comparison with their bulk counterparts [6.1, 6.2]. As a consequence of the exponential increment of ENP production and commercial applications, the probability of these particles to reach the environment (air, water, soil, and organisms) unintentionally or intentionally has risen [6.3]. One of the most abundant ENPs in the environment are silver nanoparticles (AgNPs) due to their broad use in the industry as antibacterial agents (production in 2010 ~55 tons/year) [6.1-6.4]. In the environment, AgNP behaviour is not clear due to the various factors that affect their transport, mobility, bioavailability, and toxicity. They can stay as individual particles in suspension or they can suffer several changes through different environmental processes such as aggregation, agglomeration, dissolution, deposition, phototransformation, sulfidation, oxidation, or macromolecular transformations [6.1, 6.4-6.6]. Although environmental conditions (pH, electrolyte composition, ionic strength, and organic matter) govern these particle transformations, AgNP properties (size, surface chemistry, aggregation state, and solubility) also contribute to their changes [6.5, 6.7]. Therefore, nanoparticle characterisation and quantification are important to understand their behaviour and the toxic effects that they can exert to humans and other organisms.

In recent years, several innovative analytical tools have been developed for detection, characterisation, and quantification of these emerging contaminants in different matrices. Microscopic, dynamic light scattering, and spectroscopic techniques are widely used for imaging and obtaining information about the size, shape, and aggregation state of nanosilver [6.8-6.19], so a complementary analytical tool has to be employed to get quantitative data. Typical quantitative approaches are conventional atomic spectroscopic techniques that permit to obtain total silver (Ag) concentrations, but they are not suitable for determining the Ag physicochemical form (dissolved or particulate), particle size, or aggregation state [6.20-6.23]. For this reason, the combination of the aforementioned techniques is required to characterise and quantify AgNPs. In addition to these analytical techniques, an innovative and emerging analytical method that is gaining popularity is single particle inductively coupled plasma mass spectrometry (SP-ICPMS) because it combines the benefits of an element specific atomic spectrometry technique (ICPMS) with those of a particle counting technique [6.24]. The

ability of this method to count particles is achieved when a sufficiently diluted particle suspension (number concentration below 10^8 particles L^{-1}) is introduced into the plasma and by measuring with an adequate time resolution (dwell time ≤10 ms) [6.20, 6.25, 6.26]. Under these conditions, when nanoparticles arrive into the plasma, they are vaporised, atomised, and ionised generating a cloud of ions that straightaway are detected as a single event in a mass spectrometer detector [6.27, 6.28]. Each single event represents a nanoparticle, so the frequency of events is related directly to particle number concentration while the intensity of each event is proportional to the mass of element in the detected nanoparticle. Moreover, if the shape, composition, and density of the particles are known, their size can be calculated from the signal intensities of the nanoparticles detected [6.27-6.29]. Thus, SP-ICPMS has the potential to characterise and give quantitative information of AgNPs at environmentally relevant exposure levels (concentration levels ≤ng L^{-1}). Nevertheless, challenges on this analytical method remain with respect to nebulisation efficiency (η_{neb}) measurement, which is one of the ICPMS parameters that affect the accuracy of particle size and particle number concentration calculations. Furthermore, validation approaches to calculate this parameter (η_{neb}) are scarce [6.30, 6.31]. Another difficulty of SP-ICPMS is the discrimination between signals corresponding to AgNPs and dissolved silver species (Ag(I)). The presence of Ag(I) produces a continuous constant signal given that distribution of metal ions entering into the plasma is homogeneous. At low concentrations of Ag(I), the detection of AgNPs is possible, but at high concentrations of Ag(I) is more critical, especially when the particles are small [6.4, 6.32, 6.33]. To overcome this SP-ICPMS limitation, some authors have discussed about different algorithms to facilitate the discrimination of nanoparticles from their corresponding dissolved species [6.31, 6.34-6.37]. A different strategy involves the use of hyphenated separation techniques, such as field flow fractionation [6.38], electrophoretic [6.39], or chromatographic techniques [6.40]. In addition to these sophisticated techniques, there are some sample treatments based on the separation and preconcentration of AgNPs that are applied before the analysis of the samples. Among the multiple sample treatment procedures (e.g. centrifugation, filtration, ultrafiltration, dialysis, or solid phase extraction), cloud point extraction (CPE) is a cheap and environment-friendly liquid-phase micro-extraction methodology. CPE consists of adding to an aqueous sample a non-ionic surfactant (usually 1,1,3,3- tetramethylbutyl)phenyl-polyethyleneglycol (Triton X-114)) at a concentration over the critical micellar concentration (cmc). The resulting mixture is then submitted to a temperature above the cloud point temperature (23 °C for Triton X-114). During this process, the aqueous sample becomes turbid, due to the formation of surfactant micelles that

capture the AgNPs present in the sample. The micelles containing the AgNPs are denser than water, so the nanoparticles are deposited and concentrated into a small surfactant volume, which can be separated by centrifugation. The most common analytical tools used in combination with CPE are spectrometric methods [6.20, 6.41, 6.42], among them is ICPMS. Several studies in the bibliography have combined the CPE with SP-ICPMS to quantify and determine particle size distribution of AgNPs in surface and wastewaters [6.43-6.45], but to our knowledge in the literature, there is only a work that determines nanoparticle size distribution in spiked soil extracts and it was performed with gold nanoparticles (AuNPs) [6.46].

The aims of the present work are: (1) to assess different calculation methods to determine the nebulisation efficiency, which is the parameter that has an effect on obtaining accurate particle size and number concentration, using AgNPs of different coatings and sizes; (2) to study the combination of CPE methodology with SP-ICPMS analysis to determine the size and concentration of AgNPs in samples containing high amounts of Ag(I); (3) to apply the developed methodology (CPE-SP-ICPMS) to the analysis of aqueous soil leachates contaminated with a mixture of AgNPs and Ag(I).

6.2 SP-ICPMS theoretical aspects

6.2.1 Thresholds for discrimination of AgNPs from Ag(I) signals

One of the critical aspects of SP-ICPMS methodology is the discrimination between nanoparticles and dissolved species of the same element, especially when their signal distributions are overlapped. This can occur due to the presence of small-sized nanoparticles and/or high content of dissolved species in the sample. Several authors use detection thresholds based on $n\sigma$ criteria (σ, standard deviation of the continuous signal produced by dissolved species) to discriminate both signals. Pace *et al.* proposed an iterative algorithm based on 3 times the standard deviation plus the mean of all data points obtained from the analysis ($\bar{y} + 3\sigma$). The data points exceeding this detection threshold are considered nanoparticles and are removed [6.33,6.34]. This procedure is repeated until no further particle signals are removed. Using $\bar{y} + 3\sigma$ as a detection threshold, there is the possibility of counting false positives (background-dissolved signals counted as nanoparticles) as stated by Tuoriniemi *et al.* [6.36]. Therefore, this author suggests the application of a $\bar{y} + 5\sigma$ detection limit to reduce to less than 0.1% the contribution of false positives.

In addition to these iterative algorithms, Cornelis and Hasellöv proposed an alternative procedure for improving the detectability of the nanoparticles based on removal of the distribution

corresponding to the dissolved element once it was fitted to a Polygaussian probability mass function [6.37].

6.2.2 Nebulisation efficiency determination

The nebulisation efficiency is described as the ratio of the amount of analyte entering the plasma to the amount of analyte aspirated. The value of this parameter is relevant in SP-ICPMS analysis because it can be used for particle size and particle number concentration calculations. Pace *et al.* presented three different methods for calculating η_{neb} [6.7]. The first method, called waste collection, consists of determining the total weight of the sample that entered the plasma by subtracting the weight of waste sample collected from the spray chamber to the total weight aspirated:

$$\eta_{neb} = \frac{\Delta \text{ total weight plasma}}{\Delta \text{ sample weight}} \tag{6.1}$$

The second method, known as particle frequency method, η_{neb} is obtained relating the number of particle events detected (I_p) during a determined acquisition time (t_i) to a known particle number concentration (N_{NP}) of the analysed nanoparticle suspension and the sample flow rate (Q_{sample}):

$$\eta_{neb} = \frac{I_P}{Q_{Sample} N_{NP} t_i} \tag{6.2}$$

The third method, named particle size method, is based on relating the ions counted per time unit of an ionic metal solution of mass concentration (C_M) with the total counts per reading of nanoparticles with known particle size. For determining η_{neb} by particle size method, firstly, a calibration curve using ionic metal standards has to be measured. This calibration curve relates the ions counted per time unit (R) to C_M [6.31]:

$$R = K_R C_M = K_{intr} K_{ICPMS} K_M C_M \tag{6.3}$$

where the K_{intr} ($=\eta_{neb} Q_{sample}$) is the contribution of the sample introduction system, K_{ICPMS} is the

detection efficiency, and K_M (= $\frac{AN_{AV}}{M_M}$) the contribution of the element. Secondly, a nanoparticle suspension with known particle size has to be analysed. If the analysis is performed in time-resolved mode and the analysed nanoparticles are spherical, solid and pure; the total counts per reading of one nanoparticle (r_{NP}) can be related to particle mass ($m_{NP} = \frac{1}{6} X_{NP} \rho \pi d^3$) through:

$$r_{NP} = K_r m_{NP} = K_{ICPMS} K_M m_{NP} \tag{6.4}$$

Considering that once in the plasma, the behaviour of the element from the ionic standard solution and the nanoparticle suspension is the same, Eq. (6.3) and (6.4) can be combined to obtain the following expression for calculating the η_{neb}:

$$\eta_{neb} = \frac{K_R}{K_r} \frac{1}{Q_{sample}} = \frac{R/C_M}{r_{NP}/m_{NP}} \frac{1}{Q_{sample}} \tag{6.5}$$

6.2.3 Particle size and particle number determination

Particle size and particle number concentration can be calculated when η_{neb} is known. Knowing the nebulisation efficiency, the term K_{intr} (=$\eta_{neb} Q_{sample}$) can be determined and consequently the term K_{ICPMS} of Eq. (6.3) can be calculated. Then, using Eq. (6.4) the element mass per particle and hence the size can be determined. On the other hand, particle number concentration can be calculated using the following equation:

$$N_{NP} = \frac{I_P}{Q_{sample} \eta_{neb} t_i} \tag{6.6}$$

6.3 Materials and methods

6.3.1 Chemicals, materials and apparatus

To prepare AgNP standards and spiked agricultural soils, commercial sodium citrate–stabilised (2 mM) silver nanoparticles (citrate-AgNPs) of 60 nm and 100 nm and polyvinylpyrrolidone-coated

silver nanoparticles (PVP-AgNPs) of 75 nm and 100 nm from Nanocomposix (St. Louis, MO, USA) were employed. An ionic silver stock solution (1,000 ± 2 mg L^{-1}) purchased from Merck (Darmstadt, Germany) was used to prepare calibration for ICPMS and flame atomic absorption spectrometry analysis, and to prepare the AgNPs/Ag(I) mixtures for studying the possibilities of CPE-SP-ICPMS methodology to analyse AgNPs in samples containing high amounts of Ag(I). Ultrapure water from a Milli-Q purification system (Millipore Corp., Bedford, MA) was utilised to dilute AgNP standards, mixtures of AgNPs/Ag(I), 1% glycerol, 1% isopropanol (Panreac, Barcelona, Spain), and soil leachates. Moreover, AgNP standards were also diluted with 1% glycerol.

Sodium thiosulfate pentahydrate ($Na_2S_2O_3 \cdot 5H_2O$) from Panreac (Barcelona, Spain) and non-ionic surfactant Triton X-114 ((1,1,3,3-tetramethylbutyl)phenyl-polyethyleneglycol) from Sigma-Aldrich (St. Louis, USA) were employed for performing the CPE procedure. In addition, the pH of the samples was adjusted during the CPE with 0.05 M nitric acid (HNO_3) prepared from analytical grade hiperpur quality HNO_3 (69%, Ag 0.1 ng g^{-1}, Panreac, Barcelona, Spain). An incubator Infors HT (Bottmingen, Switzerland) was used during the incubation step of CPE procedure. The resulting CPE extracts were diluted with 1% glycerol.

Batch sorption and leaching experiments were performed using a rotary mixer Dinko (Barcelona, Spain). To separate the aqueous soil leachate from the soil, a Rotofix 32A centrifuge (Hettich-Zentrifugen, Lauenau, Germany) was used after batch adsorption and leaching experiments. An ultrasound system J.P. Selecta (Barcelona, Spain) was employed to break down the possible agglomerated AgNPs.

6.3.2 Cloud point extraction procedure and sample preparation for SP-ICPMS analysis

In this study, the CPE methodology was carried out to separate AgNPs in complex aqueous matrices (soil leachates) with high contents of dissolved silver species to avoid the interference from the latter. With this purpose, 9.5 mL of aqueous solution or aqueous soil leachate containing AgNPs/Ag(I) was placed in a polypropylene tube. Then, the pH of the sample was adjusted at 3.5 with HNO_3 (0.05 M). Afterwards, 0.1 mL of $Na_2S_2O_3 \cdot 5H_2O$ (0.1 M) and 0.2 mL of Triton X-114 (5%) were added to the sample solution. The sample was vigorously shaken during 1 min and incubated during 30 min at 40 °C. After 30 min, the sample was centrifuged at 2,000 rpm (5 min) to separate the AgNP surfactant-rich phase (bottom of the vial) from the aqueous phase. Next, it was cooled down in a freezer during 15 min to increase the viscosity of the phase containing the nanosilver and facilitate the phase separation [6.42]. After separating the phases, the AgNP micelle-rich

phase was diluted with 1% glycerol (*v/v*) to 9.5 mL to enable the analysis by SP-ICPMS.

6.3.3 Silver nanoparticles soil sorption and leaching experiments

To obtain the aqueous soil leachates containing AgNPs and/or Ag(I), the soils were previously spiked with AgNPs (60 nm citrate-AgNPs and 75 nm PVP-AgNPs) performing a batch adsorption experiment. With this purpose, 0.5 g of soil (agricultural Mediterranean soil from Castellbisbal (Barcelona, Spain)) was weighed in polystyrene tubes. Then, 20 mL of 1 mg L^{-1} AgNP aqueous suspension (60 nm citrate-AgNPs and 75 nm PVP-AgNPs) was added and they were submitted to rotation with a rotary mixer (35 rpm) at room temperature (22 °C) for a period of 2 h. Next, the samples were centrifuged at 3,500 rpm (8 min) to separate the supernatant from the soil. After sample centrifugation, the supernatant was removed from the polystyrene tube and the soil was dried overnight into an oven at 65–70 °C.

After 3 weeks, desorption of Ag (as AgNPs or Ag(I)) from soils was performed using a leaching method based on the German Standard Method DIN 38414-S4 [6.47]. The leaching procedure consisted in adding 15 mL of ultrapure water to the agricultural soils and the mixture was submitted to rotary agitation (35 rpm) at room temperature (22 °C) during 24 h. After 1 day of rotation, the samples were centrifuged at 3,500 rpm during 12 min and the part of the supernatant (aqueous soil leaching solution) containing particles with a particle size lower than 0.2 µm was pipetted [6.48]. Then, the supernatants pipetted were directly analysed by inductively coupled plasma optic emission spectroscopy (ICP-OES) or were submitted to CPE procedure. After CPE, the extracts were also analysed by ICP-OES. Once the total silver concentration was determined for aqueous soil leachates and CPE extracts, the samples were diluted properly (<ng L^{-1}) to gain an adequate number of nanoparticles in the aqueous sample. The optimal dilution was obtained by an Excel spreadsheet that takes into account the nebulisation efficiency, the sample flow rate, the dwell time, and nanoparticle characteristics [6.49]. Finally, the prepared samples were analysed by SP-ICPMS.

Similarly, not spiked soils were also treated, using the same methodology as explained before, in order to be used as blank aqueous soil leachates for optimisation purposes.

6.3.4 Instrumentation and calculations

The total silver content in the AgNP surfactant-rich phase of different samples adjusted at different pH during the CPE procedure was determined with a PerkinElmer model AAnalyst

200 flame atomic absorption spectrometer (Toronto, Canada) utilising a calibration curve of ionic silver standards prepared in 1% glycerol (0.5–10 mg L^{-1}). The optimisation of the combination of CPE methodology with SP-ICPMS analysis was carried out with a PerkinElmer Sciex model

Table 6.1 *Inductively coupled plasma mass spectrometry instrumental and data acquisition parameters.*

		Agilent 7500c ICP-MS spectrometer		**PerkinElmer Sciex ELAN DRC-e ICPMS spectrometer**	
Instrumental characteristics	RF power	1,500 W		1,200 W	
	Sample uptake rate	0.3 mL min^{-1}		1 mL min^{-1}	
	Nebuliser chamber	Doublepass scott		Cyclonic	
	Nebuliser	Babington		Glass concentric slurry	
	Nebuliser gas flow rate	1.1 L min^{-1}		1.18 L min^{-1}	
	Sampling cone	Ni, 1 mm aperture diameter		Ni, 1.1 mm aperture diameter	
	Skimmer cone	Ni, 0.4 mm aperture diameter		Ni, 0.9 mm aperture diameter	
	Argon gas flow rate	15 L min^{-1}		15 L min^{-1}	
	Analyser	Quadrupole		Quadrupole	
	Detector	Electron multiplier		Electron multiplier	
Data acquisition parameters		**Standard measuring mode**	**Single particle measuring mode**	**Standard measuring mode**	**Single particle measuring mode**
	Isotopes monitored	^{107}Ag		^{107}Ag, ^{109}Ag	
	Dwell time	500 ms	10 ms	50 ms	5 ms
	Acquisition time	4.5 s	60 s	1 s	60 s
	Points per spectral peak	3	1	1	1
	Readings per replicate	3	5,730	5	12,000

ELAN DRC-e ICPMS spectrometer (Toronto, Canada). In aqueous soil leachates and in extracts obtained from CPE, the total silver content was measured with an Agilent Technologies model Vertical Dual View 5100 ICP-OES spectrometer (Tokyo, Japan) using an ionic silver calibration curve in ultrapure water or 1% glycerol medium (5–350 µg L^{-1}). For characterising and quantifying the AgNPs present in aqueous soil leachates and in CPE extracts, the SP-ICPMS was performed employing a quadrupole-based Agilent Technologies model 7500c ICPMS spectrometer (Tokyo, Japan) equipped with an Octapole Reaction System (ORS). SP-ICPMS data treatment was carried out using an in-lab Microsoft Excel spreadsheet and it was compared with RIKILT spreadsheet [6.27]. All these calculations assume spherical shape particles that present a density equivalent to

the bulk material, e.g. 10.49 g cm^{-3}. The instrumental characteristics and measurement conditions of the different instruments used in this study are shown in ***Table 6.1*** and ***Table S6.1*** from the Supplementary information of this chapter. In addition, *t* test was performed to determine if there were statistical differences ($t_{critical}<t_{experimental}$) o not ($t_{critical}>t_{experimental}$) between the results obtained. Size detection limits of AgNPs were determined in mixtures of AgNPs and Ag(I) as 5 times the standard deviation of the baseline (signal corresponding to the Ag(I)).

6.4 Results and discussion

6.4.1 Optimisation of CPE-SP-ICPMS methodology

6.4.1.1 Criteria for discriminating continuous signal contribution

The discrimination of the signals corresponding to AgNPs and Ag(I) can be a difficult task in SP-ICPMS analysis, especially when their signal distributions are overlapped. For this reason, different algorithms were tested (see ***Fig. 6.1***). The iterative algorithm to discriminate the AgNP signal from Ag(I) based on $\bar{y} + 3\sigma$ (see ***Fig. 6.1b***), which is frequently used in SP-ICPMS [6.27, 6.36], shows a significant occurrence of false positives (Ag(I) signals counted as particles). On the other hand, by using a 5 sigma threshold criteria ($\bar{y} + 5\sigma$), the discrimination of the signals is better, giving much less false positives (see ***Fig. 6.1c***). These iterative algorithms were also applied to mixtures of Ag(I)/AgNPs. The results presented in ***Fig. S6.1*** (see Supplementary information of this chapter) show that $\bar{y} + 5\sigma$ is the best threshold criterion for discrimination of Ag(I) signals, being adopted along the work.

6.4.1.2 Sample preparation for CPE-SP-ICPMS analysis

The resulting micelle-rich phase from the CPE procedure is viscous and around 100 µL of it is obtained. Standard SP-ICPMS analysis requires the introduction of several millilitres of aqueous sample. Because of that, in this work, several media were tested to find the adequate one to dilute the extract obtained in the CPE procedure and to perform SP-ICPMS analysis. Additionally, this medium should not affect the stability of the nanoparticles. With this purpose, blanks of CPE were prepared and the micelle-rich phase was diluted to 15 mL with the following aqueous media: ultrapure water, 1% glycerol (*v/v*), and 1% isopropanol (*v/v*).

All tested solvents were miscible with the CPE extract except ultrapure water, where two phases were observed (see ***Table S6.2*** in Supplementary information of this chapter). Then,

suspensions of 100 nm citrate-AgNPs (~152 ng L^{-1}) were prepared in glycerol and isopropanol (1%) to determine the η_{neb} of the particles in these media. Nebulisation efficiencies were determined by particle size and particle frequency methods. Results for the latter method

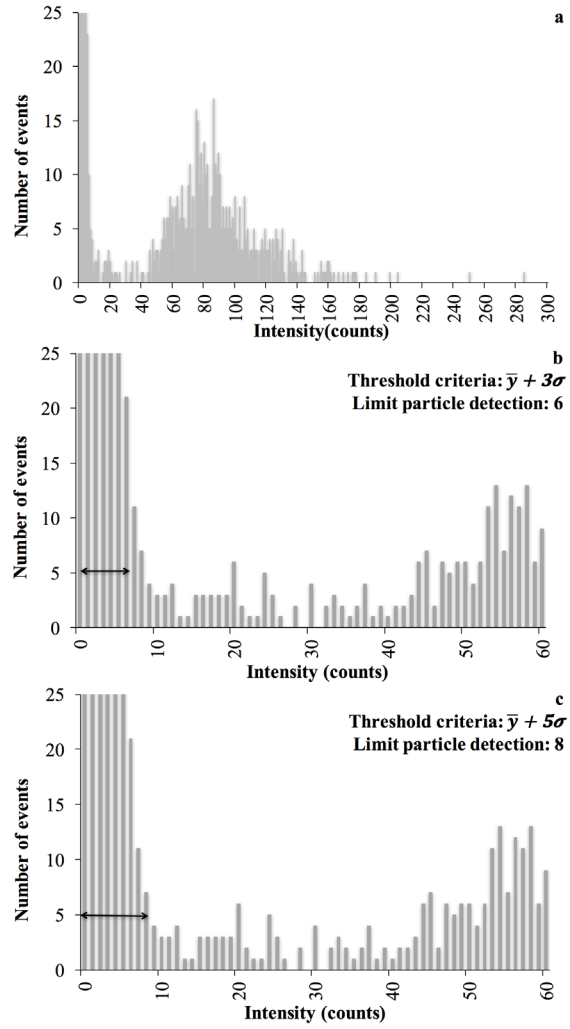

Fig. 6.1 *Signal distribution representations corresponding to 100 nm citrate-AgNPs aqueous standard solution (**a**) using different threshold criteria ((**b**,**c**)) to avoid the occurrence of false positives.*

were compared with those obtained by using the RIKILT spreadsheet, verifying that the in-lab Microsoft Excel spreadsheet was designed properly. Results demonstrated that the η_{neb} obtained in 1% glycerol were closer to η_{neb} in aqueous medium in comparison with those ones obtained in 1% isopropanol, especially the values obtained by particle size method (see ***Table 6.2***). Additionally, the tuned measurement conditions (lens voltage and nebulisation gas flow rate) were more similar between 1% glycerol and ultrapure water than 1% isopropanol (data

not shown). Therefore, 1% glycerol was selected as the medium to dilute the CPE extracts.

Table 6.2 *Nebulisation efficiencies for 100 nm citrate-AgNPs obtained by particle frequency and particle size method and RIKILT spreadsheet in different media (mean ± sd; n = 3).*

Solvent	η_{neb} particle frequency method (%)	η_{neb} particle size method (%)	RIKILT spreadsheet (%)
Ultrapure water	2.88 ± 0.02	3.35 ± 0.04	2.91 ± 0.01
Glycerol (1%)	3.11 ± 0.01	3.28 ± 0.08	3.12 ± 0.01
Isopropanol (1%)	3.20 ± 0.10	3.77 ± 0.06	3.19 ± 0.09

6.4.1.3 Nebulisation efficiency determination

To determine the particle size and the particle number concentration in unknown samples, the nebulisation efficiency has to be known. As aforementioned, nebulisation efficiency can be calculated by different methods. Here, the particle frequency and the particle size methods were evaluated with AgNPs of different coatings and sizes (100 nm citrate-AgNPs, 100 nm PVP-AgNPs, and 75 nm PVP-AgNPs). Although the waste collection method is the simplest, it was discarded because some bibliography reported higher η_{neb} values and inaccurate results in comparison with the other mentioned calculation methods [6.7, 6.50].

Several papers reported particle size and particle frequency determination methods using reference materials (RMs); nevertheless, in this study, AgNP standards characterised by the manufacturer were used as an alternative to RMs [6.7, 6.30]. For particle frequency method assessment, fresh AgNP standards with known particle number concentration were prepared in ultrapure water and 1% glycerol. The particle concentration was estimated from the measured silver concentration, the diameter provided by the manufacturer, and the bulk density of silver. The results obtained by this method are shown in ***Table 6.3***. As can be seen, no significant statistical differences were observed between the two media used. Significant statistical differences were neither observed between the results obtained by using nanoparticles of different sizes or coatings. The calculated nebulisation efficiencies by particle frequency method were verified by using RIKILT spreadsheet, which is based on particle frequency method, and no significant statistical differences were observed between the values obtained.

In addition to fresh AgNP standards, an Ag(I) calibration curve in 2% HNO_3 medium (0.2–10 ng mL^{-1}) was used to determine the η_{neb} by particle size method. Nebulisation efficiencies

obtained by this method were higher than those ones obtained by particle frequency method (see ***Table 6.3***). These differences between the two calculation methods are in accordance with the results obtained by Liu *et al.* [6.30]. In general, no significant statistical differences were observed between the η_{neb} values obtained from the different tested media. However, significant statistical differences were observed between different sizes (75 nm and 100 nm) and different coatings (citrate and PVP). These differences can be a consequence of the distinct mass sensitivity in the ICPMS of the particulate and dissolved forms of the element or the bias in the calculation of the number concentration of the element and the mean size of the particles, especially for silver because of the presence of a fraction of dissolved element. So, the use of well-sized nanoparticles is very important in particle size calculation method. Nonetheless, particle frequency calculation method relates the number of detected particles to the theoretical number of particles going into the ICPMS assuming that each nanoparticle that enters into the plasma produces an event. Hence, the factors to control to avoid errors in η_{neb} determination with this method are as follows: (1) a proper dilution of the nanoparticle standard solution; (2) particle number concentration; and (3) the sample flow rate have to be well-known [6.30, 6.50].

Table 6.3 *Nebulisation efficiencies obtained from particle frequency method, particle size method and RIKILT spreadsheet of different coated and sized AgNPs (100 nm citrate-AgNPs, 100 nm PVP-AgNPs, and 75 nm PVP-AgNPs) in ultrapure water and glycerol (1%) media (mean ± sd; n = 3).*

	η_{neb} particle frequency method (%)				**η_{neb} particle size method (%)**	
	Ultrapure water		Glycerol (1%)		Ultrapure water	Glycerol (1%)
		RIKILT		RIKILT		
100 nm citrate-AgNPs	3.1 ± 0.1	3.1 ± 0.1	3.38 ± 0.08	3.41 ± 0.08	4.15 ± 0.01	4.21 ± 0.04
100 nm PVP-AgNPs	3.3 ± 0.1	3.3 ± 0.1	3.4 ± 0.1	3.4 ± 0.1	4.83 ± 0.04	4.50 ± 0.02
75 nm PVP-AgNPs	3.18 ± 0.01	3.23 ± 0.01	3.0 ± 0.1	3.0 ± 0.1	4.23 ± 0.01	4.6 ± 0.2

6.4.1.4 Particle size and particle number concentration determination

The nebulisation efficiencies obtained in the previous Section by particle frequency and particle size methods were used to determine the particle size and the particle number concentration of the analysed AgNP standards in ultrapure water and 1% glycerol media. For 100 nm citrate-AgNPs and 75 nm PVP-AgNPs, the η_{neb} obtained for 100 nm PVP-AgNPs was

employed, and for 100 nm PVP-AgNPs, the η_{neb} of 75 nm PVP-AgNPs was used. Particle size values determined using η_{neb} calculated with particle size method were more similar to the particle diameter provided by the manufacturer than the ones obtained using η_{neb} calculated with particle frequency method (see ***Table 6.4***). Therefore, particle size method is more robust for calculating the particle size of the AgNPs than particle frequency method. The number of particles present in the AgNP standard can explain the lower particle sizes obtained by frequency-based calculation method because of dissolution of AgNPs or loss of particles in the material containing the suspension. As a consequence, the number of particles present in the suspension is lower than the expected and the determined nebulisation efficiency is underestimated. Nonetheless, no significant statistical differences were observed between the values reported by the manufacturer and the values determined with both tested calculation methods. However, in some cases, significant statistical differences were observed between nanoparticle sizes determined in the tested media. In general, the results showed that nanoparticles in 1% glycerol were slightly bigger than those determined in ultrapure water, except for 75 nm PVP-AgNPs. This effect could be due to the fact that glycerol acts as a stabilising agent and it protects the particles avoiding their partial dissolution [6.51].

Table 6.4 *Silver nanoparticles sizes in ultrapure water and glycerol (1%) media obtained from nebulisation efficiencies calculated with the different calculation methods tested in this study and particle diameter values provided by the manufacturer (mean ± sd; n = 3).*

	Particle frequency method (%)		**Particle size method (%)**		**Manufacturer value (nm)**
	Ultrapure water	Glycerol (1%)	Ultrapure water	Glycerol (1%)	
100 nm citrate-AgNPs	87.6 ± 0.2	90.7 ± 0.3	99.1 ± 0.3	99.6 ± 0.3	95 ± 9
100 nm PVP-AgNPs	88.7 ± 0.2	89.26 ± 0.04	97.6 ± 0.2	100.10 ± 0.05	102 ± 11
75 nm PVP-AgNPs	70.88 ± 0.04	70 ± 1	80.48 ± 0.05	77 ± 1	77 ± 7

Furthermore, AgNP concentrations as particle number were calculated. As can be seen in ***Table S6.3*** in Supplementary information of this chapter, particle number concentrations calculated with particle frequency η_{neb} were higher and more similar to the theoretical values than those ones acquired with particle size η_{neb}. As previously explained by Liu *et al.* [6.30], an underestimation of the particle size implies an overestimation of the nanoparticle number

concentration. Considering the results obtained, particle size method was selected for calculation of η_{neb} because the bias for the determination of particle size was smaller.

6.4.1.5 Assessment of sample pH in cloud point extraction

In a previous work, we observed that CPE extraction efficiency is pH dependent because the highest extraction efficiency was obtained at pH_{PZC} (zero-point charge pH) [6.42]. For this reason, a pH optimisation (see the "Cloud point extraction procedure and sample preparation for SP-ICPMS analysis" Section) was carried out using 75 nm PVP-AgNP standards. Considering the results obtained in a previous research [6.42], the pHs tested were 3.0, 3.5, and 4.0. pHs lower than 3.0 were discarded to avoid potential dissolution of the nanoparticles, $S_2O_3^{2-}$ decomposition, and formation of sulfur species [6.52]. As can be seen in ***Fig. 6.2***, the results obtained indicated that the highest extraction efficiency was obtained at pH 3.5.

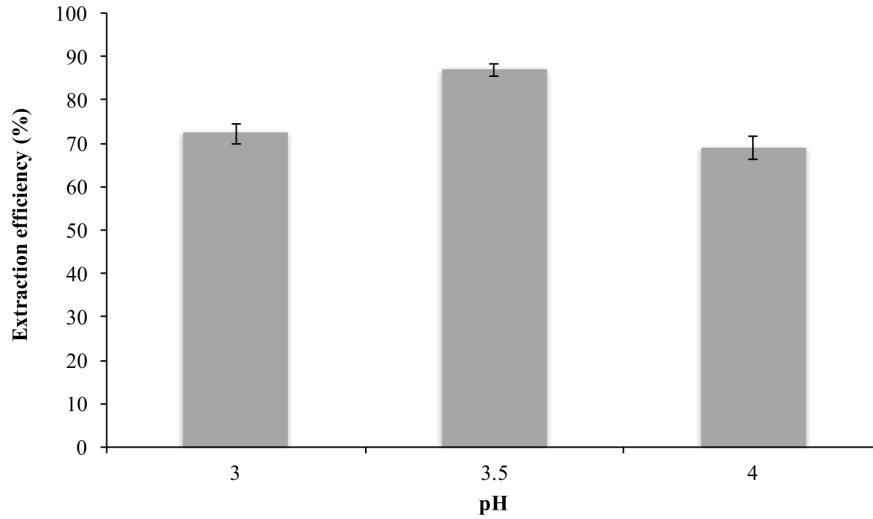

Fig. 6.2 *Extraction efficiency of cloud point extraction methodology using 75 nm PVP-AgNPs standards of 1 mg L^{-1} concentration (n = 3).*

6.4.2 Application of CPE-SP-ICPMS to soil sample extracts

In the environment, AgNPs are susceptible to interact with soil components and consequently they can suffer transformations such as oxidation to Ag(I) [6.53]. This generates the coexistence of both silver chemical forms in soils and this fact makes the determination of silver particle size and particle number concentration in these environmental matrices difficult. To avoid these problems, CPE was applied to aqueous soil leachates before SP-ICPMS analysis, to extract AgNPs. However, previously, some critical parameters were evaluated: (1) the matrix effect of

soil leachates over AgNPs; (2) the effect of CPE on particle size; and (3) the assessment of CPE for extraction of AgNPs in soil contaminated samples they can suffer transformations such as oxidation to Ag(I) [6.53]. This generates the coexistence of both silver chemical forms in soils and this fact makes the determination of silver particle size and particle number concentration in these environmental matrices difficult. To avoid these problems, CPE was applied to aqueous soil leachates before SP-ICPMS analysis, to extract AgNPs. However, previously, some critical parameters were evaluated: (1) the matrix effect of soil leachates over AgNPs; (2) the effect of CPE on particle size; and (3) the assessment of CPE for extraction of AgNPs in soil contaminated samples.

6.4.2.1 Effect of cloud point extraction and soil matrix on the sizing of AgNPs

In this study, the size determination of the silver nanoparticles in soil leachates can be affected by soil matrix because it contains diverse components with charged surfaces such as clay particles or humic acids [6.54, 6.55]. Hence, an evaluation of the potential matrix effects of soil leachates to AgNP size was also performed. For this experiment, aqueous AgNP standards (60 nm citrate-AgNPs and 75 nm PVP-AgNPs) and blank aqueous soil leachates spiked with the same AgNPs were prepared. Nanoparticle sizes obtained indicated that the matrix leached from soils did not have an effect on the determination of the particle size because no significant statistical differences were observed between the AgNP diameters determined in the aqueous standards and in the spiked aqueous soil leachates (see ***Table 6.5***).

Table 6.5 *AgNP diameter in aqueous standard solutions and in spiked blank aqueous soil leachates to determine the soil matrix effect on particle size estimation (mean ± sd; n = 2).*

Standard used to spike the different matrices	**Particle size (nm)**	
	Ultrapure water matrix	Aqueous soil leachate matrix
60 nm citrate-AgNPs	63 ± 2	65 ± 3
75 nm PVP-AgNPs	75 ± 1	80 ± 2

On the other hand, to get accurate size distributions of the nanoparticles in real samples, it is necessary to assess changes in size distribution during the extraction. For this, blank aqueous soil leachates were spiked with 60 nm citrate-AgNPs and 75 nm PVP-AgNPs and analysed by SP-ICPMS before and after CPE. As it can be seen in ***Table 6.6***, the AgNP

sizes of the silver nanoparticles did not show significant statistical differences, confirming that particle size is maintained during the extraction procedure. These results are in agreement with other authors who also observed no changes in particle size using different nanoparticles and environmental samples after the CPE procedure [6.46, 6.52, 6.56, 6.57].

Table 6.6 *Diameter of AgNPs spiked in blank aqueous soil leachates before and after cloud point extraction procedure to determine the cloud point extraction effect on particle size (mean ± sd; n = 2).*

Standard used to spike the aqueous soil leachate	**Particle size (nm)**	
	Before CPE	After CPE
60 nm citrate-AgNPs	65 ± 3	62 ± 1
75 nm PVP-AgNPs	80 ± 2	81 ± 1

6.4.2.2 Separation of AgNPs from Ag(I) in spiked aqueous soil leachates

To evaluate the selectivity of CPE towards AgNPs with respect to Ag(I) for reducing the contribution of the latter to the continuous baseline in SP-ICPMS analysis of soil leachates, blank aqueous soil leachates were spiked with a mixture of AgNPs and Ag(I) at ratios 1:10 and 1:20. As can be seen in ***Fig. 6.3***, the contribution of ionic silver in SP-ICPMS histograms was satisfactorily reduced after the application of CPE procedure (see ***Fig. 6.3b***, ***d***). Furthermore, the histograms show that the signal corresponding to AgNPs is improved because these samples were more concentrated than the ones without being treated with CPE for carrying out the SP-ICPMS analysis. As explained, the dilution of the sample for SP-ICPMS is calculated from the total amount of Ag in the extract, which is lower when applying the CPE. This indicates the ability of this micro-extraction methodology to preferentially extract these emerging contaminants. In addition, particle size limits of detection have been calculated before and after CPE using the background signal from the 1/10 diluted spiked soil leachate. Fifty-seven and forty nanometers were obtained respectively, demonstrating that this sample treatment procedure allows improving the size detection limit. Particle size and particle number concentration were also determined before and after the application of the CPE procedure. In ***Table 6.7***, similar values ($t_{critical} > t_{experimental}$) for the particle sizes of the AgNPs present in aqueous soil leachates before the CPE and after the CPE experiment can be seen. This could be a consequence of the size of the particles used that is big enough to not be affected by the presence of Ag(I) at these concentration levels. No significant statistical differences were also observed in particle number concentration obtained before and after

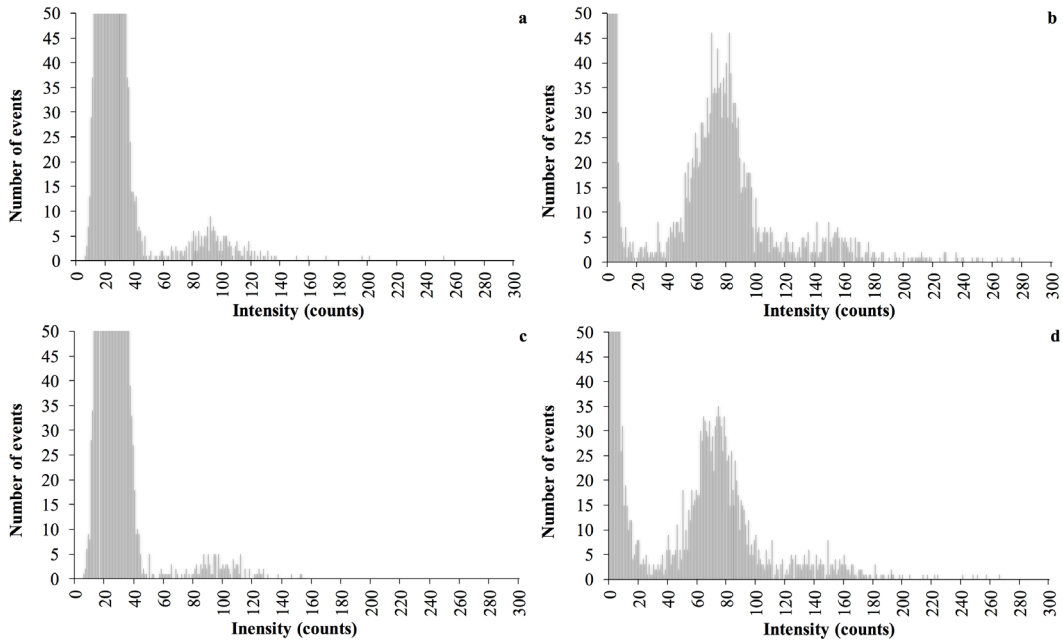

Fig. 6.3 *Histogram representations obtained before cloud poing extraction (**a,c**) and after cloud point extraction (**b,d**) of aqueous soil leachates spiked with mixtures of 75-nm PVP-AgNPs/Ag(I) (**a,b** ratio 1/10; **c,d** ratio 1/20).*

CPE procedure but concentration values were more similar to estimated ones after AgNP extraction, especially for the aqueous soil leachates containing a ratio 1/20 (AgNPs/Ag(I)) ($t_{critical}<t_{experimental}$ with estimated value before CPE).

Table 6.7 *Particle size and particle number concentration obtained before and after cloud point extraction of blank aqueous soil leachates spiked with mixtures of 75 nm PVP-AgNPs/Ag(I) at 20 µg L^{-1}/200 µg L^{-1} or 10 µg L^{-1}/200 µg L^{-1} concentration (mean ± sd; n = 2).*

	AgNPs/Ag(I) (µg L^{-1})	**Particle size (nm)**		**Particle number concentration (particle L^{-1})**	
		Calculated	Manufacturer value	Calculated	Manufacturer value
Before CPE	20/200	74.9 ± 0.6	77.7 ± 7	$9{\cdot}10^9$ ± $1{\cdot}10^9$	$8.27{\cdot}10^9$ ± $0.04{\cdot}10^9$
	10/200	75.7 ± 0.2		$8.8{\cdot}10^9$ ± $0.2{\cdot}10^9$	$4.19{\cdot}10^9$ ± $0.02{\cdot}10^9$
After CPE	20/200	76.8 ± 0.4	77.7 ± 7	$4.55{\cdot}10^9$ ± $0.05{\cdot}10^9$	$8.19{\cdot}10^9$ ± $0.02{\cdot}10^9$
	10/200	76.4 ± 0.8		$4.7{\cdot}10^9$ ± $0.5{\cdot}10^9$	$4.03{\cdot}10^9$ ± $0.02{\cdot}10^9$

6.4.2.3 CPE-SP-ICPMS analysis of spiked soils

After evaluation of the aforementioned parameters affecting CPE and SP-ICPMS procedures, the developed methodology was applied to soil leachates. Soil samples spiked with AgNPs (60 nm citrate-AgNPs and 75 nm PVP-AgNPs) and stored during 3 weeks were subjected

to CPE and the obtained extracts were analysed by SP-ICPMS. The histograms obtained showed the oxidation of the silver nanoparticles after 3 weeks due to the presence of a broad Ag(I) distribution at the low signal intensities. The AgNP signal distributions were overlapped with those ones of dissolved silver, although in a higher extent for 60 nm citrate-AgNPs (see ***Fig. 6.4***) than for 75 nm PVP-AgNPs (see ***Fig. S6.2*** in the Supplementary information of this chapter) because the signal produced by small nanoparticle is lower than the signal generated by a bigger one. Moreover, small-sized particles are more prone to get dissolved due to the large fraction of surface atoms or the low redox potential [6.3]. This overlapping of the distributions complicates the detection, sizing, and quantitation of the AgNPs. This problem was especially serious for the 60 nm citrate-AgNP particle size distributions because part of the distribution was neglected (see ***Fig. 6.4b***), generating an underestimation of the particle size as it can be seen in ***Table 6.8***. Although the AgNP and Ag(I) distributions of the 75 nm PVP-AgNPs were practically not overlapped (see ***Fig. S6.2*** in the Supplementary information of this chapter), the estimation of the particle size was also affected by the presence of Ag(I)

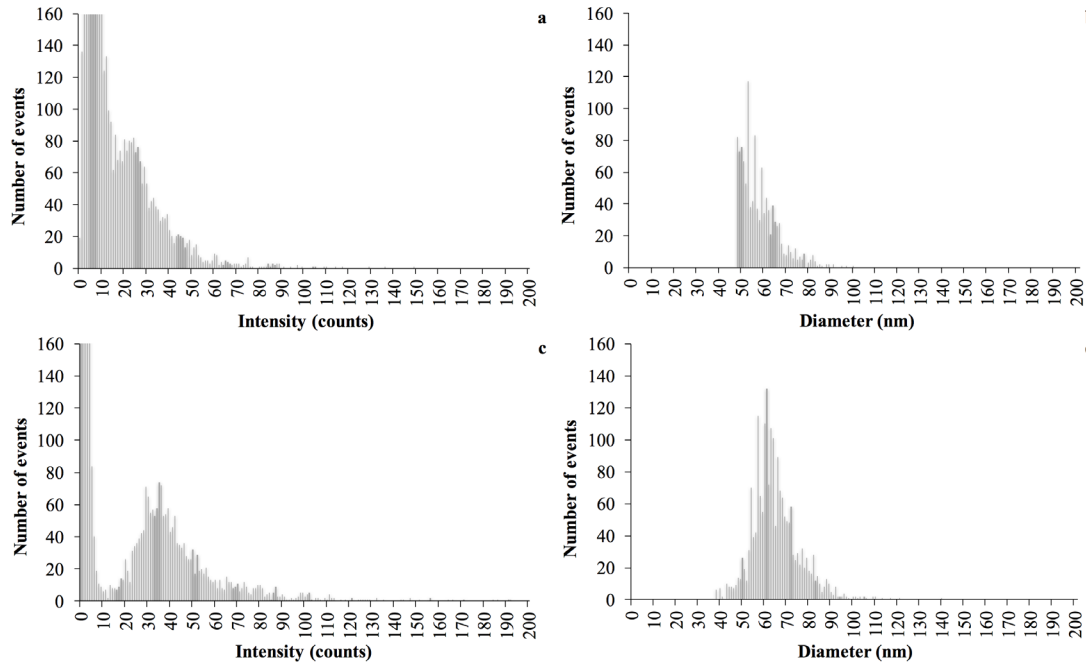

Fig. 6.4 *Histogram (**a** before CPE, **c** after CPE) and particle size distribution (**b** before CPE, **d** after CPE) representations of 60 nm citrate-AgNPs in aqueous soil leachates obtained from a soil contaminated with nanoparticles during 3 weeks.*

(see ***Table 6.8***). After applying the cloud point extraction to these aqueous soil leachates, the presence of Ag(I) was drastically reduced for both samples as it is shown in ***Fig. 6.4*** and ***Fig.***

S6.2 in the Supplementary information of this chapter, facilitating the discrimination of the signals corresponding to AgNPs from the ones corresponding to Ag(I). Additionally, complete particle size distributions were obtained allowing a better estimation of the particle sizes. The AgNP diameter values after the extraction process were higher than the ones determined without the CPE. The estimated values for 60 nm citrate-AgNPs (63.4 ± 0.4 nm) and 75 nm PVP-AgNPs (73.5 ± 0.5 nm) present in the CPE extracts were similar to the manufacturer's value (59 ± 5 nm and 77 ± 7 nm respectively) (see ***Table 6.8***). These results indicate that these particles do not suffer a reduction of the size after 3 weeks of contact with the studied soil. Furthermore, higher particle number concentration values were obtained after applying the CPE ($t_{critical}<t_{experimental}$). The lower particle number concentration obtained can be explained as a consequence of the partial overlapping of the peaks in the histogram when CPE is not carried out. The increment of AgNP ratio in the CPE extracts is due to the removal of the Ag(I) and consequently a clearer and higher AgNP peak in SP-ICPMS histograms is observed. In conclusion, these results indicate that the combination of cloud point extraction methodology with SP-ICPMS analysis could be beneficial to get accurate information of AgNPs in complex environmental samples.

Table 6.8 *Particle size and particle number concentration of AgNPs in aqueous soil leachates obtained from soils contaminated with 60 nm citrate-AgNPs and 75 nm PVP-AgNPs during 3 weeks (mean ± sd; n = 2).*

	Soil leachate			
	Before CPE		After CPE	
	60 nm citrate-AgNPs	75 nm PVP-AgNPs	60 nm citrate-AgNPs	75 nm PVP-AgNPs
Particle size (nm)	56.8 ± 0.8	63 ± 5	63.4 ± 0.4	73.5 ± 0.5
Particle number concentration (particle L^{-1})	$1.3{\cdot}10^{10} \pm 0.2{\cdot}10^{10}$	$2.0{\cdot}10^{10} \pm 0.3{\cdot}10^{10}$	$2.2{\cdot}10^{10} \pm 0.2{\cdot}10^{10}$	$4{\cdot}10^{10} \pm 2{\cdot}10^{10}$

6.5 Conclusions

In this contribution, determination of ICPMS nebulisation efficiencies for different sized and coated AgNPs with two different calculation methods has been discussed employing AgNP standards (particle size and particle number concentration proportionated by the manufacturer). Nebulisation efficiencies determined *via* particle frequency and particle size methods were slightly different, being lower the ones obtained by the frequency calculation method. Better agreement with the

manufacturer diameter values was obtained using size-based nebulisation efficiencies.

On the other hand, the use of cloud point extraction in combination with SP-ICPMS for characterising and getting quantitative information of silver nanoparticles in soil samples has been evaluated. Previous tests with spiked aqueous soil leachates indicated that particle size is not affected by CPE procedure and by the soil matrix. It is also demonstrated that the application of CPE in samples containing mixtures of AgNPs and Ag(I) before SP-ICPMS analysis facilitates the separation of the signal intensities corresponding to both silver chemical forms. Additionally, it was observed that samples containing high amounts of ionic silver generate an underestimation of the particle size and applying the CPE a more accurate particle size value can be obtained. The developed methodology has been successfully applied to samples containing high amounts of Ag(I) after 3 weeks of contact with AgNPs, improving the estimation of AgNP diameters and particle number concentrations. Although CPE-SP-ICPMS has to be assessed with other coated and sized AgNPs and also mixtures of them because in the environment several types of nanosilver can be found, the combination of these analytical tools is a promising alternative to sophisticated hyphenated techniques.

Acknowledgments

The Spanish Ministry of Economy and Competitiveness (MINECO) financially supported this work through CGL2013-48802-C3-2-R project (Program 2014) and CTQ2015- 68094-C2-1-R project (Program 2015), this last also cofounded by the European Regional Development Fund (FEDER). L. Torrent received a FPI grant from the Spanish Ministry of Economy and Competitiveness (Ref. BES-2014-070625) and a FPI mobility scholarship for her predoctoral stage in the University of Zaragoza (Ref. EEBB-I-17-12391). The authors would like to acknowledge the use of Servicio General de Apoyo a la Investigación-SAI, Universidad de Zaragoza, for ICPMS measurements.

References

[6.1] L. Goswami, K.-H. Kim, A. Deep, P. Das, S.S. Bhattacharya, S. Kumar, *et al.*, Engineered nano particles: nature, behavior, and effect on the environment, J. Environ. Manage. 196 (2017) 297–315.

[6.2] M. Bundschuh, J. Filser, S. Lüderwald, M.S. McKee, G. Metreveli, G.E. Schaumann, *et al.*, Nanoparticles in the environment: where do we come from, where do we go to?, Environ. Sci. Eur. 30 (2018) 6.

[6.3] A.D. Dwivedi, S.P. Dubey, M. Sillanpää, Y.-N. Kwon, C. Lee, R.S. Varma, Fate of engineered nanoparticles: implications in the environment, Coord. Chem. Rev. 287 (2015) 64–78.

[6.4] E. McGillicuddy, I. Murray, S. Kavanagh, L. Morrison, A. Fogarty, M. Cormican, *et al.*, Silver nanoparticles in the environment: sources, detection and ecotoxicology, Sci. Total Environ. 575 (2017) 231–246.

[6.5] S.-J. Yu, Y.-G. Yin, J.-F. Liu, Silver nanoparticles in the environment, Environ. Sci. Process. Impacts 15 (2013) 78–92.

[6.6] J.R. Lead, G.E. Batley, P.J.J. Alvarez, M.N. Croteau, R.D. Handy, M.J. McLaughlin, *et al.*, Nanomaterials in the environment: behavior, fate, bioavailability, and effects—an updated review, Environ. Toxicol. Chem. 37 (2018) 2029–2063.

[6.7] H.E. Pace, N.J. Rogers, C. Jarolimek, V.A. Coleman, C.P. Higgins, J.F. Ranville, Determining transport efficiency for the purpose of counting and sizing nanoparticles via single particle inductively coupled plasma mass spectrometry, Anal. Chem. 83 (2011) 9361–9369.

[6.8] H. Hagendorfer, C. Lorenz, R. Kaegi, B. Sinnet, R. Gehrig, N.V. Goetz, *et al.*, Size-fractionated characterization and quantification of nanoparticle release rates from a consumer spray product containing engineered nanoparticles, J. Nanopart. Res. 12 (2010) 2481–2494.

[6.9] J. Farkas, H. Peter, P. Christian, J.A. Gallego Urrea, M. Hassellöv, J. Tuoriniemi, *et al.*, Characterization of the effluent from a nanosilver producing washing machine, Environ. Int. 37 (2011) 1057–1062.

[6.10] R.D. Kent, P.J. Vikesland, Controlled evaluation of silver nanoparticle dissolution using atomic force microscopy, Environ. Sci. Technol. 46 (2012) 6977–6984.

[6.11] N. Akaighe, R.I. MacCuspie, D.A. Navarro, D.S. Aga, S. Banerjee, M. Sohn, *et al.*, Humic acid-induced silver nanoparticle formation under environmentally relevant conditions, Environ. Sci. Technol. 45 (2011) 3895–3901.

[6.12] X. Li, J.J. Lenhart, Aggregation and dissolution of silver nanoparticles in natural surface water, Environ. Sci. Technol. 46 (2012) 5378–5386.

[6.13] R. Kaegi, A. Voegelin, C. Ort, B. Sinnet, B. Thalmann, J. Krismer, *et al.*, Fate and transformation of silver nanoparticles in urban wastewater systems, Water Res. 47 (2013) 3866–3877.

[6.14] R. Kaegi, A. Voegelin, B. Sinnet, S. Zuleeg, H. Hagendorfer, M. Burkhardt, *et al.*, Behavior of metallic silver nanoparticles in a pilot wastewater treatment plant, Environ. Sci. Technol. 45 (2011) 3902–3908.

[6.15] E. Lombi, E. Donner, S. Taheri, E. Tavakkoli, Å.K. Jämting, S. McClure, *et al.*, Transformation of four silver/silver chloride nanoparticles during anaerobic treatment of wastewater and post-processing of sewage sludge, Environ. Pollut. 176 (2013) 193–197.

[6.16] S. Elzey, V.H. Grassian, Agglomeration, isolation and dissolution of commercially manufactured silver nanoparticles in aqueous environments, J. Nanopart. Res. 12 (2010) 1945–1958.

[6.17] A.M. El Badawy, T.P. Luxton, R.G. Silva, K.G. Scheckel, M.T. Suidan, T.M. Tolaymat, Impact of environmental conditions (pH, ionic strength, and electrolyte type) on the surface charge and aggregation of silver nanoparticles suspensions, Environ. Sci. Technol. 44 (2010) 1260–1266.

[6.18] B.L.T. Lau, W.C. Hockaday, K. Ikuma, O. Furman, A.W. Decho, A preliminary assessment of the interactions between the capping agents of silver nanoparticles and environmental organics, Colloids Surf. A Physicochem. Eng. Asp. 435 (2013) 22–27.

[6.19] R. Ma, C. Levard, S.M. Marinakos, Y. Cheng, J. Liu, F.M. Michel, *et al.*, Size-controlled dissolution of organic-coated silver nanoparticles, Environ. Sci. Technol. 46 (2012) 752–759.

[6.20] F. Laborda, E. Bolea, G. Cepriá, M.T. Gómez, M.S. Jiménez, J. Pérez-Arantegui, *et al.*, Detection, characterization and quantification of inorganic engineered nanomaterials: a review of techniques and methodological approaches for the analysis of complex samples, Anal. Chim. Acta 904 (2016) 10–32.

[6.21] M.C. Sportelli, R.A. Picca, N. Cioffi, Recent advances in the synthesis and characterization of nano-antimicrobials, Trends Anal. Chem. 84 (2016) 131–138.

[6.22] N.S. Tulve, A.B. Stefaniak, M.E. Vance, K. Rogers, S. Mwilu, R.F. LeBouf, *et al.*, Characterization of silver nanoparticles in selected consumer products and its relevance for predicting children's potential exposures, Int. J. Hyg. Environ. Health 218 (2015) 345–357.

[6.23] G.F. Koopmans, T. Hiemstra, I.C. Regelink, B. Molleman, R.N.J. Comans, Asymmetric flow field-flow fractionation of manufactured silver nanoparticles spiked into soil solution, J. Chromatogr. A 1392 (2015) 100–109.

[6.24] F. Laborda, E. Bolea, J. Jiménez-Lamana, Single particle inductively coupled plasma mass spectrometry for the analysis of inorganic engineered nanoparticles in environmental samples, Trends Environ. Anal. Chem. 9 (2016) 15–23.

[6.25] B. Meermann, V. Nischwitz, ICP-MS for the analysis at the nanoscale-a tutorial review, J. Anal. At. Spectrom. 33 (2018) 1432–1468.

[6.26] F. Laborda, J. Jiménez-Lamana, E. Bolea, J.R. Castillo, Selective identification, characterization and determination of dissolved silver(I) and silver nanoparticles based on single particle detection by inductively coupled plasma mass spectrometry, J. Anal. At. Spectrom. 26 (2011) 1362-1371.

[6.27] R. Peters, Z. Herrera-Rivera, A. Undas, M. van der Lee, H. Marvin, H. Bouwmeester, et al., Single

particle ICP-MS combined with a data evaluation tool as a routine technique for the analysis of nanoparticles in complex matrices, J. Anal. At. Spectrom. 30 (2015) 1274–1285.

[6.28] M.A. Gomez-Gonzalez, E. Bolea, P.A. O'Day, J. Garcia-Guinea, F. Garrido, F. Laborda, Combining single-particle inductively coupled plasma mass spectrometry and X-ray absorption spectroscopy to evaluate the release of colloidal arsenic from environmental samples, Anal. Bioanal. Chem. 408 (2016) 5125–5135.

[6.29] T.P.J. Linsinger, R. Peters, S. Weigel, International interlaboratory study for sizing and quantification of Ag nanoparticles in food simulants by single-particle ICPMS, Anal. Bioanal. Chem. 406 (2014) 3835–3843.

[6.30] J. Liu, K.E. Murphy, M.R. Winchester, V.A. Hackley, Overcoming challenges in single particle inductively coupled plasma mass spectrometry measurement of silver nanoparticles, Anal. Bioanal. Chem. 409 (2017) 6027–6039.

[6.31] F. Laborda, J. Jiménez-Lamana, E. Bolea, J.R. Castillo, Critical considerations for the determination of nanoparticle number concentrations, size and number size distributions by single particle ICP-MS, J. Anal. At. Spectrom. 28 (2013) 1220–1232.

[6.32] M. Hadioui, C. Peyrot, K.J. Wilkinson, Improvements to single particle ICPMS by the online coupling of ion exchange resins, Anal. Chem. 86 (2014) 4668–4674.

[6.33] H.E. Pace, N.J. Rogers, C. Jarolimek, V.A. Coleman, E.P. Gray, C.P. Higgins, *et al.*, Single particle inductively coupled plasma-mass spectrometry: a performance evaluation and method comparison in the determination of nanoparticle size, Environ. Sci. Technol. 46 (2012) 12272–12280.

[6.34] D.M. Mitrano, E.K. Lesher, A. Bednar, J. Monserud, C.P. Higgins, J.F. Ranville, Detecting nanoparticulate silver using single-particle inductively coupled plasma-mass spectrometry, Environ. Toxicol. Chem. 31 (2012) 115–121.

[6.35] S. Lee, X. Bi, R.B. Reed, J.F. Ranville, P. Herckes, P. Westerhoff, Nanoparticle size detection limits by single particle ICP-MS for 40 elements, Environ. Sci. Technol. 48 (2014) 10291–10300.

[6.36] J. Tuoriniemi, G. Cornelis, M. Hassellöv, Size discrimination and detection capabilities of single-particle ICPMS for environmental analysis of silver nanoparticles, Anal. Chem. 84 (2012) 3965–3972.

[6.37] G. Cornelis, M. Hassellöv, A signal deconvolution method to discriminate smaller nanoparticles in single particle ICP-MS, J. Anal. At. Spectrom. 29 (2014) 134–144.

[6.38] T.K. Mudalige, H. Qu, S.W. Linder, Asymmetric flow-field flow fractionation hyphenated ICP-MS as an alternative to cloud point extraction for quantification of silver nanoparticles and silver

speciation: application for nanoparticles with a protein corona, Anal. Chem. 87 (2015) 7395–7401.

[6.39] B. Franze, C. Engelhard, Fast separation, characterization, and speciation of gold and silver nanoparticles and their ionic counterparts with micellar electrokinetic chromatography coupled to ICP-MS, Anal. Chem. 86 (2014) 5713–5720.

[6.40] X.X. Zhou, R. Liu, J.-F. Liu, Rapid chromatographic separation of dissoluble Ag(I) and silver-containing nanoparticles of 1-100 nanometer in antibacterial products and environmental waters, Environ. Sci. Technol. 48 (2014) 14516–14524.

[6.41] I. Hagarová, Separation and quantification of metallic nanoparticles using cloud point extraction and spectrometric methods: a brief review of latest applications, Anal. Methods 9 (2017) 3594–3601.

[6.42] L. Torrent, M. Iglesias, M. Hidalgo, E. Marguí, Determination of silver nanoparticles in complex aqueous matrices by total reflection X-ray fluorescence spectrometry combined with cloud point extraction, J. Anal. At. Spectrom. 33 (2018) 383–394.

[6.43] L. Li, M. Stoiber, A. Wimmer, Z. Xu, C. Lindenblatt, B. Helmreich, *et al.*, To what extent can full-scale wastewater treatment plant effluent influence the occurrence of silver-based nanoparticles in surface waters?, Environ. Sci. Technol. 50 (2016) 6327–6333.

[6.44] A. Wimmer, A. Kalinnik, M. Schuster, New insights into the formation of silver-based nanoparticles under natural and semi-natural conditions, Water Res. 141 (2018) 227–234.

[6.45] A. Wimmer, R. Ritsema, M. Schuster, P. Krystek, Sampling and pre-treatment effects on the quantification of (nano)silver and selected trace elements in surface water-application in a Dutch case study, Sci. Total Environ. 663 (2019) 154–161.

[6.46] H. El Hadri, V.A. Hackley, Investigation of cloud point extraction for the analysis of metallic nanoparticles in a soil matrix, Environ. Sci. Nano 4 (2017) 105–116.

[6.47] German Standard legislation (1984) DIN 38414-S4: German standards methods for examination of water, waste water and sludge; sludge and sediments (group S); determination of leachability by water (S4). Berlin: Deutsches Institut für Normung E.V. (DIN).

[6.48] E. Bolea, F. Laborda, J.R. Castillo, Metal associations to microparticles, nanocolloids and macromolecules in compost leachates: size characterization by asymmetrical flow field-flow fractionation coupled to ICP-MS, Anal. Chim. Acta 661 (2010) 206–214.

[6.49] I. Abad-Álvaro, E. Peña-Vázquez, E. Bolea, P. Bermejo-Barrera, J.R. Castillo, F. Laborda, Evaluation of number concentration quantification by single-particle inductively coupled plasma mass spectrometry: microsecond vs. millisecond dwell times, Anal. Bioanal. Chem. 408 (2016)

5089-5097.

[6.50] M.D. Montaño, J.W. Olesik, A.G. Barber, K. Challis, J.F. Ranville, Single particle ICP-MS: advances toward routine analysis of nanomaterials, Anal. Bioanal. Chem. 408 (2016) 5053–5074.

[6.51] M. van der Zande, R.J. Vandebriel, E. Van Doren, E. Kramer, Z.H. Rivera, C.S. Serrano-Rojero, *et al.*, Distribution, elimination, and toxicity of silver nanoparticles and silver ions in rats after 28-Day oral exposure, ACS Nano 6 (2012) 7427–7442.

[6.52] J.-F. Liu, J.-B. Chao, R. Liu, Z.-Q. Tan, Y.-G. Yin, Y. Wu, *et al.*, Cloud point extraction as an advantageous preconcentration approach for analysis of trace silver nanoparticles in environmental waters, Anal. Chem. 81 (2009) 6496–6502.

[6.53] L. Torrent, M. Iglesias, M. Hidalgo, E. Marguí, Analytical capabilities of total reflection X-ray fluorescence spectrometry for silver nanoparticles determination in soil adsorption studies, Spectrochim. Acta Part B At. Spectrosc. 126 (2016) 71–78.

[6.54] P.S. Tourinho, C.A.M. van Gestel, S. Lofts, C. Svendsen, A.M.V.M. Soares, S. Loureiro, Metal-based nanoparticles in soil: fate, behavior, and effects on soil invertebrates, Environ. Toxicol. Chem. 31 (2012) 1679–1692.

[6.55] N.A. Anjum, S.S. Gill, A.C. Duarte, E. Pereira, I. Ahmad, Silver nanoparticles in soil-plant systems, J. Nanopart. Res. 15 (2013) 1896.

[6.56] G. Hartmann, M. Schuster, Species selective preconcentration and quantification of gold nanoparticles using cloud point extraction and electrothermal atomic absorption spectrometry, Anal. Chim. Acta 761 (2013) 27–33.

[6.57] G. Hartmann, C. Hutterer, M. Schuster, Ultra-trace determination of silver nanoparticles in water samples using cloud point extraction and ETAAS, J. Anal. At. Spectrom. 28 (2013) 567-572.

Supplementary information

Table S6.1 *Flame atomic absorption spectrometer and inductively coupled plasma emission optic spectrometry instrumental and data acquisition parameters.*

PerkinElmer AAnalyst 200 flame atomic absorption spectrometer		
Instrumental characteristics	Lamp	Hollow cathode
	Current lamp	15 mA
	Wavelength selector	Echelle monochromator
	Slit width	0.8 mm
	Air flow	10 L min^{-1}
	Acetylene flow	2.5 L min^{-1}
Data acquisition parameters	Ag wavelength	328.068 nm
Agilent 5100 Vertical Dual View ICP-OES spectrometer		
Instrumental characteristics	RF power	1200 W
	Pump speed	12 rpm
	Nebuliser chamber	Double pass glass cyclonic
	Nebuliser	Concentric glass
	Nebuliser flow rate	0.7 L min^{-1}
	Argon gas flow rate	12 L min^{-1}
	Plasma configuration	Axial (double vision)
	Wavelength selector	Echelle polychromator
Data acquisition parameters	Ag wavelength	328.068 nm
	Detector	Charge-coupled device (CCD)
	Reading time	1 s
	Readings per replicate	3

Table S6.2 *Results obtained for the different solvents tested to dilute the cloud point extraction extract (surfactant).*

Solvent	**Resulting solution appearance**	**Miscible or immiscible?**
Ultrapure water	Two phases	Immiscible
Glycerol (1%)	Transparent	Miscible
Isopropanol (1%)	Turbid	Miscible

Table S6.3 *Silver particle number concentration in ultrapure water and glycerol (1%) media obtained from nebulisation efficiencies calculated with the different methods tested in this study and silver particle number concentration estimated value of the AgNPs standards prepared (mean ± sd; n = 3).*

	Particle number concentration (particle L^{-1})					
	Ultrapure water		Glycerol (1%)		Ultrapure water	Glycerol (1%)
	Particle frequency method	Particle size method	Particle frequency method	Particle size method	Estimated value	
100 nm citrate-AgNPs	$3.36 \cdot 10^7 \pm 0.3 \cdot 10^6$	$2.29 \cdot 10^7 \pm 0.2 \cdot 10^6$	$3.6 \cdot 10^7 \pm 1 \cdot 10^6$	$2.69 \cdot 10^7 \pm 0.7 \cdot 10^6$	$3.6 \cdot 10^7$	$3.6 \cdot 10^7$
100 nm PVP-AgNPs	$3.0 \cdot 10^7 \pm 1 \cdot 10^6$	$2.27 \cdot 10^7 \pm 0.9 \cdot 10^6$	$3.1 \cdot 10^7 \pm 1 \cdot 10^6$	$2.2 \cdot 10^7 \pm 1 \cdot 10^6$	$2.89 \cdot 10^7$	$2.75 \cdot 10^7$
75 nm PVP-AgNPs	$2.552 \cdot 10^7 \pm 0.8 \cdot 10^5$	$1.743 \cdot 10^7 \pm 0.5 \cdot 10^5$	$2.52 \cdot 10^7 \pm 8 \cdot 10^5$	$1.91 \cdot 10^7 \pm 6 \cdot 10^5$	$2.65 \cdot 10^7$	$2.87 \cdot 10^7$

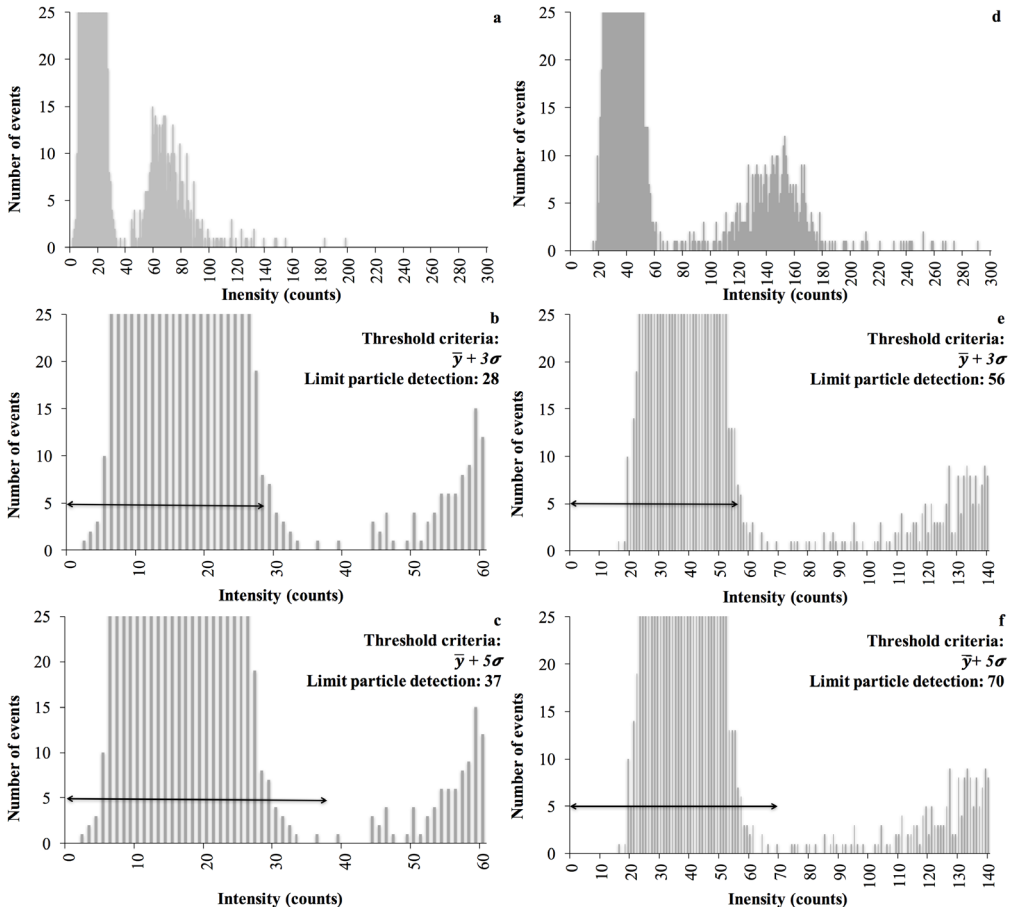

Fig S6.1 *Signal distributions corresponding to Ag(I)/60 nm citrate-AgNPs aqueous standard solution (**a**-**c**) and Ag(I)/75 nm PVP-AgNPs aqueous standard solution (**d**-**f**) using different threshold criteria (3σ (**b**,**e**) and 5σ (**c**,**f**)) to avoid the occurrence of false positives.*

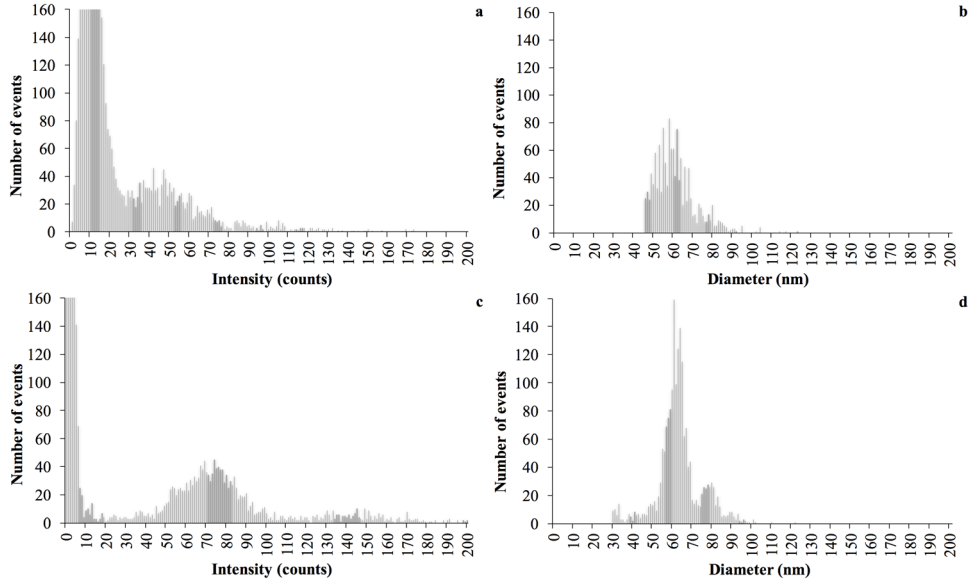

Fig S6.2 *Histogram (**a** before CPE, **c** after CPE) and particle size distribution (**b** before CPE, **d** after CPE) representations of 75 nm PVP-AgNPs in aqueous soil leachates obtained from a soil contaminated with nanoparticles during three weeks.*

CHAPTER 7

Uptake, translocation and ligand of silver in Lactuca sativa exposed to silver nanoparticles of different size, coatings and concentration

This chapter corresponds to the following publication:

L. Torrent, M. Iglesias, E. Marguí, D. Verdaguer, L. Llorens, A. Kodre, A. Kavčič, K. Vogel-Mikuš, *Uptake, translocation and ligand of silver in Lactuca sativa exposed to silver nanoparticles of different size, coatings and concentration.* Journal of Hazardous Materials (under revision)

Abstract

Silver nanoparticles (AgNPs) are broadly commercialised due to their antibacterial properties. The wide industrial fabrication of daily life products containing these particles enhances their possibilities to reach the environment and exert toxic effects. Therefore, it is important to understand the uptake, translocation and biotransformation in plants and the toxicological impacts derived from these biological processes. In the present contribution, *Lactuca sativa* (lettuce) was exposed to different coated and sized AgNPs at different nanosilver concentrations. Total silver measurements in lettuce roots indicated that accumulation of AgNPs is influenced by size and concentration, but not by nanoparticle coating. On the other hand, nanosilver translocation to shoots was more pronounced for neutral charged and large-sized NPs at higher NP concentrations. Single particle inductively coupled plasma mass spectrometry analysis, after an enzymatic digestion of lettuce tissues indicated the dissolution of some NPs. Ag K-edge X-ray absorption spectroscopy analysis corroborated the AgNPs dissolution due to the presence of less Ag-Ag bonds and appearance of Ag-O and/or Ag-S bonds in lettuce roots. Toxicological effects on lettuce plants were observed after exposure to nanosilver, especially for transpiration and stomatal conductance. These findings indicated that AgNPs can enter to edible plants, exerting toxicological effects on them.

Keywords: Silver nanoparticles, Lactuca sativa, Inductively coupled plasma optic emission spectrometry, Single particle inductively coupled plasma mass spectrometry, X-ray absorption spectroscopy.

7.1 Introduction

The global market of manufactured nanomaterials has increased in recent times generating in Europe a revenue of 2.5$ billion in 2015. This rising tendency seems to continue, expecting a compound growth rate of 20% during 2016-2022. Among the different types of nanomaterials, silver nanoparticles (AgNPs) are considered the most commercialised, forecasting a growth of the market of nearly 13% in 2016-2024 [7.1]. The main AgNP uses include diagnostic, antibacterial, conductive and optical applications because of their unique physicochemical properties given by their nanosize (1-100 nm). The broad of AgNP applications increase their chance of reaching environmental compartments (air, water or/and soil) through direct (e.g. photocatalyst during water treatment) or indirect modes such as landfills, waste incineration and effluent or sewage sludge from wastewater treatment plants [7.2-7.5]. Soils are the major sink of disposal of these emerging contaminants estimating an increase by 1.2 and 110 ng kg^{-1} per year in bare soil and soil treated with sewage sludge, respectively [7.6]. Consequently, terrestrial organisms as well as plants are exposed to these particles generating a growing concern in their toxicological effects on ecosystem and human health. AgNPs can enter into vegetal species through their interactions with plant rhizosphere (soil, water), penetrating cell walls and membranes of root epidermis and subsequently entering vascular tissues (xylem). After reaching the xylem, which is the main tissue in plants for transporting water and nutrients from roots to shoots, particles can be translocated to leaves through stems. Another way of nanosilver entry is through air, by their attachment to aerial parts of the plant [7.2,7.7, 7.8]. During their transport inside the plant, silver nanoparticles are susceptible to transformation processes such as partial oxidation, surface modification, dissolution and/or aggregation/agglomeration [7.3,7.7,7.9]. All these biotransformations may influence AgNPs toxicity to plants, especially the dissolution of metallic silver from nanoparticles that is considered to partly explain nanoparticles toxicity [7.10,7.11]. Their toxicity effects are greatly dependent on particle characteristics (coating, size and surface properties), plant species and plant growth substrates (soil, hydroponics and culture medium) [7.12]. Due to the multiple factors that contribute to AgNP effects in plants, several studies have been performed. Most of them have been conducted with *Arabidopsis thaliana* as model plant because it has a short generation time, small size, high seed production and a small fully sequenced genome [7.3]. From these works, it has been confirmed that AgNPs can be accumulated in *A. thaliana* plants cultivated in different media such as agar [7.13-7.15], Hoagland's [7.16,7.17] or soil [7.18], and that these particles provoke root, shoot and leaf growth reduction [7.13,7.15,7.18-7.22]. Plant growth reduction is typically caused by the inhibition

of photosynthesis that is affected by chlorophyll content. In fact, some studies with *A. thaliana* have shown a decrease in chlorophyll content when plants have been contaminated with AgNPs [7.14,7.15, 7.22]. Reactive oxygen species (ROS), which are the combination of molecular oxygen with surplus electrons, are also formed when photosynthetic efficiency decreases causing structural damages to chloroplasts, lipids and DNA macromolecules. However, plants have an antioxidant defence system (enzymatic and non-enzymatic antioxidants) to avoid the increase of ROS levels. An excess of ROS respect to antioxidants is called oxidative stress, which can lead to cell damage. Several studies have found an increase of ROS species, oxidative stress, cellular structural damages or gene alterations when *Arabidopsis thaliana* has been exposed to AgNPs [7.13-7.16,7.19-7.21]. Furthermore, several authors have corroborated that toxicity of nanosilver to *A. thaliana* depends on particle concentration [7.14], particle size [7.17] and silver species (AgNPs or Ag(I)) [7.13,7.21]. Because of the negative effects that nanosilver can exert to *A. thaliana*, it was also considered essential to evaluate the toxicity of these particles in aquatic [7.23], wetland [7.24,7.25] and edible plants [7.9,7.26-7.44]. Among the studied crop plants, some works have been performed with *Lactuca sativa* (lettuce), which is common in farmlands and as foodstuff. Barrena *et al.* [7.33] showed that uncoated AgNPs (2 nm) negatively affect lettuce seed germination. Larue *et al.* [7.45] determined that foliar exposure of *L. sativa* to uncoated AgNPs (38.6 nm) at different concentration levels (1, 10, 100 $\mu g\ g^{-1}$) did not lead to changes in biomass, protein content and photosynthetic parameters. Nevertheless, AgNPs (as Ag agglomerates) over the surface of lettuce leaves including stomata were detected by micro X-ray fluorescence. Moreover, it was determined by X-ray absorption near edge structure spectroscopy (XANES), that the majority of the analysed regions of lettuce leaves contained a mixture of AgNPs and secondary species such as Ag-glutathione. Doolette *et al.* [7.46] demonstrated that Ag uptake by lettuce (AgNPs (40 nm) and silver sulfide nanoparticles (152 nm)) from dosed soils depends on nanoparticles dissolution and that the bioavailability of Ag from these particles increases with the application of ammonium thiosulfate fertiliser. Furthermore, a low translocation of Ag from roots to shoots in lettuce was also reported. These previous studies with lettuce informed about the accumulation and toxicity of AgNPs, but none of them assessed the impact of nanosilver coating and size on uptake, translocation and toxicity in this crop plant. Cvjetko *et al.* [7.9] stated that AgNPs toxicity in *Allium cepa* is directly correlated to particle size, surface charge and/or surface coating. Thus, in order to better understand the behaviour of nanosilver in lettuces, the effect of these particles depending on their characteristics has also to be studied. The aims of this work were to: (1)

assess the concentration effect on uptake and translocation of AgNPs and Ag(I) in lettuce tissues; (2) evaluate the uptake and translocation of different types of AgNPs (size/coating) and Ag(I) in *L. sativa* roots and shoots; (3) evaluate the toxicity effects of AgNPs and Ag(I) by some *L. sativa* plant physiological parameters (leaf gas exchange, chlorophyll fluorescence and photosynthetic pigment content); (4) determine silver form (nanoparticle or dissolved) in roots and shoots from the studied lettuce plants; and (5) investigate Ag speciation and ligand environment in the model crop plant by Ag K-edge X-ray absorption spectroscopy (XAS).

7.2 Material and methods

7.2.1 Chemicals, materials and apparatus

Well-characterized (AgNP characteristics supplied by the manufacturer) commercial solutions of sodium citrate (2 mM) stabilised silver nanoparticles (citrate-AgNPs) of 60 and 100 nm; polyvinylpyrrolidone coated AgNPs (PVP-AgNPs) of 75 and 100 nm stabilised with sodium citrate (2 mM); and polyethyleneglycol coated AgNPs (PEG-AgNPs) of 100 nm dissolved in water were purchased from NanoComposix (San Diego, USA). These AgNP commercial stock solutions were used to dose plant growth medium for assessing nanosilver absorption by lettuces. An ionic silver stock solution of 1,000 ± 2 mg L^{-1} (Merck KGaA, Darmstadt, Germany) was also employed for spiking plant growth medium, and for preparing inductively coupled plasma optical emission spectrometry (ICP-OES) and inductively coupled plasma mass spectrometry (ICPMS) standard solutions. The Hoagland solution (nutrient solution) was prepared with the following reagents: zinc sulfate monohydrate ($ZnSO_4 \cdot H_2O$, Panreac, Barcelona, Spain), molybdenum trioxide (MoO_3, Panreac, Barcelona, Spain), calcium nitrate tetrahydrate ($(CaNO_3)_2 \cdot 4H_2O$, Panreac, Barcelona, Spain), ammonium iron (III) sulfate dodecahydrate ($(NH_4Fe(SO_4)_2 \cdot 12H_2O$, Panreac, Barcelona, Spain), manganese chloride tetrahydrate ($MnCl_2 \cdot 4H_2O$, Panreac, Barcelona, Spain), potassium nitrate (KNO_3, Merck KGaA, Darmstadt, Germany), copper sulfate pentahydrate ($CuSO_4 \cdot 5H_2O$, Panreac, Barcelona, Spain), boric acid (H_3BO_3, Merck KGaA, Darmstadt, Germany), ammonium hydrogen phosphate ($(NH_4)_2HPO_4$, Sigma-Aldrich, St. Louis, USA) and magnesium sulfate ($MgSO_4$, Sigma-Aldrich, St. Louis, USA). In addition, for preparing the Hoagland solution, sodium hydroxide (NaOH, Panreac, Barcelona, Spain) was used to adjust the pH. High purity water obtained from a Milli-Q purification system (Millipore Corp., Bedford, MA) was employed to prepare the Hoagland solution and to dilute stock solutions and sample digests. Acetone and calcium

carbonate ($CaCO_3$, Panreac, Barcelona, Spain) were employed to determine chlorophyll and carotene contents. For the microwave acid digestion of lettuce tissues analytical grade hiperpur quality nitric acid (HNO_3 69%, Ag 0.1 ng g^{-1}, Panreac, Barcelona, Spain) and hydrogen peroxide (H_2O_2 30%, Sigma-Aldrich, St. Louis, USA) was used. Macerozyme R-10 enzyme from *Rhizopus* sp. (Serva Electrophoresis GmbH, Heidelberg, Germany) and citric acid (Panreac, Barcelona, Spain) were utilsed to digest plant tissues for AgNP extraction.

Ovan magnetic stirrers (Barcelona, Spain) were employed to agitate the lettuce growth media (Hoagland solution). An ultrasonic bath J.P. Selecta (Barcelona, Spain) was employed to break down the possible agglomerated AgNPs.

Leaf gas exchange parameters were measured using a portable open-circuit infrared gas analyser system (CIRAS-2, PP-Systems Inc. Amesbury, USA) at about 400 mg L^{-1} of CO_2 equipped with a leaf chamber cuvette (PLC6–18mm of diameter, PP-systems Inc. Amesbury, USA). Chlorophyll fluorescence of the adaxial surface of attached leaves was measured using a portable modulated fluorimeter PAM-2100 (Heinz Walz GmbH, Effeltrich, Germany). Lettuce leaf chlorophylls and carotenoids concentration were determined employing a spectrophotometer Genesys 6 (Thermo electron corporation, Massachusetts, USA).

The acid digestion of vegetal tissue samples was carried out with a Berghof Speedwave Xpert microwave digestion system (Eningen, Germany) equipped with an innovative sensor technology (temperature and pressure). The enzymatic digestion of lettuce tissue was performed with an incubator Ecotron (Infors HT, Bottmingen, Switzerland) equipped with a temperature sensor. The separation of plant tissues from the supernatant during enzymatic digestion procedure was done with Rotofix 32A centrifuge (Hettrich-Zentrifugen, Landau, Germany).

7.2.2 Plant culture

Lactuca sativa seedlings obtained from a garden centre (Can Morera, Girona, Spain) were cleaned with tap water, especially their roots since they contained organic matter. After the cleaning procedure, the plants were completely rinsed with Milli-Q water. Lettuces were cultivated in polypropylene containers containing 100 mL of Hoagland solution [7.47] (pH ~ 5.7) contaminated with AgNPs or Ag(I) depending on the test to be performed as shown in ***Table 7.1.*** The growing period was 9 days with 16h/8h light/dark regime at controlled temperature (21 ± 2 ºC). In addition, hydroponic media were under constant magnetic stirring during the growing period.

Table 7.1 *Lettuce growing conditions in the different tests performed (control = 0 mg L^{-1}).*

Test	Silver form in lettuce growing media	Concentration of silver in lettuce growing media
AgNPs and Ag(I) concentration effect	75 nm PVP-AgNPs Ag(I)	0, 3, 5, 7, 10 and 15 mg L^{-1}
AgNPs coating effect	100 nm PVP-AgNPs 100 nm citrate-AgNPs 100 nm PEG-AgNPs	0, 1, 3 mg L^{-1}
AgNPs size effect	75 nm PVP-AgNPs 100 nm PVP-AgNPs 60 nm citrate-AgNPs 100 nm citrate-AgNPs	0, 1, 3 mg L^{-1}

7.2.3 Measurement of physiological parameters

After lettuces cultivation and exposure to AgNPs or Ag(I), the physiological parameters (leaf gas exchange, chlorophyll fluorescence and photosynthetic pigment content) of fully-developed lettuce leaves were measured to determine if these emerging contaminants have a toxicological effect on the studied plant. Data were analysed separately for both tests, and one-way ANOVAs were applied to test whether different Ag(I) or AgNP concentration or coated AgNPs were statistically different from controls.

7.2.3.1 Gas-exchange measurements

Foliar gas exchange parameters, including transpiration rates (E), stomatal conductance (g_s) and net photosynthetic rates (A) were measured in an attached fully-developed leaf from three (or four) different *L. sativa* plants per treatment in the concentration and coating experiments performed (see ***Table 7.1***). These parameters were analysed using a portable open-circuit infrared gas analyser system. Intrinsic (A/g_s; WUE) and instantaneous (A/E; WUE_i) water use efficiencies were also calculated.

7.2.3.2 Chlorophyll a fluorescence measurements

Measurement of chlorophyll *a* fluorescence provides an insight about the health of the photosynthetic system. Components of chlorophyll *a* fluorescence were quantified with a portable modulated fluorometer PAM-2100 (Heinz Walz GmbH, Effeltrich, Germany) using 4 plants per treatment in the concentration effect test and 2-4 plants per treatment in the coating effect test. Measurements were performed on one exposed and fully developed

leaf per plant. After a dark-adaptation period of at least 30 min, we obtained the potential photochemical efficiency of PSII or *Fv/Fm*, where *Fv* was the variable fluorescence calculated as $Fv = Fm-F_o$, being F_o the minimum and *Fm* the maximum dark-adapted fluorescence. The actual photochemical efficiency of PSII in the light-adapted state was estimated as: $\Delta F/Fm' = (Fm'-F)/Fm'$, where *F* is the steady-state fluorescence yield under the given environmental conditions, and *Fm'* is the maximum level of fluorescence obtained during a saturating flash of light. From this index, we calculated the apparent electron transport rate (*ETR*) as: $ETR = \Delta F/Fm' x\ PAR\ x\ 0.84\ x\ 0.5$, where *PAR* was the incident photosynthetically active radiation (expressed in μmol m^2 s^{-1}), 0.84 was the assumed coefficient of absorption of the leaves, and 0.5 was the assumed distribution of absorbed energy between the two photosystems [7.48]. Finally, the non-photochemical quenching coefficient (*NPQ*), which is a measure of the thermal dissipation of excess energy, was determined as $NPQ = (Fm-Fm')/Fm'$.

7.2.3.3 Chlorophyll and carotenoid concentration

To determine leaf concentration of chlorophylls (*Chl*) and carotenoids (*Car*), 0.1 g of fresh lettuce leaves per plant were ground with a mortar in presence of a little quantity of liquid nitrogen, 10 mg $CaCO_3$ to buffer the solution and 1 mL of acetone (100%). Then, 7 mL of 80% acetone were added in aliquots. When the sample was colourless and totally ground, it was transferred into 15 mL centrifuge tube, being centrifuged at 6,000 rpm during 5 min. The resultant supernatant was transferred to another centrifuge tube and it was diluted to 10 mL with 80% acetone. Finally, the absorbance was measured at 470, 646.6 and 663.6 nm wavelengths using 80% acetone as blank sample. Leaf concentrations of chlorophyll *a* and *b*, total chlorophylls, and carotenoids were then estimated using Porra *et al.* [7.49] equations for the chlorophylls and Lichtenthaler and Wellburn [7.50] equation for the carotenoids, as in Verdaguer *et al.* [7.51]. The content of pigments was finally expressed as mg g^{-1} dry weight (DW) and the ratio *Car/Chl a+b* was calculated.

7.2.4 Plant treatments

After measuring plant physiological parameters, lettuces were submitted to different sample treatments depending on the analysis to be performed. The sample treatments applied are described in the following sections:

7.2.4.1 Total sample digestion

In order to determine the total silver content accumulated in plant tissues (shoots and roots) a microwave acid digestion was performed. For that, lettuces were washed 3 times with Milli-Q water to remove the residual dosing solution and then the shoots were separated from the roots. Afterwards, shoots and roots were dried in the oven during 24 h at 60-70 ºC. After 24 h, the dried samples were weighed, placed in a polytetrafluoroethylene (PTFE) reactor and were ground with a glass rod. Next, 9 mL of HNO_3 (69%) and 1 mL of H_2O_2 (30%) were added in each PTFE reactor. After capping the vessels, the vegetal samples were digested into the microwave following a digestion program consisting on a first step of 5 min to reach 180 ºC, a second step of 10 min at 180 ºC and a third step of 15 min of cooling to room temperature [7.52]. Once at room temperature, plant digests were transferred to polystyrene tubes and were diluted to 20 mL with Milli-Q water. Finally, the samples were stored at 4 ºC until their analysis by ICP-OES or ICPMS. Data were analysed separately for concentration, coating and size tests. One-way ANOVAs were applied to all these tests separately to determine whether different Ag(I) or AgNP concentration, different coated AgNPs and different sized AgNPs were statistically different between each other.

7.2.4.2 Enzymatic sample digestion

An enzymatic digestion was performed to verify the presence of AgNPs after being accumulated in lettuce tissues. As in microwave acid digestion procedure, lettuces were washed 3 times with Milli-Q water before carrying out the enzymatic digestion. After removing the residual dosing solution, the shoots were separated from the roots and then both vegetal tissues (roots and shoots) were cut in small pieces using scissors. Then, the tissues were homogenised in 8 mL of citrate buffer (2 mM) adjusted to optimum pH range (3.5-7.0) for Macerozyme R-10 in accordance with manufacturer's information. Afterwards, 2 mL of Macerozyme R-10 (1 g of enzyme powder in 20 mL of Milli-Q water) were added. Macerozyme R-10 from *Rhizopus* sp. is a multi-component enzyme containing pectinase 0.5 unit/mg, hemicellulose 0.25 unit/mg and cellulose 0.1 unit/mg, which enables the digestion of vegetal tissues and the extraction of the nanoparticles. After adding the Macerozyme R-10, the samples were shaken in an incubator at 37 ºC during 24 h. Afterwards, the plant digests were settled during 1 h and then were filtered by gravity to remove the small pieces of plant tissues [7.53]. Finally, the samples were filtered through 0.45 µm cellulose acetate filter (Whatman, Filterlab, Barcelona, Spain) and diluted to

20 mL with Milli-Q water.

7.2.4.3 XAS sample preparation

The fresh roots were rinsed with Milli-Q water, frozen in liquid nitrogen, homogenised and fixed onto Cu holders for measurements under cryo conditions.

7.2.5 Analysis of plant digests

The plant tissue digests obtained from the two digestion methods were analysed with two different instruments as described below:

7.2.5.1 Measurement of total silver content in lettuce tissues

Lettuce root digests obtained from microwave acid digestion were analysed with an ICP-OES system (Agilent 5100 Vertical Dual View, Agilent Technologies, Tokyo, Japan) in order to determine the total silver content accumulated in the roots. This instrument is equipped with a concentric glass nebuliser, a double pass glass cyclonic spray chamber, an echelle polychromator wavelength selector and a charge-coupled device (CCD) detector. The measurement conditions were: 1,200 W RF power, axial plasma configuration, 12 L min^{-1} plasma gas flow rate, 0.7 L min^{-1} nebuliser flow rate, 25 s of stabilisation time, 1 s of reading time and 3 replicates for each reading. The silver wavelength used was 328.068 nm.

Silver concentrations in lettuce root and shoot tissues below the detection limit of ICP-OES (lettuce tissue digests obtained from enzymatic and microwave acid digestions) were determined by an ICPMS 7500 c (Agilent Technologies, Tokyo, Japan) equipped with a Babington nebuliser, a double pass scott nebuliser chamber, an octopole reaction collision cell system (ORS), a quadrupole analyser and an electron multiplier detector. Measurement parameters were: 1,500 W RF power, 15 L min^{-1} plasma gas flow rate, 1.1 L min^{-1} nebuliser flow rate, 20 s of stabilisation time, integration time of 0.1 s and 3 readings per replicate. The isotope monitored was ^{107}Ag.

7.2.5.2 Detection of AgNPs in lettuce tissues

Single particle inductively coupled plasma mass spectrometry (SP-ICPMS) was employed for analysing the plant tissue digests obtained by enzymatic digestion in order to determine the chemical form of silver (AgNPs or Ag(I)) after being accumulated in these plants. Prior to SP-ICPMS analysis, the total silver content was determined using ICP-OES or ICPMS system to

adjust the silver concentration in sample digests at <1 µg L^{-1}. SP-ICPMS analysis was carried out with an ICPMS 7500 c (Agilent Technologies, Tokyo, Japan) using a 10 ms dwell time and a total measurement time of 60 s. The raw data obtained by the analysis performed was treated using Excel software.

7.2.6 XAS analysis

The samples were measured at CLÆSS beamline of Synchrotron ALBA in Barcelona, Spain. The samples were fixed on the Cu holders and mounted on a finger cooled by a He cryostat. Ag K-edge EXAFS spectra were measured in fluorescence mode using CdTe detector (Amptek, USA) with a total collection time of ~2 h in consecutive runs, to ensure the useful interval up to k = 10 $Å^{-1}$. The spectra were analysed with IFFEFIT software [7.54]. Statistical analysis of Ag neighbourhood in plants was performed by XLSTAT software.

7.3 Results and discussion

7.3.1 Evaluation of plant growing medium conditions

A test to evaluate the best conditions for accumulating the maximum quantity of silver inside lettuce tissues (roots and shoots) during the growing process was performed before carrying out the experiments of this study. For this test, lettuce plants were cultivated during 9 days (16h/8h light/dark, 21 ± 2 °C) in 100 mL hydroponic medium containing 75 nm PVP-AgNPs (1 mg L^{-1}) under two different conditions: without agitation and magnetic stirring (~200 rpm). After 9 days of cultivation, lettuce roots and shoots were submitted to an acid digestion following the procedure described previously (Section 7.2.4.1). Then, the resulting sample digests were analysed by ICP-OES or ICPMS to determine the total silver content in lettuce tissues. As can be seen in ***Fig. S7.1*** in the Supporting information of this chapter, the highest total silver concentration was obtained in lettuce roots and shoots cultivated in nutrient medium submitted to magnetic stirring agitation. This could be due to the fact that AgNPs tend to be deposited at the bottom of the growing tank when no stirring is used during lettuce cultivation. For this reason, it was decided to agitate the Hoagland medium with magnetic stirrers during lettuce cultivation.

7.3.2 Physiological parameters

7.3.2.1 Gas-exchange

The analyses of gas exchange parameters in *L. sativa* revealed that plants were sensitive to

the different 75 nm PVP-AgNPs concentrations (0, 3, 5 and 10 mg L^{-1}) since the transpiration rate and stomatal conductance were affected. Specifically, plants subjected to the different AgNP concentrations showed lower transpiration rate values than control ones (see ***Table 7.2***), but the effect was not in dose dependent manner, since there were not statistically significant differences between the tested concentrations (statistical data not shown). The stomatal conductance was also reduced in lettuce plants, but only when they grew under 3 and 5 mg L^{-1} AgNPs concentration, although the same tendency was observed by plants under 10 mg L^{-1} ($F_{1,6}$= 5.511, p = 0.057).

Table 7.2 *Overall means ± standard errors for the studied leaf physiological parameters in Lactuca sativa plants grown under four different 75 nm PVP-AgNPs concentration (0, 3, 5 and 10 mg L^{-1}). The sample size used was n = 4 for each concentration. p-values for each physiological parameter were the result of comparing each AgNP concentration with the control one (0 mg L^{-1}) by one-way ANOVA tests. The significance level considered was p≤ 0.05 (* indicate a p-value marginally significant; E: transpiration rate; g_s: stomatal conductance; A: photosynthetic rate; WUE_i: instantaneous water use efficiency; WUE: intrinsic water use efficiency; ns: not significant; p: p-values).*

	0 mg L^{-1}	3 mg L^{-1}	*p*	5 mg L^{-1}	*p*	10 mg L^{-1}	*p*
***E* (mmols H_2O m^{-2} s^{-1})**	0.86 ± 0.03	0.45 ± 0.13	0.022	0.33 ± 0.15	0.013	0.53 ± 0.13	0.045
***g_s* (mmols H_2O m^{-2} s^{-1})**	54 ± 4.26	24.75 ± 7.55	0.015	21.75 ± 10.83	0.032	29.50 ± 9.53	0.057*
***A* (μmols CO_2 m^{-2} s^{-1})**	0.60 ± 0.07	0.50 ± 0.09	*ns*	0.48 ± 0.08	*ns*	0.50 ± 0.14	*ns*
WUE_i (A/E)	0.69 ± 0.07	1.92 ± 1.04	*ns*	3.38 ± 2.21	*ns*	1.09 ± 0.35	*ns*
WUE (A/g_s)	0.01 ± 0.00	0.04 ± 0.022 0.02	*ns*	0.06 ± 0.05	*ns*	0.02 ± 0.01	*ns*

Hence, the presence of 75 nm PVP-AgNPs in the culture medium affected negatively lettuce plant water relations being reduced the transpiration rates and stomatal conductance by nearly half of that of control plants (49.4% ± 6.5 and 53% ± 4.2, respectively). Lower transpiration rates agree with lower stomatal conductance. Stomatal closure could be the consequence of a direct PVP-AgNPs effect on guard cells, since nanosilver particles, through the xylem stream water, can reach leaves and thus stomata [7.55]. In fact, other authors stated that in cut roses nanosilver particles also reduced the stomatal conductance and transpiration rate [7.56]. Nevertheless, when those particles are coated with PVP, results could vary. For instance,

in willow and hybrid poplar cuttings the transpiration was unaffected by PVP-AgNPs [7.57], although values obtained were also lower than those of controls. The decrease in stomatal conductance could also be a consequence of an indirect effect due to an interference of PVP-AgNPs with root water uptake. In the treated lettuce plants of this study, much more nanosilver particles were found in roots than in shoots, which would support a stomatal closure due to a disruption of water uptake. Accordingly, in *A. thaliana*, AgNPs caused imbalance in the levels of water affecting the transcript levels of aquaporins [7.13]. A decrease in root water uptake could provoke plant water deficit, rising ABA in leaves and promoting stomatal closure [7.58]. Nevertheless, more studies are needed to assess in lettuce the relationship between PVP-AgNPs aquaporin root cell, water uptake, ABA levels and stomata movement.

Photosynthetic rates did not vary in lettuce plants treated with 75 nm PVP-AgNPs in comparison to control ones. Likely, because of the low light intensity conditions that limits plant CO_2 fixation. Neither the water use efficiency (*WUE* and WUE_i) of treated plants differed from control ones.

Table 7.3 *Overall means ± standard errors for the Lactuca sativa leaf transpiration rate (E) and stomatal conductance (g_s) from plants grown under 3 mg L^{-1} Ag(I) or AgNPs coated with different compounds (PEG, citrate or PVP). The sample size used was n = 4 for controls and citrate-AgNPs and n = 3 for PEG-AgNPs and PVP-AgNPs. For Ag(I) n = 2 because two of the four initial seedlings died before ending the experiment. p≤ values given for each physiological parameter are the results of comparing each treatment with the control one (0 mg L^{-1}) by one way ANOVA tests. The significance level considered was p·0.05 (ns: not significant; p: p-values).*

	0 mg L^{-1}	Ag(I)	*p*	*Citrate-AgNPs*	*p*	*PVP-AgNPs*	*p*	*PEG-AgNPs*	*p*
***E* (mmols H_2O m^{-2} s^{-1})**	1.22 ± 0.09	0.46 ± 0.04	0.004	1.39 ± 0.15	*ns*	0.78 ± 0.09	0.018	0.01 ± 0.19	*ns*
g_s (mmols H_2O m^{-2} s^{-1})	47.00 ± 4.02	16.00 ± 1.00	0.007	54.25 ± 7.39	*ns*	27.00 ± 4.04	0.019	42.67 ± 9.24	*ns*

Regarding results from the coating effect test, only data for the transpiration rate and stomatal conductance was provided. In this case, the instrument was not sensitive enough to make the photosynthesis measurements under low light exposure. Transpiration rate and stomatal conductance only diminished in *L. sativa* plants growing under Ag(I) (about three-fold reduction of *E* and g_s) and 100 nm PVP-AgNPs (about 1.5-fold reduction of *E* and g_s), in comparison to control ones (see ***Table 7.3***), being the most intense the effects for Ag(I). These results highlight the negative effect of Ag(I) on plant water relations, which could agree with a

potent inhibitor effect of silver on plasma membrane aquaporins of root cells [7.59]. Moreover, the results suggest that coated nanosilver particles reduce the negative effect of Ag(I). PVP, PEG and citrate are used as coatings in order to promote stability, avoid aggregation of AgNPs and decrease interaction between proteins [7.60] so, root water uptake disruption could, likely, be alleviated by these stabilising compounds.

7.3.2.2 Chlorophyll fluorescence parameters and leaf chlorophyll and carotenoid concentrations

In the concentration effect test, there were no significant differences among lettuce plants grown under 0, 3, 5 and 10 mg L^{-1} of 75 nm PVP-AgNPs in the parameters estimated from the chlorophyll fluorescence measurements (*Fv/Fm*, *ETR* and *NPQ*). The high values of *Fv/Fm* obtained in all the treatments (between 0.81 and 0.82) indicate that plants did not experience photoinhibition under any of the different 75 nm PVP-AgNPs concentrations assayed, which was expected taking into account the low light intensity (below 50 mol m^2 s^{-1}) applied to the plants. Accordingly, treatments did neither affect the leaf amount of chlorophylls and carotenoids nor the ratio carotenoids/chlorophylls (data not shown).

Interestingly, in the coating effect test, we found significantly ($p = 0.032$) higher *Fv/Fm* values in plants treated with 100 nm PVP-AgNPs compared to controls (see ***Fig. S7.2*** from Supporting information of this chapter), which was in agreement with the significantly lower carotenoid/chlorophyll ratio observed in these plants (see ***Fig. S7.3*** from Supporting information of this chapter). Enhanced photochemical efficiency (*Fv/Fm*) indicates that a higher number of reaction centres are able to accept electrons and carry out photosynthesis, which would be in accordance with a lower need for photoprotection *via* an increased carotenoid/chlorophylls ratio. In plants treated with 100 nm PEG-AgNPs, the leaf content of *Chl a* ($p = 0.011$), *Chl b* ($p = 0.004$), total *Chl* ($p = 0.009$) and carotenoids ($p = 0.012$) was more than twice that of controls (see ***Fig. S7.4*** from Supporting information of this chapter) and, though not significant, *Fv/Fm* values also tended to be higher compared to controls. These results are opposite to those reported on *Vigna subterranean* [7.61] or *Brassica* sp [7.62], but they are in agreement with Sharma *et al.* [7.63], who found enhanced quantum efficiency and more chlorophyll content in *Brassica juncea* leaves treated with silver nanoparticles. Salama [7.64] demonstrated a concentration-dependent effect of silver nanoparticles on the leaf amount of chlorophylls and carotenoids of *Phaseolus vulgaris* and *Zea mays*. Indeed, increasing concentration of

silver nanoparticles from 20 to 60 mg L^{-1} led to enhanced growth, photosynthetic pigment, carbohydrate and protein contents, while concentrations over 60 mg L^{-1} induced an inhibitory effect on these parameters. On the other hand, citrate-AgNPs and Ag(I) treatments did not modify significantly the studied parameters in relation to controls.

7.3.3 Total silver content in lettuce tissues

As it is stated in the Introduction, nanoparticle properties and their concentration in the environment greatly influence plant uptake and translocation, as well as toxicity for the plant. In order to better understand the behaviour of AgNPs in lettuce tissues (roots and shoots), total silver concentration was determined in vegetal samples after being exposed to different types of AgNPs (size and coating) and at different nanosilver concentrations. The results obtained for different tests performed are shown in the following points:

7.3.3.1 AgNPs and Ag(I) concentration effect

In order to determine the amount of AgNPs that lettuces (root and shoot tissues) can uptake, accumulate and translocate, Hoagland solution was spiked at different nanosilver concentrations (concentration range: 3-15 mg L^{-1}). In addition, Ag(I) was also tested at the same concentration levels to determine if there were differences in respect to nanosilver.

As it is shown in ***Fig. 7.1a***, AgNPs and Ag(I) were trapped by lettuce roots because there was an increase in the silver content in these tissues in relation to controls. Total silver accumulated in lettuce root tissues increased in dose-dependent manner for both silver forms. No significant differences (p (3 mg L^{-1}) = 0.2754; p (5 mg L^{-1}) = 0.0520) were observed between the two silver species uptake at low concentrations but at concentrations above 7 mg L^{-1} significant differences were observed (p (10 mg L^{-1}) = 0.0403; p (15 mg L^{-1}) = 0.0031) showing a higher Ag(I) uptake by root tissues in respect to 75 nm PVP-AgNPs. Cvjetko *et al.* [7.9] and Vinković *et al.* [7.31] observed also differences between Ag(I) and AgNPs uptake by root tissues at higher concentrations with *Allium cepa* and *Capsicum annuum* L. plants. It is worth mentioning that the error bars were bigger at 10-15 mg L^{-1} AgNP or Ag(I) concentration, probably because roots could not accumulate more silver and they started to suffer changes in their metabolism due to toxicological effects (e.g. a minor growth of the lettuce plant was observed).

Previous studies demonstrated that AgNPs can be accumulated in roots and be transported to aerial parts of the plant [7.6,7.33,7.62]. For this reason, the total silver content in lettuce

shoots was also determined after an acid microwave digestion. The results showed that both silver chemical species (75 nm PVP-AgNPs and Ag(I)) accumulated in lettuce roots were transported to shoot tissues that did not contain silver as could be seen in control sample (see ***Fig. 7.1b***). Nevertheless, the content of silver accumulated in lettuce roots was mainly 5000-fold higher than in lettuce shoots. In this case, statistical differences at some concentration levels (e.g. p (3 mg L^{-1}) = 0.0215; p (15 mg L^{-1}) = 0.0028) were observed between 75 nm PVP-AgNPs and Ag(I), the latter being more effectively transported to lettuce aerial parts. Vinković et al. [7.31] observed also this difference with *Capsicum annuum* L. plants and the reason of this dissimilarity was explained by the aggregation behaviour of AgNPs, which at the studied concentrations easily aggregated and consequently they were less efficiently transported. Additionally, it was observed that the silver concentration accumulated in lettuce shoots increased in dose-dependent manner for both silver forms up to 7 mg L^{-1}, especially 75 nm PVP-AgNPs. At concentrations higher than 7 mg L^{-1} the shoot tissues probably contained less silver because they started to suffer toxicological effects and their metabolism was affected (e.g. deadness of lettuce shoots as a consequence of necrosis was observed) (see ***Fig. 7.1a***).

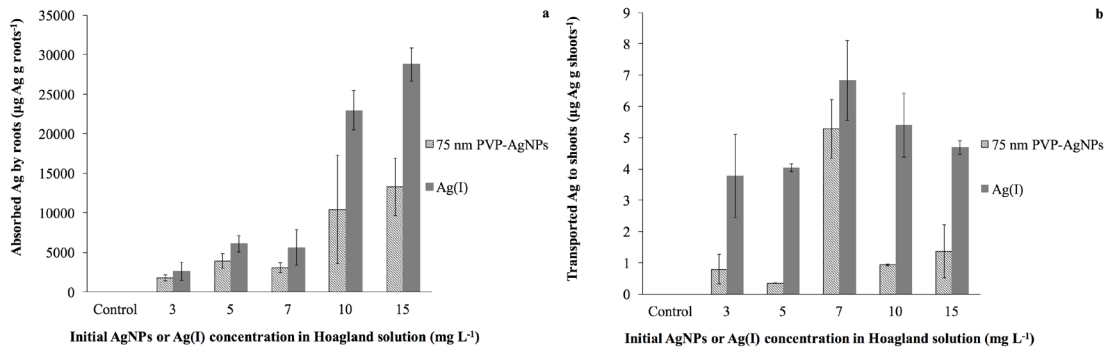

Fig. 7.1 *Total silver concentrations in lettuce roots (**a**) and lettuce shoots (**b**) obtained from concentration effect test (control (0), 3, 5, 7, 10 and 15 mg L^{-1}) with 75 nm PVP-AgNPs and Ag(I) (error bars: standard deviation (n = 3)).*

Indeed, the hydric status of lettuce leaves (E, g_s) was already affected by 75 nm PVP-AgNPs at a concentration of 3 mg L^{-1}.

7.3.3.2 AgNPs coating effect

AgNPs are synthesized with different surface coatings to improve their stability. The coat around nanoparticles modifies their surface characteristics and consequently their intrinsic behaviour. Furthermore, under environmental conditions surface coatings are susceptible to suffer changes. For instance in their superficial charge, which is an important parameter

affecting the interactions with other components [7.9,7.65]. In this work three different 100 nm coated AgNPs were tested at 1 mg L^{-1} concentration: PVP-AgNPs (negatively charged at pH 7), citrate-AgNPs (highly negatively charged at pH 7) and PEG-AgNPs (neutral at pH 7) [7.66]. In ***Fig. 7.2a*** it can be seen that the different coated AgNPs tested were similarly accumulated in lettuce roots (p = 0.9514). So, surface charge seems to have no effect on AgNPs uptake by lettuce roots although, as commented above (Section 7.3.2.1) can affect plant physiology in a different manner. Cvjetko *et al.* [7.9] studied the uptake of PVP-AgNPs and citrate-AgNPs by *Allium cepa* roots and observed a similar silver uptake, especially at higher concentrations (50 and 75 µM). In addition, Ag(I) uptake by lettuce roots was also tested to check if there were differences in respect to nanosilver. The results obtained demonstrated that Ag(I) concentration in root samples was higher although no statistical differences were observed (p = 0.1237). Published studies with other edible plants also determined that Ag accumulation was lower in treatments with AgNPs than with $AgNO_3$ [7.9,7.31,7.62].

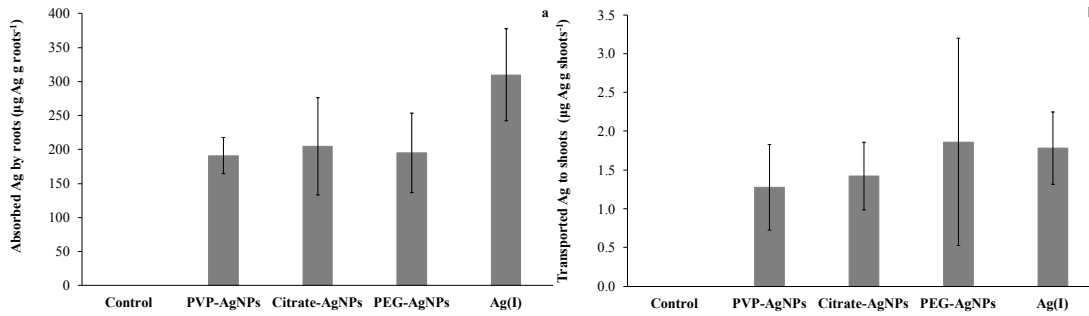

Fig. 7.2 *Total silver content in lettuce tissues (**a** roots; **b** shoots) resulting from coating effect test using different coated 100 nm AgNPs (PVP-, citrate- and PEG-AgNPs) at 1 mg L^{-1} concentration in Hoagland solution (error bars: standard deviation (n =3)).*

Total silver content in lettuce shoots was also determined. Although no statistical differences (p = 0.7700) were observed between total silver concentrations in lettuce shoots for all treatments performed (see ***Fig. 7.2b***), it seems that neutral surface charged AgNPs (PEG-AgNPs) and Ag(I) were more easily transported from roots to shoots compared to negatively charged AgNPs (PVP- and citrate-AgNPs). These results are in agreement with other works in which is confirmed that translocation of Ag(I) from roots to shoots is higher than AgNPs [7.31, 7.67]. Additionally, a stronger reduction in transpiration and stomatal conductance due to the presence of Ag(I) inside plants was already observed in comparison with other treatments (lowest E and g_s values) (see ***Table 7.3***).

7.3.3.3 AgNPs size effect

AgNPs can be synthesized at different sizes. This particle characteristic could also influence their behaviour in the environment. For this reason, the size effect on AgNP uptake by lettuce roots and their translocation to shoots was studied with two different sized PVP-AgNPs (75 and 100 nm) and citrate-AgNPs (60 and 100 nm). The results obtained showed that small-sized AgNPs (75 nm PVP-AgNPs and 60 nm citrate AgNPs) were more absorbed by lettuce roots than large-sized AgNPs (100 nm PVP- and citrate-AgNPs) (see ***Fig. 7.3a*** and ***7.3c***), observing statistical differences between the tested particle sizes (p_{PVP} = 0.0001; $p_{citrate}$ = 0.0037). The same tendency was observed in a bioaccumulation study of different sized AgNPs (20, 30-60, 70-120 and 150 nm) in *Oryza sativa* L. cv KDML 105 root tissues [7.26]. This supports the hypothesis that roots have a higher tendency of trapping smaller AgNPs rather than bigger ones. However, it is worth mentioning that in this work the same AgNPs mass concentration is used, so the number of particles present in the solutions of 75 nm PVP-AgNPs and 60 nm citrate-AgNPs is higher than the solutions of 100 nm PVP- and citrate-AgNPs. Therefore, the probability of smaller AgNPs being absorbed by lettuce roots is higher than for the bigger ones.

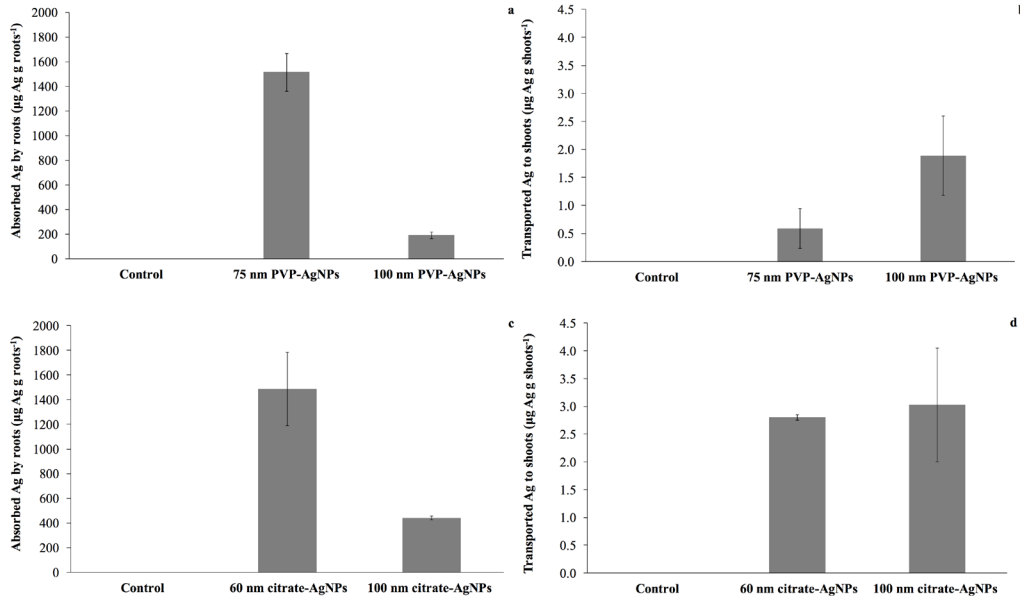

Fig. 7.3 *Content of silver in vegetal roots (**a** PVP-AgNPs; **c** citrate-AgNPs) and shoots (**b** PVP-AgNPs; **d** citrate-AgNPs) after performing particle size effect test at 1 mg L^{-1} concentration (error bars: standard deviation (n = 3)).*

The total silver content in lettuce shoots was also determined. The concentration of large-sized AgNPs (100 nm PVP- and citrate-AgNPs) was higher than small-sized AgNPs (75 nm

PVP-AgNPs and 60 nm citrate-AgNPs) (see ***Fig. 7.3b*** and ***7.3d***), exhibiting statistical differences between different sized PVP-AgNPs (p = 0.050) but none for citrate-AgNPs (p = 0.1501). These results are in agreement with P. Thuesombat *et al.* [7.26] that also determined the total silver content in *Oryza sativa* L. cv *KDML* 105 leaf tissues of different sized AgNPs (20 nm, 30-60, 70-120 and 150 nm) and they concluded that 20 nm AgNPs were less accumulated in rice aerial parts than 150 nm AgNPs. This tendency was also confirmed by calculating the translocation factor (*TF*) with the following equation [7.68]:

$$TF = C_{shoot} / C_{root} \qquad (6.1)$$

where C_{shoot} is the total silver concentration in lettuce shoots and C_{root} is the total silver concentration in lettuce roots. The *TF*s obtained were higher for large-sized AgNPs (100 nm PVP-AgNPs: 0.0099; 100 nm citrate-AgNPs: 0.0068) than small-sized AgNPs (75 nm PVP-AgNPs: 0.0004; 60 nm citrate-AgNPs: 0.0019). These results indicate that large-sized AgNPs could be transported more efficiently from root tissues to shoot tissues than small-sized AgNPs.

7.3.4 AgNPs detection in plant tissues by SP-ICPMS

SP-ICPMS is a viable methodology for detecting nanoparticles at levels down the ng L^{-1} in liquid samples, differentiating them from other forms of the same element. To obtain reliable results, just one nanoparticle must be measured during each reading period. So sufficiently diluted metal-rich particle suspensions and adequate data acquisition frequency are required [7.69, 7.70]. In this study, an enzymatic digestion was carried out in order to maintain intact the AgNPs to determine by SP-ICPMS the chemical form of the silver (as AgNPs or Ag(I)) after being accumulated in lettuce tissues. The nanoparticles transformation inside lettuce tissues was assessed at different concentrations and using AgNPs with different coatings and sizes. The results obtained from these three different tests performed are shown below:

7.3.4.1 AgNPs concentration effect

Before carrying out the SP-ICPMS analysis of vegetal tissues, the total amount of silver present in the enzymatic plant digests was determined to know the silver extracted by enzymatic digestion from lettuce roots and shoots.

After knowing the silver concentrations in lettuce enzymatic digests (shoots and roots); sample dilution was performed, when it was necessary (concentration <1 µg L^{-1}), to obtain

an adequate sample to be analysed by SP-ICPMS. The time-resolved plots obtained for the different concentration levels studied (3, 5 and 10 mg L^{-1}) are shown in ***Fig. 7.4***. A large number of peaks above the baseline were observed in ***Fig. 7.4c*** and ***7.4e***, indicating the presence of AgNPs in lettuce roots except for ***Fig. 7.4a*** where less peaks were observed (3 mg L^{-1}). This could probably be because the presence of AgNPs is smaller at 3 mg L^{-1} and the probability to get all of them partially or totally dissolved is higher than at 5 and 10 mg L^{-1}. Therefore, the amount of Ag(I) is higher in 3 mg L^{-1} in comparison with 5 and 10 mg L^{-1}, where the presence of Ag(I) was also determined (baseline counts around 100-120). This was also reflected by the calculations carried out to estimate the concentration of both metal forms (AgNPs and Ag(I)) in which it was observed that at 5 and 10 mg L^{-1} the percentage of AgNPs was higher than at 3 mg L^{-1} (data not shown). Furthermore, the histogram representations (see ***Fig. 7.4d*** and ***7.4f***) of all the concentration levels tested showed a first distribution at low pulse intensity

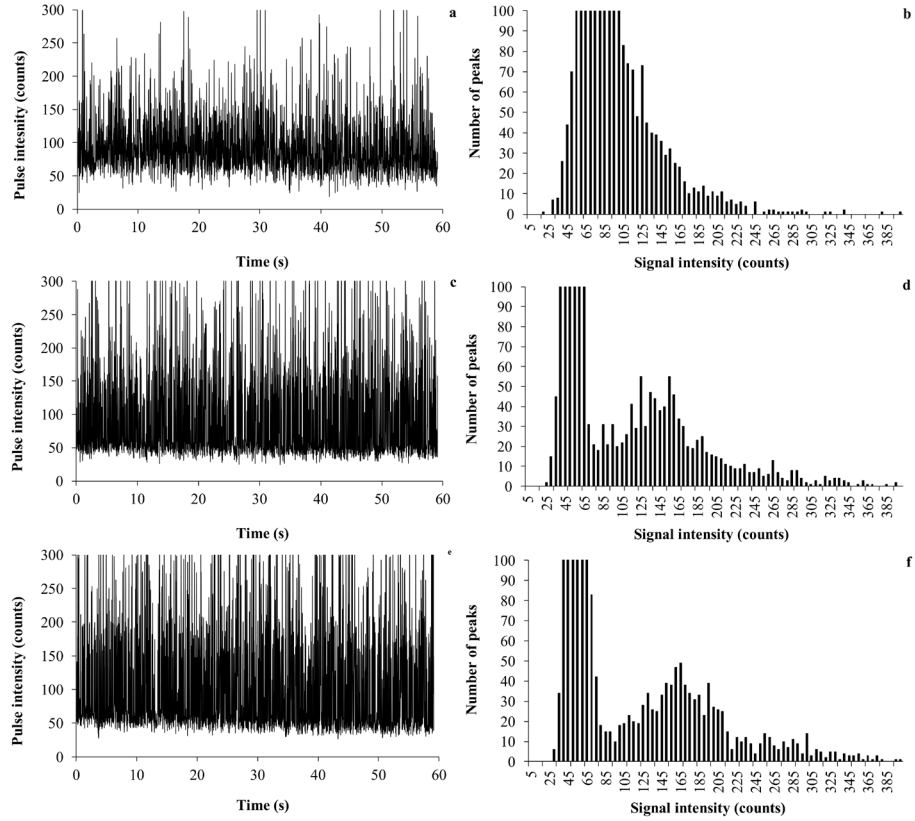

Fig. 7.4 *SP-ICPMS time-resolved plots and histograms of lettuce roots contaminated with 75 nm PVP-AgNPs at different concentration levels (**a-b** 3 mg L^{-1}; **c-d** 5 mg L^{-1}; **e-f** 10 mg L^{-1}).*

values corresponding to dissolved silver and a second distribution at high pulse intensity values corresponding to nanosilver except for ***Fig. 7.4b*** (3 mg L^{-1} concentration level) where

both distributions (AgNPs and Ag(I)) were overlapped. Ag K-edge EXAFS also confirmed the dissolution of AgNPs, where significantly higher proportion of -S and -O ligands was observed at 3 mg L^{-1} (***Table 7.4***, ***Fig. 7.8***).

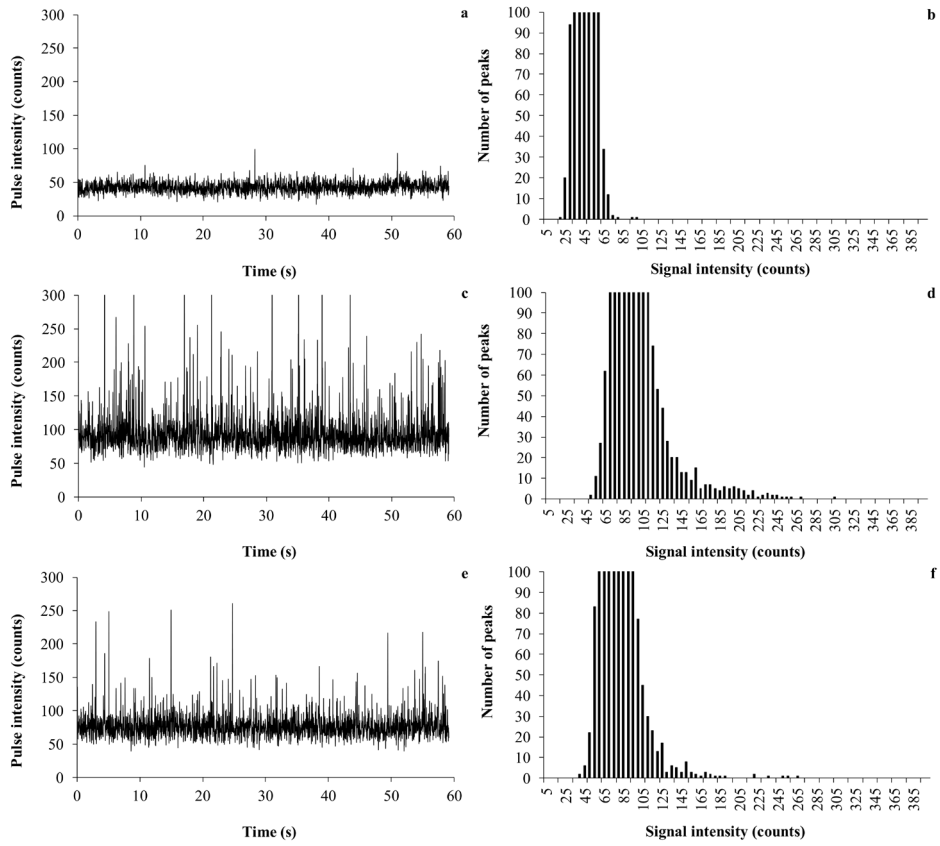

Fig. 7.5 *SP-ICPMS time-resolved plots and histograms of lettuce shoots contaminated with 75 nm PVP-AgNPs at different concentration levels (**a-b** 3 mg L^{-1}; **c-d** 5 mg L^{-1}; **e-f** 10 mg L^{-1}).*

In lettuce shoots the presence of AgNPs was also confirmed at higher concentration levels (see ***Fig. 7.5***). At 3 mg L^{-1} the baseline counts were shifted to higher values in respect to baseline (around 40-50 counts) and the signal was practically constant (see ***Fig. 7.5a***). Additionally, the histogram representation showed one distribution at low pulse intensity corresponding to Ag(I) (see ***Fig. 7.5b***). At 5 and 10 mg L^{-1} the presence of Ag(I) was also confirmed but some peaks above the baseline were observed indicating the presence of AgNPs as well (see ***Fig. 7.5c***, ***7.5e***). Although there were some AgNPs in lettuce shoots at 5 and 10 mg L^{-1}, the percentage of AgNPs quantified by SP-ICPMS was insignificant in comparison with Ag(I) percentage (data not shown). Therefore, their presence was lower than in root tissues. The presence of Ag(I) in all concentration levels, because of AgNPs dissolution, could explain the lower results obtained

in the different physiological parameters evaluated (*E*, g_S and *Fm/Fv*) in respect to controls (see ***Table 7.2*** and ***Fig. S7.2*** from the Supporting information of this chapter), indicating that the toxicity of AgNPs could be partially explained by the presence of Ag(I) as some authors stated [7.10,7.11]. However, AgNPs toxicity to lettuces cannot be only a consequence of their dissolution, since in 5 mg L^{-1} treatment more Ag-Ag bonds were observed by EXAFS analysis (see ***Table 7.4***).

7.3.4.2 AgNPs coating effect

As in the concentration test, the total amount of silver in lettuce tissues was determined by ICPMS before SP-ICPMS analysis. Silver was detected in plant roots but not in plant shoots; thus, in this latter case the SP-ICPMS analysis was not carried out. After diluting the lettuce root enzymatic digests to a proper concentration (≤1 µg L^{-1}), time-resolved plots obtained for all the coated AgNPs tested shown several peaks above the baseline indicating the presence of AgNPs in root tissues (see ***Fig. 7.6a***, **7.6c**, **7.6e**). However, the presence of dissolved silver was higher in roots treated with citrate-AgNPs (baseline around 50 counts) and PEG-AgNPs (baseline around 25 counts) (see ***Fig. 7.6a*** and **7.6e**) in comparison with roots treated with PVP-AgNPs (baseline around 10 counts) (see ***Fig. 7.6c***).

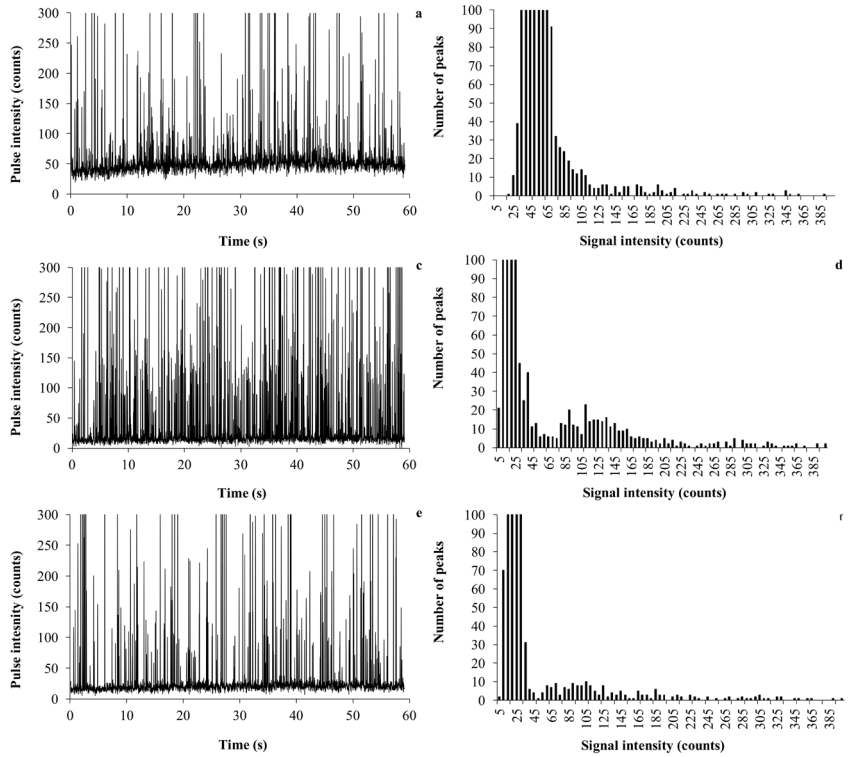

Fig. 7.6 *SP-ICPMS time-resolved plots and histograms of lettuce roots contaminated with different coated AgNPs at 1 mg L^{-1} (**a-b** citrate-AgNPs; **c-d** PVP-AgNPs; **e-f** PEG-AgNPs)*

This was also observed in histogram representation, where the first distribution corresponding to Ag(I) was at higher pulse intensity, especially for citrate-AgNPs, compared to PVP-AgNPs. Additionally, the percentage of estimated PVP-AgNPs was higher than PEG-AgNPs and citrate-AgNPs (data not shown). The same behaviour was observed with Ag K-edge EXAFS (see ***Table 7.5***). Thus, in biological environment, PVP-AgNPs would be more stable and less susceptible to suffer transformations than citrate-AgNPs and PEG-AgNPs. On the other hand, citrate-AgNPs chlorophyll (*Chl a* and *Chl b*) and carotenoid values obtained were similar to Ag(I) (see ***Fig. S7.4*** from Supporting information of this chapter) but the *E* and g_s were more similar to those obtained for PEG-AgNPs (see ***Table 7.3***). Therefore, more experiments are needed to understand citrate- and PEG-AgNPs dissolution and to confirm that they can behave similarly to Ag(I).

7.3.4.3 AgNPs size effect

In this test, as in coating effect test, silver was only detected in lettuce root enzymatic digests during ICP-OES analysis. So, lettuce shoots were not analysed by SP-ICPMS. Previous to SP-ICPMS analysis, the samples were diluted to an adequate concentration (≤1 μg L^{-1}). From 75 nm PVP-AgNPs time-resolved plot, it was observed that silver signal was constant and shifted to higher values in respect to baseline (around 100 counts) (see ***Fig.***

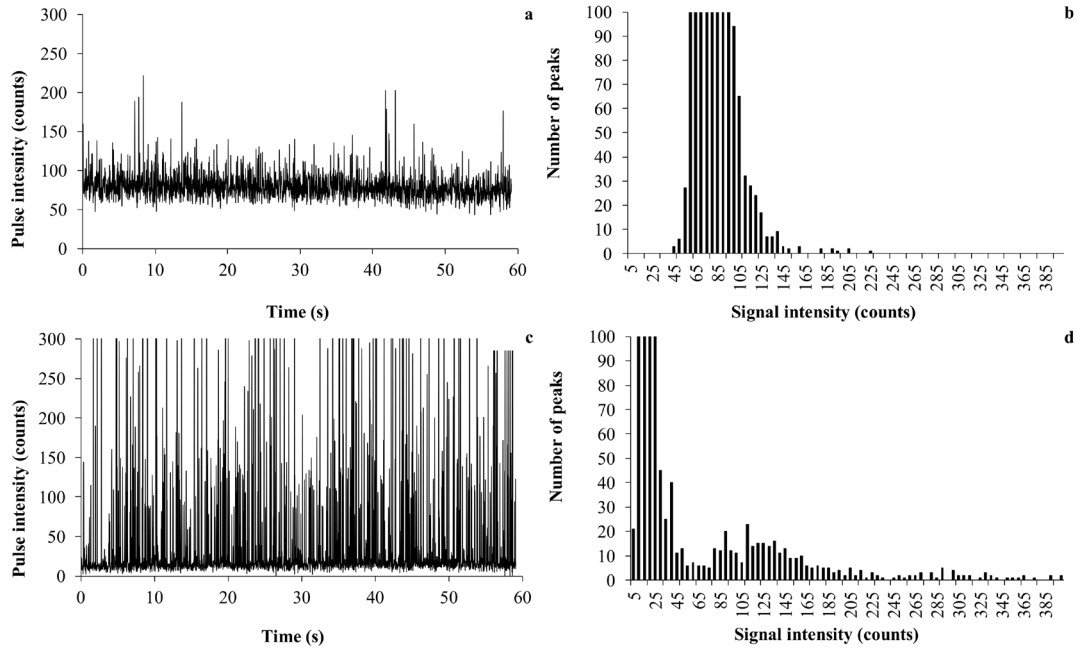

Fig. 7.7 *SP-ICPMS time-resolved plots and histograms of lettuce roots contaminated with different sized AgNPs at 1 mg L^{-1} (**a-b** 75 nm PVP-AgNPs **c-d** 100 nm PVP-AgNPs).*

7.7a), indicating that AgNPs were dissolved to Ag(I). On the other hand, 100 nm PVP-AgNPs time-resolved plot showed several peaks above the baseline, evidencing the presence of silver nanoparticles in lettuce roots (see ***Fig. 7.7c***).

Histogram representations showed only one distribution corresponding to Ag(I) in the case of 75 nm PVP-AgNPs (see ***Fig. 7.7b***) and two distributions corresponding to Ag(I) (first distribution) and AgNPs (second distribution) in the case of 100 nm PVP-AgNPs (see ***Fig. 7.7d***). Furthermore, the percentage of Ag(I) estimated for the smaller particles was higher than for the bigger ones (99% and 26%, respectively). These results are in agreement with EXAFS analysis, because a higher number of Ag-Ag bonds were found for 100 nm NPs than for 75 nm NPs (see ***Table 7.6***). Therefore, larger particles are more stable than smaller ones in lettuce roots. This fact supports the hypothesis that smaller NPs are more prone to get dissolved than bigger NPs as it is stated by some authors [7.71].

7.3.5 Speciation and ligand environment of Ag in lettuce plant

The prevailing feature in EXAFS spectra of all samples is the signal of the neighbour Ag atoms in the NPs: it follows the spectral features of bulk Ag metal up to 5 Å. The contribution of low-Z organic ligands is hardly noticeable beneath the signal of ~12 strongly scattering Ag neighbours. Two candidate ligands are identified: sulfur at 2.4 Å, and oxygen at 2.3 Å (see ***Fig. 7.8***).

In the Feff model constructed from the first 5 scattering paths of Ag metal lattice and single paths of O and S ligands, the number of required parameters is at par with the number of freedom degrees of the usable part of the spectrum. Statistically stable values of the parameters can thus only be gained in collective fitting, preferably of related groups of spectra (studying e.g. concentration effect, coating effect, size effect), so that common values can be assumed for some parameters. When parameter values for a given sample from fitting in different groups are compared, their reliability can be assessed. Those pertaining to the Ag neighbours within the NP are highly reliable, with the spread in the percentage range. The parameters of the S-shell vary typically for 25 %, and those of O-shell more than 50%.

When compared to the initial AgNPs added to the nutrient solution, the Ag neighbourhood in plant roots is characterised by lower number of Ag neighbours, indicating leaching of Ag(I), which makes the AgNPs smaller (see ***Tables 7.4***, ***7.5***, ***7.6***). Ag ions are then bound to -S or -O ligands, but de *novo* formation of Ag-Ag bonds is also possible.

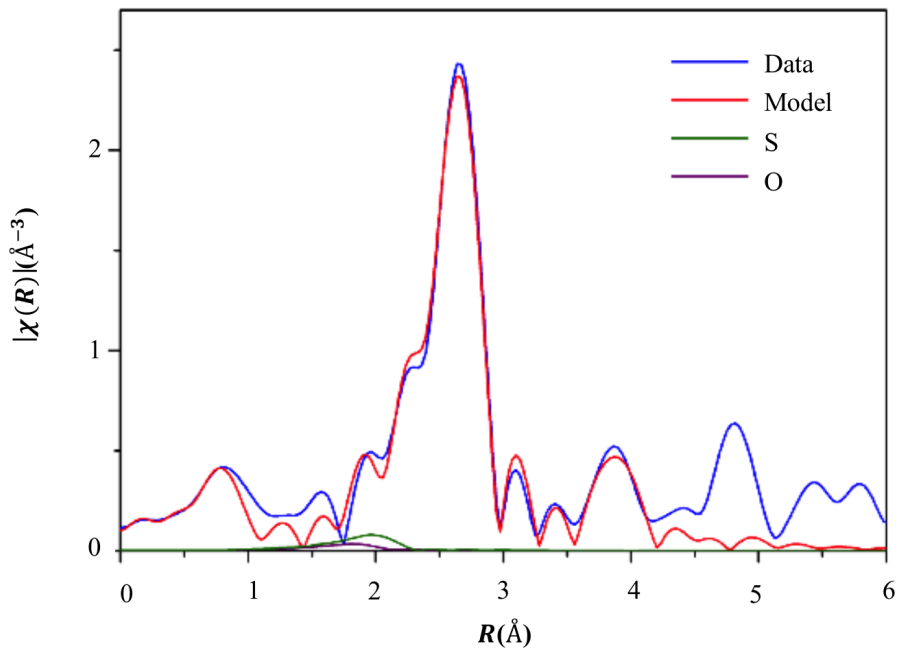

Fig. 7.8 *Fourier transform magnitudes of the k3 weighted Ag K-edge EXAFS of plant roots exposed to 3 ug g^{-1} of PVP-AgNPs.*

Table 7.4 *Best fit model parameters of Ag K-edge EXAFS spectra measured on frozen-hydrated plant roots exposed to 75 nm PVP-AgNPs at different concentrations. Rf - relative frequency, R the distance between Ag and the neighbour atom (Ag, S or O), σ^2 - the width of the radial distribution of the neighbours. E_o - effective zero energy of the photoelectron. Estimated errors in units of the last decimal place are given in parentheses.*

AgNPs concentration	**75 nm PVP-AgNPs added to the nutrient solution**	**Roots 3 mg L^{-1}**	**Roots 5 mg L^{-1}**	**Roots 10 mg L^{-1}**
***Rf* (Ag)**	**0.76(2)**	**0.38(3)**	**0.57(3)**	**0.35(3)**
***R* (Ag) [Å]**	2.875(2)	2.866(2)	2.872(2)	2.863(2)
σ^2Ag [Å2]	32(6)	32	32	32
***Rf* (S)**	**0****	**0.35(10)**	**0.0(10)**	**0.11(10)**
R* (S) [Å]	-	2.430(11)	2.430	2.430
σ^2S [Å^2]*	-	72(30)	72	72
***Rf* (O)**	**0.18(20)**	**0.60(20)**	**0.29(20)**	**0.22(20)**
R* (O) [Å]*	2.300	2.300	2.300	2.300
σ^2(O) [Å^2]**	72	72	72	72
***Eo* [eV]**	1.2(3)	0.6(3)	1.4(3)	1.0(3)

In the concentration effect study, agglomerative hierarchical clustering analysis of Ag neighbourhood in plants *vs.* intact 75 nm PVP-AgNPs shows that the Ag neighbourhood at 5 and 10 mg L^{-1} resembles that of intact AgNPs (see ***Fig. 7.9a***), while at 3 mg L^{-1} the Ag neighbourhood

is significantly different, with higher number of -O and -S ligands due to higher level of AgNP dissolution. A higher number of Ag-Ag bonds are seen at 5mg L^{-1} than at 3 and 10 mg L^{-1} (see ***Table 7.4***) which correlates with increased plant physiological parameters as WUE_i and *WUE* and lowered *E* and g_s (see ***Table 7.2***), possibly as a direct effect of AgNPs on the membrane systems of plant cells.

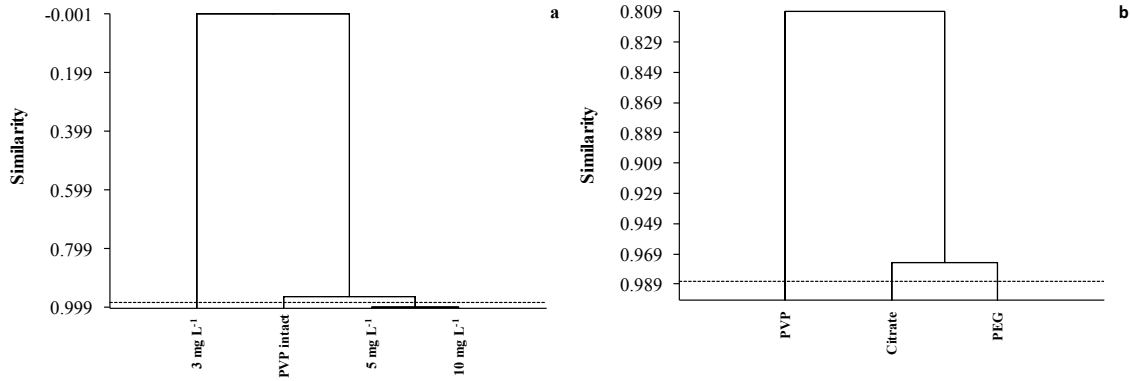

Fig. 7.9 *Agglomerative hierarchical clustering analysis based on Pearson's correlation coefficient, of Ag neighbourhood as obtained by Ag K-edge EXAFS analysis in concentrationeffect study, where the lettuces were exposed to 3, 5, 10 mg L^{-1} of 75 nm PVP-AgNPs and PVP intact (Ag neighbourhood in raw 75 nm PVP-AgNPs) (**a**), and coating effect study where the lettuce plants were exposed to 3 mg L^{-1} of 100 nm PVP, citrate and PEG coated AgNPs (**b**).*

In the coating effects study, PVP coated 100 nm NPs show the highest stability (53% Ag-Ag bonds) (see ***Table 7.5***), again correlating with lower *E* and g_s (see ***Table 7.3***).

Table 7.5 *Best fit model parameters of Ag K-edge EXAFS spectra measured on frozen-hydrated plant roots exposed to 100 nm PVP, citrate and PEG coated AgNPs. Rf - relative frequency, R the distance between Ag and the neighbour atom (Ag, S or O), σ^2 - the width of the radial distribution of the neighbours. E_o - effective zero energy of the photoelectron. Estimated errors in units of the last decimal place are given in parentheses.*

AgNPs concentration	Roots 3 mg L^{-1} PVP, 100 nm	Roots 3 mg L^{-1} Citrate, 100 nm	Roots 3 mg L^{-1} PEG, 100 nm
***Rf* (Ag)**	**0.38(3)**	**0.57(3)**	**0.35(3)**
***R* (Ag) [Å]**	2.866(2)	2.872(2)	2.863(2)
σ^2Ag [Å2]	32	32	32
***Rf* (S)**	**0.35(10)**	**0.0(10)**	**0.11(10)**
R* (S) [Å]	2.430(11)	2.430	2.430
σ^2S [Å^2]*	72(30)	72	72
***Rf* (O)**	**0.60(20)**	**0.29(20)**	**0.22(20)**
R* (O) [Å]*	2.300	2.300	2.300
σ^2(O) [Å^2]**	72	72	72
Eo [eV]	0.6(3)	1.4(3)	1.0(3)

Agglomerative hierarchical clustering confirms higher similarity of Ag neighbourhood in

the lettuce roots exposed to PEG and citrate coated AgNPs (see ***Fig. 7.9b***), characterised by a lower number of Ag-Ag bonds, while higher number of O-ligands is seen in roots exposed to 100 nm PVP-AgNPs.

In the size effects study, 100 nm PVP-AgNPs show better stability than 75 nm NPs, with higher percentage of Ag-Ag bonds (53% *vs.* 38%) (see ***Table 7.6***) correlating with lower root and higher shoot Ag concentration. This indicates that more stable AgNPs are more easily transported from the roots to the shoots, since silver ions probably react already with the cell components in the root system.

Table 7.6 *Best fit model parameters of Ag K-edge EXAFS spectra measured on frozen-hydrated plant roots exposed to 75 and 100 nm PVP-AgNPs at different concentrations. Rf – relative frequency, R the distance between Ag and the neighbour atom (Ag, S or O), σ^2 – the width of the radial distribution of the neighbours. E_o – effective zero energy of the photoelectron. Estimated errors in units of the last decimal place are given in parentheses.*

AgNPs concentration, coating and size	Roots 3 mg L^{-1} PVP, 75 nm	Roots 3 mg L^{-1} PVP, 100 nm
***Rf* (Ag)**	**0.38(3)**	**0.53(3)**
***R* (Ag) [Å]**	2.866(2)	2.868(2)
σ^2Ag [Å2]	37(5)	32(5)
***Rf* (S)**	**0.35(10)**	**0.18(10)**
R* (S) [Å]	2.430(12)	2.430
σ^2S [Å^2]*	72(30)	72
***Rf* (O)**	**0.60(22)**	**0.34(20)**
R* (O) [Å]*	2.300	2.300
σ^2(O) [Å^2]**	72	72
Eo [eV]	0.6(8)	5.8(9)

**- Constrained to common value, **- fixed value*

7.4 Conclusions

The AgNPs accumulation and biotransformation processes in plants and their subsequent toxicological effects are governed by several factors, among them nanoparticle physicochemical properties. The results showed that nanosilver absorption by lettuce roots and their translocation to shoots were concentration dependent processes. Furthermore, the accumulation of these emerging pollutants in lettuce tissues at low exposure concentrations was similar to Ag(I), but at high concentration levels Ag(I) was accumulated at a greater extent. Nanosilver concentration tests also indicated through SP-ICPMS analysis that at 3 mg L^{-1} these emerging pollutants were more prone to get dissolved compared to 5 mg L^{-1} and 10 mg L^{-1}. The same results were obtained by Ag K-edge EXAFS analysis of plant roots due to higher number of Ag-S and Ag-O bonds at low concentrations

were found, pointing to a higher level of AgNPs dissolution at lower nanoparticle concentration. Although transpiration rate values and stomatal conductance of lettuces were reduced after being exposed to AgNPs, toxicological effects were not concentration dependent in the different exposure levels tested in this work.

Particle coatings were found to have no effect on nanosilver uptake by lettuce roots. Nevertheless, 100 nm PEG-AgNPs and Ag(I) seemed to be more transported to aerial parts of the edible plant than negatively charged nanoparticles. SP-ICPMS and Ag K-edge EXAFS analysis demonstrated that PVP coated nanosilver is more stable in lettuce roots than PEG- and citrate-AgNPs. Toxicological studies showed that Ag(I) has a higher negative impact on transpiration and stomatal conductance respect to other studied AgNPs, although the differences on toxicological effects that differently coated AgNPs can exert in lettuce are not clear. On the other hand, particle size has an effect on their absorption by lettuce roots and their translocation to shoots. Small-sized AgNPs were more accumulated by roots, meanwhile large-sized nanosilver were more efficiently transported to lettuce aerial parts. Ag K-edge EXAFS results indicated that 100 nm PVP-AgNPs were more stable because the presence of Ag-Ag bonds was higher in comparison with 75 nm PVP-AgNPs. SP-ICPMS results also showed the dissolution of smaller tested AgNPs and the maintenance of nanoform for bigger NPs in lettuce roots. Although this work gives an overview of the parameters that can influence the AgNPs accumulation, biotransformation and the toxicological effects derived from these processes to lettuce plants, more research is needed to understand the behaviour and risks that can pose these emerging contaminants to edible plants.

Acknowledgments

The Spanish Ministry of Economy and Competitiveness financed this work through the project CGL2013-48802-C3-2-R (Program 2014). L. Torrent gratefully acknowledges a FPI grant from the Spanish Ministry of Economy and Competitiveness (Ref. BES-2014-070625). The authors acknowledge synchrotron facility ALBA (2016091810) for provision of the beamtime and Wojciech Olszewski for the help with the measurements. The authors are also thankful to Albert Salado and Miquel Frau for their contribution on the performance of this work.

The Slovenian Research Agency is acknowledged for financing this work through programs P1-0212, P1-0112 and projects J7-9418 and J7-9398.

References

[7.1] E. Inshakova, O. Inshakov, World market for nanomaterials: structure and trends, MATEC Web Conf. 129 (2017) 02013.

[7.2] A. Cox, P. Venkatachalam, S. Sahi, N. Sharma, Reprint of: silver and titanium dioxide nanoparticle toxicity in plants: A review of current research, Plant Physiol. Biochem. 110 (2017) 33–49.

[7.3] A. Montes, M.A. Bisson, J.A. Gardella Jr., D.S. Aga, Uptake and transformations of engineered nanomaterials: critical responses observed in terrestrial plants and the model plant A*rabidopsis thaliana*, Sci. Total Environ. 607–608 (2017) 1497–1516.

[7.4] V.L. Pachapur, A.D. Larios, M. Cledón, S.K. Brar, M. Verma, R.Y. Surampalli, Behavior and characterization of titanium dioxide and silver nanoparticles in soils, Sci. Total Environ. 563–564 (2016) 933–943.

[7.5] S. Wagner, A. Gondikas, E. Neubauer, T. Hofmann, F. von der Kammer, Spot the Difference: engineered and natural nanoparticles in the environment-release, behavior, and fate, Angew. Chemie Int. Ed. 53 (2014) 12398–12419.

[7.6] M. Rui, C. Ma, X. Tang, J. Yang, F. Jiang, Y. Pan, *et al.*, Phytotoxicity of silver nanoparticles to peanut (*Arachis hypogaea* L.): physiological responses and food safety, ACS Sustain. Chem. Eng. 5 (2017) 6557–6567.

[7.7] D.K. Tripathi, Shweta, S. Singh, S. Singh, R. Pandey, V.P. Singh, N.C. Sharma, *et al.*, An overview on manufactured nanoparticles in plants: uptake, translocation, accumulation and phytotoxicity, Plant Physiol. Biochem. 110 (2017) 2–12.

[7.8] X. Ma, J. Geiser-Lee, Y. Deng, A. Kolmakov, Interactions between engineered nanoparticles (ENPs) and plants: phytotoxicity, uptake and accumulation, Sci. Total Environ. 408 (2010) 3053–3061.

[7.9] P. Cvjetko, A. Milošić, A.-M. Domijan, I.V. Vrček, S. Tolić, P.P. Štefanić, *et al.*, Toxicity of silver ions and differently coated silver nanoparticles in *Allium cepa* roots, Ecotoxicol. Environ. Saf. 137 (2017) 18–28.

[7.10] K.-J. Dietz, S. Herth, Plant nanotoxicology, Trends Plant Sci. 16 (2011) 582–589.

[7.11] C. Levard, E.M. Hotze, G.V. Lowry, G.E. Brown Jr., Environmental transformations of silver nanoparticles: impact on stability and toxicity, Environ. Sci. Technol. 46 (2012) 6900–6914.

[7.12] S.C.C. Arruda, A.L.D. Silva, R.M. Galazzi, R.A. Azevedo, M.A.Z. Arruda, Nanoparticles applied to plant science: a review, Talanta. 131 (2015) 693–705.

[7.13] H. Qian, X. Peng, X. Han, J. Ren, L. Sun, Z. Fu, Comparison of the toxicity of silver nanoparticles

and silver ions on the growth of terrestrial plant model *Arabidopsis thaliana*, J. Environ. Sci. 25 (2013) 1947–1956.

[7.14] R. Kaveh, Y.-S. Li, S. Ranjbar, R. Tehrani, C.L. Brueck, B. Van Aken, Changes in *Arabidopsis thaliana* gene expression in response to silver nanoparticles and silver ions, Environ. Sci. Technol. 47 (2013) 10637–10644.

[7.15] A. Sosan, D. Svistunenko, D. Straltsova, K. Tsiurkina, I. Smolich, T. Lawson, *et al.*, Engineered silver nanoparticles are sensed at the plasma membrane and dramatically modify the physiology of *Arabidopsis thaliana* plants, Plant J. 85 (2016) 245–257.

[7.16] P.M.G. Nair, I.-M. Chung, Cell cycle and mismatch repair genes as potential biomarkers in *Arabidopsis thaliana* seedlings exposed to silver nanoparticles, Bull. Environ. Contam. Toxicol. 92 (2014) 719–725.

[7.17] J. Geisler-Lee, Q. Wang, Y. Yao, W. Zhang, M. Geisler, K. Li, *et al.*, Phytotoxicity, accumulation and transport of silver nanoparticles by *Arabidopsis thaliana*, Nanotoxicology 7 (2012) 323–337.

[7.18] J. Geisler-Lee, M. Brooks, J.R. Gerfen, Q. Wang, C. Fotis, A. Sparer, *et al.*, Reproductive toxicity and life history study of silver nanoparticle effect, uptake and transport in *Arabidopsis thaliana*, Nanomaterials 4 (2014) 301–318.

[7.19] E. Kohan-Baghkheirati, J. Geisler-Lee, Gene expression, protein function and pathways of *Arabidopsis thaliana* responding to silver nanoparticles in comparison to silver ions, cold, salt, drought, and heat, Nanomaterials 5 (2015) 436–467.

[7.20] S. García-Sánchez, I. Bernales, S. Cristobal, Early response to nanoparticles in the *Arabidopsis* transcriptome compromises plant defence and root-hair development through salicylic acid signalling, BMC Genomics 16 (2015) 341.

[7.21] P.M.G. Nair, I.-M. Chung, Assessment of silver nanoparticle-induced physiological and molecular changes in *Arabidopsis thaliana*, Environ. Sci. Pollut. Res. 21 (2014) 8858–8869.

[7.22] J. Sun, L. Wang, S. Li, L. Yin, J. Huang, C. Chen, Toxicity of silver nanoparticles to *Arabidopsis*: inhibition of root gravitropism by interfering with auxin pathway, Environ. Toxicol. Chem. 36 (2017) 2773–2780.

[7.23] E.J. Gubbins, L.C. Batty, J.R. Lead, Phytotoxicity of silver nanoparticles to *Lemna minor* L, Environ. Pollut. 159 (2011) 1551–1559.

[7.24] L. Yin, B.P. Colman, B.M. McGill, J.P. Wright, E.S. Bernhardt, Effects of silver nanoparticle exposure on germination and early growth of eleven wetland plants, PLoS One 7 (2012) e47674.

[7.25] L. Yin, Y. Cheng, B. Espinasse, B.P. Colman, M. Auffan, M. Wiesner, *et al.*, More than the ions: the effects of silver nanoparticles on *Lolium multiflorum*, Environ. Sci. Technol. 45 (2011) 2360–2367.

[7.26] P. Thuesombat, S. Hannongbua, S. Akasit, S. Chadchawan, Effect of silver nanoparticles on rice (*Oryza sativa* L. cv. KDML 105) seed germination and seedling growth, Ecotoxicol. Environ. Saf. 104 (2014) 302–309.

[7.27] F. Mirzajani, H. Askari, S. Hamzelou, M. Farzaneh, A. Ghassempour, Effect of silver nanoparticles on *Oryza sativa* L. and its rhizosphere bacteria, Ecotoxicol. Environ. Saf. 88 (2013) 48–54.

[7.28] M. Kumari, A. Mukherjee, N. Chandrasekaran, Genotoxicity of silver nanoparticles in Allium cepa, Sci. Total Environ. 407 (2009) 5243–5246.

[7.29] N. Saha, S.D. Gupta, Low-dose toxicity of biogenic silver nanoparticles fabricated by *Swertia chirata* on root tips and flower buds of *Allium cepa*, J. Hazard. Mater. 330 (2017) 18–28.

[7.30] H.-S. Jiang, X.-N. Qiu, G.-B. Li, W. Li, L.-Y. Yin, Silver nanoparticles induced accumulation of reactive oxygen species and alteration of antioxidant systems in the aquatic plant *Spirodela polyrhiza*, Environ. Toxicol. Chem. 33 (2014) 1398–1405.

[7.31] T. Vinković, O. Novák, M. Strnad, W. Goessler, D.D. Jurašin, N. Parađiković, *et al.*, Cytokinin response in pepper plants (*Capsicum annuum* L.) exposed to silver nanoparticles, Environ. Res. 156 (2017) 10–18.

[7.32] P. Wang, E. Lombi, S. Sun, K.G. Scheckel, A. Malysheva, B.A. McKenna, *et al.*, Characterizing the uptake, accumulation and toxicity of silver sulfide nanoparticles in plants, Environ. Sci. Nano 4 (2017) 448–460.

[7.33] R. Barrena, E. Casals, J. Colón, X. Font, A. Sánchez, V. Puntes, Evaluation of the ecotoxicity of model nanoparticles, Chemosphere 75 (2009) 850–857.

[7.34] C.O. Dimkpa, J.E. McLean, N. Martineau, D.W. Britt, R. Haverkamp, A.J. Anderson, Silver nanoparticles disrupt wheat (*Triticum aestivum* L.) growth in a sand matrix, Environ. Sci. Technol. 47 (2013) 1082–1090.

[7.35] B. Quah, C. Musante, J.C. White, X. Ma, Phytotoxicity, uptake, and accumulation of silver with different particle sizes and chemical forms, J. Nanopart. Res. 17 (2015) 277.

[7.36] C. Musante, J.C. White, Toxicity of silver and copper to *Cucurbita pepo*: Differential effects of nano and bulk-size particles, Environ. Toxicol. 27 (2012) 510–517.

[7.37] A.K. Patlolla, A. Berry, L. May, P.B. Tchounwou, Genotoxicity of silver nanoparticles in *Vicia faba*: a pilot study on the environmental monitoring of nanoparticles, Int. J. Environ. Res. Public Health

9 (2012) 1649–1662.

[7.38] V.N. Belava, O.O. Panyuta, G.M. Yakovleva, Y.M. Pysmenna, M.V. Volkogon, The effect of silver and copper nanoparticles on the wheat—*Pseudocercosporella* herpotrichoides pathosystem, Nanoscale Res. Lett. 12 (2017) 250.

[7.39] D.K. Tripathi, S. Singh, S. Singh, P.K. Srivastava, V.P. Singh, S. Singh, *et al.*, Nitric oxide alleviates silver nanoparticles (Ag-Nps)-induced phytotoxicity in *Pisum sativum* seedlings, Plant Physiol. Biochem. 110 (2017) 167–177.

[7.40] A.A. Berahmand, A.G. Panahi, H. Sahabi, H. Feizi, P.R. Moghaddam, N. Shahtahmassebi, *et al.*, Effects silver nanoparticles and magnetic field on growth of fodder maize (*Zea mays* L.), Biol. Trace Elem. Res. 149 (2012) 419–424.

[7.41] L.R. Pokhrel, B. Dubey, Evaluation of developmental responses of two crop plants exposed to silver and zinc oxide nanoparticles, Sci. Total Environ. 452–453 (2013) 321–332.

[7.42] W.-M. Lee, J.I. Kwak, Y.-J. An, Effect of silver nanoparticles in crop plants *Phaseolus radiatus* and *Sorghum bicolor*: media effect on phytotoxicity, Chemosphere 86 (2012) 491–499.

[7.43] L.V. Antisari, S. Carbone, A. Gatti, G. Vianello, P. Nannipieri, Uptake and translocation of metals and nutrients in tomato grown in soil polluted with metal oxide (CeO_2, Fe_3O_4, SnO_2, TiO_2) or metallic (Ag, Co, Ni) engineered nanoparticles, Environ. Sci. Pollut. Res. Int. 22 (2015) 1841–1853.

[7.44] U. Song, H. Jun, B. Waldman, J. Roh, Y. Kim, J. Yi, *et al.*, Functional analyses of nanoparticle toxicity: a comparative study of the effects of TiO_2 and Ag on tomatoes (*Lycopersicon esculentum*), Ecotoxicol. Environ. Saf. 93 (2013) 60–67.

[7.45] C. Larue, H. Castillo-Michel, S. Sobanska, L. Cécillon, S. Bureau, V. Barthès, *et al.*, Foliar exposure of the crop *Lactuca sativa* to silver nanoparticles: evidence for internalization and changes in Ag speciation, J. Hazard. Mater. 264 (2014) 98–106.

[7.46] C.L. Doolette, M.J. McLaughlin, J.K. Kirby, D.A. Navarro, Bioavailability of silver and silver sulfide nanoparticles to lettuce (*Lactuca sativa*): effect of agricultural amendments on plant uptake, J. Hazard. Mater. 300 (2015) 788–795.

[7.47] Classic plant media - plant tissue culture protocol, Sigma-Aldrich, (n.d.). Available at: https://www.sigmaaldrich.com/technical-documents/protocols/biology/classic-plant-media.html. Accesed date: 7 September, 2018.

[7.48] J. Galmés, H. Medrano, J. Flexas, Photosynthetic limitations in response to water stress and recovery in Mediterreanean plants with different growth forms, New Phytol. 175 (2007) 81-93.

[7.49] R.J. Porra, The chequered history of the development and use of simultaneous equations for the accurate determination of chlorophylls a and b, Photosynth. Res. 73 (2002) 149–156.

[7.50] H.K. Lichtenthaler, A.R. Wellburn, Determinations of total carotenoids and chlorophylls a and b of leaf extracts in different solvents, Biochem. Soc. Trans. 11 (1983) 591–592.

[7.51] D. Verdaguer, L. Díaz-Guerra, J. Font, J.A. González, L. Llorens, Contrasting seasonal morphological and physio-biochemical responses to UV radiation and reduced rainfall of two mature naturally growing Mediterranean shrubs in the context of climate change, Environ. Exp. Bot. 147 (2018) 189–201.

[7.52] E. Marguí, I. Queralt, M.L. Carvalho, M. Hidalgo, Comparison of EDXRF and ICP-OES after microwave digestion for element determination in plant specimens from an abandoned mining area, Anal. Chim. Acta. 549 (2005) 197–204.

[7.53] D. Bao, Z.G. Oh, Z. Chen, Characterization of silver nanoparticles internalized by *Arabidopsis* plants using single particle ICP-MS Analysis, Front. Plant Sci. 7 (2016) 32.

[7.54] B. Ravel, M. Newville, ATHENA, ARTEMIS, HEPHAESTUS: data analysis for X-ray absorption spectroscopy using IFEFFIT, J. Synchrotron Radiat. 12 (2005) 537–541.

[7.55] D.K. Tripathi, A. Tripathi, Shweta, S. Singh, Y. Singh, K. Vishwakarma, *et al.*, Uptake, accumulation and toxicity of silver nanoparticle in autotrophic plants, and heterotrophic microbes: a concentric review, Front. Microbiol. 8 (2017) 7.

[7.56] P. Lü, S. He, H. Li, J. Cao, H.-L. Xu, Effects of nano-silver treatment on vase life of cut rose cv. movie star flowers, J. Food Agric. Environ. 8 (2010) 1118–1122.

[7.57] A.B. Alicea, Phytotoxicity of silver nanoparticles to hydroponic hybrid poplar and willow cuttings, 2013.

[7.58] M.R.G. Roelfsema, R. Hedrich, In the light of stomatal opening: new insights into "the Watergate", New Phytol. 167 (2005) 665–691.

[7.59] C.M. Niemietz, S.D. Tyerman, New potent inhibitors of aquaporins: silver and gold compounds inhibit aquaporins of plant and human origin, FEBS Lett. 531 (2002) 443–447.

[7.60] N. Hadjesfandiari, A. Parambath, Stealth coatings for nanoparticles: polyethylene glycol alternatives, in: Engineering of biomaterials for drug delivery systems, Elsevier, 2018, Chapter 13, pp. 345–361.

[7.61] E.O. Nwaichi, E.O. Anosike, Plant response on exposure to Ag nanoparticles: a study with *Vigna subterranea*, Biochem. Anal. Biochem. 5 (2016) 299.

[7.62] K. Vishwakarma, Shweta, N. Upadhyay, J. Singh, S. Liu, V.P. Singh, *et al.*, Differential phytotoxic impact of plant mediated silver nanoparticles (AgNPs) and silver nitrate ($AgNO_3$) on *Brassica* sp., Front. Plant Sci. 8 (2017) 1501.

[7.63] P. Sharma, D. Bhatt, M.G.H. Zaidi, P.P. Saradhi, P.K. Khanna, S. Arora, Silver nanoparticle-mediated enhancement in growth and antioxidant status of *Brassica juncea*, Appl. Biochem. Biotechnol. 167 (2012) 2225–2233.

[7.64] H.M.H. Salama, Effects of silver nanoparticles in some crop plants, common bean (*Phaseolus vulgaris* L.) and corn (*Zea mays* L.), International Research Journal of Biotechnology 3 (2012) 190–197.

[7.65] A.M. El Badawy, T.P. Luxton, R.G. Silva, K.G. Scheckel, M.T. Suidan, T.M. Tolaymat, Impact of environmental conditions (pH, ionic strength, and electrolyte type) on the surface charge and aggregation of silver nanoparticles suspensions, Environ. Sci. Technol. 44 (2010) 1260–1266.

[7.66] Nanocomposix. Standard capping agents, (n.d.). Available at: http://cdn.shopify.com/s/files/1/0257/8237/files/Standard_Capping_Agents.pdf. Accessed date: 6 February, 2018.

[7.67] N.G.C. Soria, A. Montes, M.A. Bisson, G.E. Atilla-Gokcumen, D.S. Aga, Mass spectrometry-based metabolomics to assess uptake of silver nanoparticles by *Arabidopsis thaliana*, Environ. Sci. Nano 4 (2017) 1944–1953.

[7.68] K.K. Tiwari, N.K. Singh, M.P. Patel, M.R. Tiwari, U.N. Rai, Metal contamination of soil and translocation in vegetables growing under industrial wastewater irrigated agricultural field of Vadodara, Gujarat, India, Ecotoxicol. Environ. Saf. 74 (2011) 1670–1677.

[7.69] F. Laborda, J. Jiménez-Lamana, E. Bolea, J.R. Castillo, Critical considerations for the determination of nanoparticle number concentrations, size and number size distributions by single particle ICP-MS, J. Anal. At. Spectrom. 28 (2013) 1220–1232.

[7.70] J. Tuoriniemi, G. Cornelis, M. Hassellöv, Size discrimination and detection capabilities of single-particle ICPMS for environmental analysis of silver nanoparticles, Anal. Chem. 84 (2012) 3965–3972.

[7.71] A.D. Dwivedi, S.P. Dubey, M. Sillanpää, Y.-N. Kwon, C. Lee, R.S. Varma, Fate of engineered nanoparticles: implications in the environment, Coord. Chem. Rev. 287 (2015) 64–78.

Supplementary information

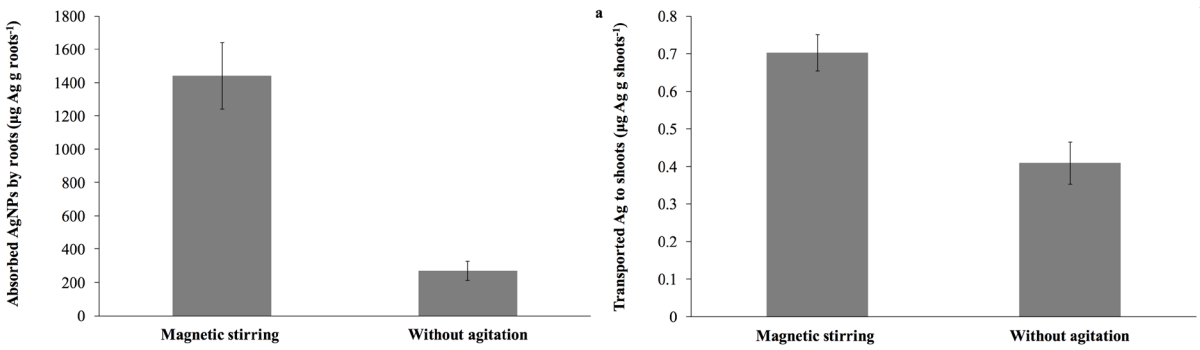

Fig. S7.1 *Total silver content in lettuce root (**a**) and shoot (**b**) tissues after testing different growing conditions with 75 nm PVP-AgNPs at 1 mg L^{-1} (error bars: standard deviation (n = 3)).*

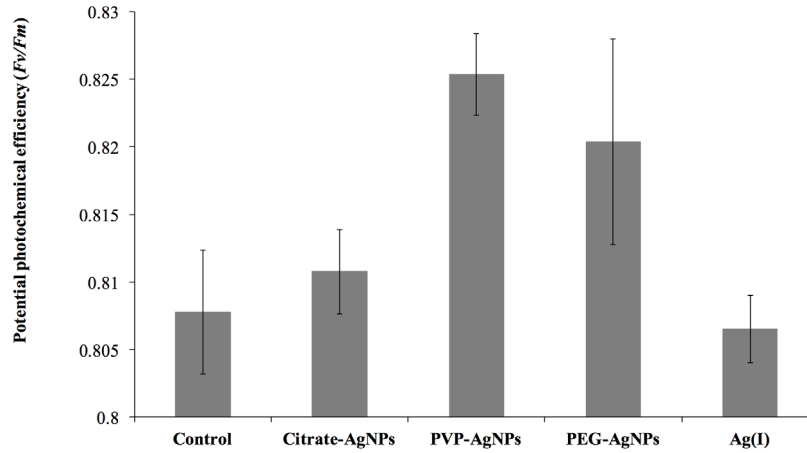

Fig. S7.2 *Foliar potential photochemical efficiency (Fv/Fm) of control lettuces and lettuces treated with different 100 nm coated AgNPs (citrate-, PVP- and PEG-AgNPs) and Ag(I) at 3 mg L^{-1} (error bars: standard deviation, n = 3-4, except for Ag(I) where , n = 2).*

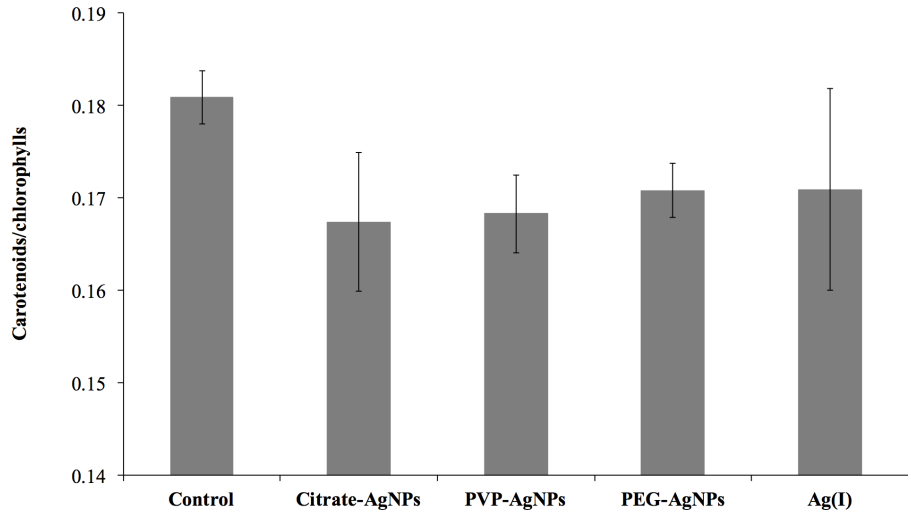

Fig. S7.3 *Foliar carotenoids/chlorophylls ratio of control lettuces and lettuces treated with different 100 nm coated AgNPs (citrate-, PVP- and PEG-AgNPs) and Ag(I) at 3 mg L^{-1} (error bars: standard error; n = 3-4, except for Ag(I) where n = 2).*

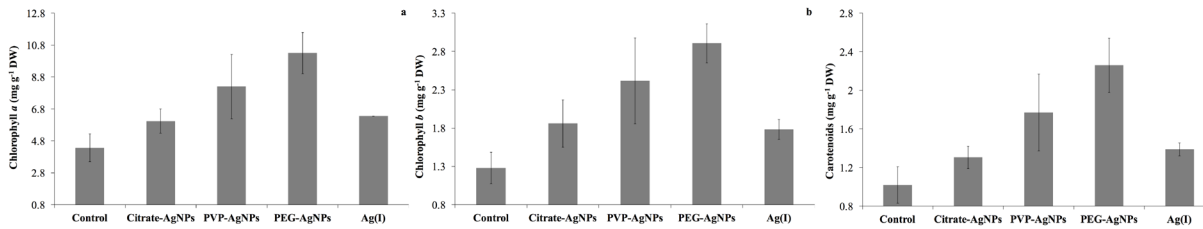

Fig. S7.4 *Foliar concentration of chlorophyll a (**a**), chlorophyll b (**b**) and carotenoids (**c**) of control lettuces and lettuces treated with different 100 nm coated AgNPs (citrate-, PVP- and PEG-AgNPs) and Ag(I) at 3 mg L^{-1} (error bars: standard error; n = 3-4, except for Ag(I) where n = 2).*

CHAPTER 8

Results and discussion

This chapter presents a global discussion of the results summarised in ***Chapters 3-7***. ***Chapter 3*** presents a study that focused on understanding AgNPs adsorption and desorption processes with soils through batch adsorption and leaching studies. The study was carried out by taking into account that soil is one of the main sinks of nanosilver disposal where NPs can undergo different transformation processes that affect their behaviour, mobility and bioavailability [8.1,8.2]. The adsorption kinetics of 75 nm PVP-AgNPs in five Mediterranean soils with different physicochemical properties was tested to determine the influence of soil properties on this environmental process. Adsorption had practically ended after 4 h for all the tested soils, with adsorption rates reaching 80% (see ***Fig. 3.1a***). Affinity coefficients were calculated for all the studied soils to determine which soil had more affinity for AgNPs, except for one soil in which the determination of this coefficient was not possible (see ***Fig. S3.4***). This soil presented a 100% nanosilver adsorption rate 10 min after the experiment started, and showed the fastest adsorption kinetics of all the different examined soils. The affinity coefficients of the other soils coincided with their adsorption rates because the soil with the lowest affinity coefficient had the slowest adsorption kinetics. The differences in the adsorption kinetics between the studied soils can be explained in relation with their cation exchange capacity and electrical conductivity, which are related to clay mineralogy. Therefore, soil physicochemical characteristics can play a key role in the adsorption processes of AgNPs into soil surfaces. Apart from soil physicochemical characteristics, NPs properties can also affect this process, as reported by several authors [8.3,8.4]. In this work, the adsorption kinetics of different coated AgNPs was evaluated using the same soil in each experiment to determine how the surface charge influences this environmental process. Citrate-AgNPs (100 nm) obtained a lower adsorption rate (80%) than PEG- and PVP-AgNPs (100 nm) (almost 100%). Generally NPs with negative zeta potential are more stable in colloidal suspensions compared to the NPs with a low negative zeta potential [8.5]. For this reason, citrate-AgNPs (highly negatively charged) were less adsorbed than PVP-AgNPs (negatively charged) and PEG-AgNPs (neutrally charged) [8.6] as they were less prone to be associated with negatively charged soil surfaces. For comparison purposes, ionic silver was also tested and showed faster adsorption kinetics than the studied AgNPs (see ***Fig. 3.1b***). Particle size effect on adsorption processes was also assessed in this research by taking into account that the smaller the particle size, the larger the surface area, and that particle interactions with soil components are more probable [8.7]. Small-sized citrate-AgNPs (40 nm) were less adsorbed than large-sized citrate-AgNPs (100 nm and 200 nm) (see ***Fig. 3.1c***). These results were quite unexpected because small NPs are more reactive than big NPs. One possible explanation for this phenomenon was that in this work, the

compared suspensions had the same mass concentration, but a different particle number concentration. This fact implies that the number of particles to be adsorbed in 40 nm AgNPs suspension is bigger than in the 100 nm AgNPs suspension. For this reason, smaller AgNPs are less adsorbed than bigger ones. Moreover, the coating and size NP effects were also evaluated for all the soils used herein, and the same previously explained trends were observed, except for one tested soil (see ***Fig. 3.2***). This soil showed better adsorption for the 100 nm citrate-AgNPs than for the other studied NPs, probably because its low organic matter content implies the presence of positive charges on soil surfaces, which would favour interactions with the citrate coating. Therefore, apart from cation exchange capacity and electrical conductivity, organic matter content can also influence nanosilver soil adsorption processes. To evaluate the mobility and bioavailability of AgNPs, leaching tests with water (DIN 38414-S4) and with DTPA were applied to soils after they had been in contact with these emerging contaminants for 3 weeks. The total silver content in the DIN 38414-S4 extracts was low (0.4-4.6%), which indicated scarce nanosilver mobility. Differences in the desorption of the different studied NPs were also observed, and the least desorbed were large-sized AgNPs (100 nm and 200 nm), PVP-coated AgNPs and ionic silver. The completely opposite pattern was obtained when DTPA was used as the leaching agent (see ***Table 3.2***). These differences between both leaching tests can be partially explained by the ability of DTPA to complex ionic silver and the capacity of organic matter to stabilise some AgNPs. The recoveries obtained by leaching tests DIN 38414-S4 and DTPA indicated that both the mobility and the bioavailability of nanosilver were low in the studied soils. Both the aqueous and DTPA leachates were analysed by SP-ICPMS to ascertain if AgNPs would maintain their nanoform after the interactions they underwent during adsorption/desorption processes. In the DIN 38414-S4 leaching solutions that contain PVP-AgNPs and citrate-AgNPs, the nanoform of most particles remained after 3 weeks of being in contact with soils, but practically all the particles in the PEG-AgNPs solution were dissolved (see ***Fig. 3.3***). Differences were also observed between the different sized AgNPs as the smaller ones were more dissolved (see ***Fig. 3.4***). This fact can be explained because smaller particles have a lower redox potential and are constituted with a larger fraction of atoms on the surface than larger NPs [8.8]. Therefore, particle coating and particle size can both play a key role in the transformations that AgNPs undergo during adsorption/desorption processes. In addition to NPs properties, soil physicochemical characteristics proved important in nanosilver transformations during the studied phenomena because the soils with less organic matter content showed less AgNPs and more ionic silver (see ***Fig. 3.5***). The DTPA extracts showed that all the tested nanosilver samples were dissolved, probably due to DTPA's

complexing capacity (see ***Fig. S3.5*** and ***Fig. S3.6***).

The common spectrometric techniques used to monitor the total silver content in adsorption/desorption processes in soils are ICP-based techniques, as presented in our study in **Chapter 3**. However, one of the main drawbacks of these techniques is that they require a previous sample treatment of solid samples, which sometimes needs toxic/corrosive reagents (e.g. acid digestion). Additionally, these analytical tools are quite expensive (e.g. a large quantity of argon is used) [8.9]. TXRF is a cost-effective technique that allows the determination of the total metal content in aqueous and solid samples. With this analytical tool, only a few microlitres of sample are needed to perform the analysis (microanalytical capacity) and solid suspensions can be directly analysed [8.10]. **Chapter 4** is about a TXRF methodology followed to determine AgNPs in aqueous (soil supernatants) and solid (soil) matrices, developed as an alternative to the most frequently used spectrometric techniques. For this purpose, sample preparation for both liquid and solid samples and the best TXRF conditions were studied. LODs were around 34-40 μg L^{-1} for the different sized (75 and 100 nm) and coated AgNP (citrate-, PVP- and PEG-AgNPs) aqueous standard solutions, which were comparable with those obtained for ionic silver (40 μg L^{-1}). Although these LODs were higher than those obtained by ICP-OES (see ***Table 4.2***) and were unsuitable for the analysis of natural waters (lower AgNPs concentrations) [8.11], they were acceptable for monitoring these emerging contaminants in lab-controlled soil adsorption studies. For the solid samples (soil), the LODs obtained from the analysis of soil and sludge CRMs suspensions were around 1.5-1.9 mg kg^{-1} and 1.66-1.83 mg kg^{-1}, respectively. Furthermore in the TXRF analysis, different quantification strategies can be employed, such as external calibration and internal standardisation [8.12]. For internal standardisation purposes, palladium was chosen as the internal standard because the frequently used internal standards (gallium and yttrium) can be present in soil. In the AgNP aqueous suspensions, external calibration was selected because the accuracy values were better (92-100%) than those determined by internal standardisation (84-108%), despite the precision of both quantification methods going below 15% (see ***Table 4.2***). On the contrary, the silver concentrations of the soil and sludge CRMs obtained by internal standardisation were similar to the certified value observed after applying a correction factor to cushion TXRF absorption effects (see ***Table 4.3***). The optimised method was applied to two soil aqueous supernatants and soil samples from AgNPs batch adsorption studies. The total silver concentrations in the soil aqueous supernatants determined by TXRF were similar to those obtained by an ICP-OES analysis (see ***Fig. 4.1***). By taking advantage of the microanalytical potential of TXRF, batch adsorption studies were also performed with only one sample tube instead of seven sample tubes (one for each time in the kinetic

study). The total metal contents using a smaller amount of sample (1 sample tube) were slightly lower than those obtained by our established soil batch adsorption methodology (7 sample tubes), probably because sample rotation was stopped several times in the adsorption kinetics experiment to remove a few µL from the sample tube (see ***Table 4.4***). The direct analysis by TXRF of the total silver in the soils from the batch adsorption studies showed that the concentration values were comparable to those obtained from the soil digests (see ***Table 4.5***). Apart from the possibility of directly analysing solid suspensions, TXRF allows information to be obtained from other elements present in the sample (see ***Fig. 4.2***). A mass balance of the entire procedure was also calculated and confirmed that some silver losses occurred during both analytical methodologies (TXRF and ICP-OES), but the differences compared to the initial silver content were acceptable (<20%) in most cases (see ***Table 4.6***).

The co-existence of nanosilver with ionic silver (e.g. from dissolution processes), together with its low concentration levels in the environment, make it difficult to acquire accurate information about the behaviour of these emerging contaminants in the environment. Therefore, the development and/or improvement of analytical methodologies to preconcentrate and isolate AgNPs from Ag(I) are of paramount importance [8.9]. **Chapter 5** evaluates the potential use of CPE in combination with TXRF for this purpose. Firstly, the experimental CPE procedure conditions were assessed. As reported in the literature, one of the most critical parameters in the CPE procedure is the sample's pH. The highest extraction efficiencies are usually obtained at the analyte's zero-point charge pH [8.13]. Several pHs were tested within the 3-10 range, which gave better extraction recoveries at pH 3.0 for PEG-AgNPs and at pH 3.7 for the other tested NPs (citrate- and PVP-AgNPs) (see ***Fig. 5.2***). As complex samples can contain a mixture of different sized and coated AgNPs, pH 3.7 was chosen. The sample treatment required for the TXRF analysis was evaluated for the different sized (40 and 100 nm) and coated AgNPs (citrate-, PVP- and PEG-AgNPs). In scientific publications on CPE, an acid digestion of the micelle-rich phase (~100 µL) is carried out before the spectrometric analysis is done [8.13-8.15]. In this work, by considering that only a small amount of sample is needed for the TXRF analysis (5-50 µL), two sample treatments were tested to avoid the digestion step: (1) the direct analysis of the surfactant-rich phase; (2) evaporation of the phase containing the AgNPs with a subsequent dissolution by employing an appropriate solvent. The direct analysis of the preconcentrated samples was ruled out because the precision of the analysis was low (RSD >30%, n = 5). This dispersion in the results could have been the result of sample viscosity that makes correct sample deposition on the sample carrier and complete sample drying difficult. Diverse parameters were tested for the second sample preparation

procedure: evaporation temperature (60 ºC and 100 ºC), solvent to reconstitute the evaporated phase (chloroform, carbon tetrachloride, methanol/nitric acid, tetrahydrofuran) and solvent volume (20 µL and 60 µL). By evaporating the AgNPs-rich phase at 60 ºC and reconstituting the evaporated phase with 20 µL of carbon tetrachloride, precision was acceptable (RSD ~12%, n=3). So this sample treatment was selected to prepare the sample before the TXRF analysis. Additionally, the surfactant volumes used in the CPE procedure were evaluated to increase the method's sensitivity. A 0.2 mL volume of surfactant gave the highest silver peak area compared to 0.1 mL and 0.4 mL (see ***Fig. 5.5***). The TXRF measurement conditions were also assessed, and 2,000 s was established as the adequate analysis time. Having established the best analytical conditions of the developed method (CPE-TXRF), LODs, linearity, accuracy and precision were evaluated. The LODs for the different studied coated AgNPs (100 nm citrate-, PVP- and PEG-AgNPs) lay between 0.7-0.8 µg L^{-1}. Although the CPE combined with other common spectrometric techniques, such as ICPMS, leads to lower LODs [8.9,8.10], the developed methodology can be used for other aqueous samples that contain larger amounts of nanosilver. CPE-TXRF is also cost-effective compared to other commonly used spectrometric techniques because of its low operation and maintenance costs [8.16]. The linearity for the PVP- and PEG-AgNPs was good and fell within the 10 to 100 µg L^{-1} concentration range ($R^2 \geq 0.99$), and it was also good for the citrate-AgNPs (concentration range: 10-1,000 µg L^{-1}; $R^2 \geq 0.99$) where, in this case, an extended linearity range was taken because these NPs are frequently employed in commercial products. Despite the different coated AgNPs presenting good linearity, the analytical response at higher concentrations differed between the PEG-AgNPs and citrate-/PVP-AgNPs (see ***Fig. 5.6***). This phenomenon could be due to the zeta potential of PEG-AgNPs being more positive than the other types of studied nanosilvers [8.6]. The accuracy of the CPE-TXRF methodology to analyse mixtures of different coated AgNPs (citrate-, PVP- and PEG-AgNPs), different sized AgNPs (40 and 100 nm) and Ag(I)/AgNPs ratio below 3 was acceptable, with recoveries of 73-114% (see ***Table 5.2***). However, higher Ag recoveries were obtained at a Ag(I)/AgNPs ratio above 3 (>100%) probably because the amount of $Na_2S_2O_3$ (added as a complexing agent) was not enough to complex all the Ag(I) present in the sample. Therefore, the free Ag(I) was adsorbed onto the NP surfaces to be extracted with nanosilver. The precision of the developed methodology was adequate (RSD = 10-15%; n = 6). The CPE-TXRF methodology was applied to aqueous soil leachates and a medical consumer product to determine AgNPs contents. For both real samples, the presence of AgNPs in the CPE extract was confirmed by SP-ICPMS (see ***Fig. 5.7***), but a higher Ag(I) content and a wide variety of NPs sizes were observed for the consumer product extract. The silver concentration values

obtained by CPE-TXRF in aqueous soil extracts agreed with the percentage of nanosilver calculated by the SP-ICPMS analysis (see ***Table 5.3***). However, the presence of a wide variety of different sized AgNPs in the consumer product could reduce CPE extraction efficiency because it is not possible to well extract some considerably sized NPs. Furthermore, the presence of larger amounts of Ag(I) makes the signal separation of both the silver chemical forms in SP-ICPMS difficult, and consequently induces non-accurate AgNPs quantification. This fact, indicated the necessity to study in more detail the effectiveness of existing methodologies (including CPE and SP-ICPMS) for the monitoring of AgNPs in complex samples.

In **Chapter 6** the combination of CPE with SP-ICPMS was investigated to characterise and quantify nanosilver in aqueous samples with high Ag(I) contents, taking into account that CPE has the capacity to isolate AgNPs from aqueous samples containing Ag(I), and SP-ICPMS has the potential to provide information about Ag(I) content, and NPs content and characteristics (e.g. particle size) [8.9,8.13]. Critical parameters of the SP-ICPMS analysis, such as separation of NPs and ionic species signals, and calculating nebulisation efficiencies, were assessed. Taking into account that millilitres of aqueous sample are required in SP-ICPMS to perform the analysis, several solvents were tested to dissolve the CPE extract (~100 µL). Of the studied solvents, 1% glycerol was chosen because the η_{neb} and measurement conditions were similar to those of the nanosilver aqueous suspensions. Several iterative algorithms are proposed in the literature to separate AgNPs and Ag(I) signals [8.17-8.20]. In this study, $\bar{y} + n\sigma$ (n = 3 and n = 5) was tested by using a AgNPs suspension and a solution with a mixture of Ag(I)/AgNPs. The 5σ criterion was found to better discriminate the signals in both samples because it resulted in fewer false positives (see ***Fig. 6.1*** and ***Fig. S6.1***). Therefore, this was the iterative algorithm selected to carry out the study. The nebulisation efficiency values were calculated by two different methods (particle frequency and particle size) to compare the particle size and particle number concentration determinations in unknown samples. The particle frequency and particle size calculation methods were evaluated for the different coated (PVP- and citrate-AgNPs) and sized (75 and 100 nm) AgNPs. The nebulisation efficiencies calculated by the particle size method differed considerably among the different studied AgNPs, and the obtained values were higher than those corresponding to the particle frequency method. However in the particle frequency method, no differences were observed between the studied NPs (see ***Table 6.3***). Bearing in mind that this work was performed with the nanosilver standards characterised by the manufacturer instead of RMs, the presence of Ag(I) could probably be the reason for the differences noted in the η_{neb} obtained by the particle size method. Both particle

size and particle number concentration were determined for all the tested NPs with the η_{neb} obtained by both calculation methods. The AgNPs sizes values calculated by the size-based η_{neb} were more accurate than those that resulted from the frequency-based η_{neb}, but the AgNP number concentrations gave the opposite results because an underestimated particle size implies an overestimated particle number concentration (see ***Table 6.4*** and ***Table S6.3***) [8.21]. Furthermore, the particle sizes obtained in the 1% glycerol medium were slightly bigger than those in the aqueous medium, which was probably due to glycerol stabilising AgNPs by avoiding their dissolution [8.22]. The particle size method was chosen to calculate η_{neb} as the determination of particle sizes was more accurate. As in **Chapter 5**, the pH adjustment for the CPE procedure was also herein evaluated because it is a critical parameter. In this case, the pH that gave the best extraction recoveries for 75 nm PVP-AgNPs was 3.5. So CPE-SP-ICPMS was applied to two synthetic aqueous soil leachates containing AgNPs to determine any possible disturbance to the particle size determination. Fortunately no soil matrix effects and changes in particle size as a result of the CPE procedure were observed (see ***Table 6.5*** and ***Table 6.6***). Another test was performed with the aqueous soil leachates spiked with a mixture of AgNPs/Ag(I) to confirm that the developed methodology was useful for separating these silver chemical forms. The presence of Ag(I) is reduced after applying CPE to synthetic aqueous soil leachates (see ***Fig. 6.3***). Additionally, its presence did not affect the AgNPs size determination as well the silver particle number concentration values after CPE had been applied (see ***Table 6.7***). The developed methodology was applied to the aqueous soil extracts containing the 60 nm citrate-AgNPs and 75 nm PVP-AgNPs obtained from the batch adsorption studies. After applying CPE, and as observed with the synthetic samples, the Ag(I) contribution drastically reduced and gave more accurate AgNPs sizes and AgNP number concentrations compared with the direct analysis by SP-ICPMS (see ***Table 6.8***). Before CPE, both AgNPs sizes and AgNP number concentrations were underestimated as a result of the AgNPs and Ag(I) signals overlapping [8.21], which was solved after applying CPE. The developed methodology allowed information on AgNPs to be obtained after being in contact with the studied soil for 3 weeks. The results indicated that nanosilver did not reduce size after this period of time.

The presence of AgNPs in soils can favour uptake by terrestrial organisms and, consequently, concerns about their ecotoxicological risks on ecosystems and human health are increasing [8.23]. **Chapter 7** reports research that focused on determining the uptake, accumulation, translocation and bioatransformation of AgNPs, as well as the toxicological effects that these emerging contaminants can have on *Lactuca sativa* (lettuce) plants. Nanoparticle properties (e.g. size and coating), and their

concentration in the environment, can affect plant uptake and translocation [8.23]. *Lactuca sativa* plants were cultivated for 9 days (16h/8h light/dark, 21±2 ºC) in Hoagland solutions that contained different sized (60, 75 and 100 nm) or coated AgNPs (citrate-, PVP- and PEG-AgNPs), or at different concentrations (0, 3, 5, 7, 10 and 15 mg L^{-1}). The growing media were subjected to magnetic agitation to maintain homogenous the dispersion of NPs. In the concentration effect tests performed with 75 nm PVP-AgNPs, the presence of silver was confirmed by ICP-OES in both plant tissues. Therefore, lettuce roots absorb AgNPs and some of these particles were translocated to aerial plant parts. More nanosilver was accumulated in lettuce roots than shoots, with increases in both plant tissues in a dose-dependent manner. However, when plants were exposed to AgNPs at concentrations above 7 mg L^{-1}, nanosilver accumulation diminished in plant shoots, probably because the metabolism of these tissues started to be affected by NPs toxicity. The precision of AgNPs measurements in lettuce roots at 10 and 15 mg L^{-1} was poor compared to the lower concentration levels, which could be due to toxicological effects (see ***Fig. 7.1***). As the transpiration and stomatal conductance values were lower for the edible plants exposed to nanosilver (see ***Table 7.2***), it can be stated that these lettuce physiological parameters were affected by AgNPs. Their toxicity can be explained by their dissolution to Ag(I) in lettuce roots and shoots, as observed in the SP-ICPMS analysis. ***Fig. 7.5*** depicts the complete dissolution of the AgNPs accumulated in plant shoots, but plant roots presented a mixture of AgNPs and Ag(I) (see ***Fig. 7.4***). The nanosilver dissolution in root tissues decreased at high concentration levels. The presence of more nanoparticulate silver at 5-10 mg L^{-1} than at 3 mg L^{-1} could be due to the higher amount of AgNPs and the lower probability of them all being partially or totally dissolved. In addition, proper nanosilver dissolution at low exposure concentrations was evidenced by the Ag K-edge EXAFS analysis of root tissues, where a lower proportion of Ag-Ag bonds was observed compared to high concentration levels (see ***Table 7.4*** and ***Fig. 7.8***). Although the toxicological effects in the studied plants seemed to be induced by Ag(I), at 5 mg L^{-1}, at which the transpiration and stomatal conductance values were comparable to the other tested concentrations, the predominant ligand environment presented Ag-Ag bonds (see ***Table 7.4***). Therefore at this concentration level, NPs probably also exerted toxicity on lettuces. For comparison reasons, Ag(I) was also studied and more accumulation in lettuce roots and shoots was observed compared to 75 nm PVP-AgNPs. Coating effect tests indicated that particle surface charges had no effect on these biological processes as no differences were observed between the different tested coated AgNPs (see ***Fig. 7.2***). Although no statistical differences were found in the silver accumulated in plant shoots, it would seem that 100 nm PEG-AgNPs (neutral charged) and Ag(I)

were slightly better transported to the aerial parts of this edible plant than negatively charged particles (100 nm citrate- and PVP-AgNPs). The uptake and accumulation of these different coated NPs were also confirmed by SP-ICPMS, and different trends in their dissolution were observed. The percentage of nanosilver estimated by SP-ICPMS indicated that citrate- and PEG-AgNPs were more dissolved in lettuce roots than PVP-AgNPs. The Ag K-edge EXAFS analysis found a similar Ag neighbourhood for citrate- and PEG-AgNPs (see ***Fig. 7.9***) and fewer Ag-Ag bonds compared to PVP-AgNPs (see ***Table 7.5***). Although the results indicated that PVP-AgNPs were more stable in root tissues than the other tested coatings, the notion that toxicological effects depended on NPs coating were not clear. The chlorophyll and caroten contents of the edible plants treated with citrate-AgNPs were similar to Ag(I), but both transpiration and stomatal conductance were comparable to the PEG-AgNPs values (see ***Fig. S7.4*** and ***Table 7.3***). Although the toxicity of the different coated NPs was unclear, the coated NPs generated a less negative impact on lettuces than Ag(I) as all the tested physiological parameters (transpiration, stomatal conductance, photochemical efficiency, chlorophyll and carotene contents) for the lettuces treated with Ag(I) had the lowest values (see ***Table 7.3***, ***Fig. S7.2*** and ***Fig. S7.4***). Particle size also affected nanosilver uptake, accumulation and translocation in the studied edible plants. The performed tests demonstrated that smaller NPs accumulated more in lettuce roots, which backs the hypothesis that smaller particles are more trapped by roots, but are less transported to lettuce shoots (see ***Fig. 7.3***). This tendency was confirmed by the translocation factor calculation. One possible explanation for the better transportation of large NPs could lie in their better stability than smaller-sized AgNPs, as corroborated by the Ag K-edge EXAFS analysis of lettuce roots (53% *vs* 38%; 100 and 75 nm PVP-AgNPs, respectively) (see ***Table 7.6***). The percentage of Ag(I) estimated by SP-ICPMS indicated that smaller AgNPs were more dissolved (99%) than bigger ones (26%) in lettuce shoots. In short, these results obtained during this thesis provide valuable information about the behaviour of AgNPs in soils (mobility and bioavailability) and in lettuce (uptake, accumulation, translocation and biotransformation) with the developed or improved analytical methodologies.

References

[8.1] S.A. Blaser, M. Scheringer, M. MacLeod, K. Hungerbühler, Estimation of cumulative aquatic exposure and risk due to silver: contribution of nano-functionalized plastics and textiles, Sci. Total Environ. 390 (2008) 396–409.

[8.2] P.S. Tourinho, C.A.M. van Gestel, S. Lofts, C. Svendsen, A.M.V.M. Soares, S. Loureiro, Metal-based nanoparticles in soil: fate, behavior, and effects on soil invertebrates, Environ. Toxicol. Chem. 31

(2012) 1679–1692.

[8.3] M. Hoppe, R. Mikutta, J. Utermann, W. Duijnisveld, G. Guggenberger, Retention of sterically and electrosterically stabilized silver nanoparticles in soils, Environ.

[8.4] M. Hoppe, R. Mikutta, J. Utermann, W. Duijnisveld, S. Kaufhold, C.F. Stange, *et al.*, Remobilization of sterically stabilized silver nanoparticles from farmland soils determined by column leaching, Eur. J. Soil Sci. 66 (2015) 898–909.

[8.5] T.C. Prathna, N. Chandrasekaran, R. Ashwathy, A. Mukherjee, Studies on aggregation behaviour of silver nanoparticles in aqueous matrices: effect of surface functionalization and matrix composition, Colloids Surfaces A Physicochem. Eng. Asp. 390 (2011) 216–224.

[8.6] Nanocomposix. Standard capping agents, (n.d.). Available at: http://cdn.shopify.com/s/files/1/0257/8237/files/Standard_Capping_Agents.pdf. Accessed: February 6, 2018.

[8.7] I. Römer, T.A. White, M. Baalousha, K. Chipman, M.R. Viant, J.R. Lead, Aggregation and dispersion of silver nanoparticles in exposure media for aquatic toxicity tests, J. Chromatogr. A. 1218 (2011) 4226–4233.

[8.8] A.D. Dwivedi, S.P. Dubey, M. Sillanpää, Y.-N. Kwon, C. Lee, R.S. Varma, Fate of engineered nanoparticles: implications in the environment, Coord. Chem. Rev. 287 (2015) 64–78.

[8.9] F. Laborda, E. Bolea, G. Cepriá, M.T. Gómez, M.S. Jiménez, J. Pérez-Arantegui, *et al.*, Detection, characterization and quantification of inorganic engineered nanomaterials: a review of techniques and methodological approaches for the analysis of complex samples, Anal. Chim. Acta 904 (2016) 10–32.

[8.10] R. Klockenkämper, Total-reflection X-ray fluorescence analysis, Wiley, 1997.

[8.11] T.Y. Sun, N.A. Bornhöft, K. Hungerbühler, B. Nowack, Dynamic probabilistic modeling of environmental emissions of engineered nanomaterials, Environ. Sci. Technol. 50 (2016) 4701–4711.

[8.12] E. Marguí, R. van Grieken, X-ray fluorescence spectrometry and related techniques: an introduction, Momentum Press, 2013.

[8.13] J.-F. Liu, J.-B. Chao, R. Liu, Z.-Q. Tan, Y.-G. Yin, Y. Wu, *et al.*, Cloud point extraction as an advantageous preconcentration approach for analysis of trace silver nanoparticles in environmental waters, Anal. Chem. 81 (2009) 6496–6502.

[8.14] J.-B. Chao, J.-F. Liu, S.-J. Yu, Y.-D. Feng, Z.-Q. Tan, R. Liu, *et al.*, Speciation analysis of silver nanoparticles and silver ions in antibacterial products and environmental waters via cloud point extraction-based separation, Anal. Chem. 83 (2011) 6875-6882.

[8.15] S.-J. Yu, J.-B. Chao, J. Sun, Y.-G. Yin, J.-F. Liu, G.-B. Jiang, Quantification of the uptake of silver nanoparticles and ions to HepG2 cells, Environ. Sci. Technol. 47 (2013) 3268-3274.

[8.16] E. Marguí, M. Sagué, I. Queralt, M. Hidalgo, Liquid phase microextraction strategies combined with total reflection X-ray spectrometry for the determination of low amounts of inorganic antimony species in waters, Anal. Chim. Acta 786 (2013) 8–15.

[8.17] H.E. Pace, N.J. Rogers, C. Jarolimek, V.A. Coleman, E.P. Gray, C.P. Higgins, *et al.*, Single particle inductively coupled plasma-mass spectrometry: a performance evaluation and method comparison in the determination of nanoparticle size, Environ. Sci. Technol. 46 (2012) 12272–12280.

[8.18] D.M. Mitrano, E.K. Lesher, A. Bednar, J. Monserud, C.P. Higgins, J.F. Ranville, Detecting nanoparticulate silver using single-particle inductively coupled plasma-mass spectrometry, Environ. Toxicol. Chem. 31 (2012) 115–121.

[8.19] J. Tuoriniemi, G. Cornelis, M. Hassellöv, Size discrimination and detection capabilities of single-particle ICPMS for environmental analysis of silver nanoparticles, Anal. Chem. 84 (2012) 3965–3972.

[8.20] G. Cornelis, M. Hassellöv, A signal deconvolution method to discriminate smaller nanoparticles in single particle ICP-MS, J. Anal. At. Spectrom. 29 (2014) 134–144.

[8.21] J. Liu, K.E. Murphy, M.R. Winchester, V.A. Hackley, Overcoming challenges in single particle inductively coupled plasma mass spectrometry measurement of silver nanoparticles, Anal. Bioanal. Chem. 409 (2017) 6027–6039.

[8.22] M.D. Montaño, J.W. Olesik, A.G. Barber, K. Challis, J.F. Ranville, Single particle ICP-MS: advances toward routine analysis of nanomaterials, Anal. Bioanal. Chem. 408 (2016) 5053–5074.

[8.23] A. Rastogi, M. Zivcak, O. Sytar, H.M. Kalaji, X. He, S. Mbarki, *et al.*, Impact of metal and metal oxide nanoparticles on plant: a critical review, Front. Chem. 5 (2017) 78.

CHAPTER 9

General Conclusions

The main aim of this thesis was to evaluate AgNPs mobility and bioavailability in soil systems and to assess their accumulation, biotransformation and toxicity in edible plants. To do so, the development or improvement of analytical methodologies for the accurate determination of AgNPs in environmental samples forms a significant part of this research.

Despite detailed conclusions being included at the end of each chapter, this section summarises the main research conclusions. Moreover, a brief discussion of the future studies that might derive from the research carried out in this thesis is presented.

Batch adsorption studies demonstrated that AgNPs can be quickly and efficiently adsorbed on soil surfaces. High cation exchange capacity and electrical conductivity values were found to be the soil properties that favoured fast nanosilver adsorption kinetics, whereas low organic matter content can can stabilise AgNPs hampering their adsorption. Nanosilver size and coating also influenced soil adsorption processes, and larger ones with a less negative surface charge were more efficiently adsorbed.

Leaching experiments showed that these emerging contaminants are well retained in soils, along with low mobility and bioavailability. During this environmental process, smaller and negatively charged AgNPs were the least desorbed in leaching test using water (DIN 38414-S4), but the opposite trend was observed in leaching procedure using DTPA. Furthermore during adsorption and desorption processes, AgNPs can be dissolved, and nanosilver and soil properties also play an important role.

The developed TXRF methodology proved to be a possible alternative to ICP-OES or ICPMS to determine Ag content dealing with AgNPs in aqueous soil supernatants and soil samples from batch adsorption experiments. Moreover with this analytical tool, some advantages over other techniques emerge, such as the possibility of analysing soil samples by means of solid suspensions, obtaining information on other elements present in samples, smaller amounts of sample and reagents are required and operation costs are lower. However, TXRF provides information on total silver content which indicates that AgNPs cannot be discriminated from Ag(I).

The CPE-TXRF combination allows analyses to be performed to quantify the total nanosilver amount in complex samples containing low nanosilver concentrations and mixtures of AgNPs and Ag(I), such as aqueous soil leachates. This fact is given by CPE, which has the potential to isolate and preconcentrate nanosilver in aqueous samples. However with this methodology, only AgNPs quantitative information can be obtained and the presence of large amounts of Ag(I) can induce inaccurate NP quantification. So further studies are required to apply the methodology to complex samples containing mixtures of NPs with different coatings and sizes.

The developed CPE-SP-ICPMS methodology enables AgNPs size and particle number concentration to be determined in aqueous soil leachates. The employment of iterative algorithm $\bar{y} + 5\sigma$ helps to discriminate AgNPs from Ag(I) in the SP-ICPMS analysis in aqueous samples containing small amounts of Ag(I), but this proves more difficult at a high Ag(I) because of the signals of both chemical forms overlapping. The application of CPE to complex samples (containing large amounts of Ag(I)) before performing SP-ICPMS demonstrated its ability to reduce Ag(I) content, which solves the aforementioned problem. Furthermore, the nebulisation efficiencies obtained by the particle size calculation method allows to calculate more accurate particle sizes. Therefore, the developed methodology appears to be a promising alternative to sophisticated hyphenated techniques to obtain accurate particle sizes and particle number concentrations.

The study of exposure of lettuces to AgNPs at different concentrations demonstrated that their uptake by lettuce roots and translocation to aerial plant parts were concentration-dependent. The amount of accumulated nanosilver also affected their dissolution inside roots and shoots, which was more dissolved and biotransformed at lower concentrations. Although transpiration and stomatal conductance of plants were affected after being exposed to AgNPs, the toxicological effects were similar at the different exposure concentrations. Nanoparticle coating had no effect on nanosilver absorption by lettuce roots, but transportation to lettuce shoots seemed more efficient for less negative charged NPs. PVP-AgNPs were more stable inside lettuce roots compared to PEG- and citrate-AgNPs, but the role of coating on the damage that these NPs can cause to edible plants remained unclear. Smaller AgNPs were taken up more by lettuce roots than larger particles, but were less translocated to aerial plant parts. Inside lettuce roots, small-sized NPs proved more suitable to be dissolved and biotransformed than large-sized NPs. Although Ag(I) from the dissolution of nanosilver seemed responsible for the toxicological effects, in some cases the NP form apparently induced toxicity. However, the worst toxicological effects were observed for the plants treated with Ag(I). Therefore, more studies are needed to completely understand the role that NPs characteristics play in the negative impacts that may affect edible plants. From these conclusions, future studies on nanosilver soil adsorption and desorption processes can focus on investigating other sized and coated AgNPs to completely understand the behaviour, mobility and bioavailability of these emerging pollutants in this environmental compartment. Conducting desorption studies at different times can help to obtain information about the aging and transformation of AgNPs in soils. Further studies could be performed using CPE with mixtures of different sized and coated nanosilver to improve our understanding of size resolved extraction efficiencies by CPE by

bearing in mind that NPs with different characteristics exist in real samples. Further research in the future could focus on the accumulation and biotransformation of AgNPs inside terrestrial animals as a consequence of their presence in roots and shoots in edible plants (lettuces). More research on the toxicological effects that AgNPs with different properties (e.g. size and coating) may have on terrestrial organisms has to be conducted.